Paleoseismology and Paleogeodesy of the Sumatran Subduction Zone:

A Study of Vertical Deformation Using Coral Microatolls

Thesis by

Judith Zachariasen

In Partial Fulfillment of the Requirements

for the Degree of

Doctor of Philosophy

California Institute of Technology

Pasadena, California

1998

(Submitted October 3, 1997)

This thesis is dedicated to

my parents,

Kerry, John, and Maddie

and Rubio

Acknowledgments

I would like to thank my three primary advisors: Kerry Sieh, who introduced me to the field of paleoseismology, gave me the opportunity to work on an exciting new project, and opened the door to Indonesia for me; Fred Taylor, who offered his considerable experience and expertise in the use of corals as sea level recorders and paleoseismological tools and persevered with me through a long and rainy 1996 field season; and Larry Edwards, who welcomed me into his lab and offered guidance and instruction in using U-Th geochronology to date corals. Each contributed from his own area of expertise, and I benefited from it all.

All the members of the Minnesota Isotope Lab - John, Hai, Kirsten, Christina, Min, Chuck, Jeff, Lynn - deserve my utmost gratitude for making me so welcome in their workplace and giving me help at all times, from explaining U-series systematics *again*, to showing me new and valuable lab techniques, to turning off hotplates, to giving up their time on the machine to let me finish my work. To all of them, thanks from "the visitor". Special thanks go to Hai Cheng who trained me in the lab techniques; John Hoff, who answered infinite questions, repeatedly saved the day when the machine went down, and generally earned the nickname "God;" and Kirsten Banks, for coffee and rice krispie bars among many other things.

I would like to acknowledge all the people who helped me in the field in Indonesia: the people from LIPI - Wahyoe Hantoro, who provided enthusiasm and support, and his colleagues and assistants, Nono, Anto, Sri, Dudi, Arief; the owner and crew of our field vessel the Dani Putra - owner Daniel Madre, Captain Tobing, and crew Doni, Bambang, Rapit, and As; and the proprietors of the Wisma Lestari, who took such good care of us while we were in Sikakap, watched our equipment and the tide gauge, and took hourly tide measurements for us in 1994.

Abstract

Corals from Western Sumatra retain stratigraphic records of relative sea-level change that can be used to infer vertical displacement rates in the hanging wall block of the Sumatran subduction zone. The upward growth of the coral "microatolls" is limited by low water levels, and fluctuations in water level produce measurable changes in the coral morphology. Furthermore, the corals contain annual growth rings, which act as an internal chronometer of coral growth history. The microatolls, which are widespread and can live for decades or centuries, can serve as natural long-term tide gauges, recording sea-level variations over wide intervals of space and time.

Relative sea-level records from living corals from the outer-arc islands and mainland coast constrain the nature of recent vertical deformation over the subduction zone. Emerged fossil corals from the islands, dated with U-Th geochronometry, constrain the paleoseismic and paleogeodetic history of the region.

Stratigraphic analysis of cross-sectional slabs cut from living coral heads reveals that the islands have been submerging at rates of 4-10 mm/yr over the last four or five decades, while the mainland has remained relatively stable. Many fossil corals died in the early 1800's. Their age and morphological signature indicate they died as a result of coseismic uplift of more than 1m during the last great subduction-zone earthquake in this region, in 1833, following decades of interseismic submergence at rates similar to modern rates.

Other sampled corals died at earlier times throughout the late to mid-Holocene. Their presence in the intertidal zone suggests that little permanent vertical deformation has occurred here over the past several thousand years, and, therefore, most of the accumulated interseismic strain is recovered during earthquakes. The temporal distribution of coral deaths suggests an average earthquake recurrence interval for subduction zone events of about 230 years. Combining sea-level histories from modern, 1833, and older corals yields partial records of co- and interseismic vertical displacement for multiple earthquake cycles. Such displacement records from the hanging wall of a major plate boundary can help constrain models of subduction-zone deformation.

Table of Contents

List of Illustrations

List of Tables

Chapter I

Introduction

1. Introduction

2. Geological Setting of Sumatra and the Mentawai Islands

    2a. Tectonic setting

    2b. Earthquake history

    2c. Western Sumatran margin and the Mentawai Islands

    2d. North Pagai, South Pagai, Sipora, and Sanding

3. Holocene sea level changes

    3a. Glacio-isostatic and hydro-isostatic effects on sea-level

    3b. Holocene sea-level records in the Indian Ocean

    3c. Models of glacio-isostatically-controlled sea-level change

    3d. Glacio-isostatic models of sea-level history in western Sumatra

4. Observations and models of subduction zone deformation

    4a. Geodetic observations from other subduction zones

    4b. Models of subduction zone deformation

5. Corals

    5a. Corals and coral reefs

    5b. Microatolls

    5c. Distinguishing tectonically and oceanographically induced sea level changes

    5d. Corals, sea level records, and tectonics - Previous work

    4e. Microatolls, tectonics and paleoseismology - Previous work

    4f. Cocos Islands tidal records and hypothetical coral growth

6. Microatolls, paleoseismology, paleogeodesy - goals of this study

1.1. Introduction

Understanding of earthquake recurrence and rupture characteristics is hampered by a paucity of observational data. Accurate characterization of earthquake processes requires knowledge of the temporal and spatial pattern of past earthquakes. This applies both to the earthquake process in general and to the behavior of individual faults and fault segments. Unfortunately, the historical and instrumental records of earthquake occurrence and associated coseismic and interseismic deformation are few and far between. Seismological records are only available for the past century, and instrumental geodetic records are similarly short. Geodetic records from leveling lines and tide gauges are, in general, sparsely distributed geographically and records more than 100 years old are rare. Historical records of seismic shaking and intensity may be longer, but are also sporadic, and very much dependent on the degree of human development in a region. The period of time for which these records are available is shorter than the average earthquake recurrence interval along most major faults and plate boundaries. Thus, in very few places is the historical record of seismic activity complete through even one earthquake cycle, let alone the many that would be needed to understand the nature of earthquake processes.

Paleoseismological techniques were developed to address this lack of instrumental records. The principle behind paleoseismology is to study the geologic expression of past earthquakes. Only in the geologic record is information available for multiple past earthquake cycles. If the nature of these former earthquakes can be discerned from the geological traces they have left, it will help characterize the timing and size of coseismic faulting events along individual faults. If this characterization is available for many faults, it can help constrain models of earthquake processes in general. This is important both for

the advancement of scientific understanding in seismotectonics and for seismic hazard assessment.

Paleoseismological techniques that have been used successfully have included tectonic geomorphology, excavation of fault scarps and traces, and documentation of uplift and subsidence of old shorelines. Paleoseismologists have studied the earthquake history of faults by analyzing old fault scarps and measuring the offset of various features across them. R.E. Wallace (1968) measured offset streams across the San Andreas Fault in the Carrizo Plain to estimate the size of coseismic displacements during past earthquakes, arguing that the smallest offsets probably represented slip in a single event, while larger offsets were probably the cumulative offset from several similar past earthquakes (Yeats and Prentice, 1996). Similar work has been done with normal fault scarps and has involved analyzing the erosional degradation of old scarp surfaces to estimate the size and number of coseismic ruptures the scarp represents (e.g. Wallace, 1977). Estimated ages of faulted Quaternary strata combined with the estimates of coseismic rupture determined from analysis of the fault scarps and offset features permitted workers to estimate recurrence intervals for earthquakes (e.g. Clark et al., 1972). K. Sieh introduced methods to date individual earthquakes and determine the magnitudes of coseismic ruptures with detailed fault excavations and ^{14}C dating of organic material contained in the faulted sediments (Sieh, 1978). These techniques, and newer ones that have built upon them, have been the cornerstones of paleoseismology, at least for subaerially exposed faults.

The problem of a lack of data is exacerbated at subduction zones. Subduction zones have generated the largest earthquakes in the historical record, yet the nature of deformation there is much less well-studied than at transform margins, primarily because they are largely inaccessible to direct observation. One cannot readily measure features offset across the fault or excavate the scarp. Understanding of slip on subduction

interfaces and deformation of adjacent blocks has been limited primarily to that gleaned from seismological and geodetic inversions. Yet, furthering the understanding of subduction-zone tectonics requires more observational data about the coseismic and interseismic cycles of deformation. Given that the slip interface itself will likely remain unobservable, we are limited to increasing our observational knowledge of subduction-related deformation at the earth's surface.

Thus far observations of vertical deformation at the surface above subduction zones are limited. GPS data are robust but scarce and limited to the very recent past. Tide gauges have been installed above subduction zones in numerous locations around the world, and they record sea-level changes that are oceanographically and tectonically induced. For example, tide gauge records have been used in both Alaska and Japan to document sea level changes associated with coseismic vertical deformation (Savage and Plafker, 1991; Savage and Thatcher, 1992; see section 4, this chapter). However, these records are unusual. In most areas, tide records are much shorter and more geographically sparse. And, of course, there are no such records for the pre-instrumental period. What is required to document both recent and older vertical deformation at other subduction zones is a long-lived recorder that extends the geodetic record into the past.

Paleoseismological methods that have been applied to study past subduction-zone earthquakes have mostly involved analysis of uplifted and submerged coastlines. Raised marine terraces in Papua New Guinea, Alaska, Japan, and New Zealand, among other places, are thought to have been uplifted tectonically (e.g. Ota et al., 1993; Ota and Chappell, 1996; Plafker and Rubin, 1967; Ota, 1985; Ota et al., 1991). Comparison of some of these older terraces to terraces developed by modern coseismic uplift in the same region has led workers to infer that each of the older terraces was formed in a similar coseismic event in the past (Pandolfi, 1994; Plafker and Rubin, 1967; Ota et al., 1993). Successive burial of old coastal lowlands by intertidal mud and sand that was probably

deposited by tsunamis have been interpreted to indicate the occurrence of coseismic subsidence events in coastal Washington, above the Cascadia subduction zone (Atwater, 1987; Atwater and Yamaguchi, 1991).

Traditional paleoseismological analyses have yielded the ages of past earthquakes and often the amount of associated coseismic offset. Rarely, however, do they shed light on the deformation that occurs between events. That record is usually lost once the earthquake occurs and releases the accumulated strain. What remains is the net displacement from the coseismic rupture.

In this thesis, I present the results of a paleoseismological and paleogeodetic study of the Sumatran subduction zone that illustrates how certain kinds of coral can be used not only to document the occurrence of past earthquakes, but also to constrain the nature of the coseismic and interseismic vertical deformation of the hanging wall above the subduction zone.

The upward growth of certain species of coral is sensitive to changes in sea level on the order of a few centimeters. Thus, these corals, many of which thrive in the equatorial waters of Sumatra, may serve as natural tide gauges, recording in their morphology changes in relative sea level, from a few centimeters to more than a meter, that have occurred during the lifetime of the coral. The average growth rate of the corals is about 1 cm/yr. Therefore, a coral 3 m in diameter contains a sea-level record of about 150 years. Dead corals have been shown to be accurately dateable with U-Th geochronometry, with precision of a few permil possible (Edwards et al., 1987a,b,c; Edwards, 1988). If the date of death of the coral is known, one can determine the relative sea-record for the period up to and including the age of death. By combining such sea-level records of corals of different ages, one could conceivably obtain a complete record of coseismic and interseismic displacement throughout multiple earthquake cycles. This technique, which can be used wherever the appropriate corals grow, can yield detailed

records of deformation throughout several earthquake cycles and help inform our understanding of the nature of subduction zone deformation.

In Chapter 2, I examine the accuracy and precision of corals as tide gauges by studying the record of ongoing relative sea-level change retained in living corals from the west coast and outer-arc islands of Sumatra. Living corals provide the best constrained data set with which to examine the quality of this paleogeodetic "instrument" because there is excellent age control, erosion is minimal and living coral is necessarily *in situ*. Chapter 3 presents the results from U-Th dating of fossil coral samples from the same region. Chapter 4 provides a paleoseismological and paleogeodetic analysis of these fossil corals. I apply the methods described and used in Chapter 2 to the dead corals whose ages are presented in Chapter 3, to find a record of several large paleo-earthquakes and the vertical displacement that accompanied and preceded them. I speculate on the complete deformational history that the records imply, from several centuries in the past into the present day. Chapter 5 presents a brief synopsis of the conclusions of the previous chapters.

The remainder of this chapter presents some background information on the tectonic and geologic setting of the trench-proximal western margin of Sumatra; average Holocene sea level history; characteristics of subduction zone deformation, observations of deformation at other subduction zones and various models proposed to describe them; and characteristic of corals and specifically the microatolls that I use to infer sea-level and tectonic displacement histories.

1.2. Geological Setting of Sumatra and the Mentawai Islands

Sumatra presents an ideal setting in which to examine coral records of vertical deformation. It sits on the overriding plate of a major subduction boundary which has

been the site of historical earthquakes with estimated moment magnitudes greater than M_W 8. Many species of coral grow in abundance along the coasts of the main and the smaller islands offshore, making west Sumatra an excellent place to examine coral records and test the value of coral as a paleoseismological tool. As such a tool, of course they are obviously best applied at low-latitude sites where corals are abundant. However, general results about subduction zone earthquake characteristics derived from such a coral study can perhaps be applied elsewhere, at high-latitude sites without coral. In addition, although seismic activity has been slight along the subduction zone since the most recent, mid-19th century earthquakes, convergence continues at a relatively rapid rate, and GPS measurements suggest the degree of locking on parts of the subduction zone is large (Prawirodirdjo et al., in prep. 1996). Sumatra is a location in which to expect large subduction zone events in the future. Given the increasing population and development in Sumatra, such earthquakes could produce significant damage and loss of life. Any information characterizing the seismic history and patterns of deformation will be helpful for regional seismic hazard analysis.

1.2a. Tectonic setting

The island of Sumatra, within the Indonesian archipelago, sits atop the Southeast Asian plate, beneath which the Australian and Indian plates are subducting (Figure 1.1). The coast is about 200-240 km from the subduction-zone trench. The outer-arc rise, about 100 km from the trench, is subaerially exposed as a series of outer-arc islands, the Mentawai chain. GPS measurements across the boundary show that the Australian and Southeast Asian plates are converging at a rate of 67 ± 7 mm/yr , with the Australian plate moving in a direction about N11E ± 4 relative to the Southeast Asian plate (Tregoning et al., 1994). The convergence direction, though nearly perpendicular to the trench in Java, is highly oblique to the plate boundary southwest of Sumatra, increasingly

Figure 1.1. Location map of Sumatra

The island of Sumatra lies parallel to the convergent boundary between the Indian and Australian plates and the Southeast Asian plate. This subduction zone is capable of producing earthquakes greater than or equal to Mw 8.5, the two most recent of which occurred in 1833 and 1861(inferred rupture zones in light and dark grey shading, after Newcomb and McCann, 1987).
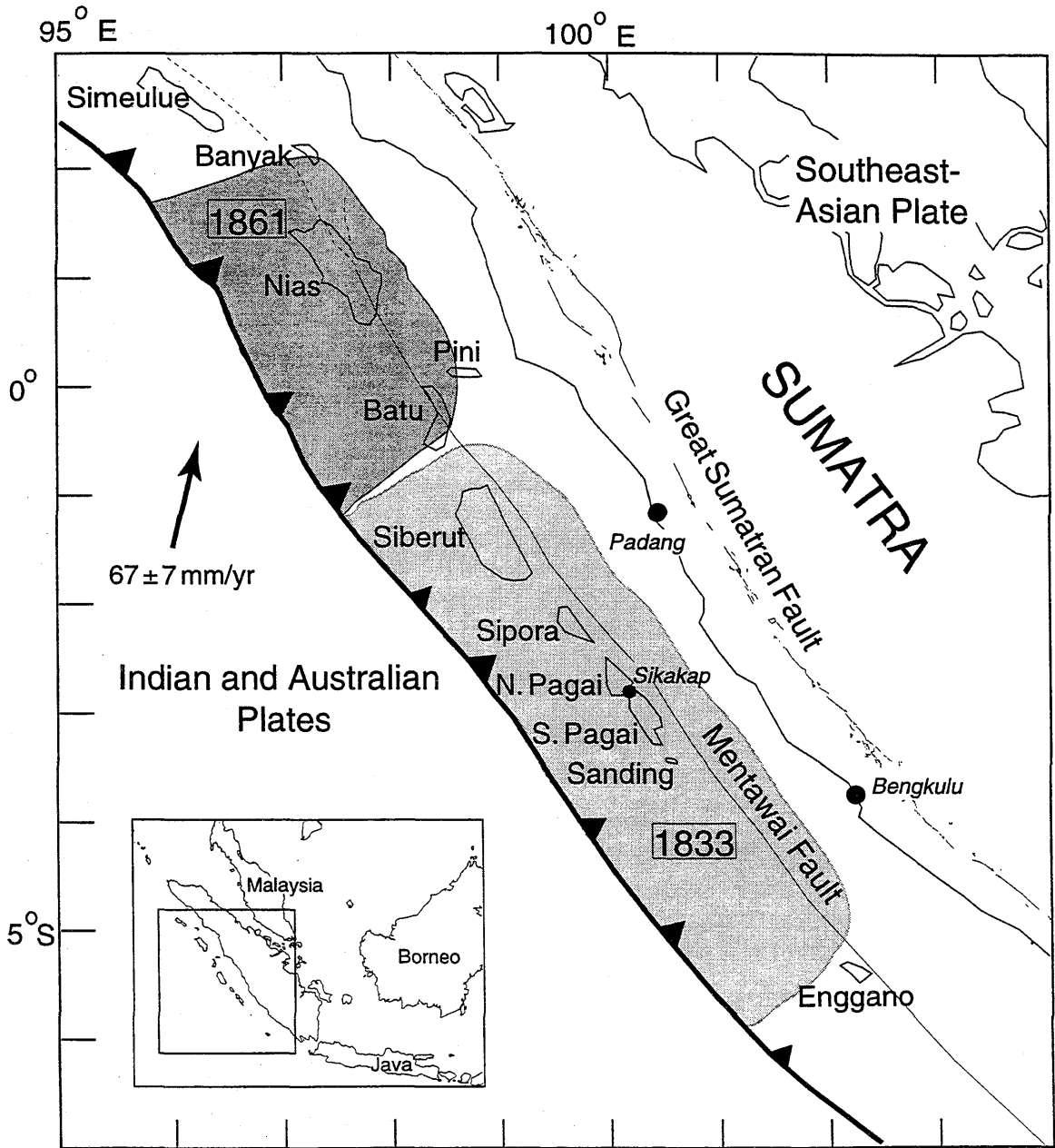
so to the northwest. Several studies (Fitch, 1972; McCaffrey, 1991,1992; Diament et al., 1992) have suggested that the convergent strain is strongly partitioned between near-orthogonal subduction at the trench and right-lateral strike-slip along the Great Sumatran Fault (GSF). The GSF is subparallel to the trench and runs the 1650 km length of Sumatra through the volcanic arc.

McCaffrey (1991) has argued that the variation in the slip vector azimuths from thrust earthquakes along the SSZ indicates that the Sumatran fore-arc sliver between the trench and the GSF should be stretching in an arc-parallel direction, with trench-parallel slip increasing from south to north. Analysis of streams and volcanic lineaments offset along the GSF, seen on Spot-images, suggest that dextral slip on the GSF in the south of Sumatra, at about 5°S, is occurring at about 2-10 mm/yr, while in the north, at 2°N the rate is about 23 mm/yr (Bellier et al., 1991; Malod et al., 1993; Detourbet et al., 1993; Beaudoin, et al., 1995). These rates are not well constrained because the offset features have not been rigorously dated; their ages are only known to be Quaternary. The remote-sensing estimates are, however, consistent with more rigorous field analyses of offsets along the GSF. Sieh (1991) measured the offset of stream channels that had incised dated volcanic deposits and found slip rates of 11 mm/yr at 3°S and 0.25°S and 27 mm/yr at 2°N. These rates are significantly lower than rates estimated from relative plate motion. The apparent stretching of the fore-arc sliver, which, based on relative plate motions, should increase from 0 in the Sunda Strait to about 50 mm/yr in the Andaman Sea north of Sumatra, has not been fully accounted for on observed structures. Diament and others (1992) suggest some of it occurs on the Mentawai Fault (MF) and possibly on other fore-arc structures. The MF, at least 600 km long, strikes parallel to the trench and the GSF but is located west of the Sumatra coast, in the ocean, and separates the forearc basin from the accretionary prism (Diament et al., 1992; Malod et al., 1993; Izart et al., 1994). There are several strike-slip faults in the fore-arc, but few extensional basins north of the

Sunda Strait, between Java and Sumatra, so apparently the structures accommodating fore-arc extension are primarily strike-slip rather than normal faults (Karig et al., 1980; McCaffrey, 1991). Seismic reflection data suggest the MF is predominantly strike-slip, though, where exposed on land, it displays little sign of lateral displacement and has been interpreted as a flexure zone or possibly a steep back-thrust (Diament et al., 1992; Karig et al., 1980).

The fore-arc is cut by three major structural features that trend northeast, oblique to the trend of the island chain. South of the island of Enggano, in the Mentawai chain, two deep sediment-filled grabens intersect the trench and cross the forearc; below the Batu Islands, which lie at the crest of the Pini Arch, a high, broad arch in pre-Oligocene basement rocks, the Investigator Fracture Zone is being subducted; at the Banyak Islands to the north, a series of vertical right-lateral oblique faults cuts across the forearc (Verstappen, 1973; Karig et al., 1979, 1980; Newcomb and McCann, 1987).

The dip of the subducting plate is not well constrained, but earthquake hypocenters and moment-tensor solutions of earthquakes in the hanging wall suggest that it is shallow (<15 degrees) near the trench and below the outer-arc rise and steepens to near 50 degrees below the volcanic arc and GSF (about 250 km from the trench) (Newcomb and McCann, 1987; Fauzi et al., 1995; Harvard CMT catalogue) (Figure 1.2). The dip of the GSF is near vertical.

Recent GPS analysis by Prawirodirdjo and others (in prep., 1996) indicates different behavior by the two parts of the plate boundary north and south of the Batu Islands - the forearc south of the Batus is moving NNE with the Australian plate at a rate about equal to the plate rate; north of the Batus, the forearc is moving NNW, in a nearly trench-parallel direction. The observed motions suggest that the southern part of the subduction zone is fully locked but the northern part only about 50% coupled.

Figure 1.2. Cartoon cross-section of the Sumatran subduction zone at the latitude of the Pagai/Sipora Islands. Black rectangles depict land, the outer-arc islands and mainland Sumatra. The black triangle depicts the volcanic arc. The dip of the slab under the islands is inferred from moment-tensor solutions of recent earthquakes near Sipora Island. The dip under Sumatra and the volcanic arc is inferred from the dip of the Benioff-Wadati zone (Newcomb and McCann, 1987; Fauzi et al., 1995).

~110 km

50°

~38

~24 km

~180 km

~115 km

12°

~120 km

50 km
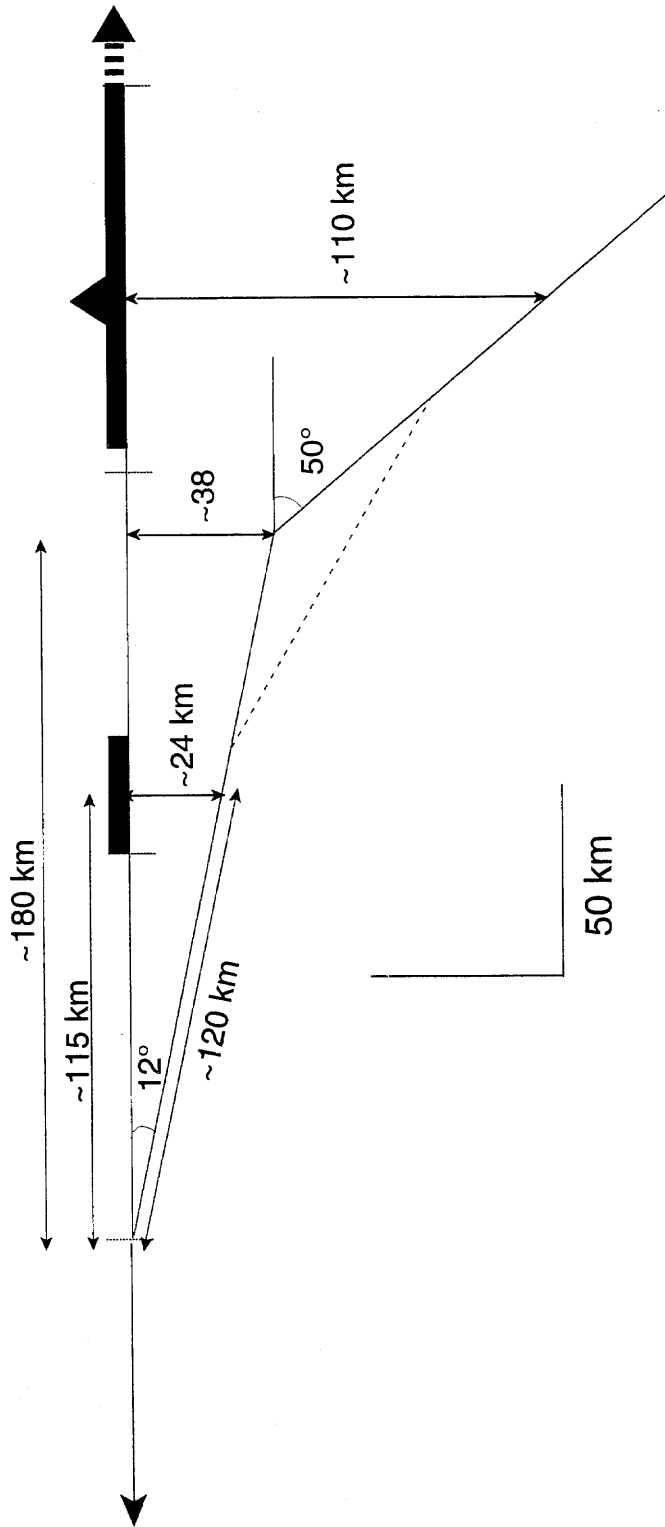
1.2b. Earthquake history

The first historically recorded earthquakes in Sumatra and Java were documented by the Dutch in Indonesia beginning in the 17th century. The Dutch accounts are of shaking and/or tsunami damage and are generally limited to events felt in areas populated by Europeans. Newcomb and McCann (1987) combined these reports with instrumental 20th century data to form their catalogue of recent subduction zone earthquakes along the Sunda arc. This catalogue excludes events judged to have sources on the mainland.

The oldest recorded event occurred in 1681 and was felt on the west coast of Sumatra and in the Pagais, Sipora, and Siberut (Figures 1.1 and 1.3). Other documented events that may have affected the Mentawai Islands or western Sumatra occurred in 1756 and 1770. Based on the intensity pattern and its similarity to an instrumentally-recorded earthquake in 1914, Newcomb and McCann (1987) believe the 1756 event did not originate on the Great Sumatran Fault, but rather under the ocean, perhaps on the subduction interface. The 1770 event was accompanied by a volcanic eruption and tsunamis. A large event in 1797 generated tsunamis that affected mainland Sumatra across from Siberut and Sipora. A very large event in 1818 generated strong shaking and a tsunami that affected the Sumatran coast near Bengkulu, across from Enggano Island (Figure 1.1).

The two largest events, estimated at greater than Mw 8.4, occurred just 27 years apart, in November 1833 and February 1861, on adjacent segments of the subduction zone below Sumatra. Newcomb and McCann (1987) estimate the earlier event ruptured a 550-km long segment from the Batu Islands south to Enganno Island and from the trench to the forearc basin and had a moment of about Mw 8.7-8.8 (Figure 1.1). It produced high intensity shaking and tsunamis on the mainland from at least the latitude of northern Siberut to Bengkulu. Historical data about damage on the Mentawai Islands is not available, presumably because of the lack of European settlement. Multiple earthquakes

occurred in conjunction with the century's second great earthquake (Mw = 8.4-8.5), in which the Sumatran subduction zone ruptured from the Batus north to at least the Banyak Islands, but there do not appear to have been any events at the latitude of the Pagais and Sipora at that time.

Two significant seismic events occurred in the decades between the two great earthquakes. Both caused damage at the latitude of Nias, in the region of the 1861 earthquake. A series of substantial aftershocks followed the main shock in 1861. The 1861 sequence, however, was followed by few events in the late 19th and early 20th centuries. Early instrumental records showed earthquakes that may have affected the region of the 1833 rupture in 1908 and 1914.

Newcomb and McCann (1987) report no earthquakes > M_S 7.0 at the latitude of North and South Pagai and Sipora between 1914 and 1970 (Figure 1.3). In the mid-1960's and again in the mid-1970's there was a spate of earthquakes in Sumatra, but most were confined to the northernmost part of Sumatra. There were two moderate events in 1970 and 1974 in the region of the Pagai/Sipora Islands that had thrust mechanisms. The nodal planes for both earthquakes were northwest-striking, one dipping shallowly (<15 degrees) northeast, the other steeply southwest-dipping. The magnitudes of these earthquakes were 6.2 and 6.8, respectively. Other events at this latitude in this period were mainland-Sumatra strike-slip events on near-vertical planes, probably on or near the GSF. The GSF has produced several historical earthquakes with 8>M_W>7 since 1892 (Katili and Hehuwat, 1967).

The Harvard CMT catalogue contains four earthquakes with magnitudes greater than 6.0 that occurred near the Pagai Islands and Sipora between 1977 and 1995. The earthquakes, one each in 1991 and 1993 and two in 1994, occurred at or just north of the island of Sipora (Figure 1.4). The dips of the nodal planes are either shallowly east-dipping or steeply west-dipping. Presumably the shallow plane represents the fault plane.

Figure 1.3. Rupture zones of historical earthquakes with Mw > 6.0 in Sumatra, inferred from reports of shaking intensity. Striped patches define the estimated rupture zone of the two 19th century Mw > 8.4 earthquakes to affect Sumatra. Lines below the map represent estimated rupture lengths of events. White lines represent regions with shaking intensity of I-IV on the Modified Mercalli Scale, dark lines greater than V. Wavy lines indicate tsunami extent and dots record reports of seaquakes. Note that in the region of the Pagai and Sipora Islands, over the 1833 rupture zone, no events were documented after 1914. From Newcomb and McCann (1987).

Figure 1.4. Focal mechanisms for earthquakes with Mw > 6.0 between 1977 and 1995.

Four thrust events occurred near Sipora Island between 1991 and 1994.
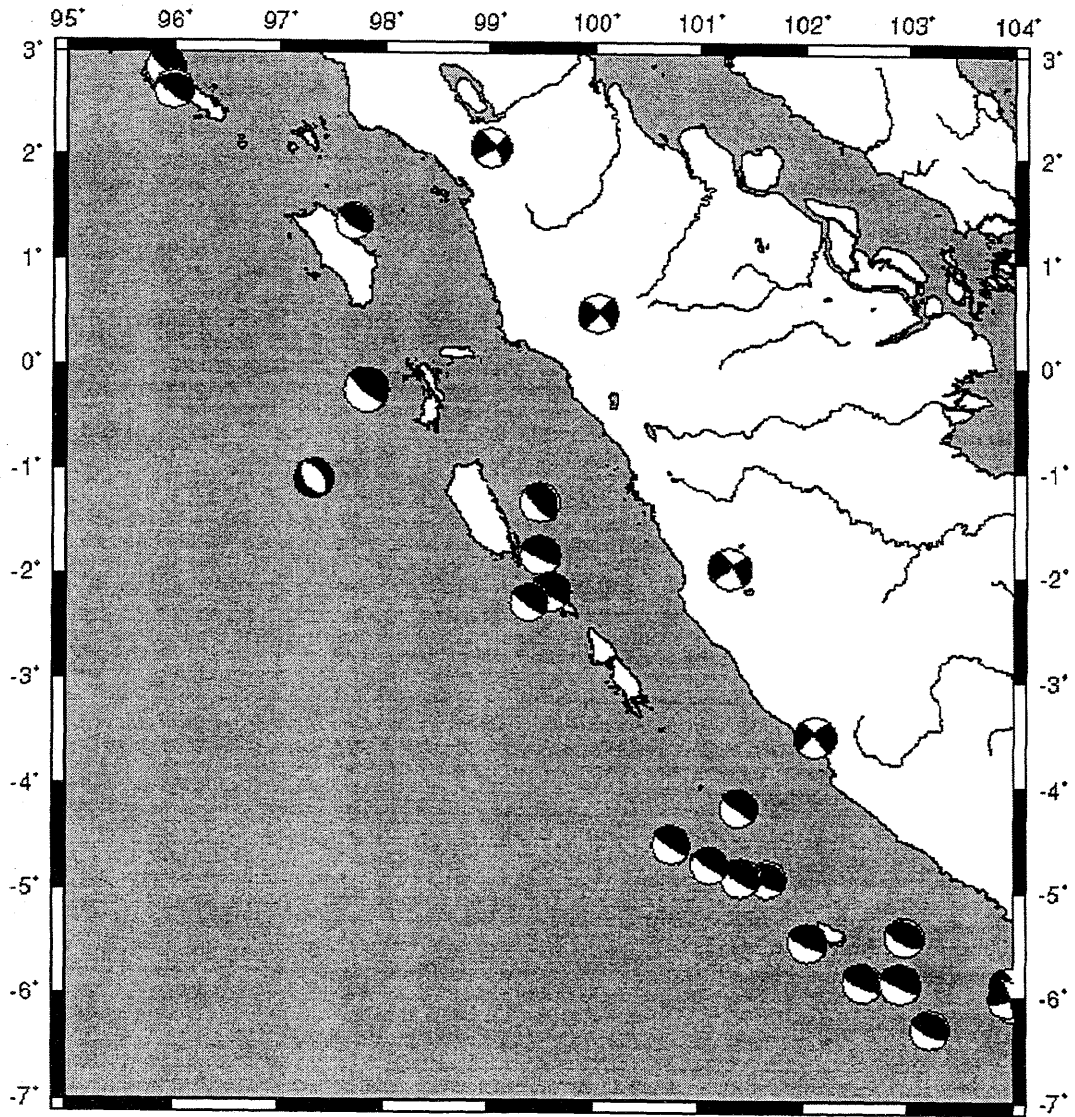
The dips for the three events nearest Sipora were between 8 and 12°; the dip for the more northerly event, east of Siberut and farther from the trench, was 20°. The slip in all cases was almost purely dip-slip.

1.2c. Western Sumatran margin and the Mentawai Islands

The Mentawai Islands are a chain of islands trending parallel to the west coast of Sumatra, about 100 km from the mainland coast and 80-130 km from the trench (Figure 1.1). They are the subaerial expression of the crest of the outer-arc rise, separated from the west coast of Sumatra by a fore-arc basin that reaches depths as great as 2400 m (Verstappen, 1973). In only a few locations, such as Barbados, does the outer-arc rise emerge above water and expose the overlying plate so near the trench (Moore and Karig, 1980).

The M_w 8.7 earthquake of 1833, which Newcomb and McCann estimate ruptured the subduction interface from the latitude of the Batu Islands to Enggano Island, probably produced significant vertical displacements in the overlying islands. If one were to search for evidence of this and earlier coseismic events in the geologic record, the Mentawai Islands are likely, by virtue of their location relative to the trench and the interface, to contain it.

The Mentawai islands are composed primarily of deformed accretionary-prism sediments topped by younger coralline limestone (Budhitrisna and Andi Mangga, 1990). Both living coral reef and preserved fossil coral are also commonly present on Mentawai coasts. The presence of these islands in tropical Sumatra, rife with numerous species of coral, provides an unusual opportunity to use living and dead corals to measure modern and ancient vertical displacements in a band some 30 km wide, approximately parallel to the trench and only 100 km away. Combining these displacement measurements with similar measurements from the west coast of Sumatra, more than 200 km from the trench,

one could conceivably obtain a series of trench-perpendicular transects of vertical displacement which could greatly help constrain the magnitude and nature of vertical deformation in the hanging wall of this subduction zone. Vertical displacements in the Mentawais could be significant because of their proximity to the trench and location over the shallowest part of the subduction zone. The dip of the subduction zone interface here, inferred from earthquake moment tensor solutions, is about 10 or 12 degrees (Harvard CMT catalogue), so the interface under the islands appears to be only 15-30 km below the surface (Figure 1.2).

Western Sumatra has been located at the edge of a convergent plate boundary at least since the late Paleozoic Era. From the Permian to late Paleocene Periods, there was an east-dipping subduction zone under Sumatra, evidence for comprises magmatic arc and ophiolitic rocks on Sumatra and the Andaman islands (Karig et al, 1979). In the early Eocene Period, perhaps in response to the collision between the Indian subcontinent and Eurasia, the relative plate motion changed and subduction slowed substantially through early Oligocene time. Basins formed west of the Sumatran coast from back-arc extension during this period (Daly et al., 1991). There are few rocks this age or older cropping out in the Mentawais (Verstappen, 1973; Karig et al., 1979). By late Oligocene time, the convergence rate had increased again (Karig et al., 1979, 1980; Beaudry and Moore, 1985).

The pre-Miocene rocks found in the Mentawai Islands are highly sheared and deformed. Moore and Karig (1980) interpret these rocks on the island of Nias to be tectonic melanges, trench turbidites, sea floor sediments and basement rocks accreted onto the overriding plate during the late Oligocene subduction episode. In the late Oligocene, possibly into the earliest Miocene, period the entire western Sumatran margin was uplifted, perhaps in response to increased convergence rate. Uplift and sea-level regression led to exposure and erosion of the melange units (Karig et al., 1980). The

location of the trench at this time was about 100 km from the coast, about where the Mentawai Islands are now located (Karig et al., 1979).

After early Miocene time, the western margin of Sumatra began subsiding, and at an increasing rate after late Miocene time. In the outer-arc islands, Miocene and later units of sandstone, siltstone, marl and tuffaceous sandstone unconformably overlie the older melange units (Moore and Karig, 1980; Budhitrisna and Andi-Mangga, 1990). These sedimentary units are substantially folded but not sheared, and are interpreted to be uplifted trench-slope sediments (Moore and Karig, 1980). The folded Miocene units are topped by an unconformity. Above this lie undeformed Pliocene shelf deposits, Pleistocene coralline limestone and Holocene reef coral (Moore et al., 1980; Budhitrisna and Andi-Mangga, 1990). East of the Mentawai chain, the fore-arc basin contains sediments up to 6 km thick. These units are primarily Sumatran-derived sediments and range in age from Paleogene to Holocene (Moore et al., 1982).

Since early Miocene time, the accretionary prism and the forearc basin have expanded, and the trench has migrated westward about 80-90 km (Karig et al., 1980). The outer-arc began to rise in response to the rapid accretion of sediment at the leading edge of the overlying plate. The nature of the fossils in the Miocene sediments of Nias suggests that the lower Miocene rocks of the outer-arc rise were uplifted 4000 m in 20 million years, an average uplift rate of 0.2 mm/yr (Moore et al., 1980). The outer-arc rise began to emerge above water and form the island chain only a few million years ago (Moore et al., 1982). Karig and others (1980) estimate that the islands may have accomplished most of their emergence within a short period in the late Pliocene, with little uplift occurring since then, although the presence on Nias of Pleistocene reef terraces more than 100 m above sea level argues for substantial Quaternary emergence. They have also suggested that the outer-arc rise/trench-slope break may still be migrating westward from the Mentawais

since the morphological crest of the Nias is apparently not rising as fast as are the western coast or small islets to the west (Verstappen, 1973; Karig et al., 1979).

On Nias, Quaternary coral terraces are as high as 130 to 300 m above sea level; in the Pagai Islands, they exist only 50 m above sea level (Verstappen, 1973; Moore and Karig, 1980; Budhitrisna and Andi-Mangga, 1990). Karig and others (1980) report 6500 yr-old reef occurring 3 m above sea level on Nias, and argue that its elevation is due to its having formed during a sea-level highstand. Vita-Finzi and Situmorang (1989) and Vita-Finzi (1995), in a study of mid- to late Holocene shells from terraces and platforms on Nias, suggest that the elevated reefs result from episodes of coseismic uplift rather than from a sea-level highstand alone. K. Sieh and F.W. Taylor found fossil reef coral in the modern intertidal zone on Nias that had ^{230}Th and corrected ^{14}C ages of about 4500 yrs (pers. comm.).

1.2d. North Pagai, South Pagai, Sipora, and Sanding

Field work for this project was concentrated on the coasts of four of the Mentawai Islands, North Pagai, South Pagai, Sipora and Sanding, which overlie the center of the inferred source region for the 1833 Mw 8.7 earthquake (Newcomb and McCann, 1987) (Figures 1.1 and 1.3). They lie about 20-30 km above the 10-12□ dipping subduction interface (Figure 1.2; Newcomb and McCann, 1987; Harvard CMT catalogue). The three northern islands range from about 30 to 70 km in length; Sanding is very small (Figure 1.5). These islands have received considerably less attention from geologists than the islands to the north, especially Nias, the Batus and Simeulue (e.g.. Karig et al., 1979, 1980; Moore and Karig, 1980; Kieckhefer et al., 1981). They, with the island of Siberut, are separated from the northern islands by the Pini Arch and Investigator Fracture Zone. Since these features may represent a major structural discontinuity, the structural and

Figure 1.5. Map of the islands of the Mentawai chain on which field work for this project was undertaken. Sipora, North Pagai, South Pagai and Sanding are four of the outer-arc islands of the western Sumatran margin. They overlie the patch of the subduction zone interface inferred to have ruptured in the 1833 Mw 8.7-8.8 earthquake.

Sipora

Pagai and Sipora
Islands

10 km

N
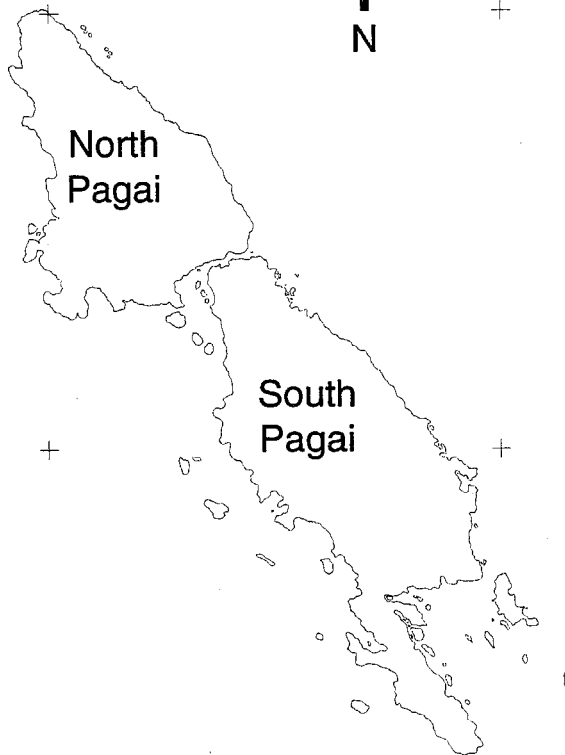
North
Pagai

South
Pagai

Sanding

tectonic character of the Nias-Batu-Banyak part of the fore-arc may differ significantly from that of the Siberut-Pagais-Sipora part.

The oldest rocks on the Pagai/Sipora islands are Oligocene to Miocene ultramafic and undifferentiated melange (Budhitrisna and Andi Mangga, 1990). Most of the older sediments are fairly unresistant and highly dissected. Older (Pleistocene) coral reef material exists on these islands but only at much lower elevations (~50 m) than on Nias and other islands north of the Batu Islands (Verstappen, 1973). Geomorphically, the three islands display a dissected highland of fairly uniform elevation, with a flanking lower apron of alluvium along the coast. The coastal region is commonly dominated by mangrove swamps. Living coral reef exists all around the islands, both as fringing reefs and as coralline islets just offshore. Southeastern South Pagai has a veritable archipelago of tiny coral islands, some so low they are completely submerged at high tide. The presence of all these islands provides an excellent source of coral with which to measure relative sea level histories.

Quaternary coralline limestone cropping out as high as 50 m above sea level in the Pagais and Sipora (Budhitrisna and Andi Mangga, 1990) suggests the islands have experienced emergence on a time scale of tens or hundreds of thousands of years. Estimated average emergences rates, then, vary from about 0.02 mm/yr, if the limestone is 2 million years old, to as high as 0.35 mm/yr, if it was deposited during the Last Interglacial sea-level high, about 125,000 years ago.

Although over the long term the islands may have been emergent, field observations undertaken for this study suggest that the Pagai/Sipora Islands have been submerging at rates of several mm/yr for at least the last several decades (Chapter 2). In many locations, salt or brackish water swamps and lagoons contain drowned trees rooted below or in the intertidal zone just behind the coastal storm berms (Figure 1.6). The

berms themselves have clearly been prograding landward in recent decades, overrunning and burying both trees and coral (Figure 1.7).

On the other hand, on intermediate time scales of hundreds to thousands of years, there appears to be little net vertical displacement. The presence of deeply-incised, 3 m-high, wave-cut notches in old, probably Pleistocene (Budhitrisna and Andi Mangga, 1990), coralline limestone at or slightly (< 1 m) above the modern intertidal zone, suggests that sea-level has not varied more than a meter or two for some time (Pirazzoli, 1979, 1986) (Figure 1.8). Holocene fossil corals are located only slightly above the elevation of live coral. Holocene coral reefs occur on these islands about 2-3 m above sea-level (Verstappen, 1973), and I found individual mid-Holocene coral heads less than 2 m above their living counterparts (Chapter 4). These observations suggest that average rates of relative sea-level change for these islands have been less than 1 mm/yr since the mid-Holocene.

1.3. Holocene sea level changes

In order to know if the apparent Holocene sea-level stability in the Mentawai Islands reflects net tectonic stability, it is necessary to understand the nature of the other contributors to local or regional sea level. The variation in relative sea-level at any location is a function of local tectonic vertical displacement, global or regional average sea-level changes caused by changes in global ocean water volume, and oceanographic/climatic fluctuations. Oceanographic fluctuations are generally most dominant on short time scales, with tidal fluctuations occurring on hourly, daily, monthly, yearly and decadal timescales. Weather, storms and droughts, can produce abrupt sea level changes that last hours, days, or even years. Oceanographic/climatic effects, such as El Niño, may introduce sea-level changes that last a year to a few years. Fluctuations in "eustatic" sea-level generally occur on longer timescales. Tectonic effects can be felt on

Figure 1.6. A salt -water swamp located just landward of the shoreline storm berm on South Pagai. The trees in the background have been killed by encroaching sea water. Such drownings are widespread throughout the Mentawais and are indicative of ongoing or recent submergence. This swamp is about 50 cm deep, indicating there has been a minimum of about half a meter of submergence since the trees were alive. The substrate itself is thick mud and may therefore have buried the tree roots an unknown amount, implying still greater submergence.

drowned trees
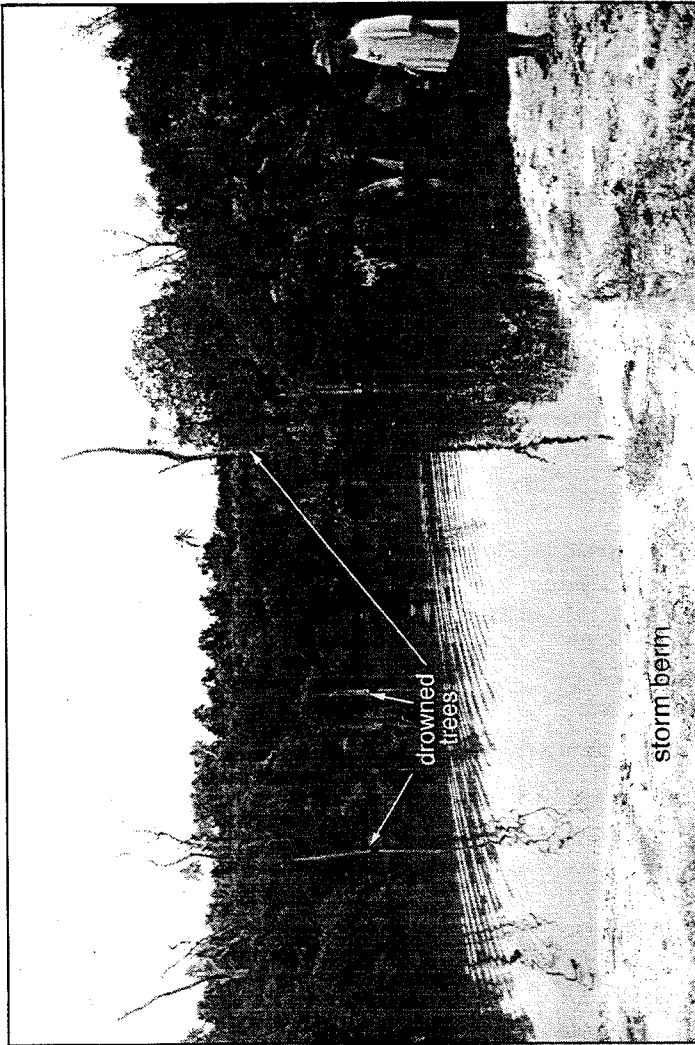
storm berm

Figure 1.7. Trees overrun and buried by a landward migrating storm berm on the coast of one of the small coralline islands flanking South Pagai. Here and elsewhere in the islands, the berms have moved landward, overrunning jungle vegetation. The trees were growing on either sand or old coral reef and have since been overtaken and killed by drowning or burial. The evident landward migration of the berm is consistent with recent submergence.
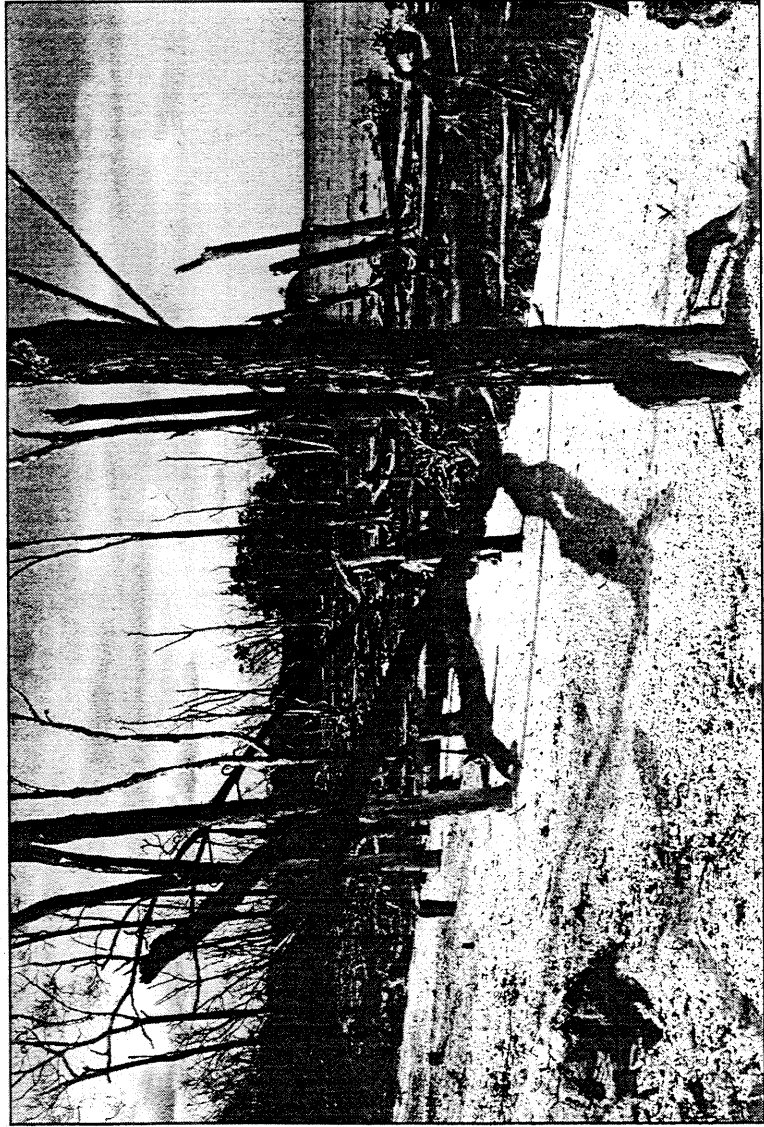
Figure 1.8. Erosional marine notch in probable Pleistocene limestone (Budhitrisna and Andi Mangga, 1990). The presence of the notch within the modern intertidal zone (this photo was taken shortly after the higher low tide of the day) indicates that sea level has remained fairly stable over time scales of millennia. The fact that the notch is slightly higher than the tidal range may imply that sea level is fluctuating around a stable mean (Pirazzoli, 1984; 1986).
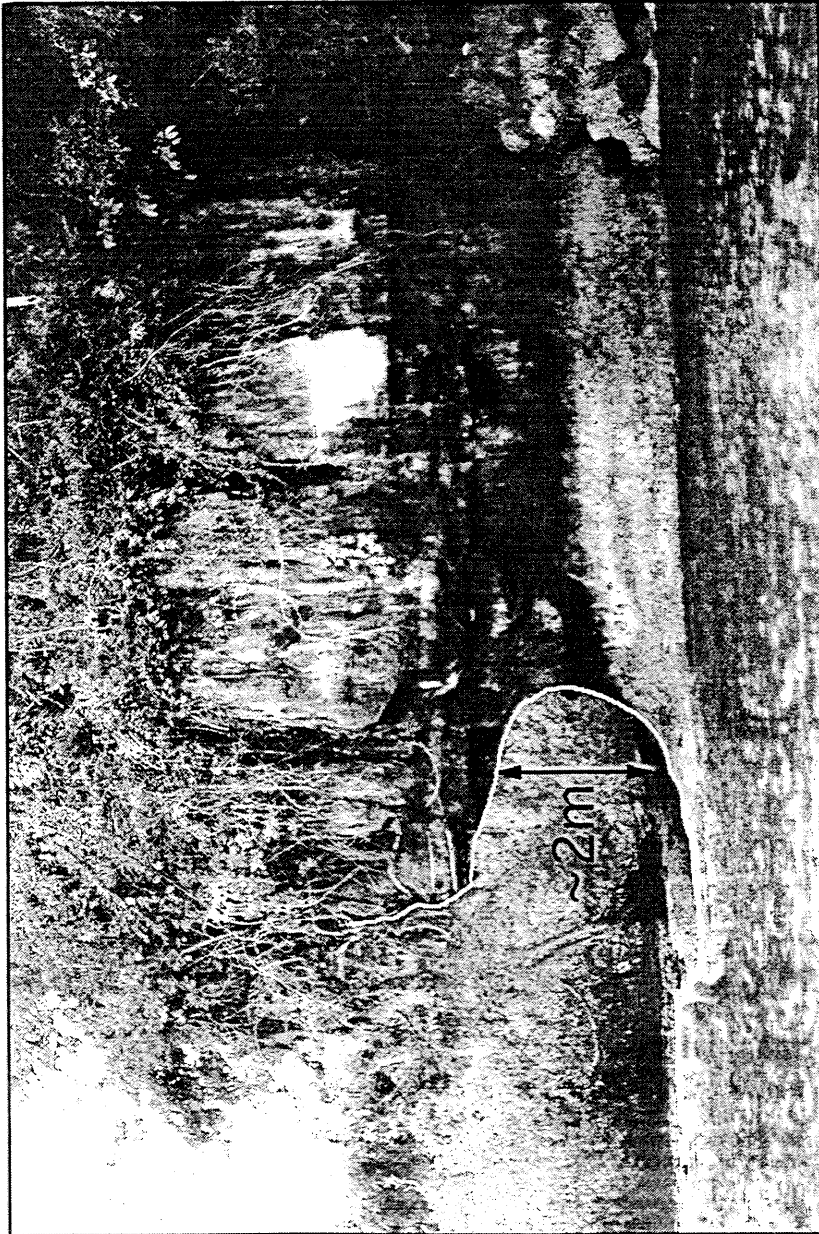
all timescales, from nearly instantaneous coseismic vertical displacements to long-term uplift or subsidence occurring over thousands and millions of years. In considering the question of net Holocene displacement, it is most relevant to focus on the long-timescale contributing factors, not tidal fluctuations or El Niño.

1.3a. Glacio-isostatic and hydro-isostatic effects on sea-level

Global sea level has risen since the last glacial maximum about 20,000 years ago, due to the melting of the ice sheets. This has been called a "eustatic " sea-level change, because it was caused by the introduction of glacial meltwater into all the world's oceans. However, the term "eustatic" is somewhat of a misnomer. Although meltwater has been distributed throughout the world's ocean basins, the magnitude of the resultant sea-level rise has not been uniform across the surface of the earth. This is because of the earth's variable isostatic response to glacial unloading and to loading by meltwater (Clark et al., 1978). The isostatic response is complex and is a function of mantle rheology and the global distribution of ice sheets and ocean basins. The isostatic adjustment has continued well after the ice itself melted and entered the oceans as meltwater. Because of this delayed adjustment, geologic or instrumental records of sea level reveal that sea-level histories differ as a function of location, depending on their proximity to the deglaciated regions and to continents and on the nature of the subjacent mantle. Thus, while the influx of meltwaters prompted sea level to rise globally more than 100 m relative to its level 20,000 years ago, some areas have recorded overall sea-level stability or sea-level decline within the last several thousand years.

1.3b. Holocene sea-level records in the Indian Ocean

Although the Indian Ocean regions have been much less well-studied than many areas in the northern hemisphere, there are some geologic data that have helped constrain

the average Holocene sea-level history for the area. Well-constrained data from coral cores in the Houtman Albrohos Islands off Western Australia and from coral reef terraces in New Guinea (Huon Peninsula) suggest that sea-level rose, in response to the melting of the glaciers, to a mid-Holocene sea-level high and have since declined to modern levels, possibly because of glacio-isostatic effects (Collins et al., 1993a, b; Eisenhauer et al., 1993; Edwards et al., 1993) (Figure 1.9). Rapid submergence in Australia is documented from at least 9800 BP when sea level was 24 m below present sea level (Eisenhauer et al., 1993). A highstand is recorded between about 6400 and 4700 BP. The differences between the records derived from the two Australian cores, the Suomi and Morley cores, reflect the different characteristics of their locations (Collins et al, 1993a). The Morley coral grew as an isolated patch of reef in a protected position behind the outer reef edge; the Suomi coral grew out on the crest of the reef. The growth rate of the former, composed mostly of fast-growing coral, apparently kept up with the rapid submergence. The Suomi corals, possibly subjected to more damage from storms, accreted material more slowly, could not keep up with rising sea level and lagged about 1500 years behind the Morley corals. The Morley coral growth curve therefore represents a record of minimum sea-level in the area. The highstand recorded by the corals is about 0.3 m above present sea level (Collins et al., 1993a; F.W. Taylor, personal communication, 1997). As there is no evidence of Holocene tectonism in this area, Collins and others (1993b) suggest that the emergence is due to hydro-isostatic rebound.

These sea level histories are broadly consistent with models of glacio-isostatic Holocene sea-level rise in this region (e.g. Peltier and Tushingham, 1991; Nakada and Lambeck, 1991; Mitrovica and Peltier, 1991), although the observed mid-Holocene high stand is somewhat lower than the modeled highstand. This may be only an apparent discrepancy between model and observation since it is very unlikely that the sampled

Figure 1.9.

U-Th ages and elevations of uplifted Holocene coral reefs from two sites from the Houtman Albrohos Islands in western Australia (data from Morley and Suomi cores - Collins et al., 1993a,b; Eisenhauer et al., 1993) and from Huon Peninsula, Papua New Guinea (Edwards et al., 1993). There is little or no tectonic uplift at Suomi or Morley; the elevations of the New Guinea corals have been corrected to exclude any component of tectonic uplift. Morley and Suomi elevations are measured in meters above living coral. The new Guinea heights were probably measured from what was thought to be mean sea level at the drill site (Taylor, personal comm.).

Late Quaternary sea level from corals in
Australia and New Guinea
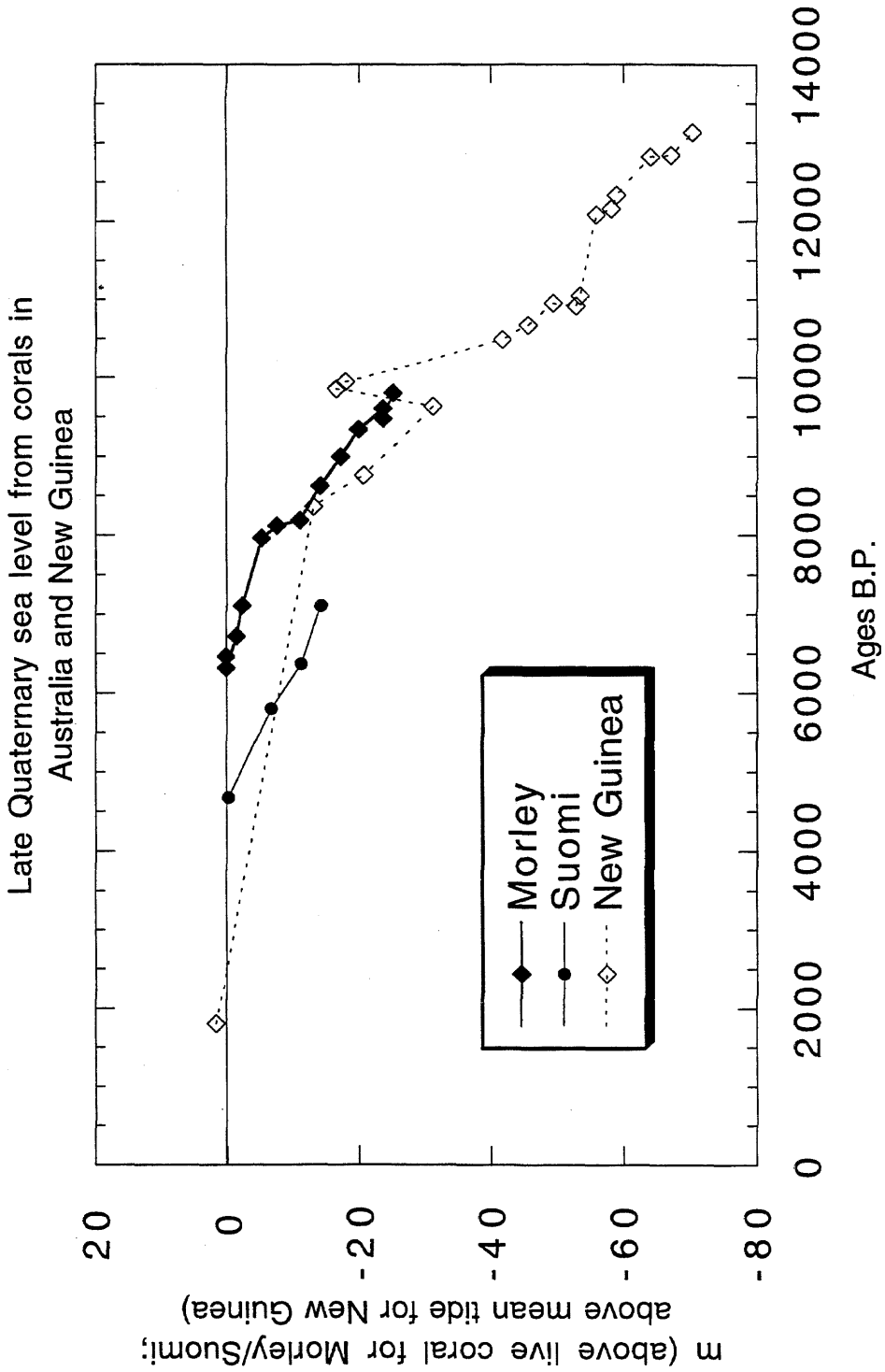
corals were the highest living corals of the youngest age. Any randomly selected coral probably lived below the shallowest possible level.

The New Guinea data, corrected to remove tectonic uplift effects, show a similar curve, though possibly shifted in time (Chappell and Pollach, 1991; Chappell et al., 1996) (Figure 1.9). The highstand is documented at about 1800 BP, but since the next youngest sample is 6600 years older, it is not clear when that highstand was first reached. Further evidence for a linear decrease in sea level from a well-defined highstand 6000 years ago to the modern level has been documented at several sites around Australia (Nakada and Lambeck, 1989; Lambeck and Nakada, 1990).

Coral reefs from the Cocos (Keeling) Islands, in the Indian Ocean, suggest the islands have emerged at least 0.5 m in the past 3000 yrs (Woodroffe et al., 1990a). Japan experienced a sea-level highstand about 6000-5000 yrs BP, with stable to decreasing sea-level since then, if tectonic contributions are removed (Yonekura and Ota, 1986).

1.3c. Models of glacio-isostatically-controlled sea-level change

Several workers (e.g. Peltier, 1988; Peltier and Tushingham, 1989,1991; Mitrovica and Peltier, 1991; Nakada, 1986; Nakada and Lambeck, 1989; Lambeck, 1990) have proposed models for the earth's isostatic response to glacial melting and sea-level change to explain observed sea-level variation. Constraining their models with sea-level data from tide gauges and geological indicators such as emerged or submerged terraces and beaches, they predict sea-level histories for the Holocene for various sites. The tide-gauge data they use are overwhelmingly from the northern hemisphere, so southern hemisphere results are probably less well-constrained (Peltier and Tushingham, 1989).

The models for areas near the Indian Ocean are fairly similar from India to Australia. In general, they suggest that a rapid rise in sea level occurred between about 20,000 to 5,000-6,000 years ago when sea level reached its present level. Along

continental margin regions far from the melting northern ice sheets, Lambeck (1990) suggests the sea-level rise should have produced a mid-Holocene high-stand a few meters above modern sea-level at about 6,000 years BP. At far-field oceanic islands, he estimates the high-stand elevation should be somewhat less pronounced. The difference in behavior between continental margins and small oceanic islands is a product of the isostatic response of the ocean basins. The meltwater load around continents or large islands forces the mantle to flow from ocean to island, generating uplift and tilting of the land; small islands don't have a differential isostatic response to additional water but act as "dipsticks", recording actual water level changes (Nakada, 1986; Nakada and Lambeck, 1988; 1991). According to these models, from the time of the highstand on, sea level should have decreased steadily to its modern value. Other models show similar results for sites in the western Pacific (very little data is available from the Indian Ocean), with highstands from 0.5 m above modern mean sea level at Reunion Island to about 1.7 m at Palau Island, Western Pacific to almost 6 m in New Zealand occurring between about 7000 and 5000 years ago (Peltier and Tushingham, 1991; Mitrovica and Peltier, 1991).

Model predictions for sites in the Indian and Pacific Oceans fit the observations of sea-level change from coral reefs and other geologic indicators of former sea-level where these are available quite well, although the observed height of the highstand is generally 2-3 m lower than the modeled height of Nakada and Lambeck (1989) and Lambeck (1990). Nakada and Lambeck (1989) suggest this may be due to Antarctic deglaciation or alpine deglaciation continuing into the present, long after the northern ice sheets had stopped melting.

1.3d. Glacio-isostatic models of sea-level history in western Sumatra

Comparison of the glacial isostatic models with data from sites in or near the Indian Ocean suggests that the models are reasonably accurate in describing the pattern of

Holocene sea level history in the region, even if absolute elevations may not be correct. Since sea level data for Sumatra are sparse, and the tectonic activity tends to overwhelm any subtle oceanographic sea level changes, these models provide the best estimates of non-tectonic sea-level history for the region. Using them can help in extracting the tectonic signal from the total signal of Holocene sea-level change reflected in the Mentawai corals.

W.R. Peltier and his colleagues produced a series of models of Holocene sea-level history (excluding tectonic effects) for sites west of Sumatra (Figure 1.10) (Peltier, written communication, 1995). They suggest that the area experienced a steady sea-level rise from 20,000 BP to a highstand at about 5000 BP of about 3-4 m above modern sea level, with steady decline to the modern level. Though there are few data from western Sumatra to compare with these models, peat deposits from Western Indonesia and Sumatra imply a marine transgression from at least 10,000 to 5,000 or 6,000 years ago, after which sea level declined (Neuzil, 1992; Cobb et al., 1989).

Although both models and observations suggest that sea-level has been decreasing for the last 4,000 to 6,000 years in the Indian Ocean, the sea-level history for the more recent past may be different. Global tide gauge data have indicated that average global sea level has been rising at rates of 1-3 mm/yr over the last 100 years, after correction for glacio-isostatic adjustment (e.g. Barnett, 1983; Peltier and Tushingham, 1991; Nakiboglu and Lambeck, 1991; Trupin and Wahr, 1991). Proposed explanations include melting of the Antarctic ice sheet and of alpine glaciers, possibly due to global warming (Peltier and Tushingham, 1989). Again, however, the tide gauges have almost all been installed in the northern hemisphere; there are few tide-gauge records of recent sea-level change in the Indian Ocean. Nevertheless, a 10-year tide gauge record from Cocos (Keeling) Islands in the Indian Ocean, a tectonically stable site, records an average rate of mean sea-level rise of about 1 mm/yr (a detailed discussion of the Cocos Islands tide gauge record appears in

section 5f of this chapter). One study of Australia suggests that modern sea level is rising 1.75 mm/yr in Northern Australia and 0.75 mm/yr in Tasmania (Bryant, 1992). A tide gauge record from Sydney shows modern sea level rising at about 0.56 mm/yr (Bryant, 1992). There are very few data from tide gauges in Sumatra, except a 4-year record from the 1980's from Padang and a 5-year record from Bengkulu from the 1920's (Clarke and Liu, 1993). Both sites are on the west coast of Sumatra. These records are too short to be useful in determining long term sea level trends.

1.4. Observations and models of subduction zone deformation

1.4a. Geodetic observations from other subduction zones

There are few subduction zones with long records of interseismic and coseismic deformation. Paleoseismic data have been collected from subduction zones in Alaska (Plafker, 1965; Plafker and Rubin, 1967), Cascadia (Atwater, 1987; Atwater and Yamaguchi, 1991), Vanuatu (Edwards et al., 1987c; Taylor et al., 1990), and New Zealand (Ota et al., 1991), among other places. However, geodetic data recording interseismic and coseismic displacements are much less common, and are relatively short-lived. The records from a few places dominate observations of the coseismic and interseismic deformational process, and these data, along with seismological data, constrain models of subduction. A robust geologic recorder of prehistoric subduction zone displacement will constrain these models further, by opening a window onto patterns of displacement through several cycles of coseismic and interseismic deformation. Comparison of newly acquired geodetic and paleogeodetic data from the Sumatran subduction zone with previously acquired data from other subduction zones can help expose features common to all subduction zone settings and those unique to each setting.

Figure 1.10. Holocene sea-level history near the outer-arc west of Sumatra, predicted from models of global glacio-isostatic and hydro-isostatic adjustment to deglaciation (Peltier, written comm., 1995). Rapid sea-level rise from about 20 ka culminated in the development of mid-Holocene sea-level highstand at 5 ka at an elevation about 3 m above modern mean sea level. Since that time, sea level in this region has steadily declined despite the continued influx of meltwater into ocean basins and an average global sea-level rise (Peltier and Tushingham, 1989).
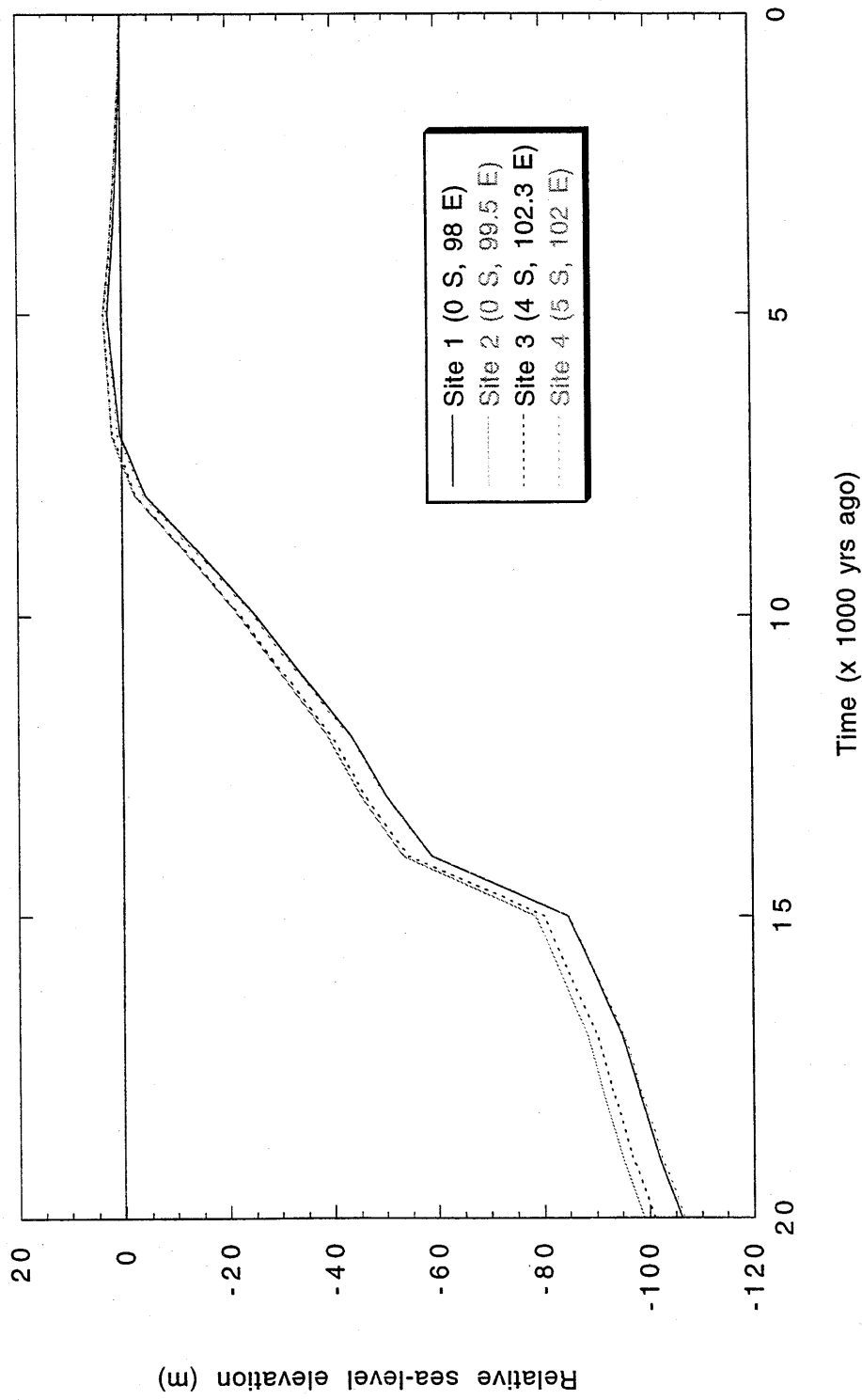
The few geodetic observations from other subduction zones in the world have shed light on the nature of displacement during the seismic cycle. One of the best geodetic records available from a subduction zone setting comes from Japan. Records from tide gauges and leveling lines were used to document vertical displacement above the Nankai subduction zone of Japan for 50 years before and after subduction zone earthquakes in 1944 and 1946 (Imamura, 1929;1945; Kawasumi, 1956; Sato, 1970; Inouchi, and Sato, 1975; Kato and Tsumura, 1979; Thatcher, 1984; Thatcher and Rundle, 1984; Savage and Thatcher, 1992; Savage, 1995). This is one of the most complete data sets of vertical displacement over a subduction zone throughout most of an earthquake cycle.

Leveling lines first surveyed in the 1880's were resurveyed at various times since then, with widespread leveling and triangulation surveys completed in the 1970's (Imamura, 1929; Thatcher, 1984). This time period spanned the 1944 M_W 8.0 Tonankai and 1946 M_W 8.2 Nankaido earthquakes, so geodetic records from all phases of one earthquake cycle were available. Thatcher (1984) and Thatcher and Rundle (1984) used these leveling data, in conjunction with tide-gauge data, to construct histories of vertical displacement in Japan.

In most regions, in the interseismic period between about 1895 and 1930, subsidence was documented within about 110-160 km of the trench, with relative uplift or stability dominating regions farther away (Figure 1.11a). The 1946 event generated vertical displacement approximately opposed to that of the interseismic period . Coseismic uplifts of up to about 80 cm were observed near the trench, with subsidence occurring over the broad regions of preseismic stability or uplift (Figure 1.11b). The immediate postseismic displacements, within 20 years after the earthquake, were large and tended to recover substantial fractions of the coseismic displacement (Figure 1.11c).

20 to 35 years after the event, displacement rates had slowed, and the vertical displacement profile was approaching the pre-1946 interseismic signals (Figure 1.11d).

While the coseismic and pre-1946 interseismic profiles were reasonably represented as abrupt slip and loading in an elastic medium, the post-seismic signals required a broader explanation. Thatcher and Rundle (1984) interpreted the rapid immediate postseismic displacement as deriving from post-seismic slip down-dip of the coseismic rupture plane, while the post-1946 interseismic period may have retained the effects of postseismic asthenospheric flow in addition to steady interseismic reloading of the rupture plane.

Savage and Thatcher (1992) analyzed the postseismic records from tide gauges from Japan, recording from 1950-1985. After estimating corrections for global eustatic sea level rise and regional oceanographic effects, they inferred that much of the coast of Japan has been rising since the 1940's earthquakes. The uplift rate in the first decade was significantly greater than the later interseismic rate. They described the full record as the superposition of a transient postseismic phase of rapid uplift and steady interseismic uplift at a lower rate. The interseismic rate was consistent with elastic dislocation models (see below) but not with the preseismic uplift rate inferred from the leveling lines. They concluded that either the steady interseismic uplift rate was not maintained throughout the earthquake cycle or the interseismic uplift rate need not be the same from one earthquake cycle to the next.

In another well-documented geodetic study, Savage and Plafker (1991) used records from eight tide gauges, the longest of which was about 65 years, to examine vertical displacement after the 1964 Alaska earthquake. After correcting for eustatic sea level rise and glacial-isostatic rebound, they determined that the nature and rates of tectonic vertical displacement at each site revealed that post-1964 interseismic displacement was occurring in opposition to coseismic displacement. In other words,

Figure 1.11. Simplified sketch of patterns of vertical displacement over the Nankai subduction zone as a function of distance from the Nankai Trough (after Thatcher, 1984). Leveling line surveys at various times before and after the 1946 Nankaido earthquake in Japan revealed the nature of vertical displacements along various transects during all parts of an earthquake cycle. Surveys encompassed the pre-1946 interseismic period from about 1900-1930 (a), the pre- and coseismic periods from 1930-1946 (b), the postseismic from about 1947-1964 (c), and the post-1946 interseismic period from about 1964-1978 (d). Magnitudes of displacement and distance from the trough are approximate. Actual values varied for different transects, but the broad configuration of displacement distribution was similar along most in that areas of interseismic subsidence experienced coseismic uplift and vice versa. Immediate postseismic rebound occurred at rapid rates, then tapered off after the first few decades to more moderate rates.
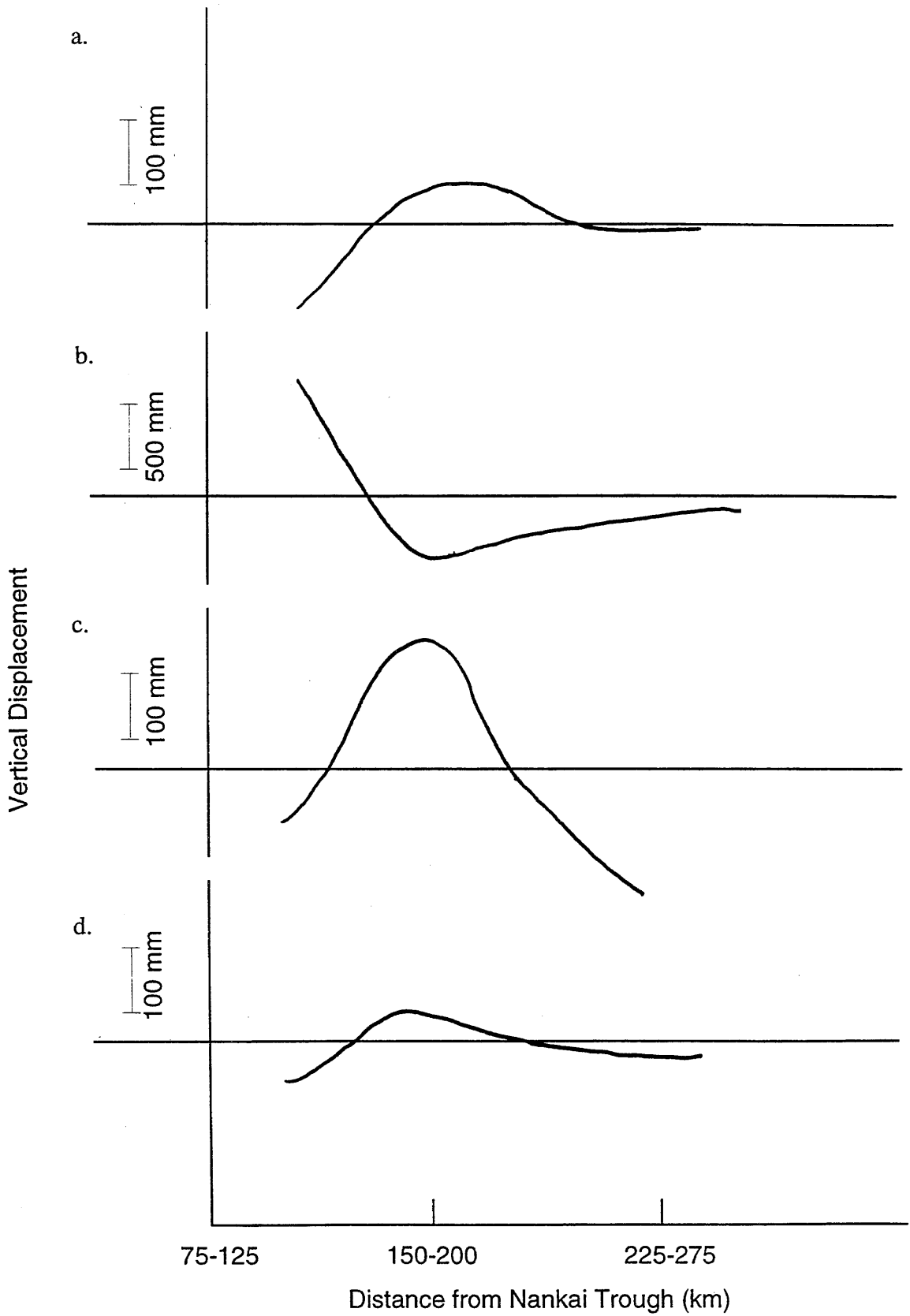
areas that had experienced coseismic uplift were subsiding interseismically, and vice versa, as was observed in Japan (Thatcher, 1984). The rates of interseismic vertical displacement were very high in several places. For example, Kodiak, near the axis of maximum coseismic subsidence in 1964, was rising at 17.5 mm/yr. The immediate postseismic displacement rates were noticeably greater than later interseismic rates. This was attributed to the occurrence of postseismic slip down-dip of the coseismic rupture zone and to asthenospheric flow. The former signal essentially damped out within a decade; the latter's effect was expected to last closer to a century or so. Savage and Plafker determined that the observed displacement rates, if maintained, suggested a much shorter recurrence interval for the 1964 event than the geologic evidence of past earthquakes suggested.

More recently, a subduction zone earthquake near Jalisco, Mexico in October 1995 was one of the few subduction zone events well-documented by a GPS network both pre- and postseismically (Melbourne et al., 1997). Eleven GPS stations were occupied about seven months prior to the M_W 8.0 Jalisco earthquake and reoccupied eight days after the event. The postseismic occupation lasted about one week. Records of the coseismic and immediate postseismic displacement were captured. The results indicated that the rupture was confined within 18 km of the surface and produced almost 1 m of total displacement at the coast. One site was continuously occupied for ten days. By day 17 after the earthquake, about 20% of the displacement measured on day 8 had been recovered (T. Melbourne, pers. comm., 1997).

1.4b. Models of subduction zone deformation

Several models have been proposed to describe subduction-related displacement in the coseismic and interseismic periods. Simple elastic dislocation models treat the plate interface as a planar fault in an elastic half-space (e.g., Savage, 1983). These models

assume that the main thrust zone of the subduction interface fails coseismically by reverse slip and is locked interseismically. The nature and magnitude of the vertical displacement of the surface at any site over the interface is dependent on the dip of the subduction zone, the amount of slip, the down-dip width of the locked zone, and the distance from the trench. The models are predicated on the basic assumption that interseismic deformation approximately recovers coseismic deformation, in other words that permanent strains are small compared to elastic strains. Insofar as the system behaves elastically, places with coseismic uplift should show interseismic subsidence and vice versa.

The pattern of coseismic vertical displacement calculated for such a planar fault, dipping 10 degrees, is illustrated in Figure 1.12. The uplifted region overlies the rupture zone, while subsidence occurs farther from the trench. The site of maximum subsidence occurs almost exactly above the down-dip terminus of fault rupture. The hingeline between the regions of coseismic uplift and subsidence is approximately trench-parallel and lies about 80% of the way from the projection of the up-dip terminus to that of the down-dip terminus of the rupture zone.

In the interseismic period, the rupture zone is locked, but the down-dip section continues to slip. This interseismic locking of the main rupture zone and steady-state subduction of the rest of the slab is represented in the calculation as normal slip at the plate convergence rate on the locked portion of the interface, superimposed on steady-state subduction of the whole slab, or reverse slip on the entire plate interface, also at the plate convergence rate. The steady-state component produces little or no strain accumulation in the overlying plate, so the vertical displacement at the surface in the interseismic period is generated only by the "normal" slip on the locked portion. In the absence of long-term permanent deformation, the cumulative uplift due to interseismic

Figure 1.12. Pattern of coseismic and interseismic vertical displacement of the overriding

plate above a 10°-dipping subduction interface in an elastic half-space as a function of

distance from the subduction zone trench (D). The fault is assumed to be planar and much

larger than the rupture patch. The down-dip width of the rupture patch is W; the

coseismic slip is x. The coseismic vertical displacement at the surface, h (solid line), in

units of x, varies with distance from the trench (D), which is calculated in units of W. The

cumulative interseismic displacement (dashed line) is equal in magnitude and opposite in

sign to the coseismic displacement. This configuration can similarly be used to describe

interseismic convergence rates simply by changing the units of slip (x) and displacement

(h) to units of slip rate ($\dot{x}$) and displacement rate($\dot{h}$). This scenario shows the rupture zone

reaching the surface. If the slip patch is shifted down-dip so that it does not reach the

surface, the deformation pattern will be shifted away from the trench, and there will be a

gradual rise to the maximum coseismic uplift, or interseismic subsidence, rather than the

step seen here. (After Savage, 1983).

vertical displacement rate (ḣ)

vertical displacement (h)
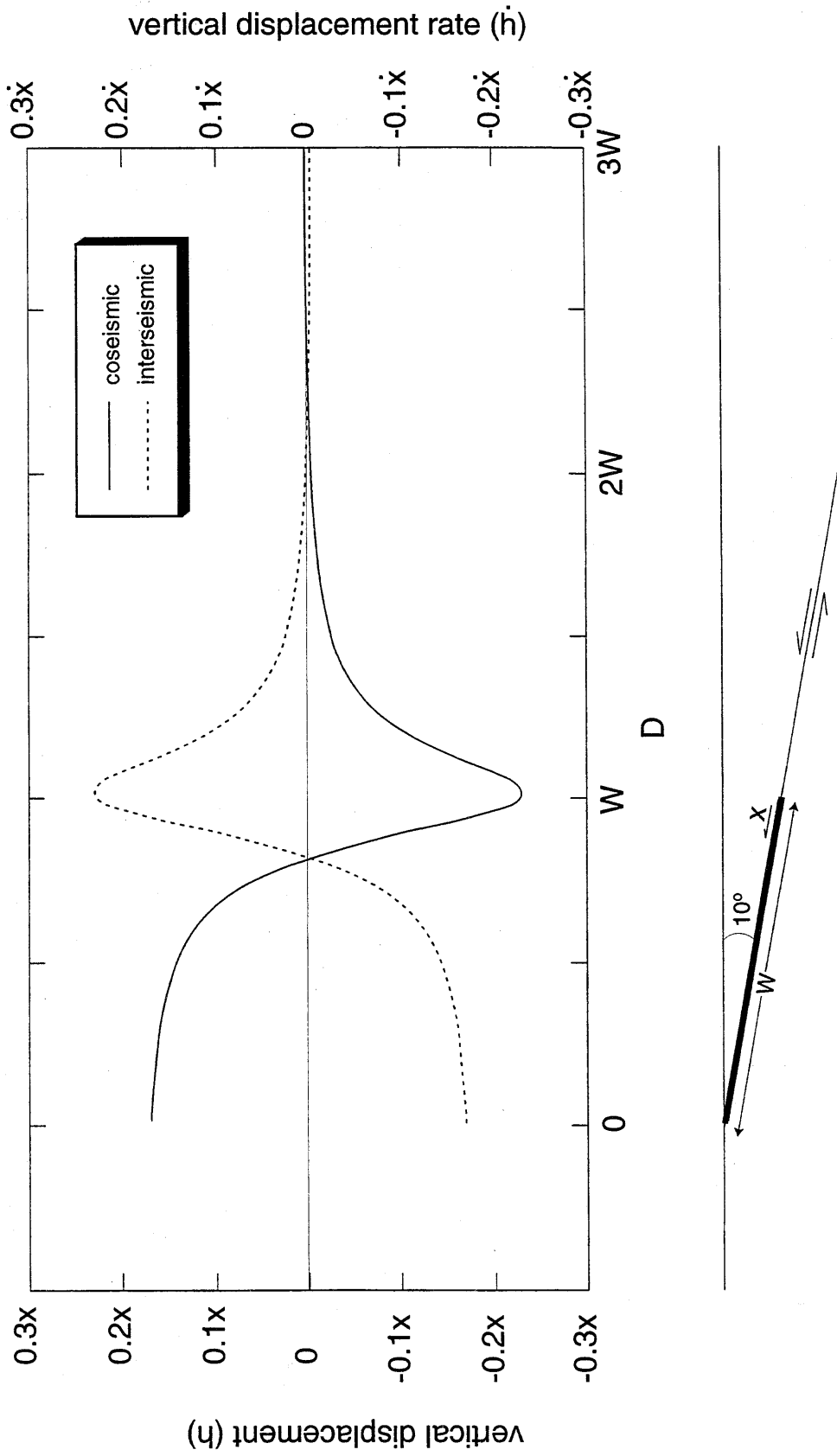
strain accumulation, or "normal" slip, is the exact reverse of the uplift due to coseismic slip (Figure 1.12).

Variations on the elastic model incorporate effects of subduction on the viscous asthenosphere, such as relaxation following a slip event and asthenospheric flow in response to steady subduction. Such models have been proposed to account for the time-dependence of the displacement pattern which the elastic model disregards, to explain observations that the elastic model fails to fit such as the non-linear transient postseismic deformation observed in Japan, Alaska, and Jalisco (e.g. Thatcher and Rundle, 1984; Savage and Thatcher, 1992; Savage and Plafker, 1991; T. Melbourne, pers. comm., 1997).

Observations from other subduction zones, and models such as the above, even if oversimplified, help to illustrate the kind of vertical displacements one might expect to see in the plate over a subduction interface throughout the earthquake cycle. Given their proximity to the trench, one might expect the outer-arc islands of western Sumatra to experience substantial coseismic uplift in a large subduction zone earthquake, and conversely to experience interseismic subsidence. At sites farther from the trench, for example on the west coast of Sumatra, the vertical displacements in both the coseismic and interseismic periods might be expected to be more subdued. The extent to which observation confirms or refutes these predictions can help to refine the models and illustrate the variations that are possible in the real world.

1.5. Corals

Indicators of past tectonic activity must retain records of the magnitudes of past deformation and chronological records of when the displacement occurred. For paleoseismic indicators, the records must be distinguishable on time and space-scales relevant to individual coseismic events. In other words, the geologic expression of

coseismic displacement must be distinguishable from long-term cumulative tectonic deformation. Uncertainties in age must be significantly smaller than the recurrence interval between earthquakes. Corals have the necessary characteristics. They are living organisms that accrete material at rates of millimeters to centimeters a year. Their growth patterns are controlled by sea level. Since vertical tectonic displacement in coastal environments is revealed by relative changes in sea level, the growth patterns of corals are thus in part controlled by tectonic displacement. And, coral growth is sensitive to changes in sea level on the same order as the magnitudes and rates of both coseismic and interseismic displacement in tectonically active areas like Sumatra. Finally, the age precision afforded by U-Th dating techniques on corals is well within the range of earthquake recurrence intervals, at least through the Holocene. Thus corals are strong candidates to be used as paleoseismic tools in marine environments, specifically at subduction zones.

1.5a. Corals and coral reefs

Corals are marine animals of the order Scleractinia (Veron, 1986). They are composed of polyps, most families of which secrete hard aragonitic skeletons. Hermatypic varieties are reef-building corals that require sunlight to grow and are thus found in shallow waters. Ahermatypic varieties require no sunlight and are able to grow beneath the photic zone, even in the deep sea. Hermatypic corals live in a symbiotic relationship with photosynthesizing zooxanthellae algae that live within the coral polyps. The algae provide almost all the coral's food and enhance its rapid growth.

Reef-building corals grow in colonies of polyps that reproduce by "budding," or asexual division and duplication. The colonies can live hundreds of years and expand to many meters in size. Coral growth rates vary from a few millimeters per year to 15 cm/yr. Coral polyps also reproduce sexually by motile gametes and so can disperse over a broad

territory. Reefs are produced by the coalescence of coral colonies and calcareous algae. The nature of reef development depends not only on the types of coral comprising it, but also on bathymetry, water temperature, wave action, turbidity and sedimentation and salinity. Types of reef include fringing reefs which border islands or coastlines and are primarily shallow-water features, barrier reefs which develop on the edge of the continental shelf, and platform reefs which develop on the continental shelf but apart from island land masses.

Because they are constrained to grow below water, coral reefs near the sea surface respond to changes in relative sea level. In times of declining sea level, reefs will be exposed above water and killed. If water level remains low, the fossil reefs often remain, emerged above sea level, as testaments to former sea level highs. Coral reefs that grew during the last interglacial sea level high, about 125,000 years ago, are exposed presently in low-latitude regions throughout the earth, often hundreds of meters above modern sea level. Rising sea levels also affect the development of reef corals, by freeing the corals to grow upward. Coral atolls are formed as a result of rising relative sea level. Coral reefs that were originally fringing reefs around an island continue to grow upward as the island sinks. Ultimately the land itself disappears below water, but the fringing coral reef can remain above water, forming the coral ring of an atoll. The actual rate of reef development is a function of the rate of coral growth and the rate of sea-level change. If the rate of coral growth cannot keep up with the rate of sea level rise, the atoll will sink below water and may drown (Darwin, 1842).

1.5b. Microatolls

Certain genera of coral, including *Porites*, *Goniastrea*, and *Cyphastrea*, which grow in abundance in Sumatra, can, if they grow in the intertidal zone, become coral "microatolls." The term "microatoll" was coined to describe corals or colonies of coral

with dead, flat tops and a live outer edge (Scoffin and Stoddart, 1978; Stoddart and Scoffin, 1979). The name arose because of their morphological similarity to large atolls. They are primarily developed in massive coral species, which, when unimpeded, grow as hemispherical mounds, or heads. The microatoll morphology develops in these corals when their upward growth is impeded by prolonged exposure at low water levels. Because microatolls reflect low water levels in their growth patterns, they can be used to document changing sea level.

Head corals that ultimately become microatolls begin growth with the attachment of a single polyp to a rocky or sandy substrate. Subsequent growth is approximately hemispherical, with new skeleton accreting onto the existing head in concentric shells. The growth rate of the head coral depends on a variety of factors including species, water temperature, water depth, turbidity, salinity, available nutrients and pollutants (Scoffin and Stoddart, 1978; Buddemeier et al., 1974). In general, rates range from a few millimeters per year to 1 or 2 centimeters per year (Knutson et al., 1972; Taylor et al., 1987; Priess et al., 1995; and this study).

Growth rates are commonly distinguishable in the coral heads because of the presence of annual growth bands similar to tree rings. Seasonal climatic changes produce density variations in the coral skeleton as it grows throughout the year (Scoffin and Stoddart, 1978; Lough and Barnes, 1990). The exact nature of the correlation between density and specific seasonal climatic characteristics is not well-established, and studies of coral in different areas yield different relationships. For example, higher density skeletal growth occurs during times of higher rainfall and warmer water temperatures in the Marshall Islands (Buddemeier et al., 1974), in drier periods in Fiji (Fallon et al., 1990), and in the summer in Vanuatu (Buskirk et al., 1981; Taylor et al., 1987). X-radiographs of cross-sectional slabs of the corals can often reveal these density

differences which appear as dark and light annual bands (e.g. Buddemeier et al., 1974; Weber and White, 1977; this study - Figure 1.13).

The coral grows upward and outward until it reaches its upper limit of growth. This upper limit, the "highest level of survival" (HLS) is controlled by a combination of subaerial exposure, sunlight intensity, and perhaps water temperature (Scoffin and Stoddart, 1978; Taylor et al., 1987), although the specific nature of these controlling factors is not well understood. The sensitivity of corals to exposure under various seasonal climatic and weather conditions has been discussed in detail by Taylor and others (1987). Many corals can survive short exposures above water, and can survive longer if exposed at night rather than during the day. The level above which the degree of exposure becomes fatal is defined as the HLS. Only that part of the coral above HLS dies; live coral below HLS continues to live and to grow.

The elevation of HLS relative to absolute sea level is not strictly defined and may vary according to genus or species. It appears, in the Mentawais at least, to be a few centimeters to over twenty centimeters above low low tide (Chapter 2). Nevertheless, it appears that HLS "tracks" sea level. Water level and sun exposure together constrain HLS. Sun intensity and angle do not change on time scales of years, while very short term variations due to weather will average out on the same time scale. It is likely that annual changes in HLS are caused primarily by changes in water level rather than sun exposure. Thus, changes in HLS can reasonably be used as a proxy for changes in sea level.

The tectonic value of the coral heads lies in their retention of an internal record of changes in HLS, and by inference, in sea level. A sea level change produces a concomitant change in the morphology of the microatoll as it adjusts its growth to the new upper limit. At the same time, annual growth bands provide an internal chronometer. The morphological expression of HLS change and the coral clock together produce an annual record of sea level not unlike that of a tide gauge.

Figure 1.14 illustrates the changes in coral morphology that changes in sea level can produce. The coral grows hemispherically, its entire surface alive, as long as it remains below HLS (Figure 1.14a). HLS at this point is somewhere above the top of the coral head, but there is no constraint on how far above, except insofar as individual species occur only down to certain depths. If, at some point the coral reaches its HLS, it will, for the first time, record the HLS as an unconformity in its morphology. From this point on, if sea level and HLS remain constant, the coral grows only laterally, impeded from further upward growth. The coral morphology changes from hemispherical, with a living shell, to a cylindrical head, with only the outer vertical ring of the coral surface alive and the flat top dead at the HLS (Figure 1.14b and Figure 1.15). If sea level drops, the HLS is correspondingly lowered and the coral can no longer grow as high as before. Lateral growth continues below the lower level defined by the new HLS. The coral thus develops a "hat" shape in response to the change (Figure 1.14c and Figure 1.16). The change in sea level should be the same as the difference in height between the former and new HLS.

If, by contrast, sea level rises after the coral has been growing at HLS for some time, HLS rises too, and the coral has a new, higher, upper limit of growth. Thus freed, it begins to grow upward toward its new HLS, producing a "cup"-shaped morphology (Figure 1.14d and Figure 1.17). It was the similarity of this shape and origin to that of atolls described by Darwin that led Scoffin and Stoddart (1978) to use the term "microatoll" in describing these coral colonies. When the coral reaches the level of the new HLS, it is once again restricted to lateral growth below that level (Figure 1.14e).

With an HLS rise, in addition to growing up to the new HLS, the coral grows laterally as well, over the top of the old, dead HLS surface and inward toward the center. Even when the coral has reached its new, higher HLS and can no longer grow up, the lateral growth can still continue in toward the center as well as outward, so that two

Figure 1.13

a. Photo positive of an x-radiograph from a *Porites* microatoll, illustrates the annual bands caused by seasonal density variations. The lighter bands are denser than the dark bands. The bands, partly traced with pen, serve a purpose similar to tree rings, providing an annual record of coral growth.

5 cm

Figure 1.14. Model of coral growth in response to sea level changes. The solid black ring is the living coral band. The solid gray rings are dead coral that grew under the same sea level conditions as the living. The dashed rings are dead bands that grew under different, older sea level conditions. Modified from Scoffin and Stoddart (1978).

a. The coral grows in hemispherical shape while below highest level of survival (HLS). Sea level (SL) stays constant; the coral does not record SL while below HLS.

b. Sea level remains constant. Upward coral growth is limited by exposure at HLS. Horizontal growth of the part of the coral below HLS continues unchanged.

c. Sea level drops and then stabilizes. The coral, initially at or below HLS, emerges partially. That part of the coral now exposed above HLS dies. The coral still below the new HLS continues to grow laterally, developing a lower outer rim around a higher center and producing a "hat" morphology. The elevation difference between the two HLS flats is a measure of the amount of emergence.

d. Sea level rises after the coral has reached HLS. Upward growth is no longer impeded by sea level. The coral grows outward and upward to a level governed by coral growth rate, producing a raised outer rim. This "cup" morphology is indicative of submergence. The exact amount of submergence cannot be determined immediately from the coral morphology. The height of the rim above the central flat provides a minimum constraint on the submergence, but no clear indication if that submergence was sudden or gradual.

e. Sea level having risen and then stabilized, the "cup" microatoll eventually reaches the new, higher HLS and is once again constrained to grow only laterally. Both the outer ring and the inner ring may be alive. If the inner ring stays alive, the coral may grow inward until it completely covers the old HLS surface in the center.

f. Sea level rises before the coral has reached HLS. Coral grows upward to the new HLS. The former HLS and the SL rise are not recorded by the coral. Only the new SL will be recorded, should coral reach HLS.

a.

b. Cylindrical coral head

c. "Hat" microatoll

d. "Cup" microatoll

e. Microatoll with 2 HLS surfaces

f. Sea level rise *before* HLS impingement

HLS

Living coral surface

"Hemi"spherical coral head

SL
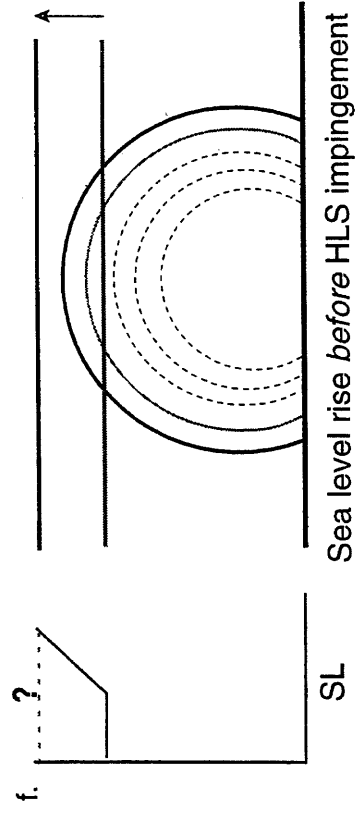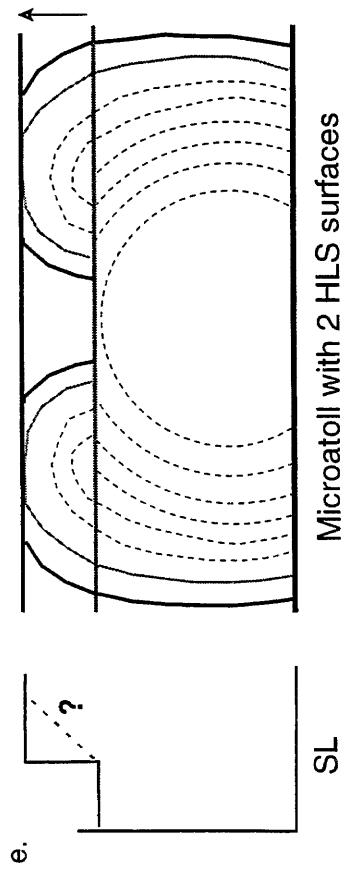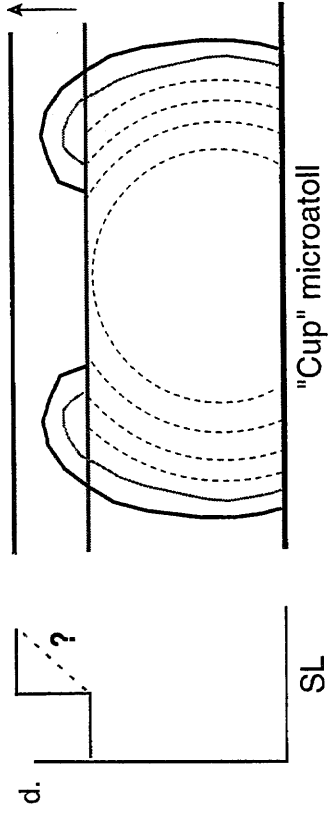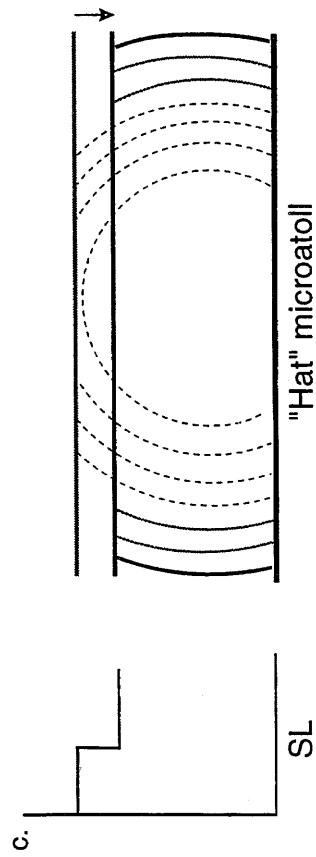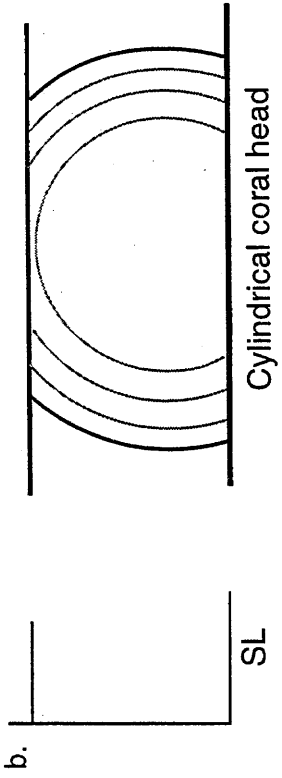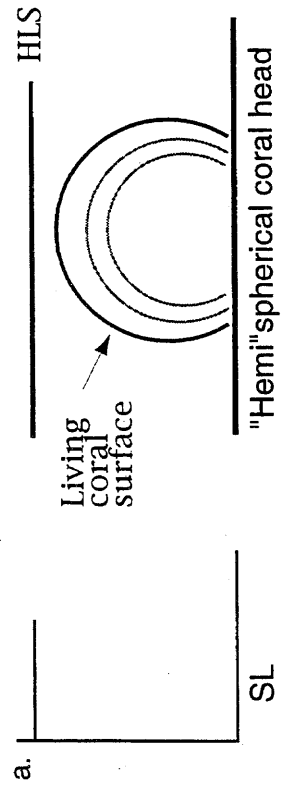
Figure 1.15. A low, flat-topped *Porites* coral with a classic microatoll shape (Scoffin and Stoddart, 1978.) The flat top is dead and only the outermost, vertical edge, under water, is living. Upward growth of the coral is prohibited by exposure above sea level so the coral is constrained to grow only laterally. The flat top is indicative of sea-level stability.

Figure 1.16. A partially emerged fossil *Porites* microatoll on North Pagai. A lower outer flange surrounding a higher, central dome is indicative of partial emergence. The rounded cap in the center of the coral indicates that the coral had not reached HLS before its emergence. The coral emerged to the point where HLS was at the level of the top of the flange. The elevation difference between the top of the dome and the top of the flange gives a minimum measure of the amount of emergence. The flat to slightly raised flange indicates that sea level was either stable or rising slightly after the partial emergence. Evidently, based on the size of the rim, after a short period of growth at the new HLS, the coral emerged again, this time completely, and died.
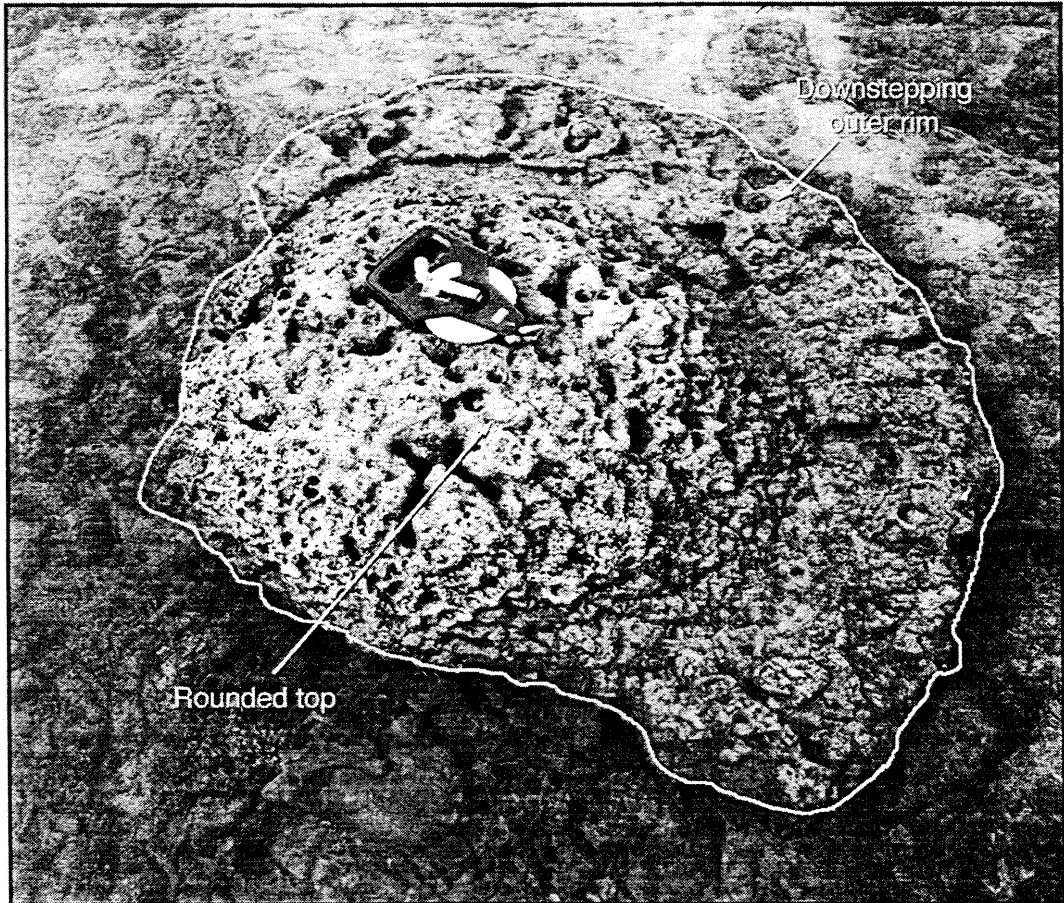
Figure 1.17. A live *Porites* microatoll from North Pagai. This coral has the high rim surrounding a lower dead central flat that is indicative of submergence. The living portion of the coral forms still another small raised rim above the dead flat top of the larger rim. Most live corals in the Pagais and Sipora expressed this submergence morphology.

Outer living raised rim

Dead HLS surface on outer rim

Older deeper HLS surface
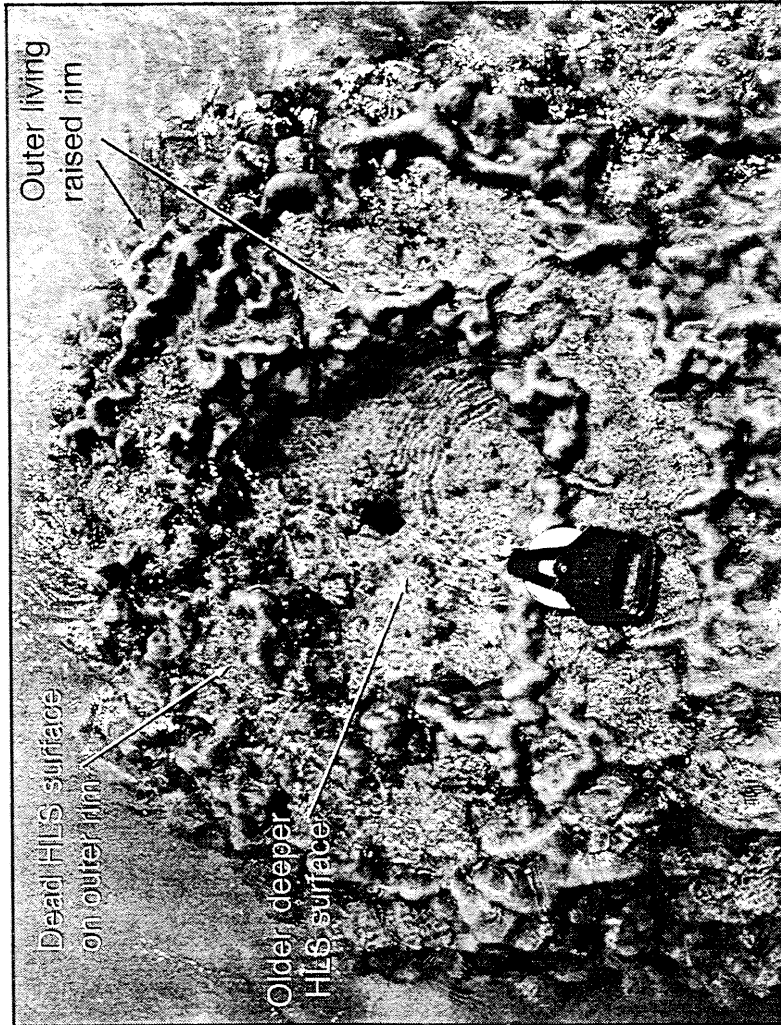
separate surfaces are alive. Sometimes inward growth continues until the old HLS surface is completely grown over, and the old flat is invisible from the surface. In many cases, however, the interior surface dies after the rim reaches HLS, perhaps because the water pooled in the cup gets too warm to support coral life.

It should be noted that a rise in sea level will be recorded by a coral only if it has already reached and been growing at HLS. HLS, and by extension sea level, can fluctuate up and down any amount before the coral has reached HLS and it will not be recorded in the coral as long as it stays above the level at which the coral is growing (Figure 1.14f).

Microatolls as sea level indicators are asymmetrical in their sensitivity and precision. Both the amount and the timing of emergence are precisely recorded by a coral originally at HLS. If the coral is at HLS both before and after the emergence event, the difference between the two elevations can be easily measured. Furthermore, the death of the emerged part occurs relatively rapidly, on time scales of days to a year or so, if the emergence is large (> 10 cm). The coral may require a couple of years to respond to smaller emergences. The rapidity of the coral's response to emergence may depend on seasonal, tidal, and weather factors (Taylor et al., 1987). Within these constraints, the new HLS will be generally recorded virtually immediately in the coral morphology.

Submergence, by contrast, is much more imprecise in both timing and amount, primarily because upward growth of a coral is limited both by HLS and by its own growth rate. A sudden submergence cannot be distinguished from a gradual submergence at a rate higher than the growth rate of the coral. If, for example, the coral grows at 1 cm/yr, its morphologic response to a sudden 10 cm submergence event will not differ from its response to gradual submergence over a 10 year period at a rate just above 1 cm/yr. Thus, by looking at the morphology, sudden and gradual emergence can be distinguished, but not sudden and gradual submergence.

Theoretically, given a vertical slice through a microatoll, by counting growth bands and measuring the changes in the elevation of flat surfaces produced by growth at HLS, one can generate a sea-level history for the time in which the coral lived based on coral morphology and stratigraphy alone (Figure 1.18). From that sea level history, one can then infer a history of vertical deformation. In principle, by finding microatolls dating back from the present and overlapping in age, one could develop a continuous sea-level record through the entire history of microatoll growth. Developing such a record at various geographic locations might therefore provide the data necessary to interpret the long-term history of deformation throughout the region. This is the goal that motivates this study of corals in western Sumatra. The living corals can both test the sensitivity and quality of the recorder and provide the first link in the chain of long-term sea-level history. Fossil corals can carry the record of sea-level fluctuations and vertical displacement into the past.

1.5c. Distinguishing tectonically and oceanographically induced sea level changes

Coral microatolls are simply a recorder of HLS and, by inference, of sea level - they do not, *ipso facto*, distinguish the cause of sea-level change. Corals may record oceanographic, climatic or geodynamic signals as well as tectonic ones. One of the difficulties in using the coral record as an indicator of tectonic vertical deformation is distinguishing tectonic causes from oceanographic or climatic causes of sea level change. In addition to the earth's isostatic response to changes in ice and water loads through the past few tens of thousands of years, shorter-term oceanographic sea-level variations may affect local and regional sea-level histories. The occurrence of El Niño is also associated with changes in sea level that may last one or a few years (e.g. Barnett, 1977; Kawabe, 1994). Other short-term oceanographic sea-level variations include tidal cycles, which fluctuate on daily, monthly, annual and greater time scales.

Figure 1.18. Schematic cross-section through a hypothetical coral head. The flat surfaces are HLS's. The rings illustrate the morphology that develops from growth under conditions of fluctuating HLS. The graph is the sea-level curve that can be inferred from the coral head. The lines with question marks offer another equally possible sea level history, illustrating the difficulty in distinguishing between sudden and gradual sea-level rise. The line patterns on the graph are pattern-coded, corresponding to those on the cross-section, to illustrate which part of the curve represents which part of the coral.

71

Sea level history inferred from the stratigraphy
of a hypothetical coral microatoll

Sea-level curve corresponding
to coral growth morphology
("color"-coded)

Alternative sea-level record
inferred from coral morphology

?
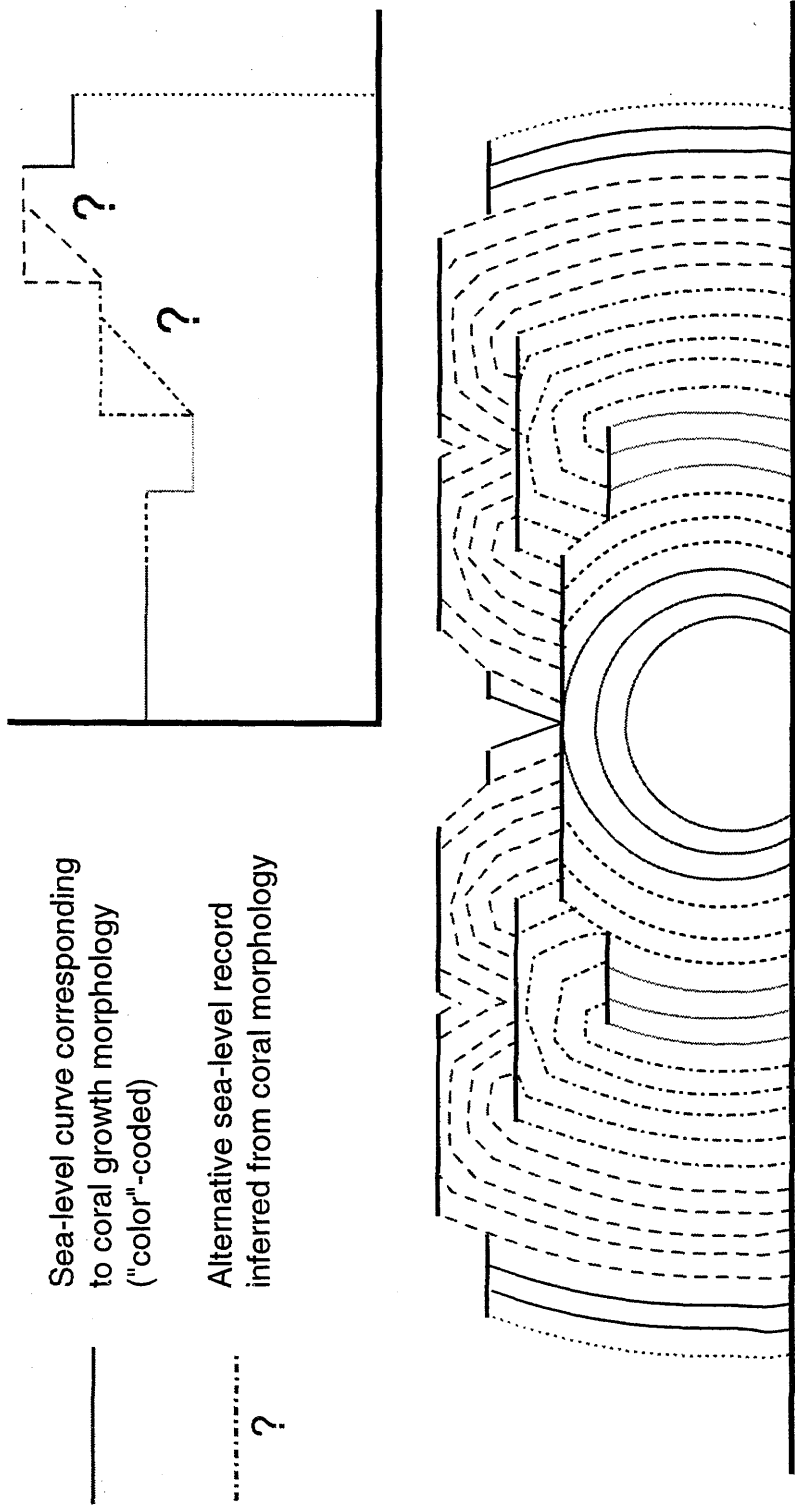
Geodynamically and oceanographically induced sea-level changes may be distinguishable from tectonically induced changes by virtue of the magnitude, shape and extent of the perturbation. Taylor and others (1987) recognized four primary distinguishing features: 1) geographic distribution of the effect, which is likely to be wider for an oceanographic cause and more localized for a tectonic cause; 2) longevity of the effect - tectonically induced sea level changes are more likely to persist through time, as a step function, while oceanographic changes will likely reverse or damp out within a few years, as a delta function; 3) coincidence in time between known earthquakes and changes in sea level which favors a tectonic cause; and 4) the tectonic nature of the site of sea level change - a sea level change that occurs in a tectonically active area that is not observed in a stable area is likely to be tectonic.

To these distinguishing features one can add a fifth, the size of the vertical change. Short-term sea level changes caused by oceanographic/climatic sources such as El Niño may be greater than 50 cm, although this is not common (e.g. Wyrtki, 1977, 1979; Taylor et al., 1987). Perigaud and Delecluse (1993) analyzed Geosat data from 1985-1989, and determined that average sea level in the Indian Ocean north of 20°S rose only about 1 cm during the 1986-1987 El Niño. However, a change of much more than a few tens of centimeters, especially if it is long-lived, is probably more likely to be tectonic in origin.

There are other factors, neither tectonic nor oceanographic, that can produce changes in relative sea level that will be recorded as HLS changes in coral heads. Distinguishing these can be difficult but may be possible by recognizing other features that accompany the changes. These factors include compaction or erosion of the substrate below the coral, which would lower the coral and raise relative sea level. Such changes in the substrate level are often recorded in the growth patterns of the base of a microatoll, with a sawtooth pattern developing on the underside of the coral in response to

fluctuating substrate levels as sediment is deposited against and eroded from the base of the microatoll (Scoffin and Stoddart 1978). Storms, anomalously strong wave action and certainly tsunamis can move microatolls, tilting them and/or transporting them laterally. I observed large coral blocks lying uprooted on some beaches, presumably torn from the sea floor and deposited on land by a tsunami (Figure 1.19). Tilting can be easily recognized and severely tilted microatolls rejected as indicators of sea level change. If the coral is tilted or overturned, the growth pattern will adapt to the new relative water level and reflect the changed orientation in its morphology (Figure 1.20). Lateral transportation is less obvious, although presumably most lateral movement would be accompanied by some tilting.

It is local water level that controls the coral growth. Ponding of water on reef-flats, behind coralline or clastic ramparts, may produce microatolls with HLS histories unrepresentative of sea-level history (Scoffin and Stoddart, 1978). If the rampart is breached, and a connection to open water established, the microatoll will display a sudden emergence. If the rampart accretes, the microatoll may display signs of submergence. This problem can be avoided by concentrating on open-water sites.

1.5d. Corals, sea level records, and tectonics - Previous work

Corals, both whole reefs and microatolls, have been used to document long-term sea level changes associated with glaciation and deglaciation as well as much shorter-term climatic and oceanographic variations of sea level. Reef corals have been studied in Australia (e.g. Collins et al., 1993a, 1993b), Papua New Guinea (e.g. Chappell, 1974; Chappell and Polach, 1991; Stein et al., 1993; Ota et al., 1993; Ota, 1994), the Caribbean (e.g. Bard et al., 1990), Indonesia (e.g. Pirazzoli et al., 1993) and elsewhere, to examine the timing and nature of sea-level changes during and since the last interglacial sea-level maximum about 125,000 years ago. Woodroffe and McLean (1990) studied slabs cut

Figure 1.19. Large blocks of coral, both partial and virtually complete coral heads, appear out of place and strewn along a beach on the east side of the southern peninsula of South Pagai. These corals were probably lifted out of growth position and deposited on the beach by a tsunami. The large pieces are on the order of 2 to 3 m across.

Figure 1.20. This living *Porites* coral microatoll had been growing at an orientation defined by the inner flat top. At some time probably about a decade or two ago, the coral was tilted and began to grow at its present orientation, defined by the outer flange. Only that part of the coral that remained under water after tilting continued to grow. The tilted, emerged part died and serves as a clear indication of the tilting. The growth rings from this coral would indicate the year in which this tilting event occurred.

from living *Porites* microatolls at several island sites in the Indian and Pacific Oceans to obtain annual records of sea-level fluctuations over the last few decades.

Emerged reefs have also been used to document average tectonic uplift rates for the Quaternary period and coseismic uplift events in several regions. The numerous high emerged reef terraces of the Huon Peninsula of Papua New Guinea, which rise to elevations as great as 1000 m, have been especially well-studied (Ota and Berryman, 1994). Ota and Chappell (1996) have argued that emerged regressive Holocene terraces on the Huon Peninsula record individual coseismic uplift events over the last 6,000 years. Jouannic and others (1988) studied a suite of emerged coral reef terraces in West Timor and calculated an average uplift rate of 0.3 mm/yr for the region since the last interglacial. By comparing the elevations of coeval reefs at different locations they documented the existence of differential uplift and block faulting. Microatolls, too, have been used to document tectonic uplift and individual coseismic uplift events (Edwards et al., 1987c; Taylor et al., 1987; 1990)

1.5e. Microatolls, tectonics and paleoseismology - Previous work

The analysis of living and dead microatolls has been utilized successfully in the southwest Pacific to document tectonic uplift (e.g. Taylor et al., 1987 and 1990; Edwards, 1988; Edwards et al., 1988). In Vanuatu, where the coastline has been rising above a subduction interface throughout the Holocene, significant emergence events in 1946, 1965, 1971 and 1973 were documented using partially emerged living coral microatolls (Taylor et al., 1987). The dates of these emergence events coincided with the dates of known earthquakes, leading these workers to conclude that coseismic uplift during these events had caused the emergence. These studies illustrated that coral microatolls could be used successfully to document the time and amount of uplift associated with recent earthquakes.

Edwards and others (1987c; 1988) and Taylor and others (1990) used the same techniques to measure the timing of paleoseismic events by analyzing fossil corals in the same region. By analogy with the partially emerged corals, they inferred that the fossil corals had emerged as a result of coseismic uplift similar to that of the modern events. They obtained ^{230}Th ages for the emerged corals. Using these ages in conjunction with annual growth bands, they determined the dates of the old uplift events and established that microatolls could also be used as recorders of paleoseismological events.

Most previous work using corals to document vertical tectonic movements has focused on uplift, in which corals emerge into or above the intertidal zone and die. But, microatolls also record submergence, so they can also be used to develop sea-level histories in subsiding and stable areas.

1.5f. Cocos Islands tidal records and hypothetical coral growth

Ideally, corals at HLS should record any fluctuations in sea level in the morphology of their HLS flats. To test the fidelity with which HLS changes reflect sea level changes, one should compare the HLS record in corals to a known sea level record. This has been done at Tarawa Atoll in the western Pacific, where the 3-month running mean from a 15-year tide gauge record was compared to the sea-level record of a microatoll (Woodroffe and McLean, 1990). The timing and sign of sea level changes was consistent between the two records, but the magnitude of the change was much more subdued in the microatoll record than in the tide gauge record. Unfortunately, the lack of a similar long-term tide gauge record in the Mentawai Islands precludes such a direct comparison.

The nearest relatively long-term tidal record to the Mentawais is from the Cocos (Keeling) Islands (12°7.0'S/96°54.0'E; about 1000 km SSE from the Pagais), an atoll in the eastern Indian Ocean. This region is tectonically stable, as judged by its intraplate

location and the observation that the atoll has undergone submergence at a low average rate of about 0.1 mm/yr since the last interglacial period, about 125,000 years ago (Woodroffe et al., 1991). The presence of emerged mid-Holocene coral microatolls more than 50 cm above sea level (Woodroffe et al., 1990a, 1990b) is consistent with the glacio-isostatically induced post-mid-Holocene drop in sea level widely observed at low to moderate latitudes and modeled by Peltier (1988) and Peltier and Tushingham (1991). This tide gauge has been recording sea level since 1986.

I compared the Cocos record with that of temporary tide gauges that were installed in Sikakap Harbor, in the strait between North and South Pagai, in July 1994 and again in February 1996, to see if the record from the nearest tide gauge to the Mentawais provided an adequate measure of Mentawai sea level history (Figure 1.21). The two Sikakap records are similar in phase and amplitude to the Cocos record. Given the similarity, it is possible that the corals in the Mentawais and Cocos are exposed to similar tidal fluctuations and would display similar morphologies, were it not for the different tectonic settings of the two locations. Thus, I can use the Cocos record to examine how a coral in the Mentawais might look if it grew under such oceanographic conditions at an elevation near its HLS.

From the hourly Cocos record, I extracted the record of lowest monthly sea level occurring near midday, the time when the corals are most likely to be killed by exposure and to record HLS impingements. Figure 1.22a shows hypothetical coral growth under the sea-level conditions represented by the Cocos monthly lowest midday tide record. The hypothetical coral was allowed to grow at 10 mm/yr, beginning slightly below HLS in 1986. In a tectonically stable area like the Cocos Islands, the only causes of sea level change are oceanographic/climatic and glacio-isostatic sea-level change. The glacio-isostatic effect there is very slight (<1 mm/yr) and short-term oceanographic effects dominate the record (Woodroffe et al., 1990a, 1990b). In particular, note that low low

tides occur about once a year, usually in the first part of the year, and that they vary by as much as 25 cm. In the 10 years of the Cocos record, the upward growth of the hypothetical coral was "clipped" or impeded by lowest low tide four times: mid-1988, mid-1989, mid-1993, and early-1995.

Figures 1.22b and c show the HLS impingements on synthetic corals growing at 10 mm/yr at hypothetical localities, where 7 mm/yr of submergence and emergence, respectively, are superimposed on the Cocos record. The submerging coral was clipped less often, twice in 10 years. Its HLS was about the same height at the end of the decade as at the start. If the extreme 1995 depression had not occurred, the coral's top would have been higher in 1996 that in 1986. The emerging coral was clipped almost every year and its 1996 HLS height ended up some 13 cm lower than its 1986 height. Such a coral would show a gradual outward downstepping.

If sea level fluctuations in the Mentawais are similar to those at Cocos, then Mentawai corals should display evidence of non-tectonic effects like those illustrated in Figure 1.22. At tectonically stable sites, subaerial exposure should produce stratigraphic and morphologic expressions of HLS impingement in microatolls several times each decade. Heads at localities characterized by steady submergence should display less frequent HLS clips. One should expect in the Mentawais to see low-amplitude die-downs due to oceanographically controlled annual fluctuations in lowest low sea level, which must be kept distinct from death and regrowth related to tectonic uplift and subsidence.

1.6. Microatolls, paleoseismology, paleogeodesy - goals of this study

In this thesis, I use microatolls from the Mentawai Islands and the west coast of Sumatra to derive records of relative sea-level change for the modern and premodern periods. The modern records are contained in living microatolls, which reveal a history of ongoing submergence. The premodern records are preserved in fossil microatolls,

Figure 1.21. Tidal records from a permanent tide gauge on the Cocos Islands, Australia (12°7.0S/96°54.0E) and a temporary tide gauge installed at Sikakap, North Pagai in July 1994 (a) and February-April 1996 (b) (times are GMT and elevations are relative to an arbitrary datum). Because of the close coincidence of the two records over short time periods, the long term Cocos Island record was used to explore the influence of tidal fluctuations on coral morphology in the Mentawai Islands. The small differences in phase and especially in amplitude would produce significant differences in the corals at the two locations on long time scales, but the general character of the coral morphology should be similar. The vertical scales are relative to arbitrary datums and should not be used to compare absolute elevations between the two sites.

Tides at Cocos Island and the Mentawai Islands
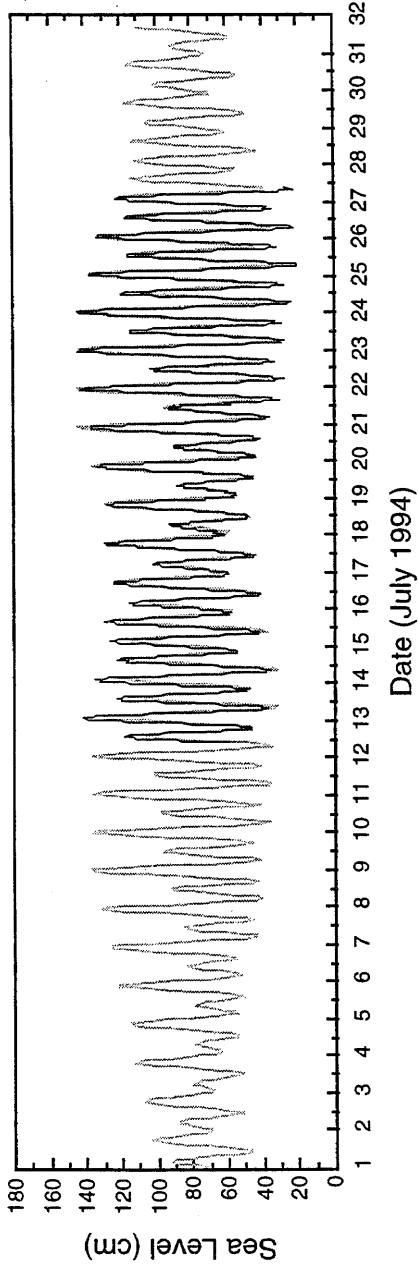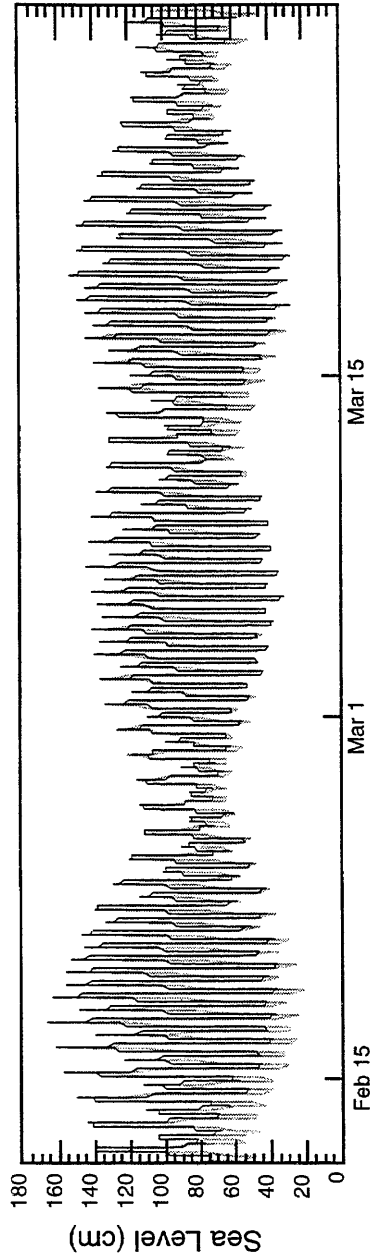
Figure 1.22

a. Hypothetical coral growth based on a ten-year Cocos Islands tidal record of the lowest low tide of the day occurring during the midday hours when sun exposure is greatest (thick black line). Elevations are relative to an arbitrary datum. A hypothetical coral, growing at a rate of 1 cm/yr under these tidal conditions, was generated (dashed line). The effect of normally fluctuating sea level on the coral growth, under conditions of tectonic stability, is to impinge on upward growth of the coral three times in a decade. Each impingement produced a slight down drop in the coral which was followed by immediate regrowth upward at the limit of the coral's natural growth rate.

b. Similar hypothetical upward growth of a coral as in Figure 1.22a, but with 7 mm/yr submergence superimposed on the Cocos record. The impingements by HLS drop to once in eight years.

c. Similar hypothetical upward coral growth , but with a 7 mm/yr tectonic emergence rate superimposed on the Cocos tidal record. The impingements increase to nearly once a year.
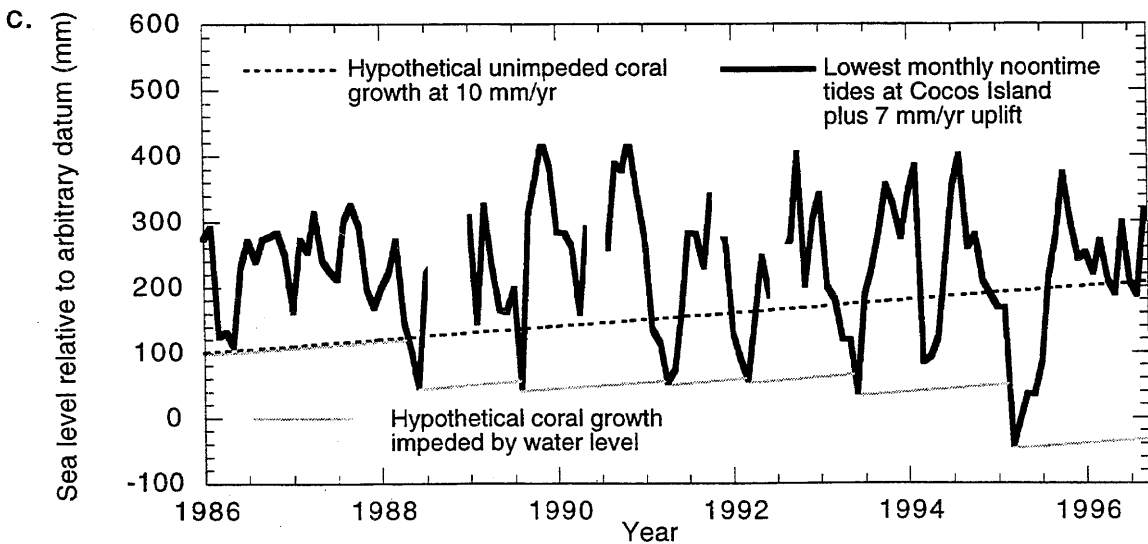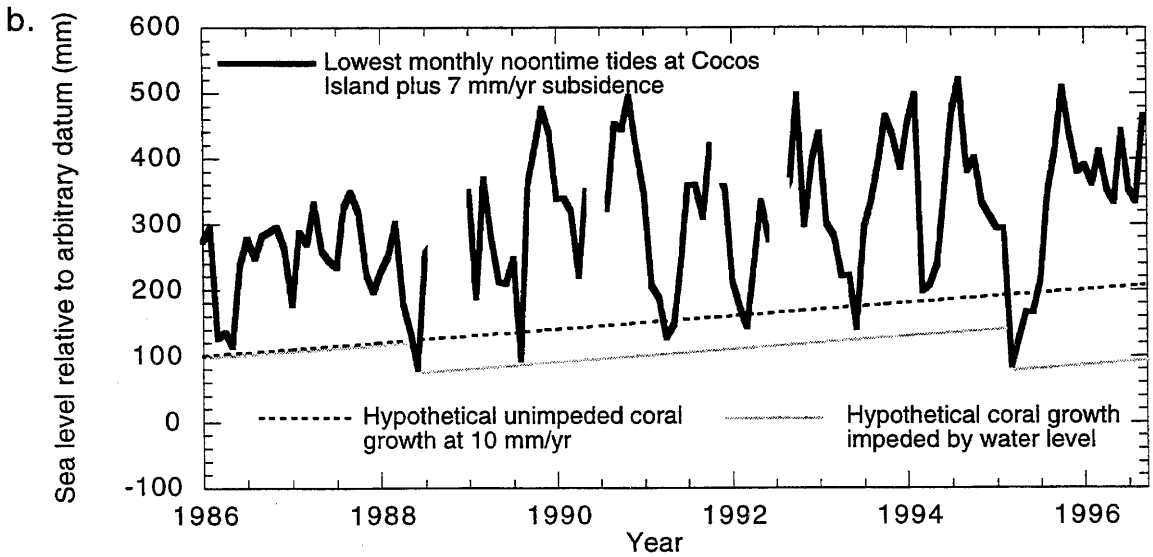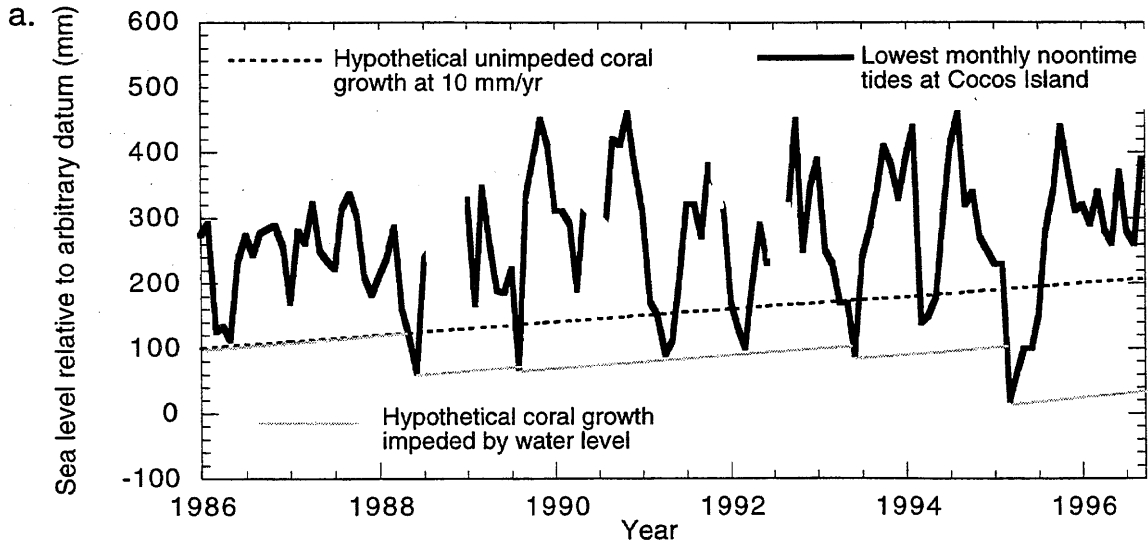
emerged and killed as a result of coseismic uplift. The corals can be dated to yield the age of death and hence the age of the paleoseismic uplift event. The sea level record from these fossil corals can be used to infer past interseismic and coseismic displacements. This coral geodetic and paleogeodetic history can ultimately aid in the development and constraint of models of subduction zone deformation and earthquake characteristics.

Chapter II

Modern vertical deformation at the Sumatran subduction zone

2.1 Introduction

2.2 Results

>*2.2a. General field observations*

>*2.2b. Surveys*

>>*Surveying methods*

>>*Survey results*

>>*Summary - Surveys of living corals*

>*2.2c. Coral slabs*

>>*Sampling and collecting slabs*

>>*X-ray analysis of slabs*

>>*Sample Sd96-C-1*

>>*Other living slabs*

>>*Submergence rates*

>>*Summary of slab analysis*

2.3 Discussion

>*2.3 a. Using corals as geodetic measurement tool*

>*2.3b. Modern vertical displacement*

2.4 Conclusions

2.1 Introduction

Historical records of seismic activity along the western margin of Sumatra have revealed that a large earthquake, probably Mw 8.7-8.8, occurred in 1833 (Newcomb and McCann, 1987; Chapter 1). It is inferred to have resulted from rupture of the interface below the outer-arc Mentawai Islands, from the Batu Islands to Enggano Island (Figure 2.1). This is the most recent earthquake of its size documented to have occurred in this region. The coseismic slip, accompanied by substantial shaking and tsunami activity on the outer-arc islands and on the Sumatran coast, probably produced uplifts of a meter or more on the outer-arc islands. Since that earthquake occurred 164 years ago, the area is well into the interseismic part of the earthquake cycle. The presence of mid-Holocene coral only slightly above modern sea-level suggests that there is little permanent vertical deformation occurring in the outer-arc islands (Chapter 1). Therefore, most of the coseismic vertical displacement should be recovered in the interseismic period. One would therefore expect to see interseismic subsidence occurring in the Mentawai Islands

In this chapter, I examine the modern interseismic vertical displacements in the hanging wall of the Sumatran subduction zone that are revealed in the geomorphic and stratigraphic signature of recent sea-level fluctuations in coral microatolls from western Sumatra. If the microatolls are to be useful as geodetic and paleogeodetic recorders, as we hope, the expression of recent sea-level change resulting from interseismic displacements should be visible in the living corals of the Mentawai Islands.

This chapter presents only the results of a study of live corals. The purpose of the examination of living coral is twofold - first, to determine the quality of the coral "instrument" and its limitations, and second, to constrain modern and recent vertical displacement in this area. Living corals provide the most well-constrained samples with

which to test the method, because the ages are known, the corals are in place, and recent tectonic and tidal histories are better known than for fossil corals. Constraints on use of this method and its limitations, derived from this study, can be used to inform and guide the study of fossil corals, described in Chapters 3 and 4. The modern vertical displacement results can ultimately be used in conjunction with results from fossil corals to constrain the long-term history of vertical deformation above the subduction zone.

Field work for the study of living corals was concentrated on the western coast of Sumatra, on Tikos Island, a small island slightly offshore of the town of Bengkulu, and on North and South Pagai and Sanding Islands, in the outer-arc Mentawai Island chain. The Pagais and Sanding are about 115 km from the subduction zone trench, and Tikos Island is about 215 km away. The crest of the volcanic arc of Sumatra is about 250 km from the trench. I expected to find indications of submergence occurring in the outer-arc islands because of their proximity to the trench. I visited Tikos Island, near the coast of Sumatra, in order to compare the nature and magnitude of vertical displacement at a site 100 km farther from the trench. Models of subduction suggest that vertical displacements there might be significantly less than farther out toward the outer-arc rise.

2.2 Results

2.2a. General field observations

I visited numerous sites around the Pagai Islands in July 1994 and mid-January to mid-February 1996, and in 1996 also went to Tikos Island (Figures 2.1 and 2.2). During both seasons, I collected samples and HLS elevation data from both living and dead corals. Coral HLS elevations were measured relative to each other and to water level. In 1994, I took measurements with a meter stick; in 1996, I also used a surveying instrument

Figure 2.1. Location map of Sumatra

Map of the subduction boundary of western Sumatra. The islands west of Sumatra form

the Mentawai chain and are the subaerial expression of the outer-arc rise. The inferred

rupture zones of two historical giant earthquakes (Mw > 8.4) are shown in light and dark

grey shading (after Newcomb and McCann, 1987).
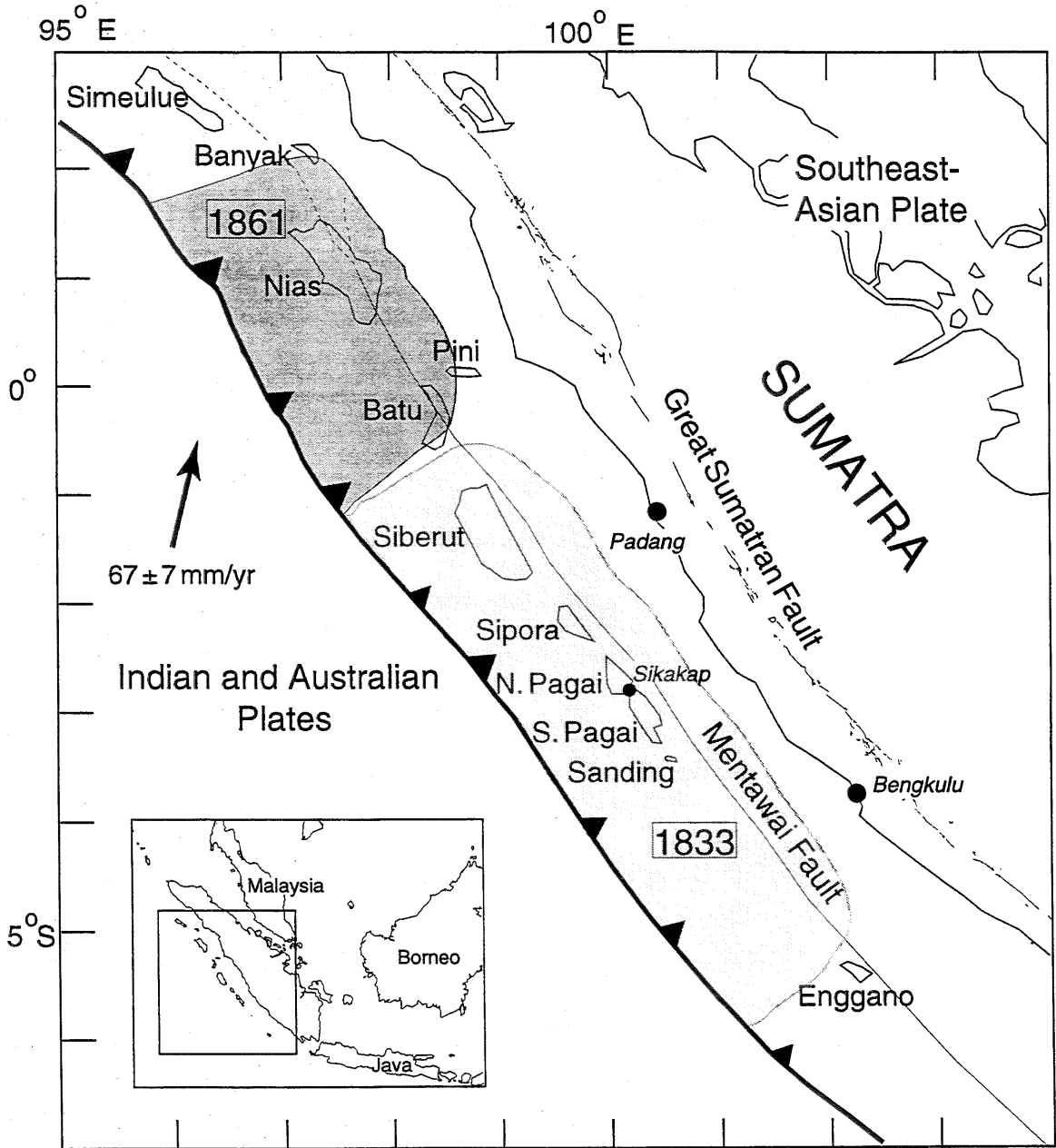
Figure 2.2. Map of sites visited in the 1994 and 1996 field seasons. In 1994, Tikos Island, just west of Bengkulu on the west coast of mainland Sumatra (see Figure 2.1) was also visited. Sites at which surveys were performed and where large slabs of living coral were collected are indicated by name. I also collected live slabs from Tikos Island. Only at site P96-J were both slabbing and surveying conducted.

Mentawai Islands

Sipora

Tuapejit

⊚ 1994 Sites
● 1996 Sites
NP96-B Survey sites
P96-B Slab sites

10 km

N

NP96-B

NP96-A

North
Pagai

NP96-C

Sikakap

P96-Q

P96-B

South
Pagai

P96-P

P96-O

P96-K

P96-J

P96-L

P96-N

Sd96-A

Sanding

Sd96-C
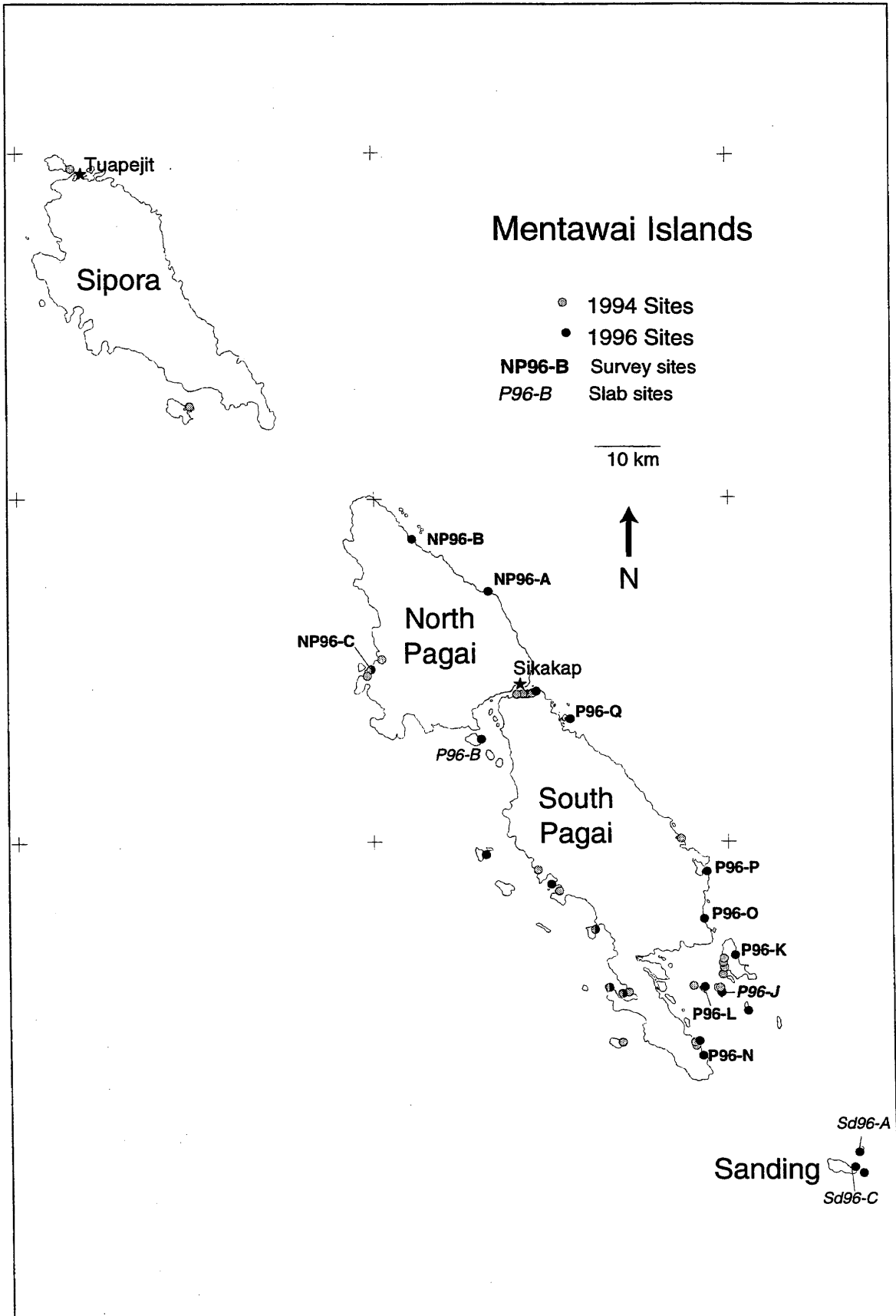
to take precise relative elevation measurements. Samples were collected either with a hammer and chisel or a concrete-cutting chain saw.

Sampling and observation were facilitated by low daytime water levels in July 1994 and inhibited by substantially higher water levels in early 1996. The mean monthly tidal record at the Cocos Islands indicates that mean tides in July 1994 were higher than in early 1996 (Figure 2.3). However, the hourly record indicates that daytime low tides in July 1994 were the lower of the day's two low tides and were about 25-50 cm above an arbitrary datum. In early 1996, daytime low tides were the higher of the two low tides and were about 35-60 cm above the datum (Figure 1.21 in Chapter 1). Certainly, from our observations, the daytime water levels in the Mentawais in 1994 were much lower than in early 1996. Between July 20 and 22, 1994, living *Porites sp.* were growing as much as 18 cm above water during the daytime low tide, whereas in 1996 living corals were not observed higher than 20-25 cm *below* water. However, the Cocos record indicates that lowest midday tides were higher in July 1994 than in early 1996 (Figure 1.22 in Chapter 1). If the Cocos tides exactly mimicked the Sikakap tides, one would expect to have seen living corals at or above water level in the third week of January, but in fact they remained well below water. Evidently, for all the short-term similarities in the two records, there are significant differences that preclude direct application of the Cocos tidal record to the Mentawais.

Another notable difference between the 1994 and 1996 seasons was in the morphology of the living coral heads. In 1994, most corals showed signs of slight recent submergence. The overall morphology was cup-like, with a lower central flat surface surrounded by a high raised rim. Superimposed on this was a smaller, secondary rim, a slight raised lip around the inner and outer edges of the main rim, which was otherwise flat and dead on its top (Figure 1.17 in Chapter 1). This lip implied unimpeded upward growth for the one or two years prior to 1994. In 1996, by contrast, the living ring of coral

was about 5 cm lower than the top of the main rim. This implied that a slight emergence had occurred sometime in the year and a half between the two field seasons. It may indeed have occurred during the first field season. As mentioned above, the living coral in July 1994 was exposed more than 10 cm in the middle of the day in sunny, hot weather. However, the Cocos Islands record indicates that a substantial sea level drop occurred in early 1995, and this may have been the event represented by the die-down (Figure 2.3 and Figure 1.22 in Chapter 1).

A third difference between 1994 and 1996 lay in the apparent health of the reef. The living reef in 1994 appeared much more robust and healthy than it did in 1996. In 1996, I observed many dead coral heads at the same elevation and exhibiting the same morphology as living corals. Furthermore, there were numerous corals that had only small patches of living coral on a mostly dead head. In 1994, this was not observed, except in Sikakap Strait. Near the town of Sikakap (population about 2000) and across the strait near a lumber operation, live corals appeared very unhealthy, some with only small patches of living material. I attributed this unhealthiness to pollution, which was clearly substantial in the area. Perhaps an increase in pollutants contributed to the poorer health of the reef exhibited in 1996, although the sick coral was not localized around Sikakap and there are no other towns of its size and degree of development in the Pagais. Fishermen have used cyanide in these waters to stun fish, and the cyanide may have killed or contributed to the death of the coral. Or perhaps some other environmental stress was imposed between the two field seasons to explain the difference.

Two general observations from the two seasons are difficult to explain. Although I observed the small, slightly raised lip on live corals at most locations in 1994, I did not see this lip as a remnant on the dead rims of living coral in 1996. Observations at most sites in 1996 showed the living coral down-dropped from a fairly smooth large rim. Little evidence of the older lip was seen. It seems unlikely that a lip about 1 cm high would

Figure 2.3. Record of mean monthly tides at Cocos Island (12°7.0S/96°54.0E; elevations relative to arbitrary datum.) Although the Cocos mean tide of July 1994 is higher than that of January-February 1996, in the Mentawais the daytime water levels were at least 35 cm higher in 1996 than 1994. The lowest mean tides of the decade, which occurred in March 1995, may account for the slight emergence, recorded in all observed living corals, between the 1994 and 1996 field seasons.
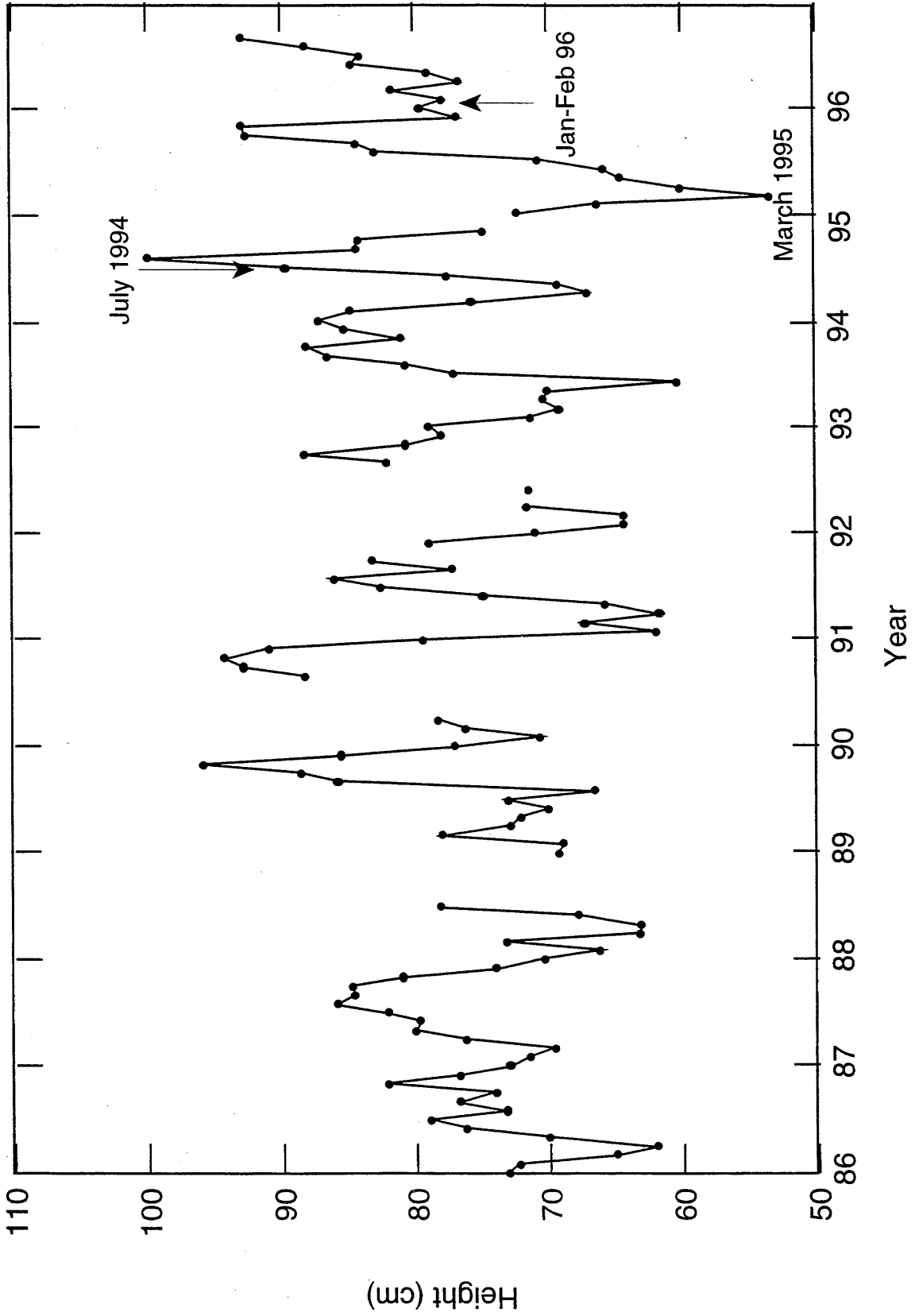
have shrunk to nothing upon dying. Possibly the lip was eroded shortly after its death, though it seems unlikely that there should be no remnants of it remaining. The other curious observation is that, in general, many of the corals observed in 1994 appeared to have one or two additional older HLS rims inside and lower than the most recent upraised rim, while in 1996 most observed corals showed just one rim surrounding a flat. Only occasionally were multiple rims noted. There is no ready explanation for these differences between 1994 and 1996 corals. It may just be coincidence that more corals of one type were observed in one year than the other, or perhaps unrecognized observational biases existed and differed between the two seasons.

2.2b. Surveys

In 1994, in order to determine the magnitude of variation in HLS elevation between corals of the same age, I surveyed live corals in one bay at Tuapejit, Sipora (Figure 2.4a). The average 1994 HLS of seven corals varied as much as 8 cm in elevation (Figure 2.4b). Duplicate measurements of modern HLS in any one head indicated that variations of 5 cm in modern HLS height could exist even within a single head. Other flats, which, based on morphology, were determined to be older HLS's, were all lower than the 1994 HLS and varied by even more than 8 cm. However, not all corals had the same number of older levels so there was no sure way to correlate these older HLS's or know their relative ages in the absence of either U-Th dates or of complete cross-sectional slabs revealing annual growth and morphology.

To understand more fully the variations of HLS within and between coral heads, in 1996 I took a Wild-Heerbrugg TC2000 "total station" surveying instrument to the islands for more precise surveys. I surveyed several sites in the islands (Figure 2.2),

measuring the location and elevations of various levels on the numerous dead and living corals at each site.

Surveying methods

I determined a rough location for each site with a single handheld GPS receiver. These locations have an absolute precision of about ±50 m. The total station was erected on a tripod, usually within about 20 or 30 m of the GPS measurement, on eroded dead coral reef, beach rock, or firm sand. A north azimuth was determined with a compass prior to surveying. In most cases, I surveyed the beach, either the top of the storm berm, the high-tide mark, or the beach-water contact. Elevations were measured relative only to the instrument at the site and to water level at the time of the survey.

At many sites time permitted the surveying of only a fraction of the corals present. I surveyed several heads that I considered representative at each site. These surveys provide a general picture of coral morphology and the basis for determining a sea-level history for the whole site. I neglected individual live corals that were radically different in morphology from all the others. However, corals that had the same general morphology but had, for example, similar levels at different depths were included, since such variations could be relevant to understanding the coral response to sea level at the site.

At most sites, I found at least 5 or 6 appropriate living corals. In some areas, I recorded only modern HLS at a few points on several heads. Elsewhere I included older levels, both higher and lower, which I interpreted to be former HLS's. In several cases, I surveyed a complete profile across the top of a living corals from substrate to substrate to provide a clearer view of the morphological similarities and differences within and between corals.

Figure 2.4

4a. Map of living corals in Tuapejit Harbor, Sipora surveyed in July 1994.

4b. Elevations of 1994 and older HLS levels of living corals in Tuapejit Harbor, Sipora. 1994 HLS's are at the same level to within about ±4 cm. Other, older, levels have greater variability, which increases with age. Although 1994 HLS is certainly the same age for each coral head, it is not certain that the other levels correspond in time from head to head. In other words, Level 4 in Coral 4 may not be the same age as Level 4 in Coral 7.

Tuapejit Bay, Sipora
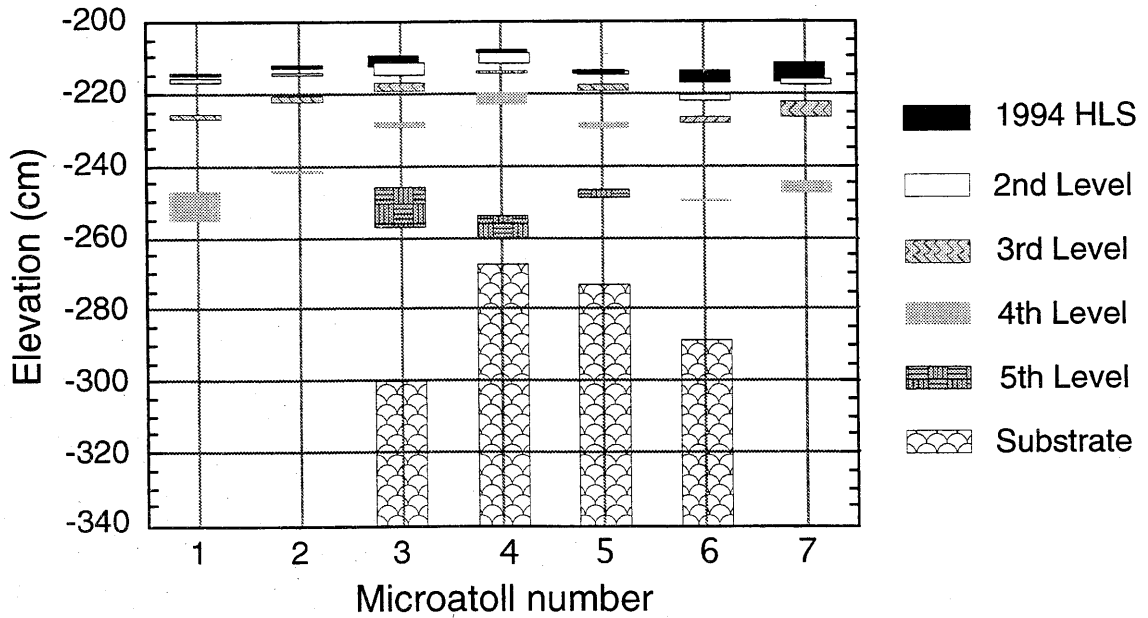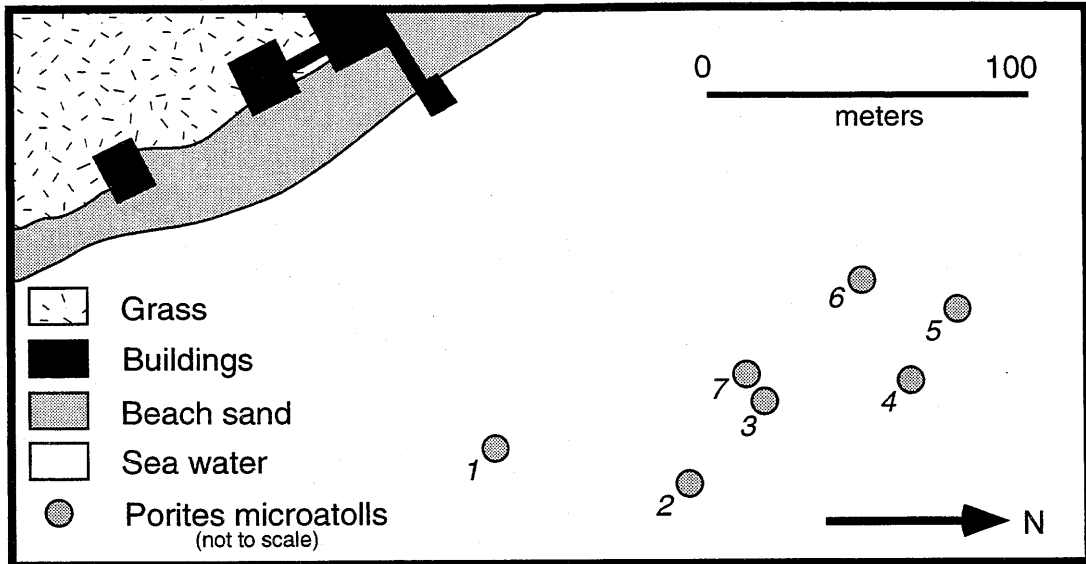
<u>Survey results</u>

Most sites with head corals were quiet water environments, in small bays or next to protected islands, though branching and platy corals could often be found in rougher areas. Microatolls lived next to sandy beaches with coconut palms, in beachless, murky bays dense with mangroves, and near rocky outcroppings of old reef or beachrock. The corals at most sites tended to be grouped in communities, relatively closely spaced and localized to a bay, or small area of the coast (Figure 2.5). Live corals that had reached HLS grew between 10 and 200 m from shore at most sites. In general, living coral was farther from shore than dead, emerged coral, at least well-preserved dead microatolls, although occasionally, broken or eroded dead coral was plentiful in the outer reef. It may be that near-shore dead corals were buried and only recently exhumed and are thus minimally eroded compared to those farther offshore that may never have been buried and that have been exposed longer to the ravages of surf, tide and bioerosion. Almost all corals surveyed were *Porites sp.*

Elevations

1996 HLS - Intrahead Variation

The elevations of HLS in 1996 of live corals at various sites are shown in Figure 2.6. At site P96-J, I measured the 1996 HLS of four living *Porites* heads about 10 m from the beach berm. For each of the four corals, I took between 3 and 7 measurements of 1996 HLS elevation. The elevations in one head were generally within ±2 or 3 cm of the average HLS elevation of the head. The intrahead range of elevations for 1996 HLS was between 4 and 6 cm. At site P96-L, I made between 2 and 4 measurements of 1996 HLS

on each of nine living coral heads. The intrahead range in 1996 HLS elevation here was between 1 and 7 cm. At P96-P, the range was as high as 10 cm in one coral, but was more commonly between 0 and 6 cm. The ranges in each of the other sites are listed in Table 2.1. If these data are representative of Mentawai corals in general, it appears that the intrahead variation of HLS of living coral is usually less than ±3 cm within a head, though occasionally some heads show ranges as high as 10 cm.

I calculated the standard deviation for intrahead variation for each head from multiple HLS measurements. First, I determined the mean elevation of 1996 HLS for each head. Then, I calculated the deviation from that mean of each measurement on the head. After normalizing the head means to zero, and calculating new elevations of each measurement relative to the normalized mean, I calculated the standard deviation of the elevation measurements around the normalized mean for each site and for all sites together. The results are presented in Table 2.1. The standard deviation for all the sites together is 1.8 cm. Thus, based solely on HLS variability *within* a head, most heads have HLS's that vary by less than ±4 cm (2σ), although larger variations may occur.

The variability in HLS within one head in the Pagais appears to be random, and therefore cannot be corrected for. I examined the possibility that HLS might differ from the seaward to the beachward side of a coral head. Such systematic variations might be expected if, for example, the seaward side were kept moist by splash during low tides and thus survived longer than the beachward side while exposed above water, or if water backed up higher behind the coral on the seaward side and was relatively depressed on the leeward side, like an eddy forming behind a rock in a river. These could produce a higher overall HLS elevation on the seaward side. Systematic variations might also be caused by water flow. Scoffin and Stoddart (1987), for example, saw asymmetric HLS height in Great Barrier Reef microatolls when there was a strong water flow in one direction. The windward side often grew slightly higher than the leeward side. However,

Figure 2.5. Surveyed maps of sites that had living corals. Both living and dead corals were surveyed. Lines across some heads show the direction along which profiles were surveyed. The locations of these survey sites appear in Figure 2.2.

a. P96-J

N

10 m

1

2

3

4

P96-J

b. P96-P

N

50 m

P96-P

2

1

1

5

6

3

2

4

7

8

9

c. P96-L

N

1

2

3

4

5

6

8

7

9

2

1

50 m

P96-L

d. P96-Q

N

2

3

4

5

6

1

4

3

2

1

50 m

P96-Q

e. NP96-B

N

7

4

3

2

6

5

8

1

25 m

5

3

2

1

NP96-B

f. NP96-A

N

1

2

3

4

7

6

5

9

8

1

2

3

4

5

7

6

50 m

NP96-A

g. P96-N

N

5

2

1

3

4

1

2

4

3

5

50 m

P96-N

h. NP96-C

N

6

5

4

3

1

2

NP94-A-9

9

8

10

7

1

2

9

3

14

15

16

4

13

8

12

5

10

11

7

6

NP94-A-6

50 m

NP96-C

4 — dead coral head* with surveyed profile line

2 — live coral head* with surveyed points

*size exaggerated 2x (except fig. a.)

sandy beach

sea water

• surveyed point along beach edge

✶ total station

Figure 2.6. Elevations of 1996 and older HLS surfaces on living corals at each of the sites

surveyed and shown in the maps of Figure 2.5. In each plot, the vertical axis is relative

elevation in centimeters. The horizontal axis shows the number of the living coral head;

the numbers correspond to the numbers in the maps of Figure 2.5. Plots for sites P96-J

and P96-N show the relative locations of the coral heads, P96-J parallel to the beach and

P96-N approximately perpendicular to the beach. The other plots just indicate the corals

by number, with no location information. Elevations are relative to an arbitrary datum at

each site and cannot be related site to site. There are no absolute elevations available for

any site, although elevations of water level at the specific times were measured in most

cases.

a. P96-J

b. P96-L

c. P96-P

d. P96-N

e. NP96-A

f. P96-Q

g. NP96-C

h. NP96-B

Current HLS	——	Multiple Measurements	—•—
Old HLS - down	—•—		
Old HLS - up	⋯⋯	Substrate	----
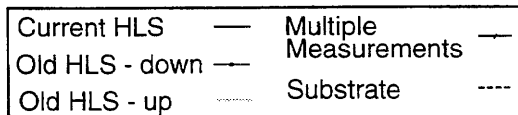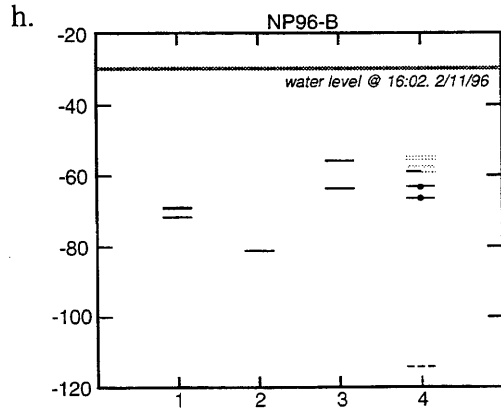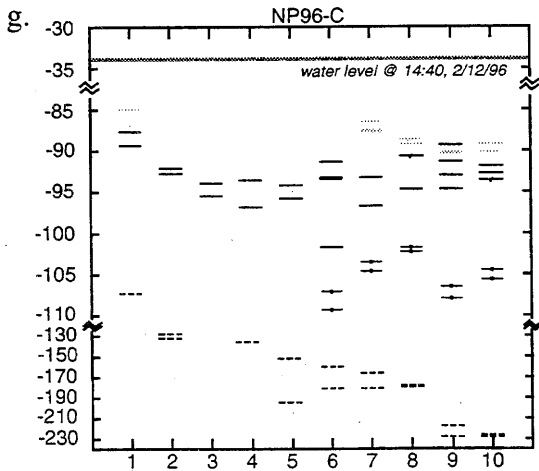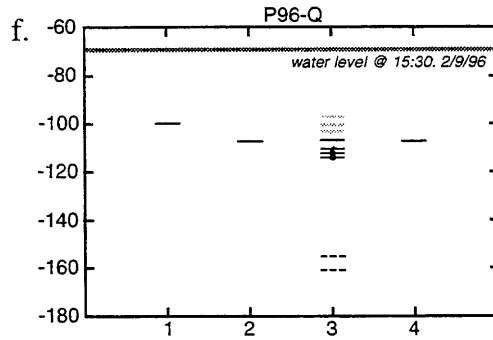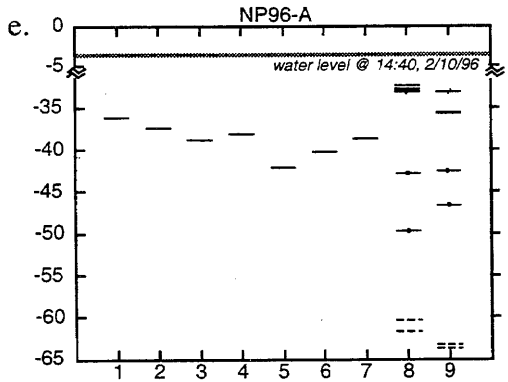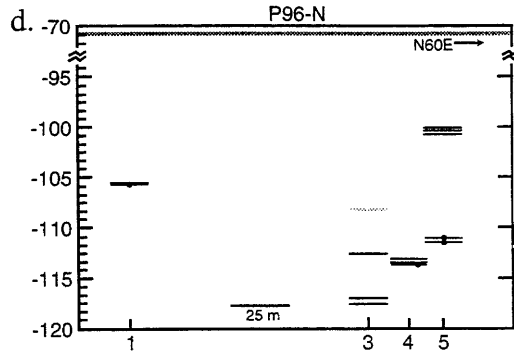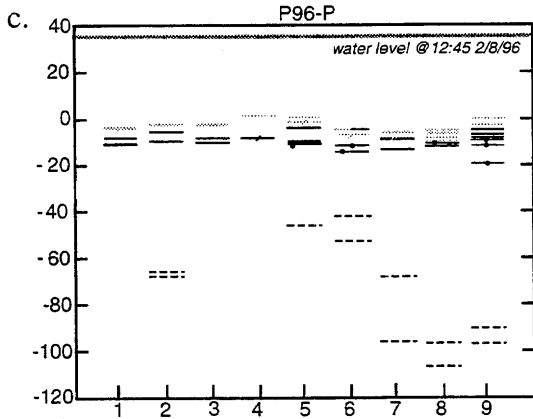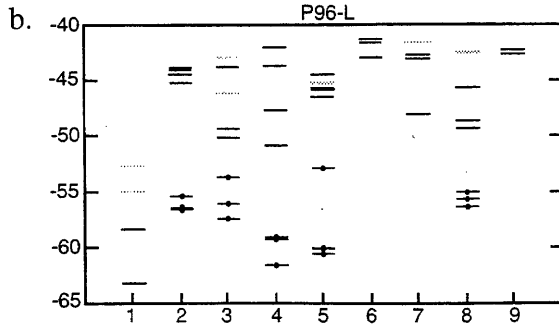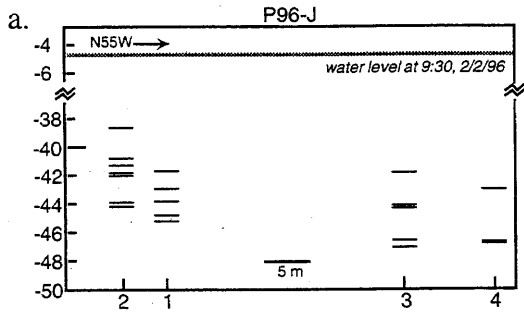
Table 2.1

Table of elevations of modern HLS in 1996 from living corals in North and South Pagai. Elevation data were gathered in detailed surveys of live coral heads performed with a TC2000 "total station" surveying instrument. The first column lists the site at which the surveys were undertaken. The locations of these sites appear in Figure 2.2. The second column shows the range living HLS elevation within individual coral heads, and the thrid column shows the standard deviation from the intrahead mean. The fourth and fifth columns show the range and standard deviation in HLS elevations between different coral heads at the same site.

Table 2.1.

Site Name	Maximum range of intrahead HLS elevations	Intrahead standard deviation (2σ)	Maximum range of interhead/intrasite mean HLS elevations	Interhead standard deviation of mean HLS elevations (2σ)
P96-J	6	3.4	4	3.2
P96-L	7	4.0	19	11.2
P96-N	5	2.8	15 (38)**	14.2 (33.4)**
P96-P	10	4.6	5	3.4
P96-Q	*		9.0	8.2
NP96-A	2.5	2.0	9.5	5.8
NP96-B	3	2.2	14.5 (25.5)**	12.4 (20.0)**
NP96-C	10.5	24.0	7	4.2
All Sites		3.6		7.4 (12.0)**

* Only one coral at this site had more than one measurement of 1996 HLS.
** Numbers in parantheses are standard deviations if one outlier at each of the two sites is included in the calculations. These outlying measurements are suspect because it was not certain based on field observations that they in fact represented a modern HLS surface.

the Pagai measurements showed no such systematic unevenness in the living corals. Vertical exaggeration in the graphs of 1996 living HLS height versus distance perpendicular to the beach at sites P96-J and P96-L illustrates that the seaward side is neither more nor less likely to be high than the beachward side (Figure 2.7). This lack of correlation appears at the other sites as well. When shown without vertical exaggeration, the most striking aspect of HLS elevation is not its variation, but the lack of it (Figure 2.8). The curves are virtually flat. This flatness is consistent with the contention that HLS is, within several centimeters, a reasonable representative of sea level.

The variation of HLS height also does not appear to be obviously related to sun angle, a phenomenon observed among *Goniastrea retiformis* microatolls in Vanuatu (Buskirk, et al., 1981). Other possible explanations for the variation are not readily apparent and have not been tested.

1996 HLS - Interhead/Intrasite Variation

The next issue I examined was the variability of HLS between heads at one site. Across a single site, one would not expect water level, sun intensity or tectonic motion to vary spatially. Thus, observed differences in HLS between corals should be a measure of how HLS in different heads at the same site varies in its response to sea level rather than a measure of differential relative sea-level. To determine intrasite variability, I compared the mean 1996 HLS's individual coral heads (the "head mean") at one site (Figure 2.9). The range of mean elevations at one site was usually between 5 and 15 cm. In one case, it was 45 cm, which was due to one head being substantially lower than the other four. The next largest range observed at a site was 25 cm. This is consistent with the findings of Taylor and others (1980,1987) in Vanuatu, who found a standard deviation of ±10 cm in the elevations of emerged corals.

To calculate the intrasite standard deviation of HLS elevations between heads, I found the mean of all the head means at each site (the "site mean"). Since the datum against which elevations were made differed from site to site, I normalized the site means to zero. I then calculated the standard deviation of the head means around the normalized site means for each site and for all the sites together. The results are in Table 2.1. At the 2σ level, this deviation varies from about 3 to 15 cm at any site. The 2σ standard deviation for all the sites together is about ± 7 cm.

1994 HLS - Interbay Variation

It would be useful to compare HLS in living corals between bays as well and see if the variation is the same or greater than that at a single site. One might imagine the variation between absolute elevations to be greater because water and sun conditions, while probably constant at one site, could vary considerably from site to site. For example, the water level conditions in a strait with active flow could be quite different from those in a quiet, protected bay, and one might expect the absolute maximum height to which a coral could grow would be different under those different conditions. Furthermore, the Mentawais and their offshore islands occupy a large area, and tidal conditions could vary noticeably from one end of the islands to the other, resulting in a different absolute elevations for HLS's of the same age.

Comparing elevations between sites is difficult in the absence of absolute elevation measurements. The surveys measured relative locations and elevations within a site only. The sites were not in view of each other, so surveys at different sites could not be directly linked. However, I attempted to compare absolute vertical elevations indirectly by way of a tide gauge. A tide gauge was installed in Sikakap harbor in 1994 and 1996 that recorded while field studies were undertaken. After the 1996 field season,

Figure 2.7. Elevations of 1996 HLS for each living coral head surveyed at sites P96-J (a)
and P96-L (b) plotted as a function of relative distance from the beach. The vertical scale
is exaggerated (degree of exaggeration varies from head to head) to emphasize any
possible correlation between HLS height and location on the seaward or beachward side
of the coral head. No relationship is evident, and the variation in HLS height within one
head appears to be random.

HLS Variations at sites P96-J &P96-L [Height(cm) vs.distance(m)] with vertical exaggeration

a. P96-J
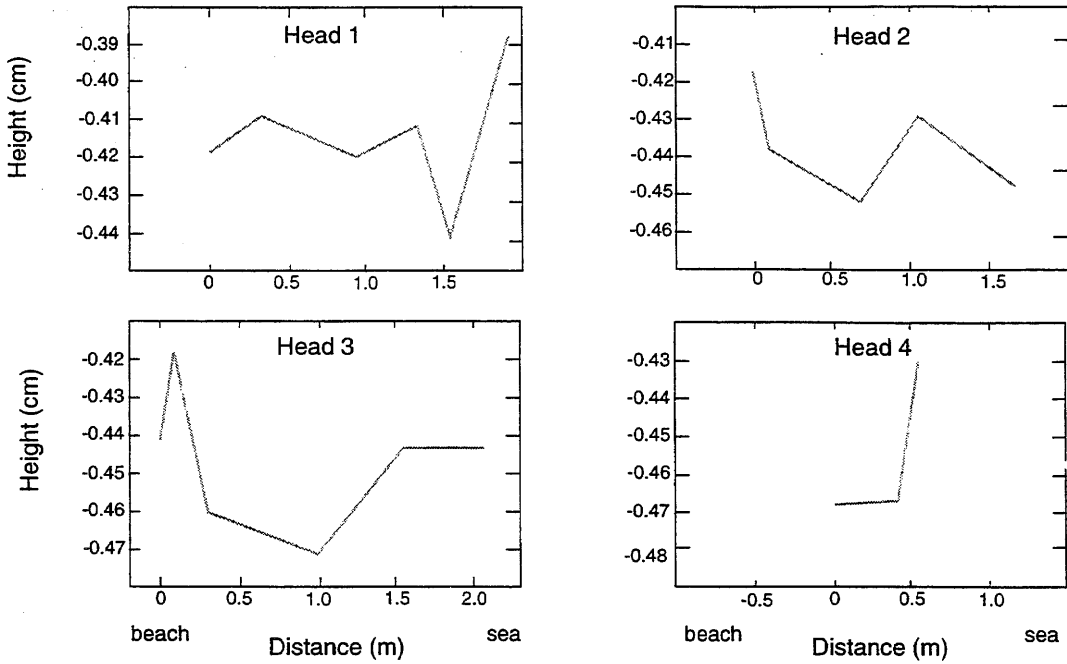
b. P96-L
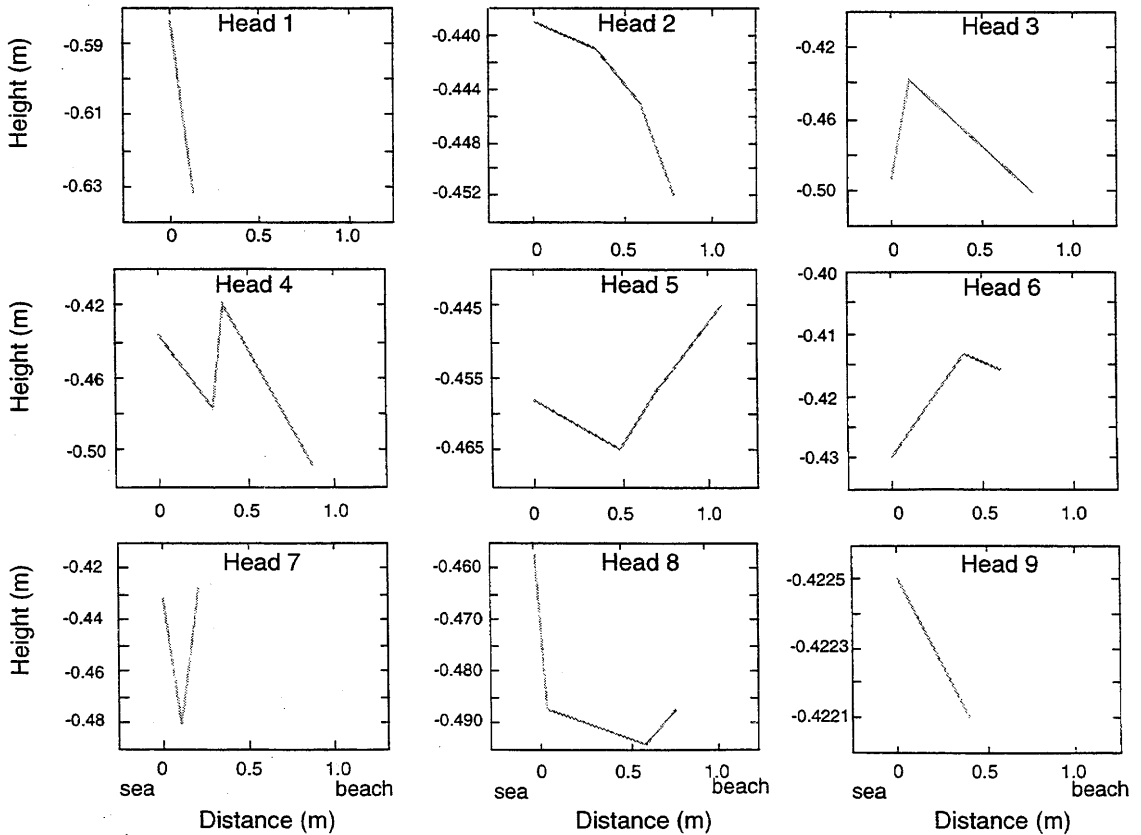
Figure 2.8. The same HLS elevation versus distance from beach as in Figure 2.7, but without any vertical exaggeration. The variations are almost imperceptible and the overall flatness of the heads and uniformity of HLS heights within each head dominate.

HLS Variations at sites P96-J &P96-L [Height(cm) vs.distance(m)] without vertical exaggeration

a. P96-J
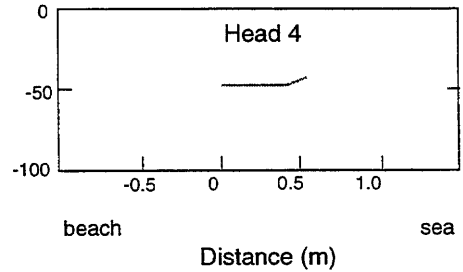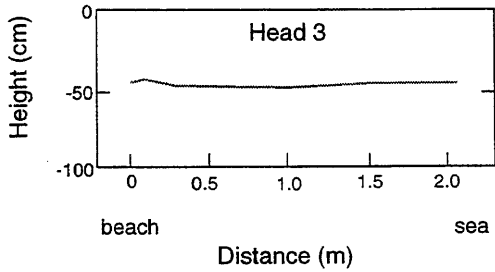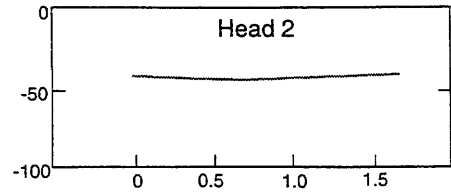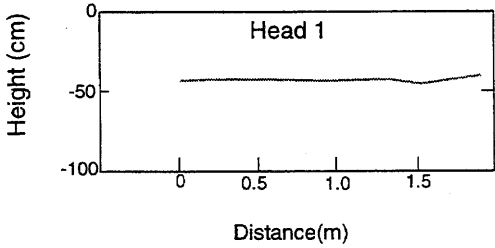
b. P96-L
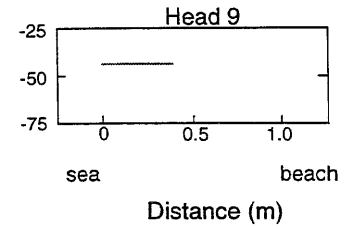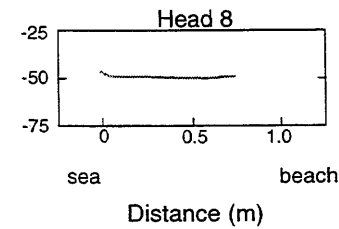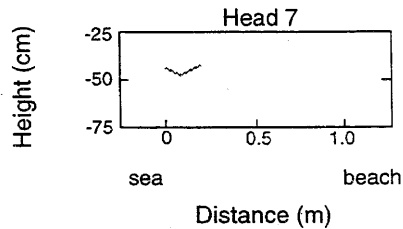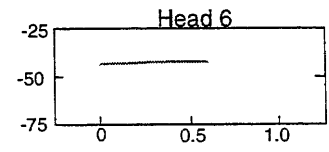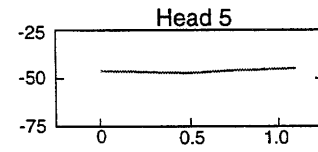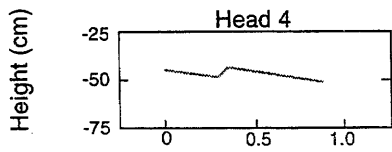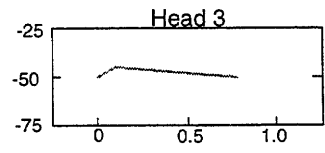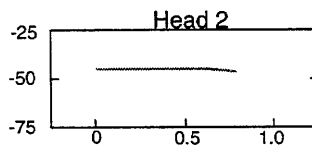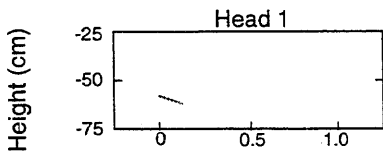
Figure 2.9. Plot of mean elevations of 1996 HLS for each coral head at all sites. The elevations of the heads at each site are located only relative to other heads at the same site and not to those at any other site. At each site, the mean elevation of each head was calculated from multiple intrahead elevation measurements (the head mean). The mean of those head means (the site mean) was then calculated. In the plot, the site means are normalized to zero and the head means for each site plotted relative to the normalized site mean

Mean HLS elevations - site means normalized to zero
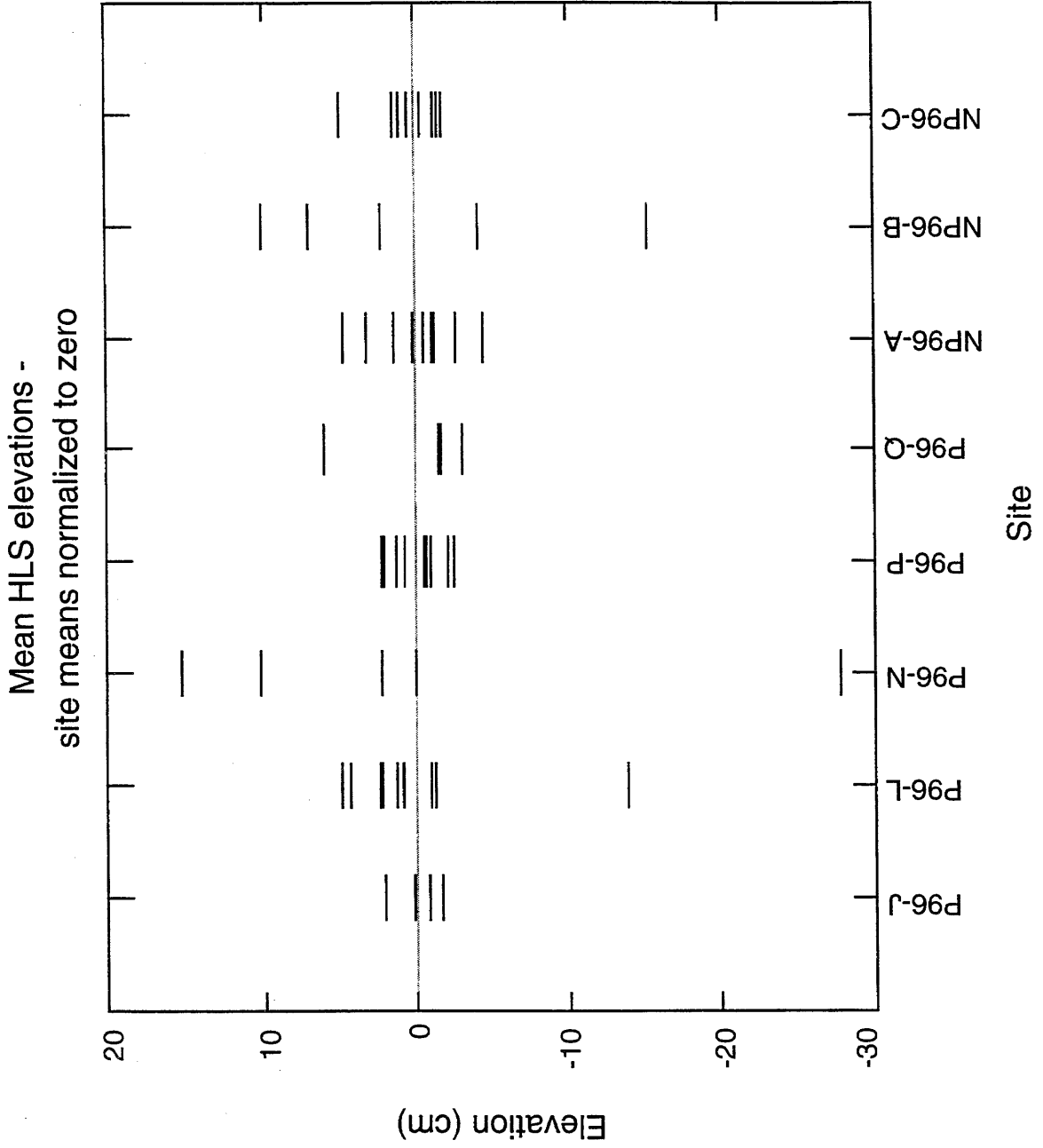
the gauge was left in place recording, the data downloaded once in September 1996. The data from July 1994 and February-April 1996 appear in Figure 1.20 in Chapter 1. Unfortunately, due to an equipment failure, the tide gauge record during the 1996 field season was lost.

The tide gauge was deployed to get an independent record of sea level variations to compare with the coral record. It was also hoped that the tide gauge could be used to correlate elevations between sites throughout the Mentawais. At each site, I measured the elevation of the corals with respect to water level, noting the time of day. I either measured elevations with a ruled stick held between the top of a coral head and average water level, or I measured water level as part of a survey. Clearly this method of measuring elevations involves some inherent uncertainty because the water surges with the influx of waves, and the water level fluctuates. In general, except in a few very rough areas, the uncertainty on water level measurements was about ±5 cm.

Tidal fluctuations prohibit direct comparisons of elevations relative to water level between different sites at different times. The tide gauge, however, provided a timed record of those fluctuations. I used that record to normalize the elevation measurements to a common height and then compare elevations from site to site. I did this in 1994 at sites throughout the Pagais and Sipora. Due to the lost tidal record in January 1996, I could not compare 1996 elevation measurements between sites.

The comparison of modern HLS between sites in 1994 indicates that HLS occurs at the same absolute elevation within a range of ±10 cm (Figure 2.10). This range does not include the contribution of estimated ±5 cm uncertainty in measuring to water level. The range does probably encompass other uncertainties due to phase differences in tidal fluctuations between the tide gauge and sites far from it, localized site characteristics like open beach versus protected bay, or tidal variability from east to west across the islands. The average elevation of HLS in 1994 determined with this method is about 22 cm above

lowest low tide of the month. This is consistent with our observations of living corals exposed by as much as 18 cm above water at low tide during the day in late July 1994.

Morphology of Living Corals

Although HLS elevations of corals of the same age clearly vary by several cm relative temporal changes in HLS might be similar from one coral to the next, if indeed HLS is governed by sea level. In other words, contemporaneous corals might display similar morphologies representing the same relative sea level history. To test this hypothesis, I surveyed cross-sectional profiles of numerous living corals (Figure 2.11). These profiles provide a rough outline of each head's morphology but do not illustrate the full detail and complexity that exists in a coral head. The profile points were chosen to depict the primary elevations and basic shape, but exclude bumps, knobs, and pits caused either by natural growth or by organisms growing or feeding on the surface (e.g. Figure 1.17 in Chapter 1). The profiles do not enable us to link different levels by age. Such correlations require more detailed stratigraphic analyses such as were performed on a few corals discussed later.

I surveyed several living corals at sites P96-P and NP96-C. At site NP96-C (Figure 2.11e), the corals possess a similar gross morphology. Each has the cup shape indicating overall submergence. Each also shows a few centimeters of emergence in the last year or two. On all the corals, the rims of the cups rise about 15-20 cm above well established flats, implying that this site has undergone a recent net submergence of some 20 cm or so. Whether that was a gradual submergence lasting until the emergence of 1995, or sudden submergence several decades ago, followed by stasis, cannot be ascertained from the morphology.

Figure 2.10. Elevations of 1994 HLS of living coral, measured relative to the lowest low tide of July 1994, as recorded by a tide gauge installed in Sikakap Harbor, North Pagai. The average elevation of the HLS was just over 20 cm above lowest low tide, consistent with field observations of living coral exposed as much as 18 cm above water. The variation in living HLS in 1994 corals was ±10 cm (at the 2σ level.)

HLS of Living Corals
Relative to Lowest Low Tide of July 94

Average Height of Living Coral ~ 22 ± 10 cm

Height above Lowest Low Tide (cm)

Coral Samples
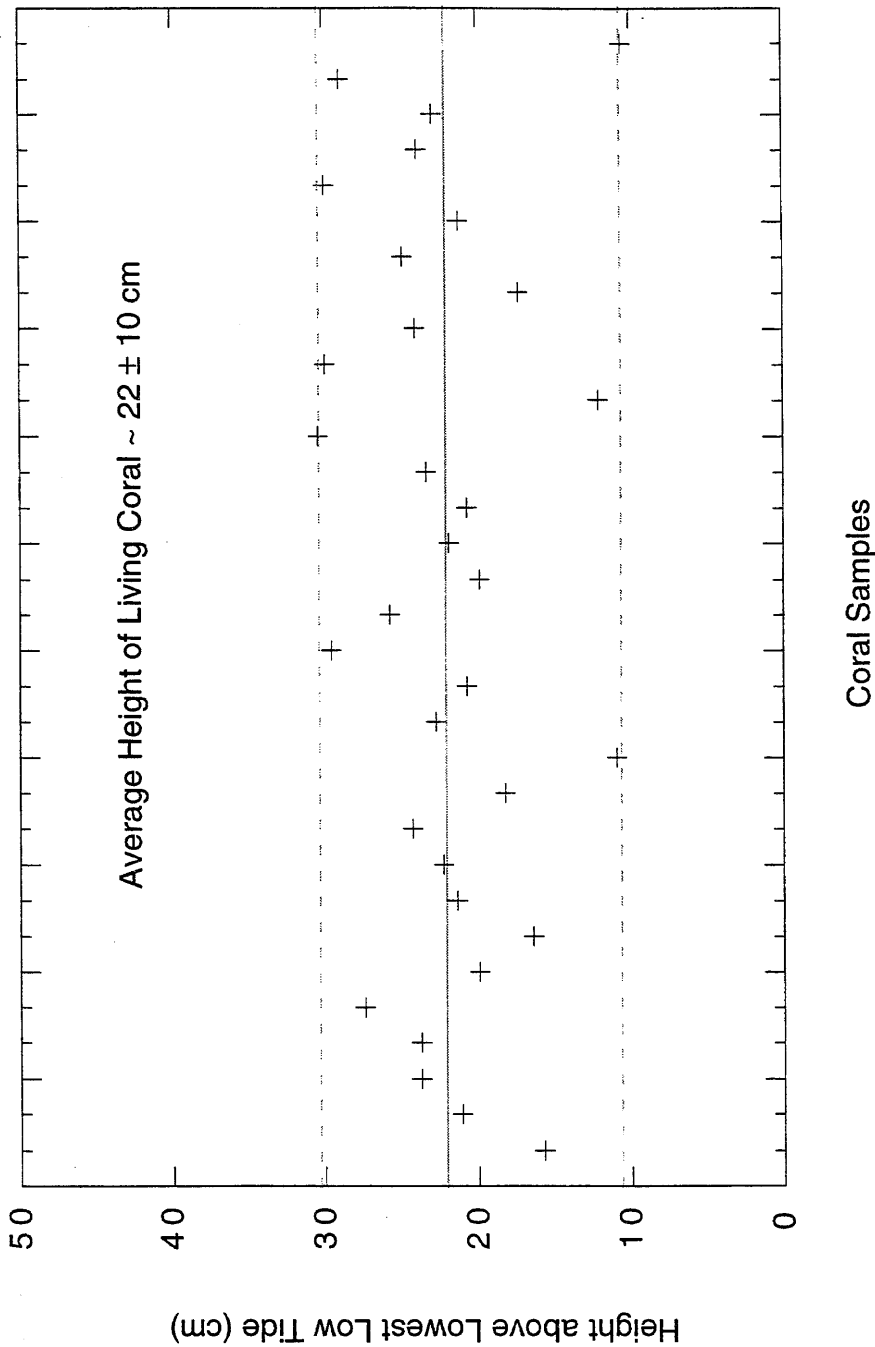
Figure 2.11. Profiles across the tops of living corals at 5 sites. Elevations are measured relative to an arbitrary datum at each site. Elevations cannot be compared site to site. The profiles show only the main HLS surfaces of the coral head and not all the fine scale topography that actually exists on any uneroded head (topography is on the order of 1 to 5 cm of relief.)

a. P96-P - Most of the six profiled living corals show morphological evidence of submergence. Heads L5, L6, and L9 show well-developed raised outer rims, whereas L7 and L8 have smaller, more subdued rims. Only L2 appears to have no rim at all. One possible explanation for this is that the rise in sea level which allowed for the development of a rim in the other heads occurred before L2 had reached HLS, so that it experienced continuous growth and has not been impeded by the exposure that produced the central flat surfaces in the other corals.

b. P96-Q - This head clearly indicates submergence of about 15 cm since the development of the central HLS flat. The rough edges of the rim may indicate several episodes of submergence and stability or even emergence within the period of overall submergence.

c. NP96-B - This head exhibits the "cup" morphology of submergence, with a raised outer rim 10 to 15 cm above the central HLS surface.

d. NP96-A - Both heads at this site have central HLS flats surrounded by raised rims about 15 cm high, again consistent with submergence.

e. NP96- C - The five live corals profiled at this site together offer a consistent record of submergence of about 18 cm illustrated by the raised rims on each head. However, slight variations on the morphology may illuminate the nature of the growth history of the corals or the variations in HLS between corals of the same generation. Possible growth scenarios to explain the morphological differences are presented in Figure 2.12.

123

P96-P

b. P96-Q
water level @ 15:30, 2/9/96
N72W

c. NP96-B
water level @ 16:39, 2/11/96

d. NP96-A
water level @ 14:42, 2/10/96

e. NP96-C
water level @ 14:32, 2/12/96

modern HLS
old HLS - lower
old HLS - higher
old HLS - lower different generation?
substrate
water level
horizontal
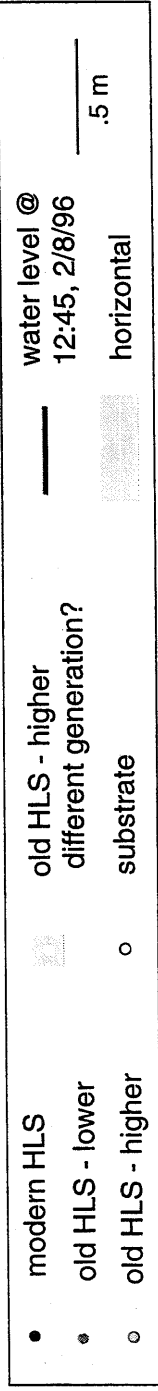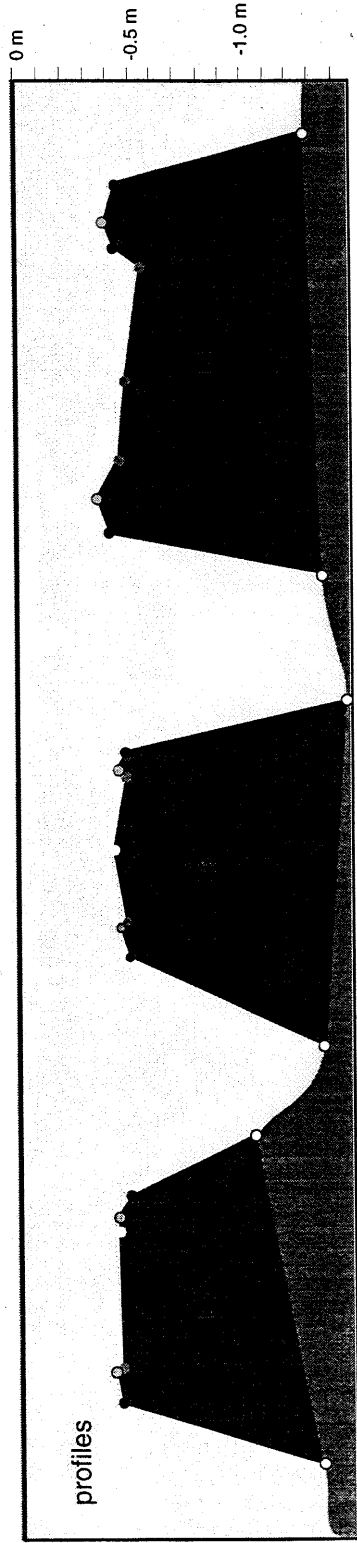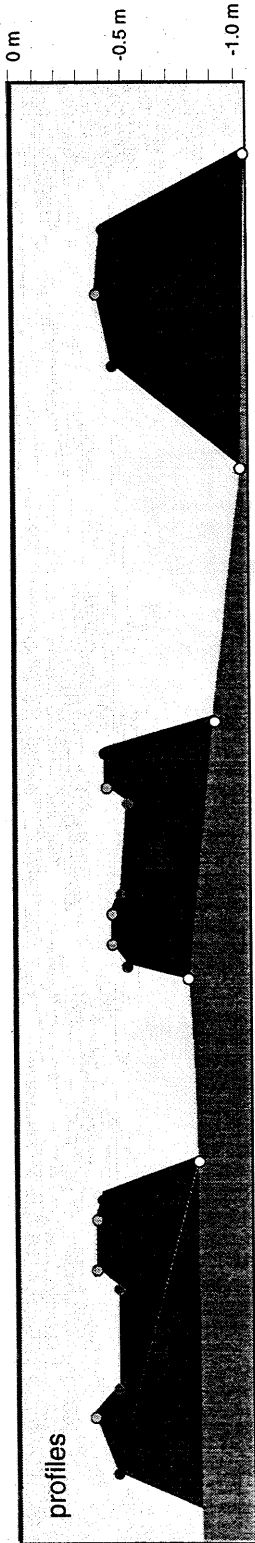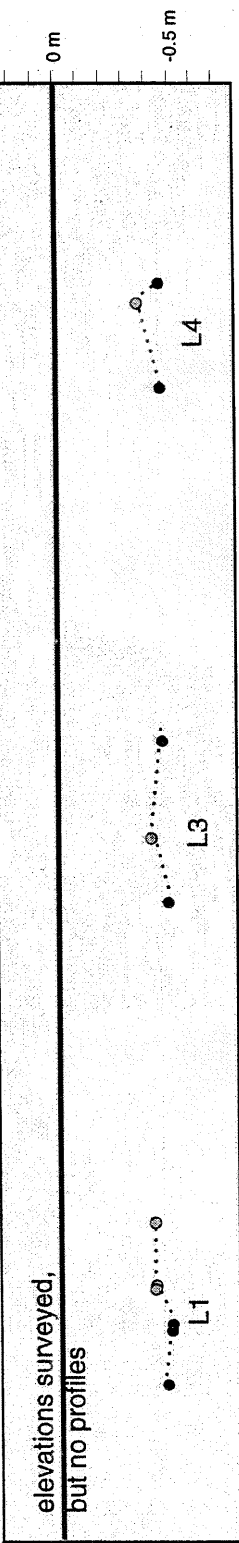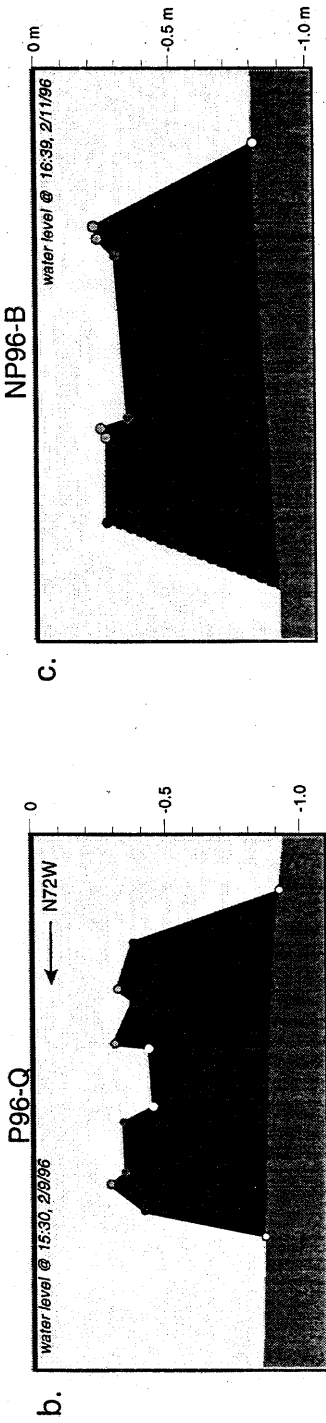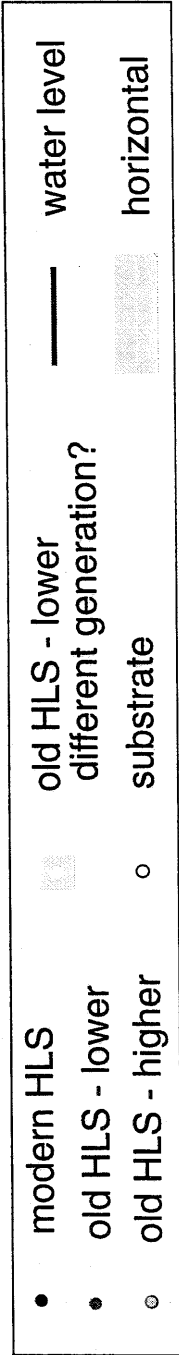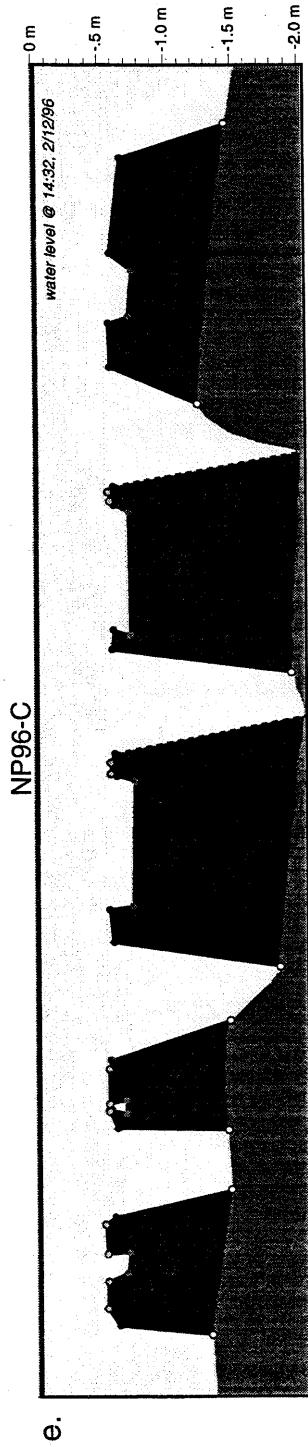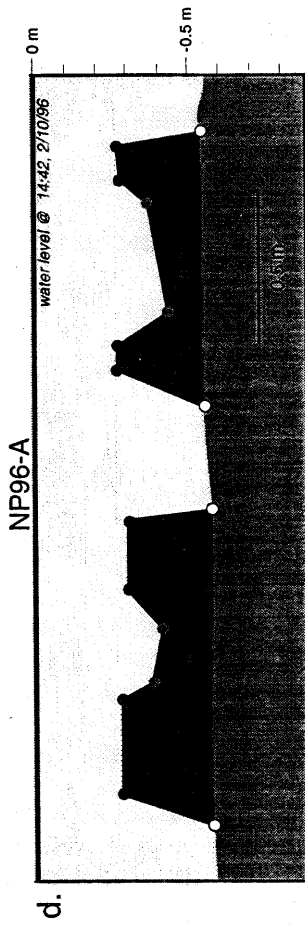
Whereas the depth of the central depression is similar among the five corals, other aspects of the morphology are not. For example, the height-to-width ratio of coral heads L7 and L8 is significantly greater than that of the other three. Likewise, the diameter of the central flat, the old HLS surface, varies dramatically from head to head. The diameter of L8 is just over 10 cm while that of L9 is almost a meter. Possibly the corals L9 and L10 are older and have had a chance to grow out more. L7 and L8 are nearer the shore and rest on a shallower substrate than L9 and L10. If the islands are submerging and the beach is retreating landward, it is reasonable that corals farther out from shore might be older . The site of L9 and L10 would have been denuded earlier than that of L7 and L8, and coral growth could have commenced earlier.

Several scenarios to explain the difference in aspect ratios are possible (Figure 2.12). The presence of a raised rim in all corals implies at least one submergence event in the past few decades. Assume L7 and L8 at NP96-C grew steadily without impingement until exposed at that HLS (time t_2 in Figure 2.12a), where they stayed for some time before submergence freed them to grow higher. At time t_1, they would have only recently begun growth and been below HLS. If L9 and L10 are older, they might have reached HLS at time t_1, and grown only laterally for some time, followed by submergence and further upgrowth until time t_2, when, with L7 and L8, they were again exposed (Figure 2.12b). In this scenario, the corals grew over the old HLS's, rendering them invisible from the outside. Furthermore, they would have reached the recent former HLS about the same time as L7 and L8 (t_2), with all corals remaining at that HLS for the same amount of time. Another possibility would involve no earlier HLS impingement for any coral. Rather L9 and L10, also below HLS at time t_1, would have reached the level of the central flat earlier than L7 and L8, and grown laterally at that elevation longer before HLS submergence occurred and all corals grew upward (Figure 2.12c). Both of these possibilities could account for the different aspect ratios without requiring vastly

Figure 2.12. The morphologies of two populations of live corals at site NP96-C differ slightly. This figure illustrates several possible growth scenarios to explain the difference. (a) is a model of the tall narrow population which is assumed to be younger and grows steadily below HLS until it reaches the main central flat. (b),(c) and (d) are models of the wider population. (b) and (c) have growth rates similar to those in (a), but are assumed to be older. In (b) upward growth was inhibited when the coral reached HLS at time t_1; a period of only lateral growth then occurred, allowing the development of a wider base. The old HLS surface was overgrown by later growth. In (c), the coral had no earlier HLS impingements but reached the main HLS flat earlier than (a) and grew laterally for a longer period before again growing up to form a rim. (d) assumes the ages of both populations are the same, and the difference in width rises from differences in growth patterns, with the (d) population growing with broad, flat bands relative to the (a) population.

a.

b.

c.

d.
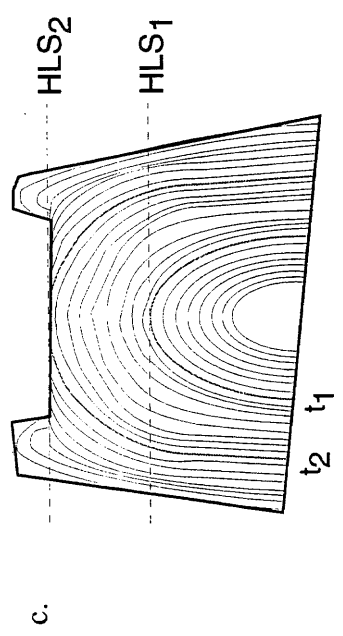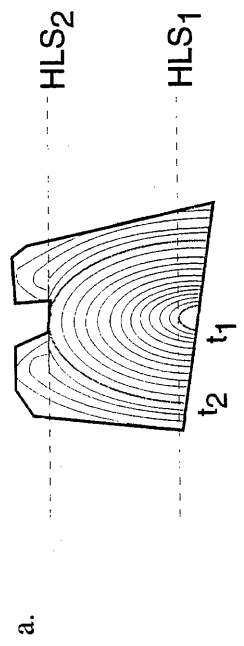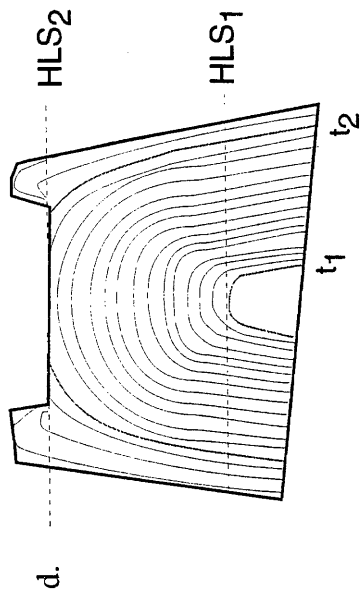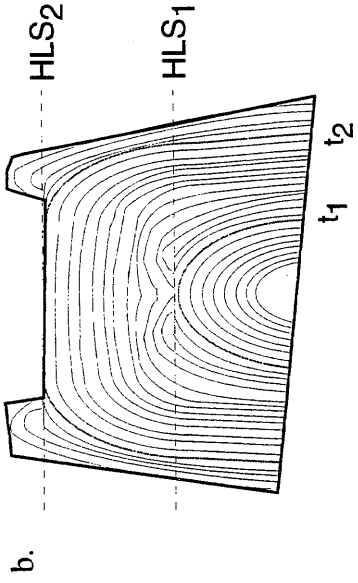
different growth characteristics. Then again, perhaps most likely, the differences could simply have arisen from different growth patterns - L7 and L8 grew faster vertically than horizontally, while the vertical and lateral growth rates of L9 and L10 were more even (Figure 2.12d).

Coral head L6 has yet a lower height to width aspect ratio than L9 and L10 and is farther out to sea. However, the substrate here seems anomalously shallow compared to the others, considering how far it is from shore, and it is possible that sand has simply built up and buried the deeper parts of the coral. Because of the strong possibilities of burial of the substrate below the coral, depth to modern substrate is not a necessarily a good indicator of the true height of the coral.

At site P96-P, the morphology of the corals is still more varied (Figure 2.11a). Three of the six corals surveyed, L5, L6 and L9 have a clear cup shape like those at site NP96-C, albeit somewhat more asymmetric. The depth from rim to central flat in the three corals ranges from about 4 to 16 cm. Coral L7, though almost flat-topped, has the slightest hint of an outer rim , a scant 2 cm above the central flat. L8 has an outer rim, but the top is domed rather than flat, and L2 lacks any rim but has a central peak. The shape of L2 need not be inconsistent with the other corals if it only reached HLS after the last rise in sea level which produced the rims in the other heads. In that case it should record only the most recent die down to modern HLS. The dome in the center of L8 is, however, harder to reconcile with the pronounced flats or slightly sloped central sections of the other corals. If the slight rim on L8 was produced by the same rise in HLS that created the other rims, as it ought to be since these corals are all the same age, then the dome in the center is more likely a product of idiosyncrasies in coral growth characteristics than representative of a sea level variation. Thus L8 illustrates the degree to which corals under the same exposure conditions can vary in their gross morphology.

Surveyed profiles of one or two corals at other sites are broadly consistent with those at NP96-C and P96-P. One live coral at NP96-B showed an outer rim, about 11 cm above an inner flat (Figure 2.11c.). The rim was strikingly asymmetrical, one side being several tens of centimeters wider than the other. Since living corallites existed only on the wide side of the coral, the asymmetry may well indicate that corallites on the narrow side were killed several years before 1996, after the submergence that enabled growth of the rim. This example serves to illustrate that subaerial exposure is not the only thing corals can die from - disease, water toxicity, starfish, chitons, and other scavengers, and burial by sand, can also cause partial or total death of a coral head.

At NP96-A, two living corals each had an outer rim about 10 or 15 cm higher than a central flat (Figure 2.11d.) The diameters of the heads were similar (1 m and 80 cm). However, L8 had a wider central flat and narrower rims than L9. This difference might have arisen because L8 experienced bioerosion which widened the central bowl. Alternatively, the coral rim on L9 may have grown inward over an old HLS flat originally the same diameter as that of L8, while that of L8 did not. It is impossible to tell from a survey look at outer surface morphology alone. However, examination of the interior of the two heads might expose the reasons for the variation. These examples show the value of examining the interiors of coral heads to reveal their detailed stratigraphic history.

The surveyed profiles of living corals illustrate the variation in morphology one can expect to see in corals of the same age growing under essentially the same exposure conditions. This variation constrains the degree to which gross morphology can be used to infer sea level fluctuations. For example, the above observations clearly indicate a rise in sea level some years ago after a period of relatively stable sea level since almost all living corals have a central flat surrounded by a raised rim. That sea level rise was approximately 10-20 cm. It is unlikely that any more precision than that can be obtained with surveys alone. Furthermore, the variations illustrate that, in using this method to

interpret HLS histories of dead coral, one could not, for example, justifiably infer that two fossil corals, one with a 5 high rim over a central flat and the other with 15 cm high rim, represent two different generations of coral experiencing two different submergence events without further substantiating evidence. Only dating the corals could establish that with certainty, while examination of the interior stratigraphy could provide supporting evidence. External morphology alone will not distinguish the sea level histories of two corals with morphological differences on the order of 10-20 cm.

To gain a more quantitative insight into the degree of variation in morphology between corals of the same age, I performed a statistical analysis of all living corals with an outer rim to see what the variation really was in the height of the rim above the most recent flat. The data include both surveyed elevations and those measured with a meter stick. Of course, one cannot know for certain that the older flats are all the same age but given that the gross morphology was similar, I made that assumption. For the 1996 corals, the outer rim sat at 19.4 ± 9.0 cm (error is 1σ), while the recent downdrop from maximum rim height to 1996 HLS was 5.1 ± 1.6 cm. In 1994, the average drop from the highest rim to the next rim down was 11.3 ± 4.0 cm, whereas the drop from the upper rim to the flat was 27.2 ± 11.0 cm. The differences in the heights to the central flat from 1994 to 1996 may reflect the as yet unexplained difference in the observation of an additional interior rim that was so much more often seen in 1994 than 1996. If the corals observed in 1996 had interior rims nonexistent or so muted as to pass unnoticed, then the average 1996 height could simply be a blend of the elevations of the double 1994 rim. The surveys were undertaken only in 1996, so a closer examination of the differences between the two years' observations is not possible.

Summary - Surveys of living corals

Although variation in living HLS height within one coral head is about ±4 cm, variation between heads, both at one site and between sites, is more on the order of ±10 cm. This range in variability approaches the size of significant seismic displacements. Therefore, in trying to determine vertical tectonic deformation from the coral record for fossil corals, it is probably not safe to infer significant sea level changes using only the difference in height between coral heads. For example, it is probably not reasonable to look at two heads of different height and assume they are of different ages and represent different sea level conditions if the difference in height is less than 10 or 20 cm.

The morphology of living corals is broadly the same, in that most exhibit the cup shape of submergence along with a small emergence in the year and a half between July 94 and January 96. Those that do not have such cup shape probably had not reached the HLS represented by the older central flat before HLS rose to its 94-95 level. However, there is variability in the rim elevation and width, diameter of the central flat, presence of a double rim, even the size of the 1996 downdrop on the order of ±10 cm. Again this seems to represent the limit of sensitivity of the method at least on the scale afforded by examining only the exterior of the corals.

2.2c. Coral slabs

The survey results show that although variation in living HLS height within one coral head is about ±4 cm, variation between heads, both at one site and between sites, is more on the order of ±10 cm. Given the variability between heads, it is probably best to focus on the variations that take place within one head rather than on comparisons between heads unless the elevation differences are greater than 20 cm. A more detailed analysis of a given head than that provided by surveys and profiles across the top, could reduce the uncertainty and provide a more detailed glimpse of its sea level history.

Such detailed histories of coral growth can be obtained by analyzing vertical cross-sectional slabs cut through several coral heads. Using annual bands and the shape of the coral head, one can find an annual record of HLS variation without having to rely on the assumption that an old HLS in one coral is coeval with that in another coral. Furthermore, by cutting a slab out of the coral, any hidden HLS surfaces that have since been grown over and are invisible from the outside will be exposed for analysis. Finally, large slabs provide a longer record than hand samples do.

Sampling and collecting slabs

I collected coral samples by two means. Small samples, usually just a small piece from the outermost part of a large coral head, were knocked out with a hammer and chisel. These were relatively easy to collect and I usually gathered several from each site. However, they were usually too small as to provide a record more than 10-15 years long.

The second method was to collect large vertical cross-sectional slabs, representing 40 or more years of growth, with a chain saw (Figure 2.13). The saw, an ICS hydraulic chain saw designed to cut concrete above or below water, was powered by an engine that drove a pump sending high pressure hydraulic fluid along about 100 ft of hose out to the chain saw. The hose length was the limiting factor in gathering samples far from shore. The saw cut by abrading with diamond chips embedded in inch-long metal teeth distributed along the length of the chain. The chain was cooled with sea water pumped into the interior of the chain saw bar with a small water pump and expelled through several small holes distributed around the edge of the bar. The saw bar was 19 inches long, effectively limiting the depth of the cuts to about 15 inches.

To collect a sample, I cut two parallel vertical slices about 10-12 cm apart along a radius of the coral head. At the end of the radial cuts, I made a vertical crosscut

perpendicular to the radial cuts. I either broke the sample out with chisels or cut it at the base with the saw. In many, even most, instances, the slab broke into several smaller pieces upon removal or during sawing. As long as the pieces were relatively few, it could be saved and put back together like a puzzle.

I cut 10 cm-thick slabs so that they would not break in transport. Once back in the United States, I had them sliced into thinner slabs for x-raying with a 36" diameter diamond table-saw blade designed to cut marble tile. This saw was capable of cutting 13" deep into a coral. The thin slabs, 3-10 mm thick, were the appropriate thickness to best bring out the density contrast in the annual bands under x-ray while still maintaining their structural integrity. Because the x-rays show an average density through the slab rather than preferentially sampling one depth, bands are more likely to show up clearly in thinner slabs (Barnes et al., 1989). I x-rayed the slabs with medical x-ray film in a medical facility, and developed them to achieve the highest contrast. Photographic positives were made from the x-radiograph negatives and both were used for analysis.

X-ray analysis of slabs

The x-radiographs of coral slabs show dark and light bands, each pair representing an annual cycle (Figure 2.14). Most annual bands among the corals sampled in the Mentawais are about 1.0±0.5 cm thick. By selecting each pair of dark and light bands, one can effectively draw in the coral's annual rings (Figure 2.14a). In some samples it can be difficult or impossible to distinguish the annual bands. In others, smaller subannual bands of varying shade within the larger bands are not easily distinguishable from the annual bands (Figure 2.14b). Even where the bands are unclear, one can sometimes make

Figure 2.13. Slabbing

a. Set-up for using hydraulic chain saw to collect large vertical cross-sectional slabs through coral heads. Hoses carried hydraulic fluid and water to the chain saw. The saw was lubricated with sea water.

b. Vertical cross-sectional chain-saw cut through a dead coral head..

a.
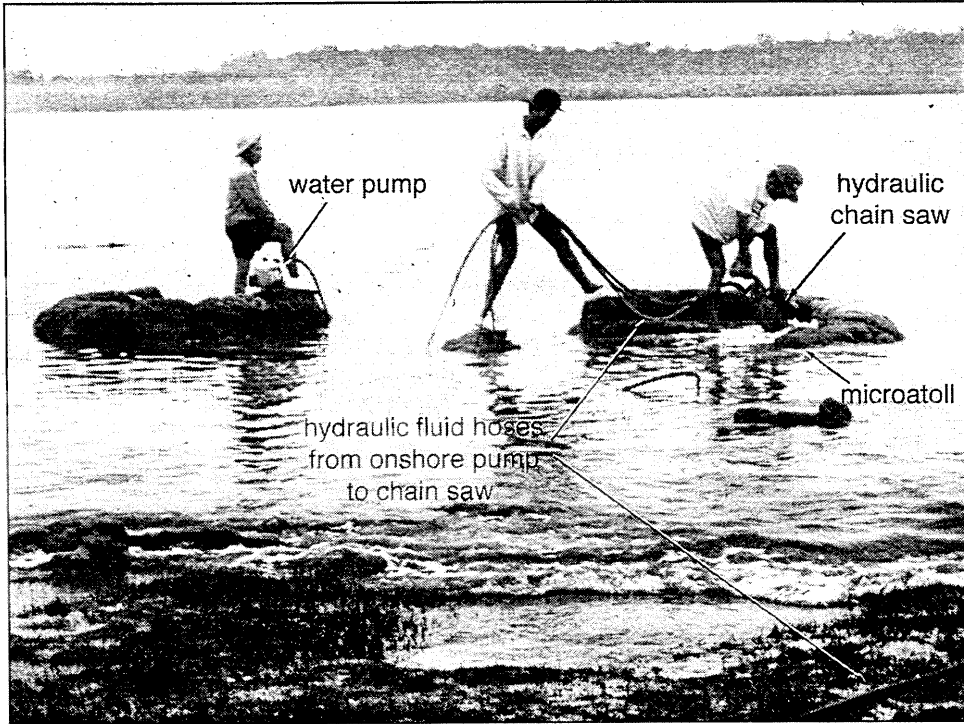
b.
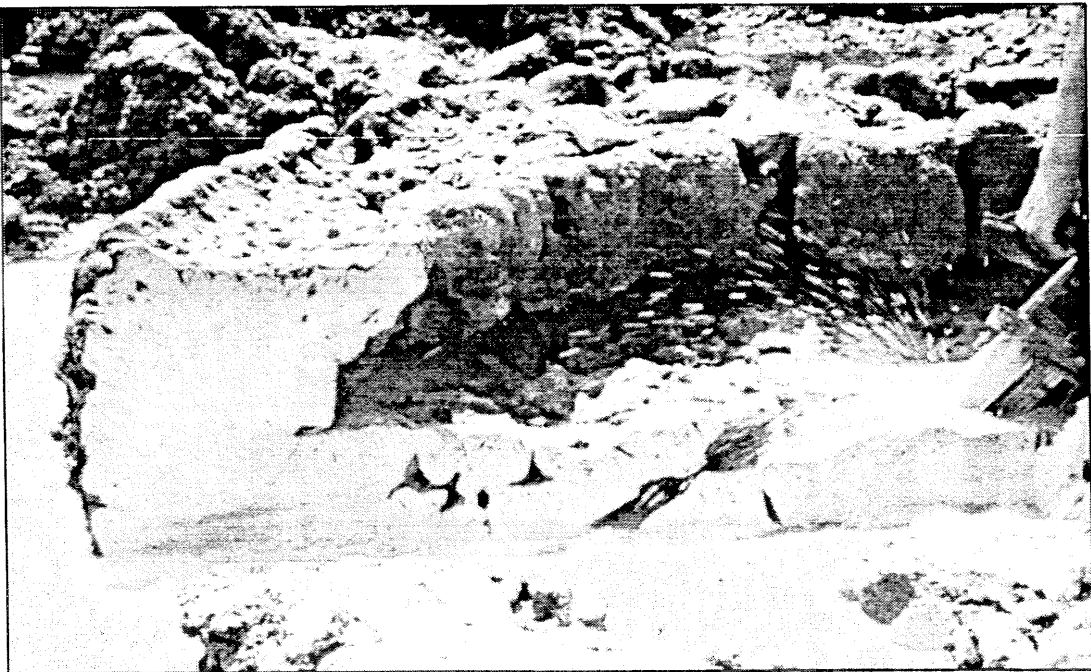
Figure 2.14. X-radiographs of coral slabs revealing annual bands

a. Photo positive of an x-radiograph from a *Cyphastrea (?)* microatoll, illustrates the annual bands caused by seasonal density variations. The lighter bands are denser than the dark bands. The bands, partly traced with pen, serve a purpose similar to tree rings, providing an annual record of coral growth. The degree to which bands are clear and well-defined varies between corals. This coral has relatively clear rings.

b. X-radiograph from a *Porites* microatoll. The annual bands are very indistinct in this coral. Also evident in this sample are smaller subannual bands that can complicate identification of annual banding.

a.
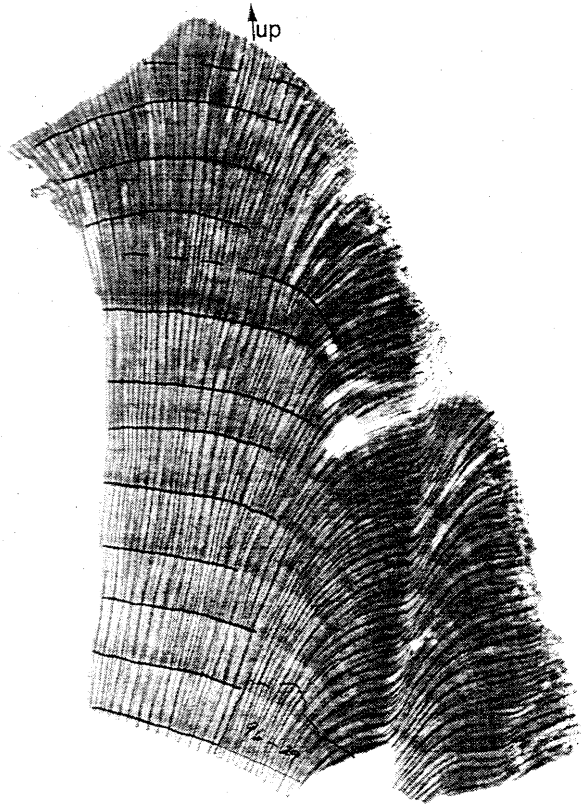
b.
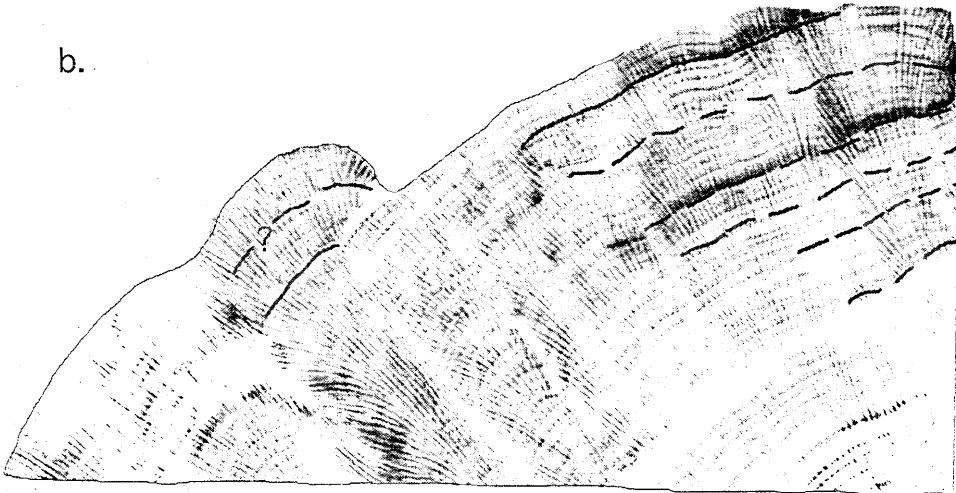
reasonable estimates of their location or at least presence. Often a band will be clear in one part of the slab but fade away in another part. In these instances, especially when the bands on either side are clear, one can reasonably extrapolate the missing band from where it is clear, through the ambiguous section. In cases where there is no partial band, it may be reasonable to assume the presence of a band between two clear bands if the distance between the two clear bands is twice the average distance between other clear bands in the sample. This is based on the assumption that the coral growth rate did not double in one year, and then return to its original growth rate. Clearly the uncertainty in ring counting increases in these instances. Occasionally, the rings are simply too indistinct to be identified with any certainty, and the sample cannot be used for stratigraphic analysis. In most cases, however, the rings are clear enough that one can date the oldest ring in a 50-year sample with an uncertainty of less than about ±5 years.

Sample Sd96-C-1

The analysis of sample Sd96-C-1, cut from a living *Porites* sp. coral head at site Sd96-C on Sanding Island, the small island south of South Pagai (Figure 2.2), provides an example of the coral tide gauge method. The head was about 185 cm in diameter, with an outer rim about 30-35 cm above a central flat and 75 cm above the substrate. HLS in 1995-96 had clearly dropped from the year before, as the top of the living ring was about 5 cm below that of the previous ring at the top of the coral. The sample includes part of the raised rim and associated outer edge of the coral head and a piece of the large central flat.

Stratigraphy

From the x-radiograph (Figure 2.15), I identified and traced the outline of the coral, the annual bands, and any former HLS surfaces or unconformities (Figure 2.16). I assigned each band an age by counting back from the outside ring which was alive in early 1996. The elevations of the tops of the annual bands were measured relative to the top of the outer living ring, to determine how relative HLS height changed with time. Rings that were clipped and impeded from upward growth represent true HLS's. Where there were complete rings, it is clear their upward growth was limited by the coral's natural growth rate, not by exposure, and therefore the tops of these rings are not HLS's. They do, however, provide a record of minimum HLS, since obviously HLS was somewhere above the top of the ring.

An annual ring is composed of a dark (denser) and light (less dense) pair of rings. The dark rings are thinner than the light bands. The outermost, living part of this coral, is light. Since this slab was collected in January, in southern winter, in the latter part of the rainy season, it suggests that less dense growth occurs in that season, and that denser occurs in the drier season. The thickness of this light band is about the same thickness as the light parts of loder bands, suggesting that dense growth may have been about to begin soon after this sample was collected. The small emergence that occurred between July 1994 and January 1996, and which appears in this sample, appears to have occurred during or just prior to the growth of the dark, dense portion of an annual ring. The Cocos record indicates asea level drop in March 1995. If the Cocos drop was the same drop as that recorded in this coral, it indicates that dense growth began during or just after March.

From the drawing of the slab, it is clear that the coral only occasionally reached HLS. During the last 10 or 12 years, represented by the uppermost part of the outer rim, it appears that HLS changed only slightly. However, there were clearly fluctuations during that decade that produced the irregular, saw-toothed surface of the rim. From 1984 to 1985, the coral seems to have been at HLS, and to have produced the small flat surface in

Figure 2.15. Photo positive of x-radiograph of sample Sd96-C-1. This sample came from a coral head living offshore of Pulau Sanding, a small island to the southeast of South Pagai. By counting annual rings and measuring the elevation of the tops of annual bands, one can produce a history of sea level variations at this site during the life of the sampled coral. Flat surfaces, where lateral growth continues but upward growth does not, are usually old HLS surfaces, marking the elevation at which exposure above sea level has prevented further upward growth. The HLS surfaces track sea level, marking its fluctuations in their relative elevations.

raised outer rim

inner living ring

outer living ring

central flat

10 cm

Figure 2.16. Drawing of sample Sd96-C-1 from the x-radiograph shown in Figure 2.15.

Annual bands are drawn in, solid where clear, dashed where uncertain or diffuse. The

lower piece on the right, connected by a small wedge to the higher, outer rim, is a

remnant of an old HLS flat which continued farther into the center of the coral but could

not be reached with the saw for sampling. The tops of the inner and outer living surfaces

are marked "1996." In this interpretation, the two pieces of living ring are not at the same

elevation, perhaps because the interior ring could not grow as fast in the higher water

temperatures that may have occurred inside the central pit during periods of greatest

exposure. In this scenario, older rings are used to determine the horizontal, and the top of

the outer living ring is defined as 0 elevation. By an alternate interpretation, the inner and

outer living rings would be assumed to be at the same elevation, and older HLS surfaces

and ring tops would therefore be tilted slightly outward from horizontal. The former

interpretation is preferred because it is more consistent with orientation of most of the

older rings; the living ring is somewhat anomalous.

Sd96-C-1
Sanding Island

10 cm
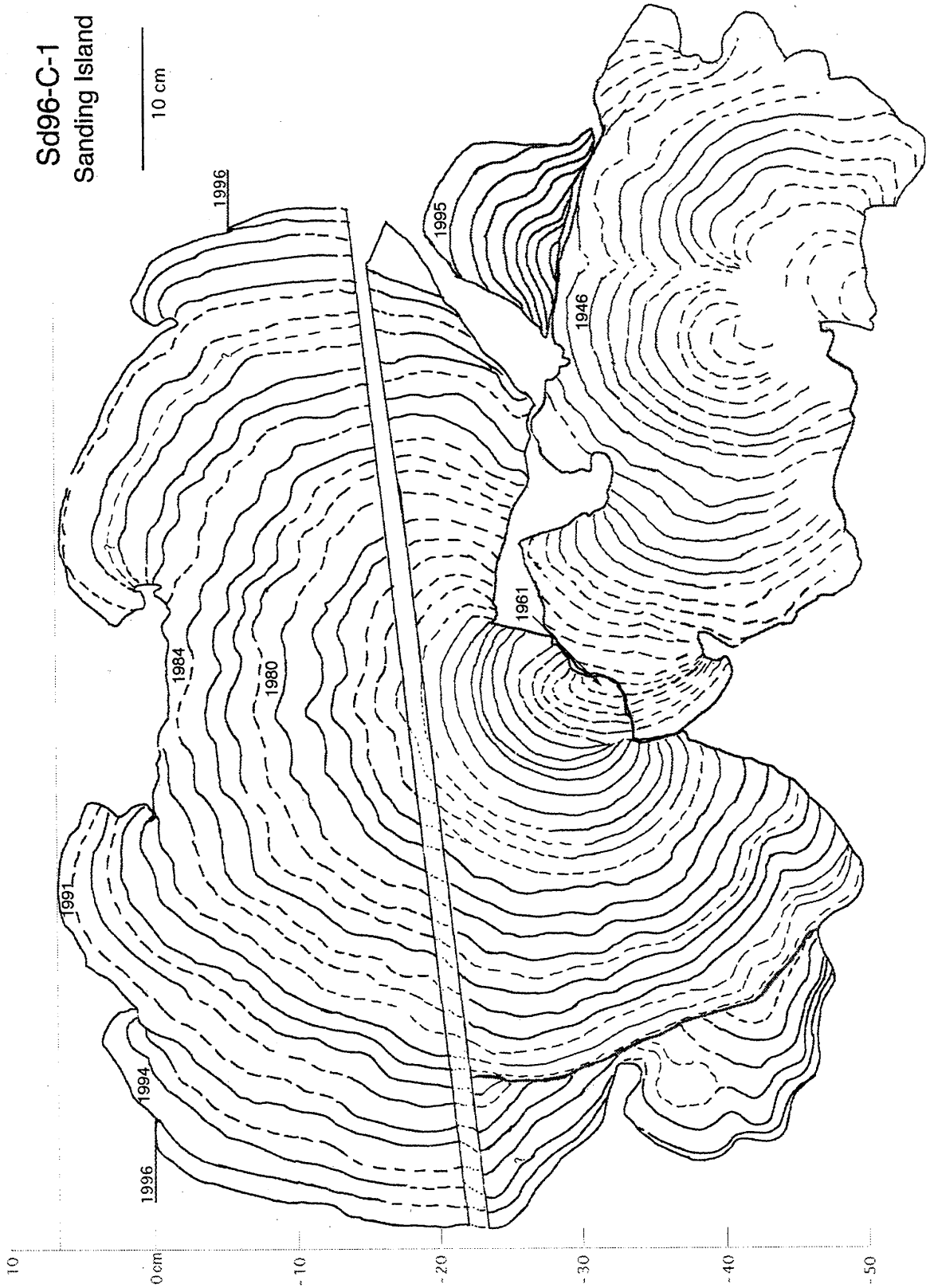
the center of the outer rim. Following that period of stability, HLS rose, freeing the coral to grow upward, which it did until 1992 when it dropped several centimeters, to near its 1985 level. It immediately began to grow up again until 1995, at which time it dropped to the level at the time of sampling.

The last two small emergences occurred when the coral was still below HLS, so there is no record of how large the true emergences were. The distance from the top of one unimpeded ring to the new HLS provides only a minimum measure of emergence. Nevertheless, those minima are rather small, no more than a few centimeters, and it seems implausible that there could actually have been a meter of emergence each time that just happened to clip the top few centimeters of the coral head. It is rather more likely that the minimum values of emergence are close to the real values, and each emergence was in fact only a few centimeters. Furthermore, the previous two emergences were followed immediately by regrowth up above the newly established HLS. There is every reason to expect that the most recent down-drop will be equally short-lived. There have been no earthquakes in the area that might indicate a tectonic source for the emergence.

The HLS behavior represented in the last ten years growth of this sample is consistent with the model of HLS impingement and oceanographically induced emergences and submergences derived from the hypothetical coral grown under Cocos Islands conditions. The hypothetical Cocos coral showed small emergences of 1 to 6 cm every 2 to 3 years under stable tectonic conditions, and every 4 or 5 years under subsiding conditions. Given the Cocos record, one would expect to see the kind of small and short-lived fluctuations in sea level represented by the last 10 years of coral record.

The sea level stability implied by the last decade of coral growth is not representative of earlier parts of this coral record. The 1984-85 growth at HLS was preceded by at least 20 years of growth below and unimpeded by HLS. The majority of the outer rim has no clips by HLS, and, based on the record of the last few years, it is

reasonable to suspect that HLS stayed substantially above the top of the coral throughout the period 1961 to 1984. The presence of the large central flat some 30 cm below the top of the outer rim testifies to significant submergence just before or during these two decades of unimpeded growth. The fact that HLS didn't clip the surface at all in this 20-year period suggests that the submergence may have been sudden rather than gradual, such that HLS rose about 30 cm in 1960 and upward coral growth did not again reach it until 1984. However, gradual submergence at a rate at or slightly above the natural coral growth rate is also a possible explanation. Submergence histories intermediate between these two end members are also possible.

The morphology of the outer rim and the central flat have certain differences that may bear on their accuracy as recorders of sea-level change. As discussed above, the small ups and downs of the coral rings probably reflect annual to subannual tidal fluctuations superimposed upon a decade of tectonic stability or slight submergence. The central flat by contrast is much flatter, with fewer fluctuations. Furthermore, while rings in the outer rim that are at or near HLS seem to taper as they approach the HLS surface, those in the central flat appear truncated where they reach the top of the flat. The most reasonable interpretation is that the outer rim presents a still largely uneroded surface while the central portion has been somewhat eroded to its current flat surface.

It is difficult to tell exactly how much erosion has occurred. The small 1984-85 HLS surface shows signs of slight erosion that has produced small divots in the flat surface, but it has not made significant inroads into the head. Because the erosion is occurring only in the low of the outer rim, it is likely biogenic and not mechanical erosion. The central flat too has probably been eroded primarily through bioerosion since the coral rim continued to grow up above the flat surface, unaffected by erosion. It is likely that the erosion is probably only on the order of a couple of centimeters at most. The growth bands of the outer rim indicate that growth occurred up and over the pre-1961

central flat from the start. It is unlikely that bioerosion removed 30 cm off the top of a high rounded coral in the space of a few years and eroded it to a flat surface over which the continuously living coral could grow. On the other hand, Spencer (1985) and Hudson (1977) have documented erosion of intertidal coral at rates of 1.5 - 6.7 mm/yr. However, sites with high erosion rates seem to occur in areas with more wave action and splash, so rates in the quiet water bays of the Mentawais are probably on the low end of the scale. This suspicion is supported by the presence in the same bays of fossil corals up to several thousand years old that still retain most of their original morphology.

Thus, it is likely that the flat does in fact approximately represent an old HLS surface, with bioerosion muting some of the original topography and perhaps lowering the average elevation slightly. Presumably, the HLS was near that level throughout the five-year period represented by the five truncated rings (1947-1951), although it may have fluctuated up and down as it has in the past decade. It is possible that the original uneroded surface of the flat looked like the younger outer rim. Any interpretation of morphological surfaces should take into account the possibility of erosion having erased some original variability. Nevertheless, in the case of Sd96-C-1, it appears that the erosion has not been great enough to erase the broad HLS history that the slab exposes.

HLS history and submergence rate

Once I had identified the old HLS's, I combined the ages and elevations of the annual rings and HLS surfaces to produce a plot of HLS versus time, which is to serve as a proxy record of sea level versus time (Figure 2.17). I assumed the central flat is a real HLS surface, albeit with uncertainties of a few centimeters in elevation, and used the elevation of the eroded flat as its HLS height. I calculated submergence rates by measuring the slope of the best-fit line through the HLS points. The plot indicates that the

coral head has recorded an average submergence rate of about 7.7 mm/yr. If the HLS represented by the central flat was slightly higher originally, in other words prior to erosion, the average submergence rate would be somewhat less than 7.7 mm/yr. It is possible that 1996 HLS has risen relative to that of 1995, a year of emergence, but is not yet evident in the morphology. This would lead us to slightly underestimate the submergence rate. Nevertheless, the rate calculations are probably fairly accurate since HLS has apparently been hovering around the same elevation for the last decade or so.

It has been suggested that the HLS record of this coral may indicate that submergence has occurred episodically, as sudden submergence events or periods of rapid submergence, interspersed with periods of stability, rather than gradually. If one divides the HLS record into three periods, 1946-1960, 1960-1984, and 1984-1996, one finds submergence rates based on HLS clips of -0.3 mm/yr, 1.3 mm/yr, and 0.0 mm/yr respectively.

The analysis of Sd96-C-1, then, yields the results that the coral has undergone significant and rapid submergence within the last half century at an average rate of about eight mm/yr. Although this was the only live coral head at this site that I sampled and slabbed, a reconnaissance of the area showed that it was representative of the numerous other live corals in the area, most of which had an interior flat about 30-50 cm deep. A few corals had no such flat - without a slab, one cannot know if these had no deep interior HLS surface or if there was one hidden by subsequent regrowth.

Uncertainties

Figure 2.17 shows no error bars. However, there *are* uncertainties in both age and elevation. In Sd96-C-1, most rings are fairly clear but in places the rings are indistinct. The rings near the cores of both the outer rim (about 1960-1970) and the central flat are

Figure 2.17. HLS curve derived from Figures 2.15 and 2.16. The dots show the elevations of actual HLS surfaces; the arrows mark minimum HLS only. the minima are the elevations of the tops of annual bands whose upward growth appears unaffected by HLS, indicating only that HLS was somewhere above the top of the coral in that year. The three oldest measured minima (shown as dots in the figure), from the central flat surface, are represented as minima rather than HLS because those rings are eroded an unknown amount. However, given the morphology of the coral head as a whole, in which the central flat is quite well defined, and the fact that probably only minor erosion could have occurred before the outer rim began to grow up and over the central flat, it is likely that these minima are approximately equal to the actual HLS elevations. This is the curve resulting from using the horizontal depicted in Figure 2.15, in which the interior and exterior living rings are at slightly different elevations. The curve that results from using a horizontal based on the 1996 rings being at the same elevation (not shown) has approximately the same shape but is higher by 1 to 2 cm throughout all but the last few years of the coral's life.

Sd96-C-1
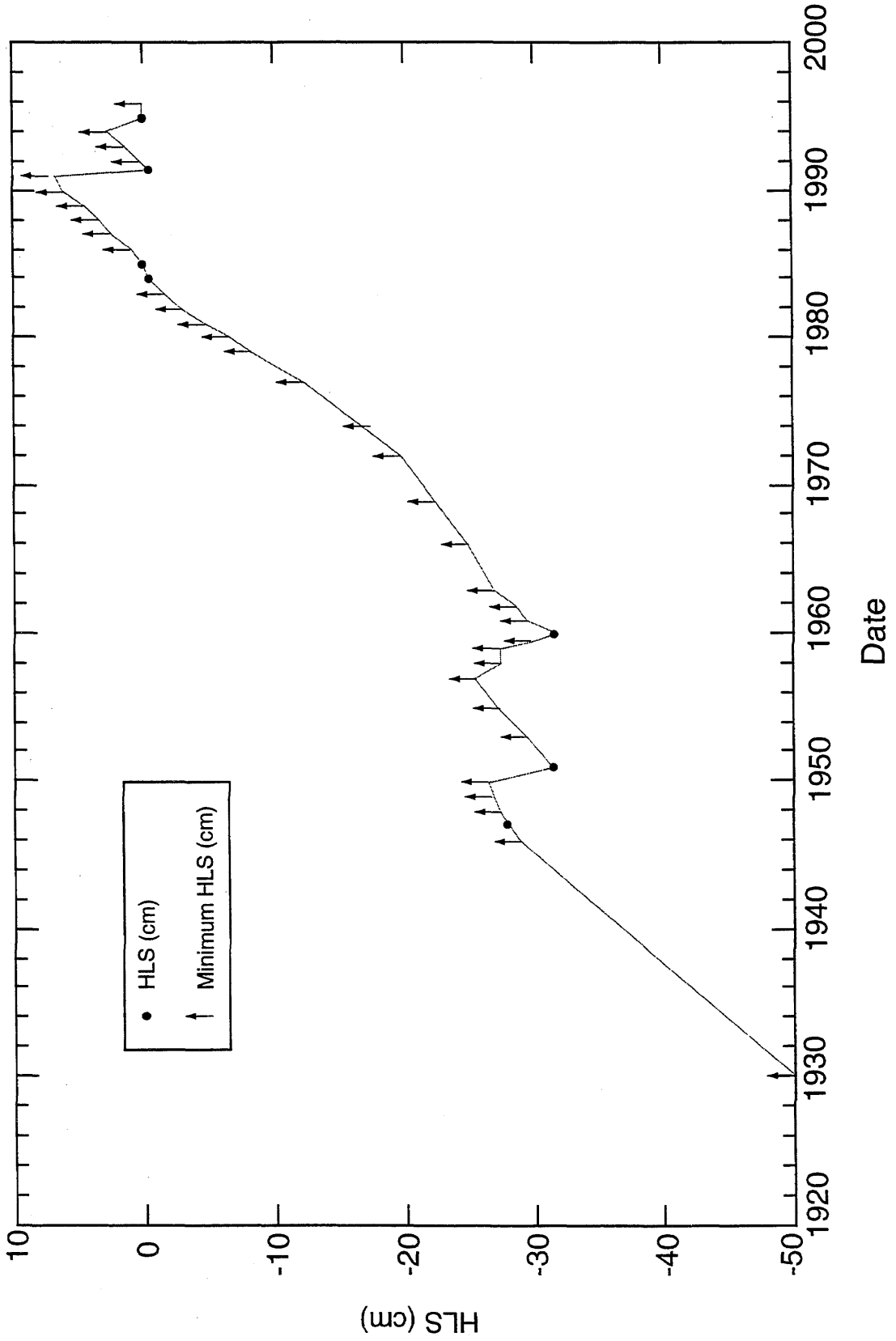
hard to distinguish and may introduce ring errors of as much as ± 50% there. The complication arises because uncertainty in ring identification translates into uncertainty in both age and elevation. A misidentified ring not only skews the age, but all the elevation data are shifted from then on. Nevertheless, in an average 40 to 50 year coral record, the ring uncertainties are less than about ±5, so the sea level histories derived from analysis of the coral slabs are unlikely to be grossly incorrect.

Errors arise in orienting the slab with respect to horizontal. The coral was under water when sampled and, although the top of the coral was marked, horizontal was not recorded. One can estimate horizontal based on the noted flat surfaces and by matching HLS levels, though probably with no better accuracy than ±5°. The variation in horizontal as determined by matching rings of equal age across a flat is a function of the variability in living HLS height, shown by the surveys to be ±4 cm. I estimated horizontal in Sd96-C-1 by using an average of the lines across the tops of annual bands within the last decade, excluding the band living in 1996. I measured elevations relative to the more robust outer living band.

Finally, there is also the uncertainty introduced by erosion, which is not easily quantifiable. Because of the interdependence of age and elevation, and the difficulty in quantifying and combining each contributing error, the overall error is not shown in the plot of HLS history. Nevertheless, a qualitative assessment of those errors indicates that the combined error in most cases will be of order ± 2 or 3 cm in elevation and ±5 years in age in a 50-year sample. These elevation uncertainties are within the same range as those of living HLS heights within one head as determined by the surveys of living coral, about ±4 cm. At any rate they are probably not enough to invalidate the broad conclusions of the analysis, in the case of Sd96-C-1, that the coral and presumably the site has experienced about 30 cm of net submergence within the last 50 years. In the same period,

no major earthquakes have been reported within 100 km of the site (Newcomb and McCann, 1987; Harvard CMT catalogue).

Other living slabs

I performed similar analyses of x-rayed slabs for six other samples collected at various sites around Western Sumatra and South Pagai (Figure 2.2). The morphology of those corals from South Pagai were broadly similar to Sd96-C-1. Each showed the cup shape indicative of submergence, with a central flat surrounded by a raised rim. Each also recorded the most recent five cm drop in HLS that occurred in 1994 or 1995. Detailed examination of the slabs confirms the gross morphologic interpretations and indicates substantial submergence of the sampled corals within the last few decades.

Sd96-A-1

Site Sd96-A was near Stupai Island, a small island about 1 km north of Sanding Island (Figure 2.2). Living *Porites* head corals there all showed signs of a recent 5-10 cm emergence superimposed on a larger older submergence. Some of the living coral appeared to have a tiny (~ 1 cm) upward regrowth implying that HLS had risen again from the low that caused the emergence. The tops of most corals were irregular or rounded rather than flat. Sample Sd96-A-1 (Figure 2.18a) came from a large (2-3 m wide)*Porites* microatoll. Our sample includes only the wide outer rim - I was unable to retrieve a piece of the interior flat, though the base of the sample toward the interior overlay the flat. Therefore, the bottom of the sample gives some measure of the elevation of that old HLS surface.

Figure 2.18. Drawings of slabs cut from living corals at several sites around South Pagai and the west coast of Sumatra. The site locations are shown in Figure 2.2.

Figure 2.18a. Sd96-A-1 - This coral head was located only about 1 km from Sd96-C-1, just offshore Stupai Island, 1 km north of Sanding Island. Only the raised outer rim of this coral could be collected. The bottom, rounded core was attached to the top and outside of a lower flat surface of dead coral, probably a former HLS surface, about 32 cm below the living level. The submergence that made the upward growth above that old flat possible occurred or began probably some time in the late 1940's or early 1950's. The rings at the base of this sample are not clear enough to discern the age more precisely.

Sd96-A-1
Stupai Island

1996

1990

1985

1980 ± 1

1970 ± 2

1960

HLS ?

10 cm
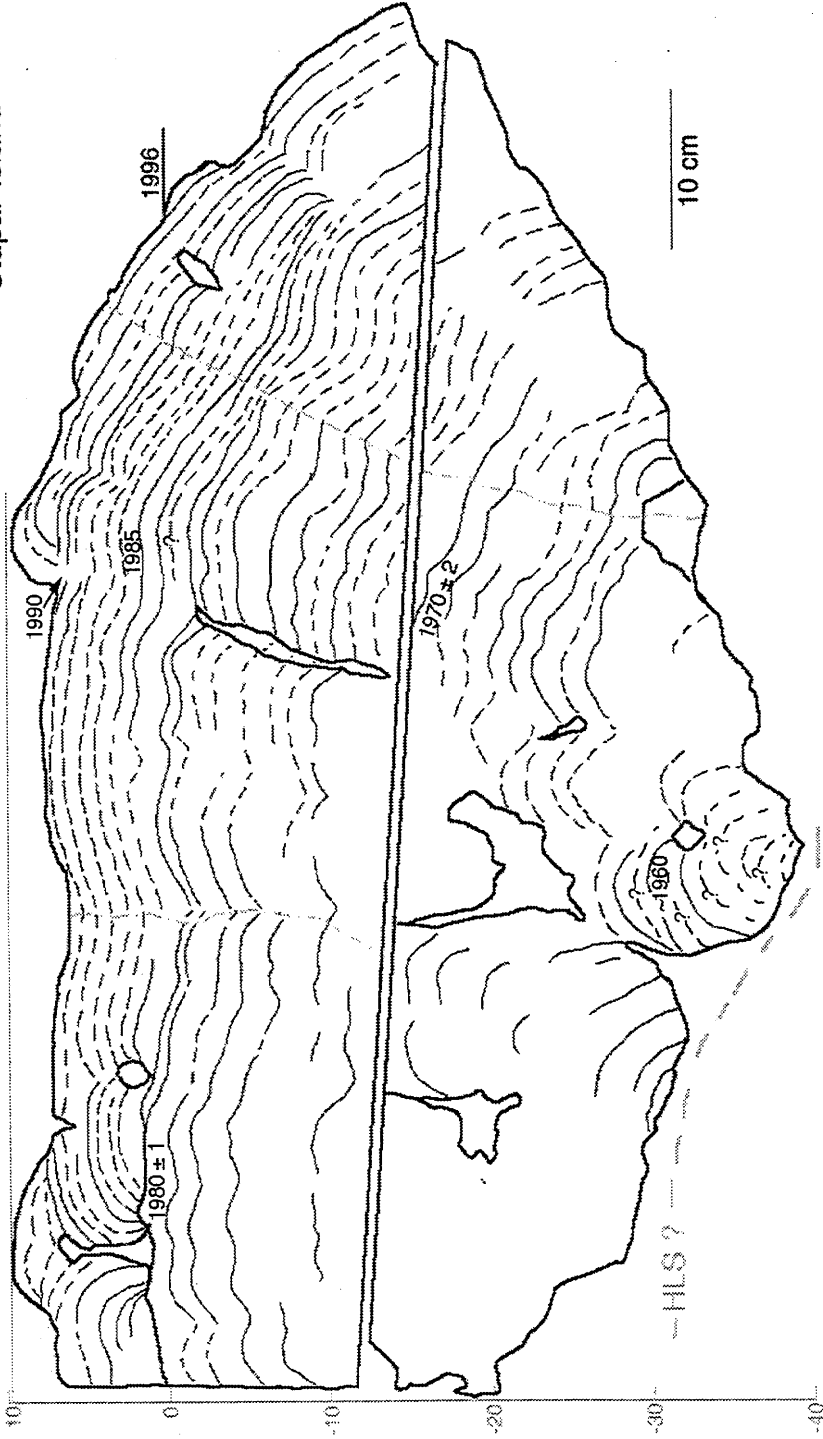
The 1995 emergence was somewhat greater on this coral head than on other sampled corals, closer to 10 than 5 cm. A submergence in about 1991 allowed the development of two small bumps on the otherwise flat rim. The flat top of the rim below these bumps was about 35 cm wide. However, my field hypothesis that this wide flat probably indicated many years of HLS stability at that level was not borne out under close stratigraphic examination. In fact, the flat represents only two years of stability for certain, and was produced primarily because the growth bands in the coral were broad and flat rather than hemispherical. Clearly, then, one cannot necessarily estimate the length of time sea level remained stable by simply dividing the radius of an HLS flat by a reasonable growth rate, as I had originally thought. Determining an accurate HLS history requires stratigraphic analysis of x-rayed slabs.

Like Sd96-C-1, Sd96-A-1 indicates that the last decade of generally constant but fluctuating HLS height was preceded by a period of substantial submergence. Though the rings near the bottom of the sample were indistinct and hard to trace across the sample, there was only one HLS impingement, in about 1981 and 1982 (±2), since about 1951 (±6). Although the lower part of the coral is missing from the sample, it appears that in that year, the coral began to grow upward from about 38 cm below the modern level. Based on field observations of the underlying flat surface, I interpret the bottom of the innermost part of the sample to have been at approximately the level of that old HLS flat. If that was the case, then it seems that the 1951 submergence was immediately preceded by an emergence of about 6 cm from the level of the central flat.

P96-J-3

Sample P96-J-3 (Figure 2.18b) lived next to one of the islands making up the SE South Pagai archipelago (Figure 2.2). The diameter of this coral head was 240 cm, and it

had a rim about 30 cm wide. The top of the coral was about five cm higher than the top of the living ring. The slab from this sample came in three discontinuous pieces - the large outermost rim and two smaller pieces from the interior. Like Sd96-A-1, there was a lower central flat surface below the sample that I could not retrieve. The two smaller pieces of the sample were part of an upper flat surface that had grown over the old HLS surface. Therefore, again I assume that the base of these samples approximates the level of that older HLS.

The history derived from P96-J-3 is similar, though not identical, to that of the Sanding and Stupai samples. A 5 cm emergence in 1995 followed a period of submergence, beginning in 1983, during which the coral grew up about 10 cm from the 1983 HLS. The 1983 submergence occurred immediately after an emergence event of several cm. That the emergence was immediately followed by submergence is consistent with its being caused by oceanographic fluctuations, although a tectonically induced uplift that was rapidly recovered is not precluded. Another HLS clip occurred in about 1982. Prior to that, growth was apparently unimpeded at least as far back as 1955.

The connection of the rim to the central flat was lost from this sample, but, it appears from the shape of the rings from the late 1950's and early 1960's, that they were growing up and over an old HLS about 25 cm below the modern HLS. From the elevation of the base of the two smaller pieces (whose location relative to the larger piece is not precisely determined since there is no direct growth connection, but rather is estimated from field observations of the coral head), one can infer the top of the large central flat to have been about 18 cm below the modern HLS. This in turn implies that an emergence event of about 7 cm occurred between the development of the central flat and the mid-1950's submergence. One can only estimate the age of the central flat to be about 40-45 years old. Furthermore, although it is not clear how much time the flat represents, one can infer from its presence across the whole head, that it was probably greater than one year.

Figure 2.18b. P96-J-3 - This coral head was growing near an island southeast of South Pagai. It records a recent (1994/95) emergence and overall submergence for several decades prior to that. An old HLS surface from the early 1950's was covered over by regrowth in the intervening years. This older surface was not sampled, but its location and age can be estimated from the rim and overgrowth that followed it.

P96-J-3
Siatanusa Island
South Pagai

1996

1990

1982

1980

1967

1955

Old HLS

10 cm

0
-10
-20
-30
-40
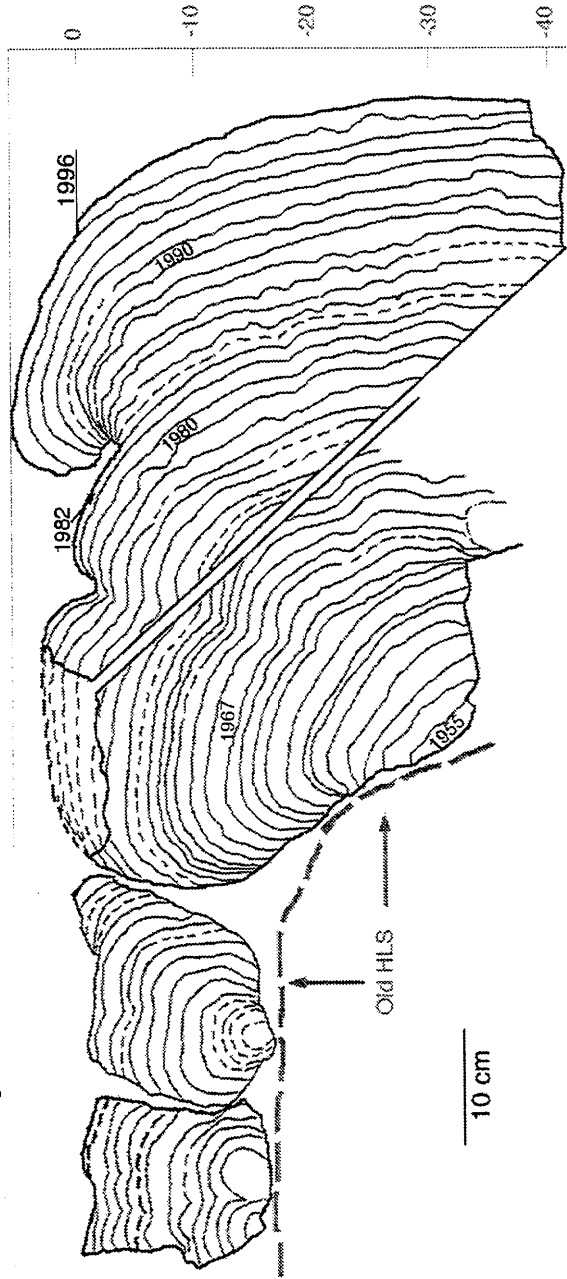
P96-K-2

Site P96-K, also in the South Pagai archipelago (Figure 2.2), contained numerous living and dead microatolls. There was much greater morphological variation among the living corals at this site than others, for reasons still not understood. In the bay where P96-K-2 was collected, the live *Porites* corals had noticeably smaller, lower raised rims than were observed at most other sites. Most were on the order of 5-10 cm above the central flat rather than the 30 cm observed elsewhere. Other genera of coral had higher rims. Similarly, the 1995 emergence signal in *Porites* corals was much subdued, usually only 2 or 3 cm. In another finger of the bay about 200 m farther south (still considered site P96-K), living *Porites* microatolls had much higher raised rims and a slightly greater recent emergence.

P96-K-2 (Figure 2.18c) came from a small *Porites* head, about 92 cm in diameter and about 22 cm high above the substrate. The slab indicates a 1995 emergence of only 1-2 cm. Upward growth was clipped by HLS from at least 1969 to 1975, 1983, 1989, possibly 1994, and 1995. Submergence followed each of the clips in 1976, 1983, and 1989. From 1969 to 1975, HLS was stable at about 9 cm below modern HLS. The sample shows no HLS impingement on growth before 1969. P96-K-2 stands out from the other corals both because its total apparent submergence over the last 30 years is smaller than that of the others, and because the record of the last 20 years shows several HLS interactions, but no emergence events until 1995, just clips followed by further submergence.

The submergence history recorded by this coral is not inconsistent with a sudden submergence event occurring in the 1950's. This event would have affected corals P96-J-3, Sd96-C- and Sd96-A-1 because they had already reached HLS at least once by that time, hence one can see that submergence recorded in those samples. P96-K-2, however,

was probably not alive at the time and thus never recorded the submergence event. If the submergence had been gradual over three decades, the coral might have recorded the later years of the submergence. A sudden submergence would not appear at all. The stability experienced by P96-K-2 from 1969 to 1976 may also have occurred at the other sites, but they did not record it because they had not yet grown back up to HLS.

P96-B-2

Site P96-B was on Siruso Island, at the western entrance of Sikakap Strait (Figure 2.2). Most of the living *Porites* microatolls there had a raised rim about 20 to 25 cm above an older dead flat, with the living ring 3 to 4 cm below the top of the rim. Sample P96-B-2 (Figure 2.18d) came from a small *Porites* microatoll with the central flat substantially overgrown by the outer rim. The slab shows a 3 cm emergence in 1995. The coral was apparently still below HLS just prior to the emergence because the top of the rim does not appear to have been clipped. However, it is thin, and may have been near its upper limit of growth.

The HLS history of this coral, like the others in the Pagais and Sanding, is one of submergence. The oldest HLS impingement that can be dated precisely occurred in late 1980 or early 1981. The HLS surface is unclear in the x-radiograph but stands out in a photograph of the sample (Figure 2.18d- inset). In the photograph, the overgrown older flat appears as a dirty band across the middle of the sample. The old HLS surface then may be only about 15 years old, in contrast to the primary flats on corals at sites Sd96-C, Sd96-A, and P96-J. The establishment of this flat, which apparently developed over one or two years (1980?-1981), was followed by an emergence of about 2-4 cm. From 1982 to 1984, HLS seems to have stayed approximately constant. After 1984 it rose, permitting upward growth of 14 cm over the next 10 years, until the emergence of 1995.

Figure 2.18c. P96-K-2 - This coral came from a site that showed significant variability in the morphology of living corals. It is also shows the most subdued HLS topography of the Mentawai corals. It is possible that this small coral did not begin to grow until after the submergence that was recorded in most of the other Mentawai corals.

P96-K-2
Taitanopo Island
South Pagai

1965

1975

1983

1988

1996

10 cm
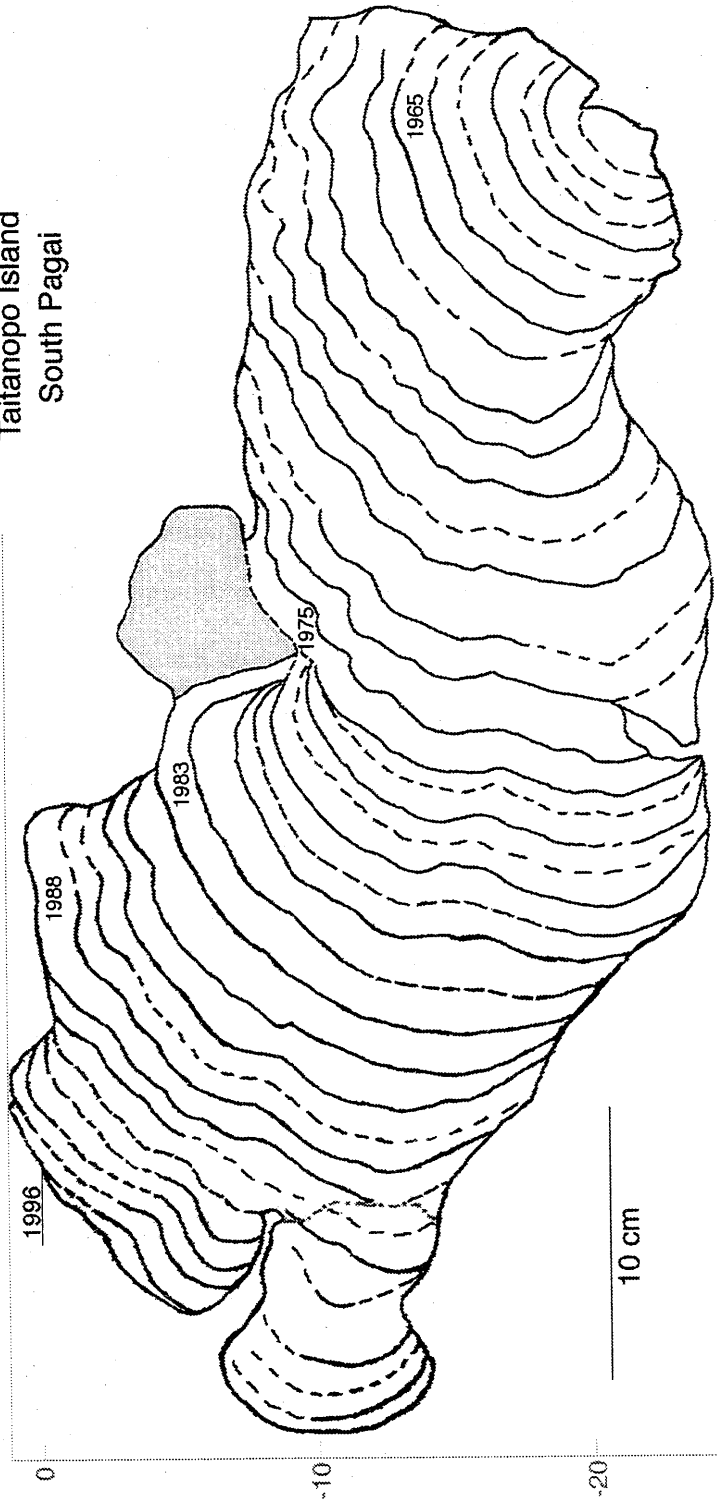
Figure 2.18d. P96-B-2 - This microatoll was one of several similar-looking corals in a bay of Siruso Island, in the western part of Sikakap Strait, between North and South Pagai. It shows, as did the others, a recent emergence of at least 3 cm, as illustrated by the youngest annual band, down-dropped about that much from the top of the head. The most recent bands form a high rim around the lower flat surface that occurs about 10 cm below the living level.

P96-B-2
Siruso Island
South Pagai

1996

1990

1980

1970

10 cm

Old HLS surface?
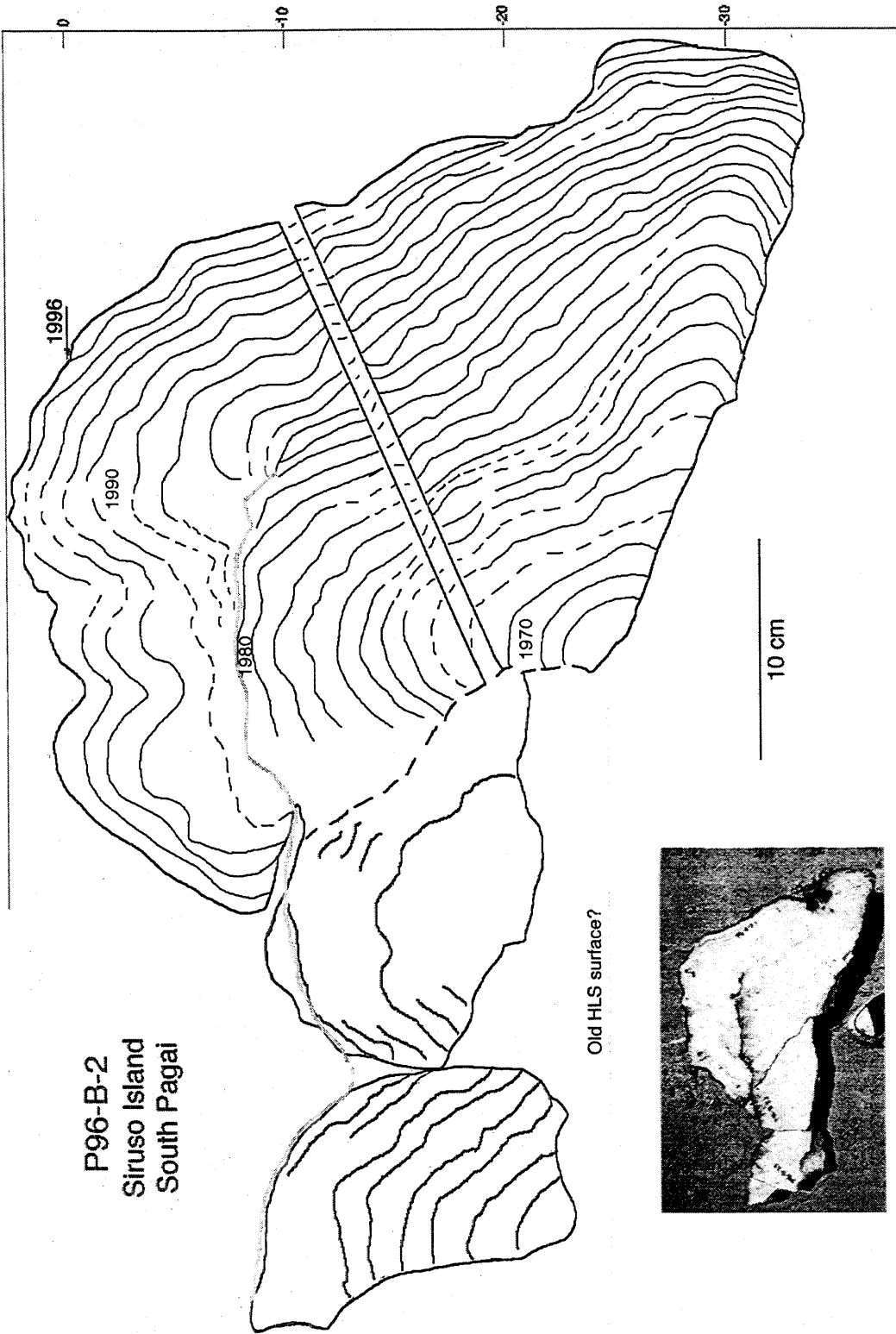
The HLS record in this sample only goes back to 1980. Prior to 1980, growth appears to have been unimpeded by HLS back to at least 1968. There is no record of an earlier HLS, but the shape of the oldest rings, which curl up and over the missing part of the head with a tight radius, is similar to that of rings growing up and over an old death surface. Perhaps not far below where this sample broke off, maybe 30 cm or so down, there is an older HLS surface that could be the contemporary of the 1950's flats in most of the other samples. The 1981 HLS clip and emergence would then be of the same vintage as the early 1980's clips observed in Sd96-A-1 and P96-J-3.

T96-A-1 and T96-A-2

These two samples came from the same site, within 50 m of each other, on the small island of Tikos, just west of the Sumatran coast near Bengkulu (Figure 2.1). The island is about 210 km from the subduction-zone trench. Most corals were not more than 30 cm high, even when several meters in diameter, in contrast to the numerous corals of similar diameter in the Mentawais that were 1 m tall. Almost all were noticeably flat topped, with only 2-4 cm of relief across the surface. All showed the same 1994-1995 emergence of a few cm observed in the corals of the outer-arc islands. Many, though not all, had a small raised ring, about 2-3 cm high and 2-4 cm wide, a few centimeters in from the living ring, as if a short period of submergence had preceded the 1994-1995 emergence. The living ring in these cases was at about the same elevation as the interior flat surface inside the raised annulus. The moderate thickness of coral heads combined with the lack of substantial rim development suggest that sea level (HLS) had been much more stable at this site than at the sites on the Mentawai Islands.

Stratigraphic analysis of the two slabs bears out the contention that submergence on Tikos Island has been slight to non-existent over the recent past. Both samples came

from the outer edge of essentially flat *Porites* microatolls. Their records are unfortunately short, but they show more impingements on the surface by HLS in that short period than do the Mentawai coral records.

T96-A-2 (Figure 2.18e) came from a flat-topped coral with a raised annulus inside the depressed living ring that is about 4 cm above the central flat surface. About 4 cm of emergence in 1994 are recorded in this coral, so the living ring is at almost exactly the same elevation as the central flat, a typical morphology at this site. The first ring in this sample to interact with HLS was the 1980 ring. HLS from this point on remained stable for about six years. The raised annulus developed after a submergence event in about 1986 permitted new upward growth. With two minor HLS clips in 1988 and 1990, the coral again reached HLS in late 1992 and remained there until the small emergence of 1994. Since the 1994 emergence almost exactly recovered the 1984 submergence, this coral shows reveals evidence of little or no net vertical displacement over the past decade and a half.

T96-A-1 (Figure 2.18f) has more subdued topography, than T96-A-2, although its gross morphology in the field did not seem remarkably different. A similar 4 cm emergence in 1994 was preceded by only minor fluctuations of about 2 cm or less back to the mid-1970's. The level of the coral remained above its 1996 level throughout this period. Prior to about 1974, the bands appear truncated and the surface slopes gradually toward the interior, suggesting that perhaps erosion hollowed out the center of the coral slightly. This coral record does not indicate a distinct submergence event occurring in 1986 like that in T96-A-2. There is a small submergence that occurred in 1984, but it was slight, and apparently merely recovered a small emergence of about the same magnitude earlier in the same year. Small fluctuations of less 1 cm or less in HLS elevation dominated the record from 1984 to 1996.

Figure 2.18e. T96-A-2 - This microatoll from Tikos Island grew within a few tens of meters of T96-A-1. This was a large, flat-topped coral head, with a slight raised rim just inside of the down-dropped living ring. Although it has a more well-developed raised rim than T96-A-1, it too yields a record of stable sea level.

T96-A-2
Tikos Island,
Western Sumatra

1979
1970
1961
1984
1992
1996

10 cm
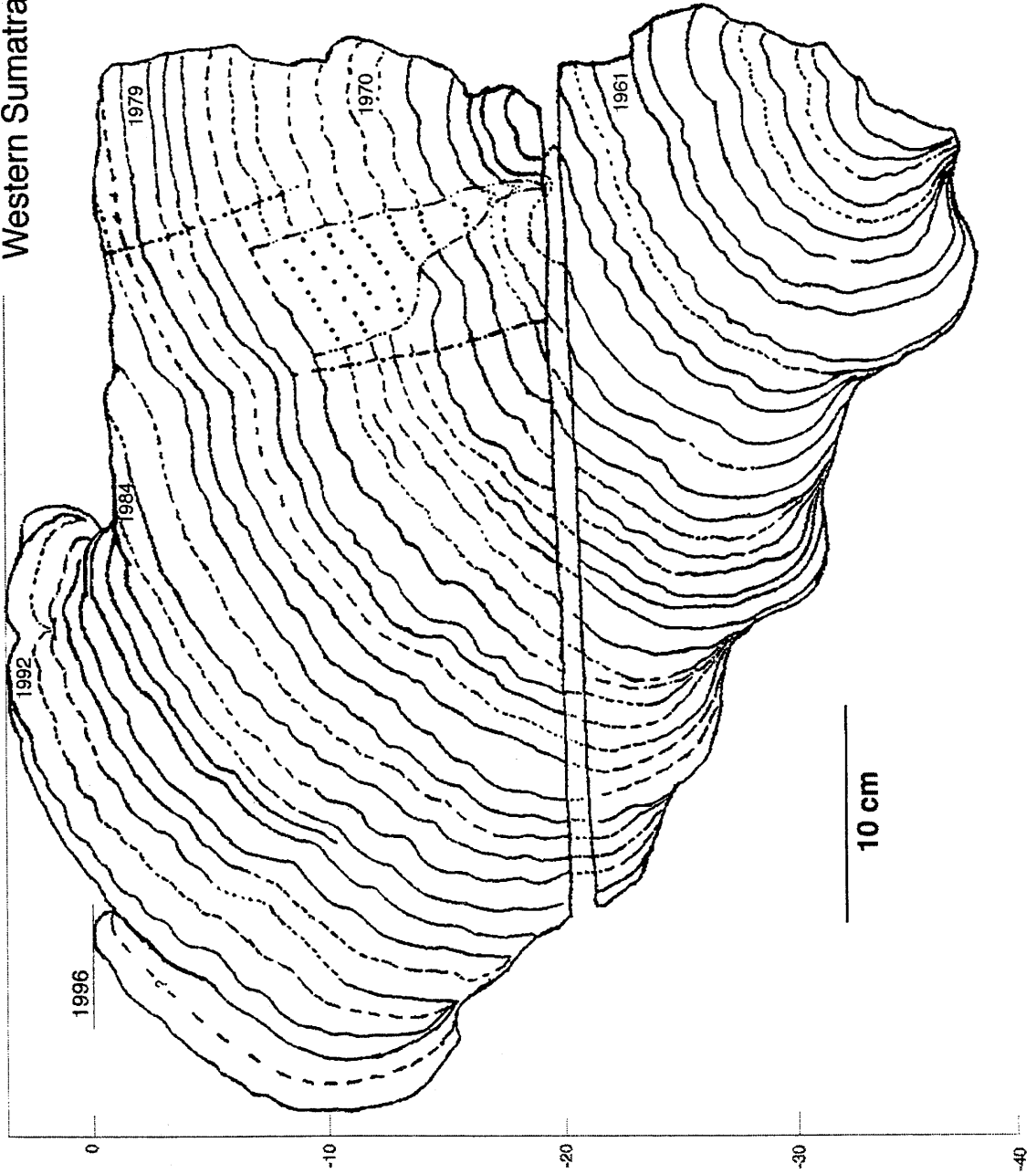
Figure 2.18f. T96-A-1 - This coral came from Tikos Island, a small island a few km west of Bengkulu on the western coast of Sumatra. The coral and this sample were flat-topped and have numerous HLS impingements that imply sea level stability.

T96-A-1
Tikos Island
Western Sumatra

10 cm

1996
1991
1986
1982
1971
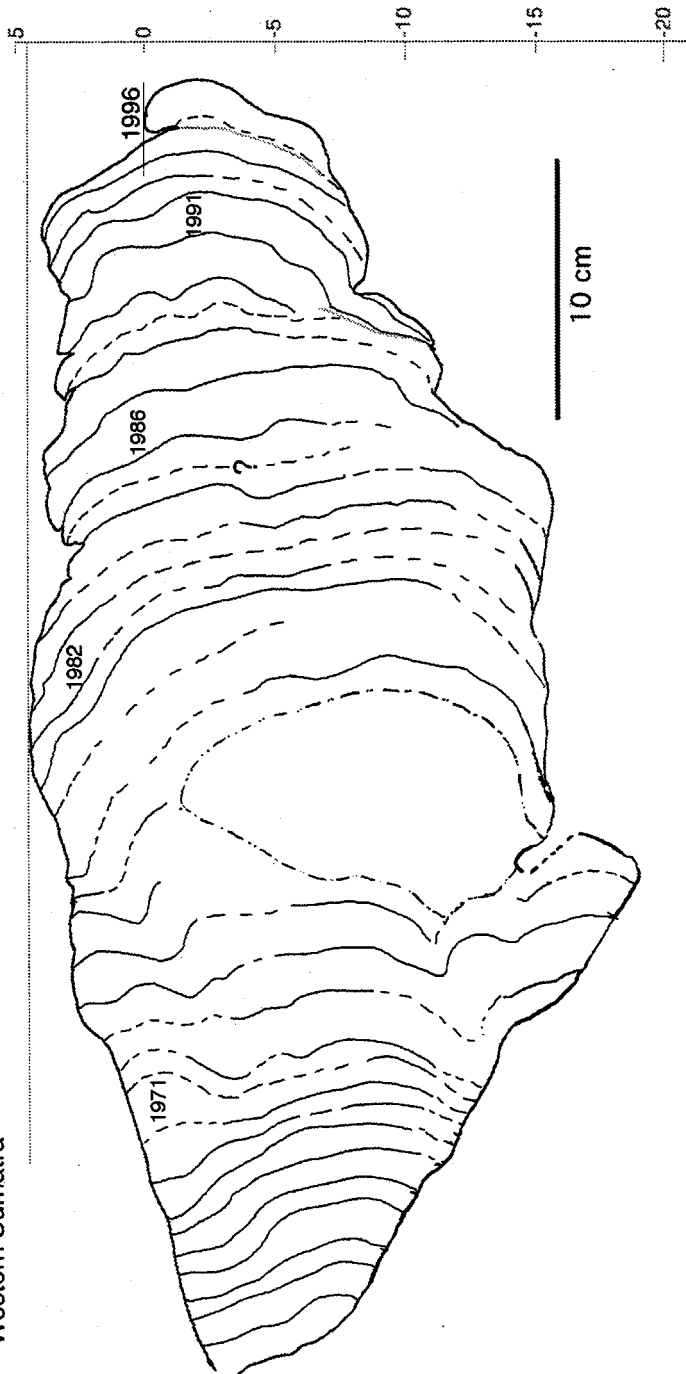
HLS histories

Plots of relative HLS elevation versus time for these six slabbed microatolls are presented in Figure 2.19. Again, the dots represent actual HLS clips, while the arrows represent the elevations of the tops of the growth rings, indicating that HLS was somewhere above these elevations. As with Sd96-C-1, most of the other slabs from South Pagai were clipped by HLS only rarely, as appears to be consistent with a rapidly subsiding coral. And, most corals that were impinged upon by HLS were affected for only one or two years before growing freely again. The rings of the past decade show more HLS clips than in previous decades. Plotting the sea level curves for each coral together illustrates the similarities and differences best (Figure 2.20.) All the curves show the latest drop in HLS, though the size of the drop is noticeably greater in Sd96-A-1 than in the others. And all show an HLS impingement in about 1981. Slight differences in the dates may be due to errors in ring identification, so impingements recorded between 1980 and 1983 may represent the same event at all sites. Or the differences could result from the fact that small HLS changes (< 5 cm) may not be recorded in the coral for a couple of years after the change (Taylor et al., 1987). HLS history between 1981 and 1995 varied somewhat from site to site. For example Sd96-C-1 had an emergence in 1991 or 1992 that did not appear in the other corals, including Sd96-A-1 which comes from a site only a few kilometers away. Sd96-A-1 shows an HLS clip at that time but no clear emergence. It is most likely that the 1992 emergence in Sd96-C-1 was due more to the individual characteristics of growth and sensitivity to HLS unique to that coral than that it represents a tectonic event localized in the 1 km around that site.

Submergence rates

I calculated average submergence rates for each head based on the plots of HLS elevation versus time (Table 2.2 and Figure 2.20). The first estimates were made by calculating the slope of the best-fit line through only HLS points, the elevations of actual, uneroded HLS surfaces. The rates range from emergence of 0.9 mm/yr on Tikos Island to submergence at 9.5 mm/yr at site Sd96-A, near Sanding Island. Focusing only on HLS and ignoring the minimum HLS data may distort the true rate of submergence by preferentially excluding high HLS's that are not explicitly recorded in the coral. Therefore, I also calculated submergence rates using HLS's and minima combined (Table 2.2.) By and large, this calculation yielded rates higher by less than a millimeter per year.

How accurate are the rates? An absolute test would require that they be compared with geodetic or tide gauge data, which are not yet available for these sites. However, one can make an internal test by comparing corals. T96-A-1 and T96-A-2 come from coral heads only a few tens of meters apart. Any sea level variations, whether oceanographic or tectonic in origin, should have affected both corals equally. Therefore, any difference in the records between the two must be explained either through measurement errors and uncertainties, by internal coral growth characteristics unique to each head, or by movement of one of both of the heads.

The broad sea level interpretation from this site, that sea level has remained largely constant over the past several decades, is fully supported by stratigraphic evidence from both of these corals. But there are noticeable differences between the two corals. The main differences are the difference in their submergence rates and the evidence of submergence in 1984 that appears clearly in T96-A-2, but not in T96-A-1. The rates differ by about 2.3 mm/yr. That discrepancy could arise from errors in establishing horizontal, distinguishing rings, or slight erosion of the surface. With such limited relief anyway, even small errors of this nature could have a large influence on the estimated submergence rate. The elevation differences that generate the submergence rate are less

Figure 2.19. Sea level curves derived from analysis of slabs shown in Figure 2.18. Figures 2.18a-d are from the outer-arc islands and all indicate submergence at various average rates for the last few decades. T96-A-1 and T96-A-2 are from Tikos Island, near mainland Sumatra and south of the Pagais. Their HLS's have remained at approximately the same elevation throughout the period represented by the sample, and support an interpretation of relative sea level stability at Tikos Island.
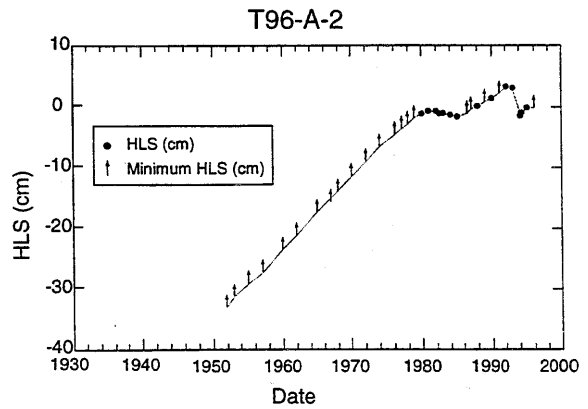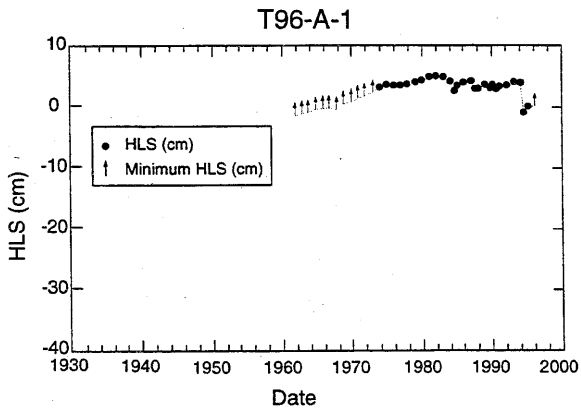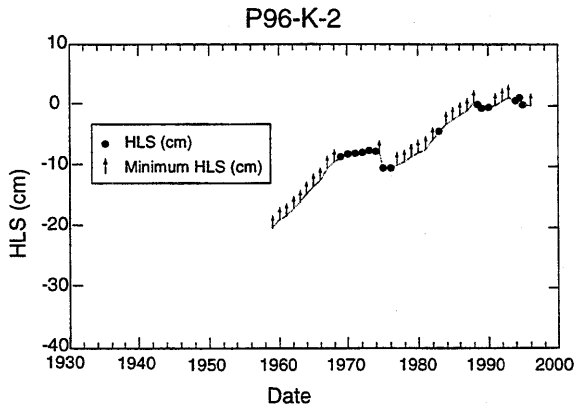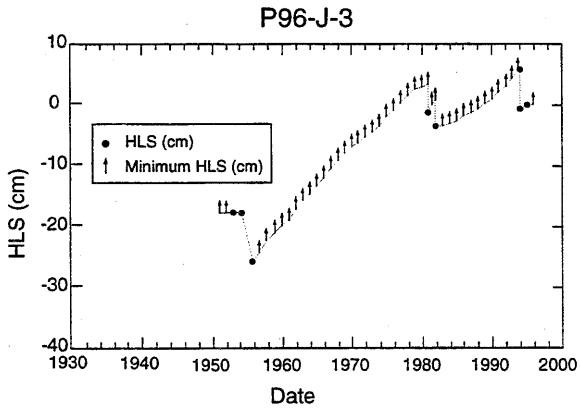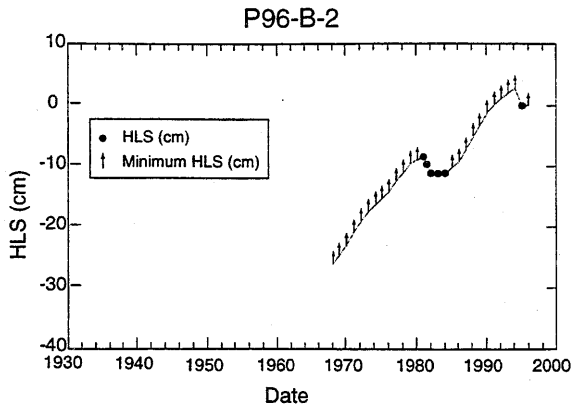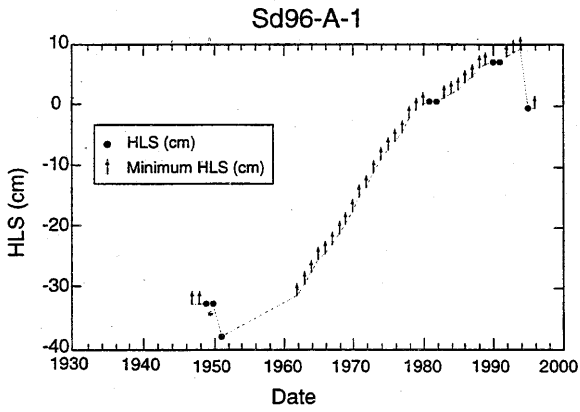
Figure 2.20. The sea level curves of Figures 2.17 and 2.19 plotted together. The dates are

the same for all curves. There are no absolute elevations available for these samples. The

points plotted are relative elevations of actual HLS impingements on the coral's upward

growth. The lines run the through the minimum HLS defined by the tops of unimpeded

growth bands. Also shown are the submergence rates calculated from the curves using

only the HLS points. These and the submergence rates derived from the HLS and the

minima are shown in Table 2. The samples from the islands have rates between 4 and 10

mm/yr. The samples from the Sumatran coast show little or no submergence.

Modern Submergence Rates
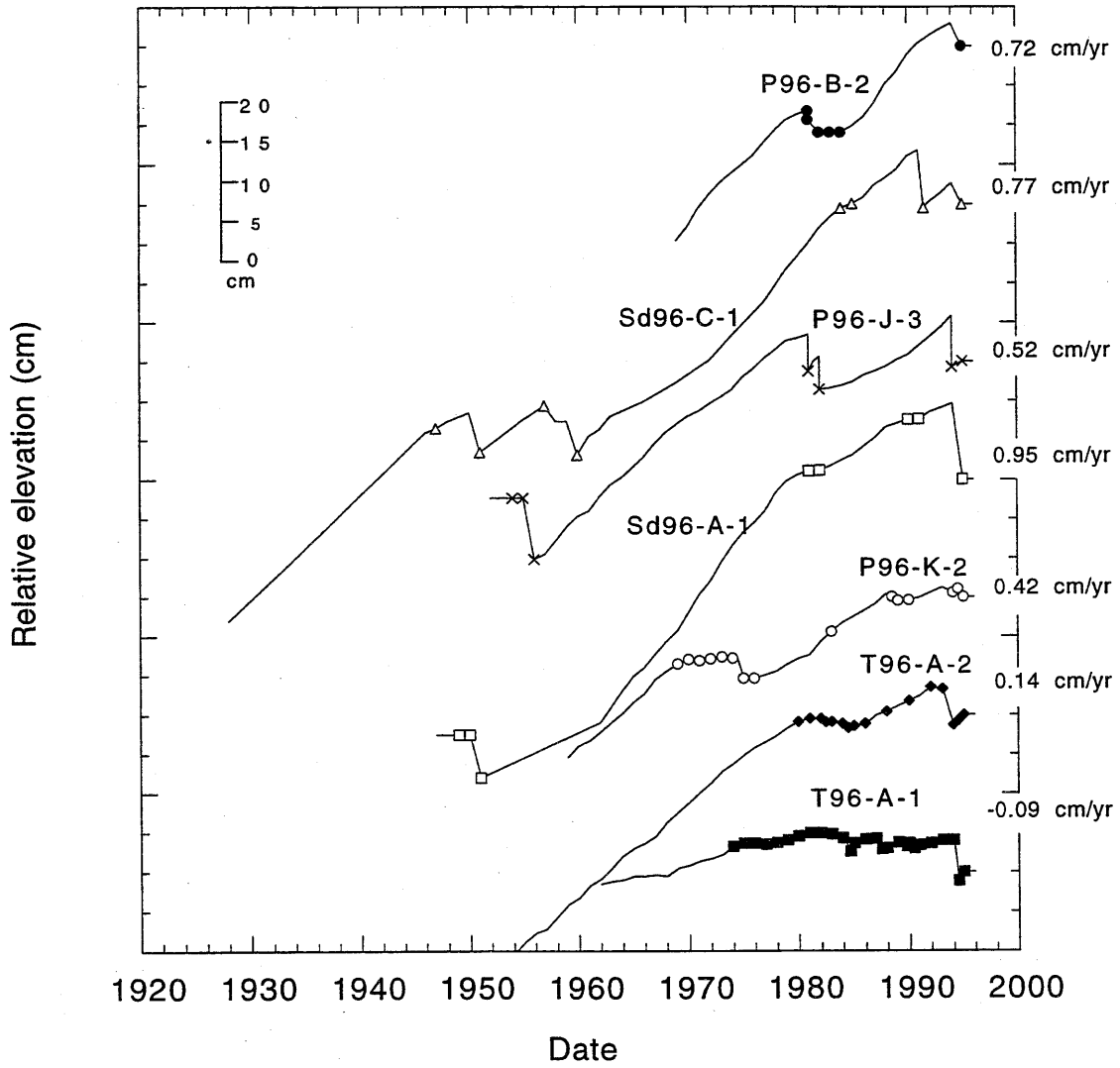
Table 2.2

Table of submergence rates derived from stratigraphic analysis of cross-sectional slabs cut from coral microatolls in Sumatra. "P" and "Sd" sites were on South Pagai and Sanding Islands respectively; "T" samples were from Tikos Island, near Bengkulu on the west Sumatran coast. South Pagai and Sanding site locations appear in Figure 2.2. Column 2 shows the distance between the site and the subduction zone trench. Column 3 shows the submergence rates derived from meaured HLS elevations only. Rates are the slope of the best fit line through the points. Column 4 shows the rates derived from measured HLS elevations and minimum HLS elevations, determined by measuring elevations of the tops of unimpeded growth bands. The last column shows rates derived from the slope of by drawing a line between the modern and the oldest HLS.

Table 2.2 - Submergence rates from coral stratigraphy.

Site	Distance from Trench (km)#	Submergence Rate - from HLS only (cm/yr)	Submergence Rate - from HLS and minima* (cm/yr)	Submergence Rate - first and last HLS (cm/yr)
P96-B	110.7 (119.1)	0.72	0.96	0.58
Sd96-C	111.6 (120.6)	0.77	0.84	0.58
P96-J	112.7 (122.6)	0.52	0.62	0.41
Sd96-A	113.4 (122.9)	0.95	1.08	0.71
P96-K	118.2 (128.2)	0.42	0.46	0.32
T96-A-1	215	-0.09	0.10	-0.23
T96-A-2	215	0.14	0.08	0.06

* Minima included only after the first HLS impingement.
# Distances are measured orthogonally from each site to the trench itself. Distances in parentheses are measured from the sites to a line best fit to approximate the strike of the trench.

than 5 cm. This is the same order as the variation one finds in the HLS elevation of the living ring on one coral head.

Although the morphologic variations between these two samples were apparent among all the corals at this site, in that there is a great degree of variability in how prominent the interior raised annulus was, and both samples expressed a 4 cm drop in HLS in 1994, the details of their stratigraphically determined HLS histories differ. The raised ring on T96-2-A appears to have developed because of a substantial increase in HLS elevation that kept pace with the coral's growth rate for about eight years, starting in about 1986. There is no seemingly abrupt increase in HLS in T96-A-1. A couple of explanations seem possible. The submergence "event" may have been caused by scouring of the substrate below T96-A-2 which lowered the coral and created a sudden local submergence affecting the coral but not representing sea level change at the site. Another possibility is that the "event" was not so much a sudden increase in elevation, but a sudden increase in submergence rate (from near zero to about one half cm/yr). That rate of submergence would be enough to permit the slower growing T96-A-2 to grow upward virtually unimpeded for eight years, just brushing HLS twice in that interval. T96-A-1 had a higher average growth rate than T96-A-2. The horizontal growth of T96-A-1, from 1985 to 1996, was about 14 cm while that of T96-A-2 was only 10 cm. T96-A-1's growth rate was almost half again that of T96-A-2. An increased submergence rate beginning in the mid-1980'a might permit T96-A-2 to grow relatively freely until the rate slowed again, while still forcing the faster T96-A-1 into almost yearly infringements by HLS. However, this still does not explain everything. Even if T96-A-1 was growing laterally at HLS, 4 cm above 1996 living level, while T96-A-2 was still growing up toward that height, not reaching it until 1992, it does not explain why T96-A-1 was able to grow at 2-4 cm above 1996-level for almost a decade prior to 1986 while T96-A-2 was constrained to grow at an HLS nearly exactly at the elevation of 1996 coral. The elevation differences

are small, well within the range of HLS variation even within a single head, let alone between heads. Nevertheless they suggest that some mechanism, such as substrate scouring or changing water flow, may have caused a rise in T96-A-2's HLS relative to that of T96-A-1 after 1985.

Whether the stratigraphic variations are a product of different growth characteristics or slight differential motion between the two heads, the difference in the average record over a couple of decades is not substantial. Just as the comparison of HLS elevations and gross morphological characteristics did, the stratigraphic comparison of T96-A-1 and A-2 illustrates the kind of variations that are possible among microatolls of the same generation at the same site. Thus variability of this order, if observed in fossil corals at one site, or between two corals at different sites need not be indicative of differential sea level histories. However, if the stratigraphic differences are borne out in a number of corals from each site, it may indeed be physically significant.

The Tikos discrepancy can give us some idea of the uncertainty involved in using coral stratigraphy to establish rates of vertical deformation. Because rates from corals in stable areas like Tikos are most sensitive to errors in measurement, one might expect that the uncertainties in the rates for the Mentawai corals are probably no greater than those at Tikos. Since the difference between the two Tikos rates is about 3 mm/yr, one can apply 3 mm/yr uncertainty to the average Tikos rate. One can therefore expect that uncertainties of about ±3 mm/yr might apply to rates throughout the region. Collecting more samples, several from each site, will establish the uncertainties better and should be a goal of future field work.

For the sites on South Pagai itself, the calculated rates vary between 4.2 and 9.5 mm/yr. The lowest rate, 4.2 mm/yr, occurs at site P96-K, the farthest Mentawai site from the trench. The fastest recorded submergence rate is from Sd96-A, next farthest from the trench after P96-K. The average rate, then, is 6.8 ± 4.2 mm/yr for HLS's only and 7.9 ±

5.0 mm/yr for HLS's plus minima. The error here, which is just the 2σ standard deviation of the rates and does not include the uncertainty in each rate, is slightly larger than the uncertainty estimated from the Tikos comparison. Either the Tikos-based uncertainty is just too low, or the difference in rates between the Mentawai sites is physically significant and not simply a relic of the uncertainty.

Summary of slab analysis

Slabs from seven living corals at various sites on the Mentawai Islands and the Sumatran coast were analyzed to determine the HLS histories recorded in the coral morphology. Most slabs provided a record from 25 to 60 years long. Though the results have slight uncertainties in both elevation and time, the broad picture provided by all the corals is consistent. The corals on the outer arc islands show clear evidence of submergence at varying rates in the modern period, while those on the Sumatran coast indicate overall stability. The submergence rates gleaned from the Mentawai slabs vary from about 4 to 10 mm/yr. Submergence rates on the coast are essentially zero.

2.3 Discussion

2.3a. Using corals as geodetic measurement tool

People have long used corals to document relative changes in sea level on various time scales. Long term eustatic sea level change has been illuminated with corals (e.g. Edwards et al., 1987c; Bard et al., 1990) as has coseismic uplift associated with historical and paleo-earthquakes (Taylor et al., 1987; Edwards et al., 1988; Zachariasen et al., 1995). It is clear that corals can be successfully used to document individual uplift events. This study attempts to test how well they act as steady, long-term annual recorders of sea

level change, as natural tide gauges to document interseismic as well as coseismic sea level variations. The value of such recorders is that they are ubiquitous in tropical waters. The density of such coral gauges promises a great advance in constraining vertical displacement so as to better understand subduction zone tectonics.

This study indicates that the method is promising. Surveys and field observations of *in situ* corals suggest that the HLS sea level indicator is precise to within a few centimeters within one coral head. Modern HLS of different heads of the same species vary by about ±10 cm. The greater precision provided by HLS records in an individual head implies that it is probably best to focus on analysis of one head at a time rather than base conclusions on a broad morphological analysis of many corals at once. Surveys and rough field measurements are appropriate for reconnaissance, but the most useful data for precise sea level histories will come from the detailed analysis of x-rayed slabs.

The study of living corals was intended both to illuminate the nature of modern deformation and ascertain the value of using corals to retrieve long term sea level records. To use corals as a paleoseismological or paleogeodetic tool and to extend the sea level record back beyond the range of living corals, the method that shows promise in live corals must be equally applicable to dead corals. The results of the analysis of one coral that died in 1834±6, probably just after the last great subduction zone earthquake in this area (Newcomb and McCann, 1987), are shown here. (Further results about this and other large earthquakes in the Pagais and Sipora are discussed Chapter 4) The drawing of the slab and associated sea level history appear in Figure 2.21. The coral stratigraphy shows a rapid minimum preseismic submergence rate of almost 1.2 cm/yr, and about 1.5 cm/yr in the last decade, followed by a sudden emergence of at least 34 cm. The emergence is a minimum because the entire coral emerged and died; the post-emergence HLS is not recorded in the coral.

Figure 2.21. Interpretation of slab NP94-A-9, cut from a fossil coral from North Pagai whose outermost ring and death by emergence date to 1834±6. 1833 was the year of the last great subduction zone earthquake at this latitude.

a. Drawing of the slab and the annual rings.

b. Sea-level curve derived from analysis of the slab. The error bars represent only the radiometric age error, not any errors from ring identification. This curve combined with a sea-level curve for a live coral from the same location would provide a sea-level history for a good fraction of a complete earthquake cycle.

a.

1830 ± 6   Date from U-Th analysis and ring counting

1834 ± 7   Date from U-Th analysis, corrected for initial
Th-230 contamination, and ring counting

[1829 ± 1]   Date from ring counting, assuming final emergence
and death occurred during 1833 earthquake

Location of dated sample

NP94-A-9
P. Silabusabeu,
North Pagai

Final emergence and death
1834 ± 6
1837 ± 7
[1833]

[1830]

[1830]

1830 ± 6
1833 ± 7
[1829 ± 1]

[1825]

[1825]

[1819]

erosional surface

[1815]

HLS
1819 ± 6
1822 ± 7
[1818 ± 1]

HLS
1820 ± 6
1823 ± 7
[1819]

10 cm
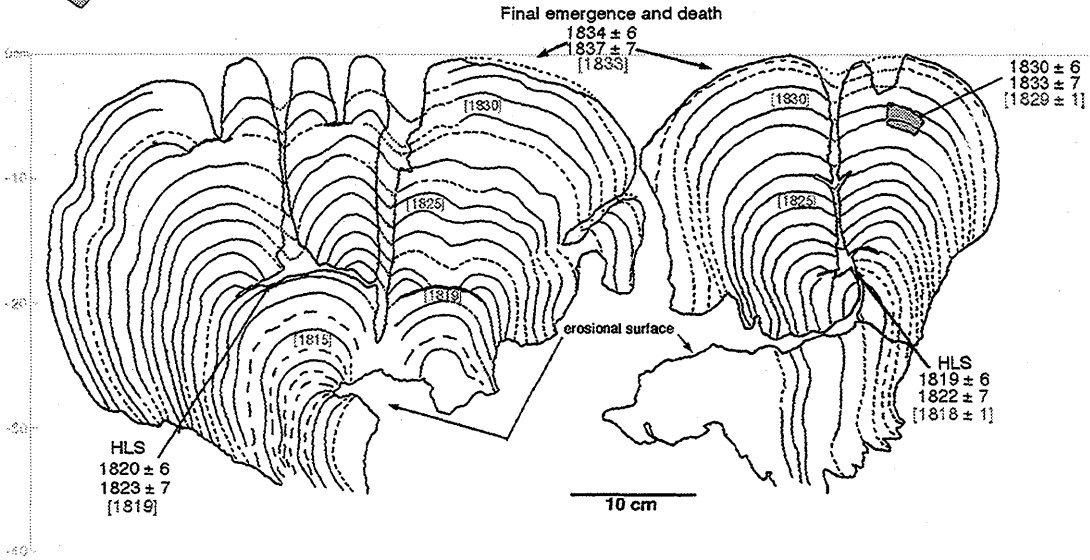
b.
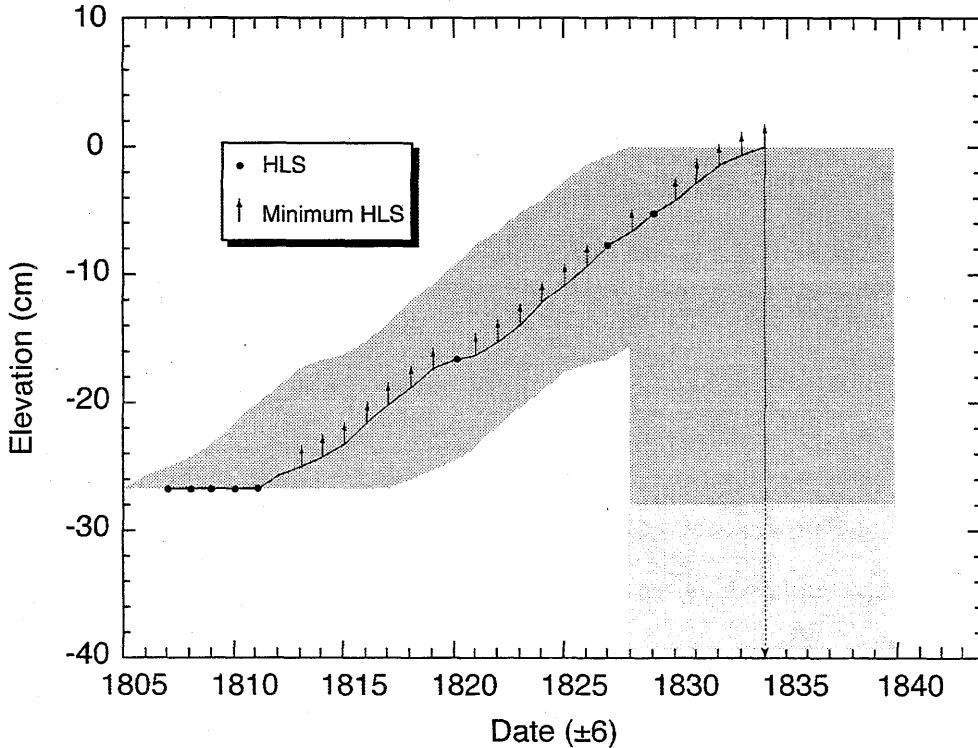
Given that the date is precise and that it coincides with a known earthquake, it is likely the coral died as a result of coseismic uplift during the 1833 event. If so, x-ray analysis of the dead coral slab provides an annual record of sea level in the immediate preseismic and coseismic periods of the last great earthquake affecting the site. Combining this record with that of a living coral at the same site would provide a good fraction of the history of vertical displacement at this site throughout the earthquake cycle. To improve the record, one would want to extend the interseismic record back to 1833, to include the immediate postseismic period, and also extend the preseismic record further back. The former requires finding a coral head that was only partially emerged during the earthquake and continued to live restricted by the new post-seismic HLS. The former requires a bigger coral or several corals that overlap in time from the 1833 event back to perhaps the previous uplift event.

2.3b. Modern vertical displacement

The stratigraphic analysis of live coral microatolls has provided a quantitative measure of recent vertical displacement rates in the hanging wall of the subduction zone. The outer-arc ridge of the Mentawai Islands is experiencing significant ongoing submergence at rates of over a half-centimeter a year, while the western coast of Sumatra, at approximately the same latitude, has remained relatively stable with respect to sea level over the past few decades. Near the mainland, every coral observed was low, wide and flat. Furthermore, corals farther up the coast near the town of Padang (Figure 2.1) also had nearly flat tops and showed few sign of submergence. It appears that, for the coast of Western Sumatra from 1°S to 4°S, the average rate of sea level change has been less than 1 mm/yr or so for the last several decades. The high rates of subsidence at the islands, the longevity of the average submergence signal, the difference in rate between islands and

coast, the tectonic setting, and the lack of similar submergence at non-tectonically active sites in the Indian Ocean all suggest that this submergence is primarily tectonic and is caused by vertical deformation of the Southeast Asian plate near the plate boundary. Regional vertical deformation at the surface over a subduction zone is usually a result of subduction-related slip in the subsurface, primarily along the plate interface. In principle, if vertical deformation is well constrained, one could use it in conjunction with information about slab location and orientation, convergence rate, and seismic history to constrain the slip on the interface.

Geographic distribution of interseismic displacements

The last great earthquake on this part of the subduction zone occurred 164 years ago, in 1833. Plate convergence rates and microatoll analysis (Chapter 4) suggest that the recurrence interval for such great earthquakes is on the order of 200-300 years (Tregoning et al., 1994; Chapter 4). If that is the case, then Sumatra should now be in the second half of an average earthquake cycle. Any transient post- or preseismic effects should be negligible, and the modern rates of deformation should be an almost purely interseismic signal. The 1833 great earthquake was accompanied by significant coseismic uplift in the islands (Chapter 4). Therefore, we should expect to see interseismic subsidence there since most of the coseismic slip is recovered interseismically, as testified by the presence of mid-Holocene corals in the intertidal zone (Chapter 1; Chapter 4).

The coral-derived submergence rates plotted as a function of distance from the subduction zone trench appear in Figure 2.22a. In principle, one could use this spatial distribution of submergence rates to constrain the interseismic deformation. The islands occupy a swath, 30 km wide, which could show significant variations in submergence rates across it. The points, as expected, fall in two clusters, one site on the Sumatran

Figure 2.22. Comparison of vertical deformation rate with distance from the trench.

a. Submergence rates derived from stratigraphic analysis of coral microatolls from the Mentawai Islands and the west coast of Sumatra. The dip of the subduction zone under the islands is inferred from earthquake moment-tensor solutions to be about 10°. Distances are measured normal to the trench at each site.

b. Plot of elastic dislocation model of vertical displacement rates as a function of distance from the subduction zone trench. The curve depicts vertical displacement rates for convergence at 6.7 cm/yr, with a 12° east-dipping planar interface locked from the trench to 170 km down-dip. The observed submergence rates derived from the corals on the Pagais and at Tikos Island are also plotted.

a.

Submergence rates in South Pagai and Western Sumatra relative to distance from the subduction zone trench
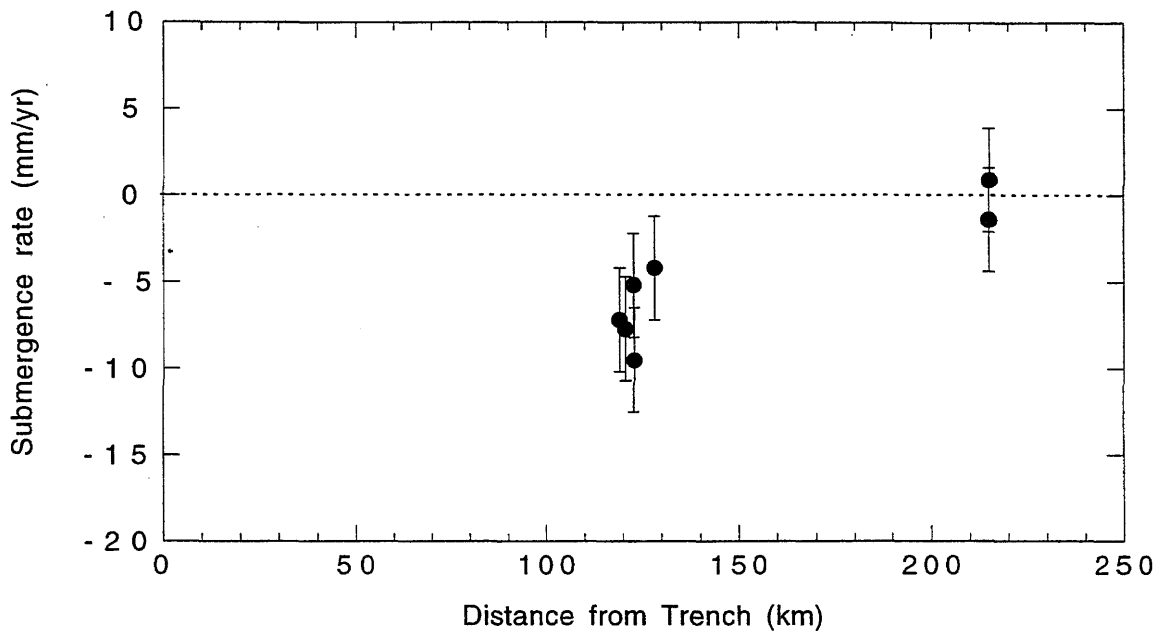
b.
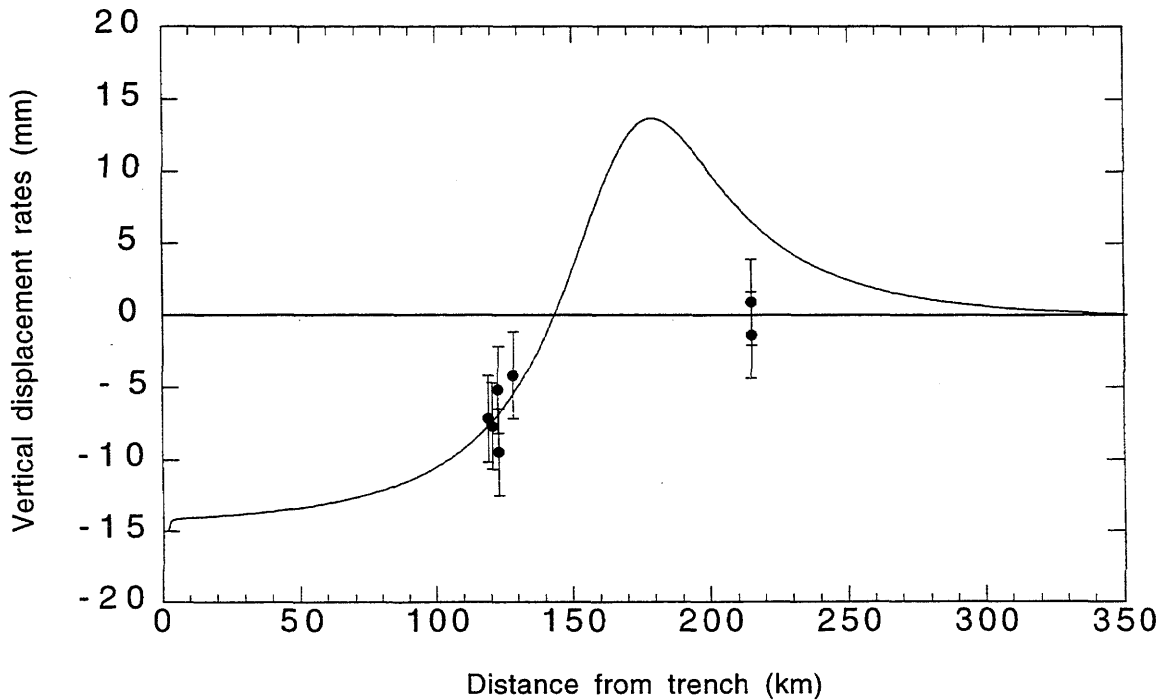
coast, about 215 km from the trench, and five on the islands about 120 km from the trench. The rates on the coast are near zero. The sites on the island plot tightly, in a window about 10 km wide. Within that window, and disregarding rate uncertainties, there appears to be an increase in submergence rate from east to west. The exception comes from Sd96-A, a site with coral recording a high submergence rate (almost 1 cm/yr) but relatively far from the trench.

The 10 km window into which the island sites project is narrow. The uncertainties on the submergence rates are about ±3 mm/yr and the surface projection of the subduction zone interface is not necessarily located well-enough to differentiate distances on the order of a kilometer or so. If the locations are not precise to within a few kilometers and the rate differences are not much greater than their uncertainties, it may not be appropriate to treat the apparent spatial distribution of rates within the islands as physically significant. With such a conservative approach, the island sites could be treated as a single site, and the Tikos site as a second site. In this case, one finds an average rate of submergence of about 7±4 mm/yr at the islands and an average rate of 0±3 mm/yr on the mainland coast.

These general results are too limited to fully model the interseismic deformation. Nevertheless, the data can provide some qualitative preliminary insights into the nature of the subduction process in Sumatra. The plot shows rapid submergence at 120 km and near-stability at 215 km. This is broadly consistent with observations at the Alaskan and Nankai subduction zones (Savage and Plafker, 1991; Thatcher, 1984; Thatcher and Rundle, 1984; Savage, 1995). The trench-orthogonal distribution of vertical displacement is opposite in sign from the coseismic displacement recorded on the islands where uplifts of more than a meter in 1833 are probable (Chapter 4). This is consistent with both elastic dislocation models and subduction models incorporating viscoelastic relaxation response.

Dead coral along the coast have not been sampled, so there are no constraints on 1833 deformation there.

Possible gradient in submergence rates across the Mentawai Islands

Although the conservative approach deems that the uncertainties in location and submergence rates may be too great to permit rigorous distinction between rates at the island sites, it is nevertheless likely that there is a real change in submergence rate across the Mentawai Islands. Although the sample sites project onto a strip only 10-km wide, the islands themselves are up to 30 km wide. In addition to the slab results, the morphology of living corals throughout the Pagais suggested that submergence rates on the west side of the islands were greater than that on the east side, consistent with the apparent distribution of rate shown in Figure 2.22a. If one abandons the most conservative approach and considers the observed spatial distribution of rates significant, it yields some interesting possibilities regarding the nature of modern deformation in the region.

In this case, the data indicate that there is a steep gradient across the islands, with lower rates, in general, occurring at sites farther from the trench. This suggests that the islands are landward of the peak amplitude of submergence. Secondly, since the coastal sites show essentially no vertical displacement, the peak interseismic uplift must be occurring somewhere between the east coast of the islands and the west coast of Sumatra, probably closer to the islands than the mainland. If the signal is real, the gradient across the 10-km swath is quite high, going from almost 10 mm/yr to less than 5 mm/yr in 10 km. Although very high displacement rates and gradients due to asthenospheric response to coseismic slip are observed postseismically, these usually have substantially dissipated by midway through the interseismic period, so this does not seem a satisfactory explanation for the high gradient. It is more likely a function of interseismic deformation that a post-seismic transient.

If simple tilt produced this gradient, and the gradient were then projected linearly to the trench, it would suggest a submergence rate at the trench of about 60 mm/yr at the trench, which is quite high, and well beyond what would be expected from convergence at 7 cm/yr on a 12°-dipping interface. Of course, the gradient probably does not project linearly to the trench, but that does offer an outer limit of possible displacement rates.

A simple elastic dislocation model, though oversimplified, is somewhat more revealing than considering simple tilt. Figure 2.22b shows a model of vertical displacement rates at the surface generated by plate convergence with a locked interface. As per Savage (1983), the convergence and interseismic locking is modeled as normal slip on the locked interface (Chapter 1). The curve was generated to model orthogonal convergence at a rate of 6.7 mm/yr, the full plate convergence rate, with a plate interface dipping 12°, the plate locked from 0 to 170 km down-dip. These conditions do not account for steepening of the fault plane east of the Mentawais, although this clearly occurs since the Wadati-Benioff zone suggests a 50° dip below the volcanic arc (Fauzi et al., 1996). The observed displacement rates are also plotted on this curve, with uncertainties.

The modeled curve passes through the island-rate points and shows a gradient in rate, with rates decreasing west to east, suggesting that the *a priori* assumptions about fault dip, slip rate and size of the rupture patch are roughly appropriate. However, a number of discrepancies are evident. First, though a rate gradient appears in the model, it is not as steep as the coral data suggest. This may simply be a function of the uncertainties in the coral-derived rates - the curve does pass through all the points within the uncertainties - but since we are here disregarding the uncertainties, the modeled curve does appear slightly less steep. It does not easily accommodate the high rate of Sd96-A, although this rate is "out of sequence" for the simple case considered here. The second discrepancy, is that, if the locked patch is chosen so that the displacement curve passes

through the island points, it suggests significant uplift should be occurring at the coast, in contrast to the observations. Although in the model the locked patch can be moved up and down the interface since, unlike the convergence rate and slab dip, that component is relatively unconstrained by independent data, it is difficult to model both the submergence rates on the islands and the stability on the coast with a locked interface on a planar fault.

There are a number of possibilities to explain the discrepancies between the simple model and observation. The high gradient in rates across the islands could be due to reverse slip on the up-dip section of the supposedly locked interface, at a point west of the islands. If a small section were slipping rather than locked, it could generate a short-wavelength displacement distribution, with peak uplift occurring well west of the islands and peak subsidence occurring at or just west of the islands. This contribution could enhance the degree of submergence on the west coast of the islands and contribute to the higher gradient.

Another plausible explanation for the gradient is that it is caused in part by slip on another structure in the hanging wall, or folding within the accretionary prism. Even moderate subsurface offsets on a steep backthrust running east of the islands could produce tilting in the outer-arc, generating a westward increase in submergence. The Mentawai Fault is a candidate for this postulated structure. Although seismic reflection data have been interpreted to suggest that the Mentawai Fault is strike-slip, sediments to the west of the fault are steeply west-dipping (Diament et al., 1992). If thrusting on, or folding above, this fault is still ongoing, it could account for some of the gradient. In that case, however, one would expect to see permament tilting.

A third possibility is that the rate differences are attributable not so much to differences in displacement perpendicular to the trench, but rather to differences parallel to the trench. Thus the lower submergence rates at sites P96-J and P96-K are a function

of their trench parallel position relative to the other sites, rather than the fact that they are slightly farther to the east.

The discrepancy between observed and modeled rates at the Sumatran coast may be due to a number of things, including the above possibility of strike parallel variation. Tikos is about 150 km southeast along strike of the subduction interface than the Pagai Islands (Figure 2.1), so it is conceivable that displacement patterns would differ between the two latitudes. If this is not the case, then it may be attributable to down-dip variation. Certainly the slab dip is different in fact than in the simple model. It may be too that there is partial locking down-dip of the fully locked zone. This could counteract the uplift expected if there were no locking, producing the stability observed at Tikos.

Episodic vs. gradual submergence

Another issue raised by the coral data which has implications for the nature of interseismic subduction is the question of whether the modern submergence is gradual or sudden and episodic. I have discussed the possibility that the observed submergence occurs episodically. The lack of HLS clips for a 20-30 year period in several corals suggests the possibility that submergence occurred suddenly, taking the top of the coral out of the zone of tidal fluctuations. However, this might also be caused by a decrease in the amplitude of the fluctuations which would in turn cause fewer interactions with low low tides. This could occur during steady state submergence. Or submergence rates could fluctuate.

Whether submergence occurs gradually or episodically is significant in interpreting the nature of the subduction zone deformation. If submergence is gradual, an aseismic steady-state process in which the main thrust zone is locked and down-dip and/or up-dip slip is steady appears likely. Interseismic loading and/or relaxation gradually counteracts the coseismic deformation. The episodic scenario implies that the

interseismic steady-state is punctuated by small earthquakes or aseismic slip events. Thus slipping parts of the interface are not freely slipping but rather experience stick-slip failure. Distinguishing between the gradual and episodic scenarios could illuminate the nature of the interseismic deformation.

In order to see if the HLS record found in the Mentawais might be evidence of episodic submergence, I compared two models of tidal fluctuation, represented by a sine wave, superimposed on overall submergence (Figure 2.23). The first case involves gradual subsidence (Figure 2.23a), the second, episodic submergence (Figure 2.23b). The resulting sea level records are noticeably different and significantly, the interactions of coral growth (shown by the dotted line in the combined signals) with the tidal record are more irregular in the episodic case than the gradual case. The models suggest that, while HLS clips are fairly regular in the gradual submergence scenario, one might expect to see long periods without an HLS clip if the region is submerging episodically. Thus, the ~20 years of impingement-free growth in Sd96-C may indeed be indicative of episodic submergence.

On the other hand, real tide records are not regular sine waves. The Cocos record implied that in a subsiding environment one might expect HLS impingements every few years. However, it does not preclude much longer periods of impingement-free coral growth. Certainly, irregularity in tidal records is not uncommon, as tides and relative sea-level are affected by weather, storms, rainfall, variations in ocean circulation patterns, and other factors that fluctuate on short time scales. A similar experiment to the above (Figure 2.23), but using a more realistic curve than a sine wave, reveals the possible differences in HLS signal that might arise in the cases of episodic and gradual submergence (Figure 2.24). Instead of a sine wave, I use a model tide record derived from a 20-year mean monthly tide gauge record from the Solomon Islands (Figure 2.24a). The range of tidal fluctuations is about 50-60 cm, slightly higher than is observed in the low tide record

Figure 2.23. Cartoon models of the effects of interseismic deformation on sea-level records.

a. Oceanographic sea-level fluctuations, modeled as a sine wave, with gradual tectonic subsidence. The dotted line in the combined signal is the coral growth curve, showing regular HLS clips and small emergences.

b. Oceanographic sea level fluctuations with sudden, episodic submergence events. The coral growth curve is clipped less often and more regularly than in the gradual subsidence scenario.

a. Elevation / Time

tide + steady submergence = combined signal
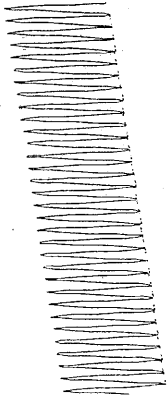
b. Elevation / Time

tide + episodic submergence = combined signal
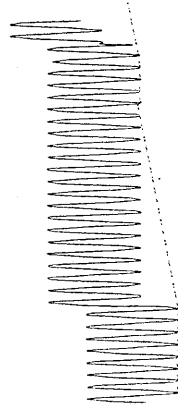
Figure 2.24.

a. Models similar to those depicted in Figure 2.23 except that the tidal fluctuations are represented by a real 20-year tide record from the Solomon Islands, doubled to give a 40-year record. Curves representing gradual and episodic submergence at 7 mm/yr are shown below the tide record. Above these are the tidal curves resulting from the addition of the tide record and the submergence curves. Dashed lines reflect coral growth at 1 cm/yr under these conditions. Interactions between the coral growth and low tide provide an idea of the HLS history that might be produced in each scenario. ,

b. Same model as Figure 2.24a. except that the tidal amplitudes have been decreased to 20% of their values in Figure 2.24a

a. Gradual vs. episodic submergence
high amplitude tidal fluctuations

~50 cm range

tidal fluctuations +
episodic submergence

tidal fluctuations
+ gradual submergence

tide record
(no net change)

episodic submergence

50 cm

gradual submergence
@7 mm/yr

coral growth @ 1 cm/yr

Elevation (cm)

Time (yrs)
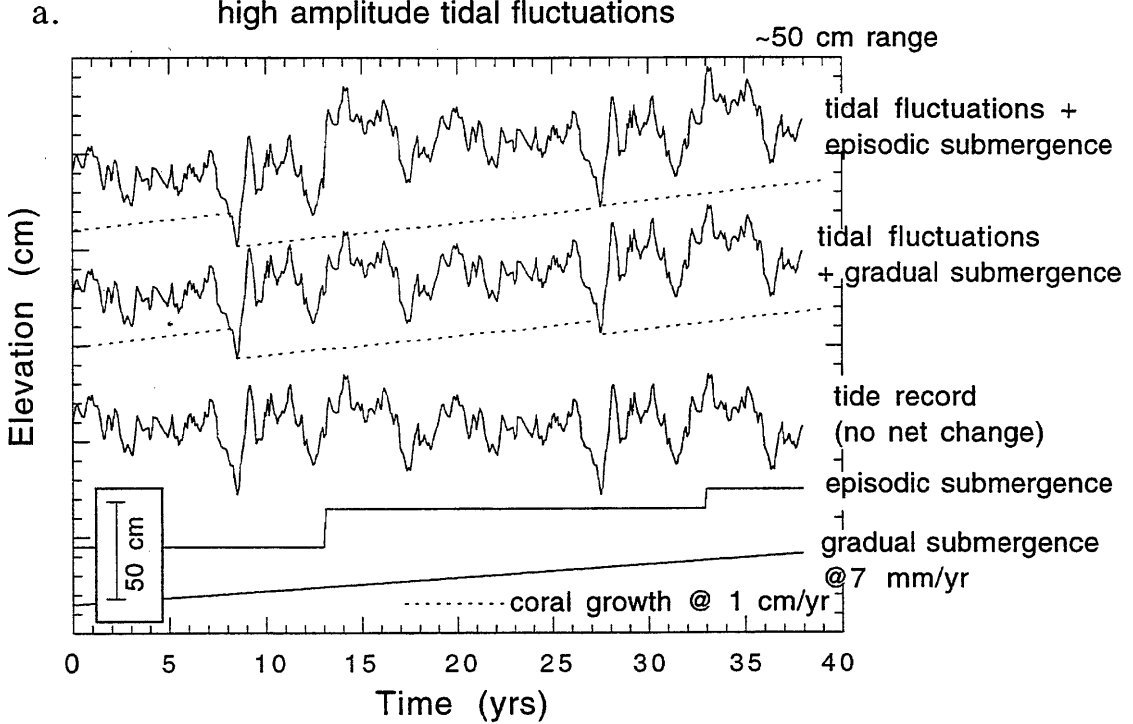
b. Gradual vs. episodic submergence
low amplitude tidal fluctuations

~10 cm range

20 cm

tidal fluctuations +
episodic submergence

tidal fluctuations
+ gradual submergence

tide record (no net change)

episodic submergence

gradual submergence
@7 mm/yr

coral growth @ 1 cm/yr

Elevation (cm)

Time (yrs)
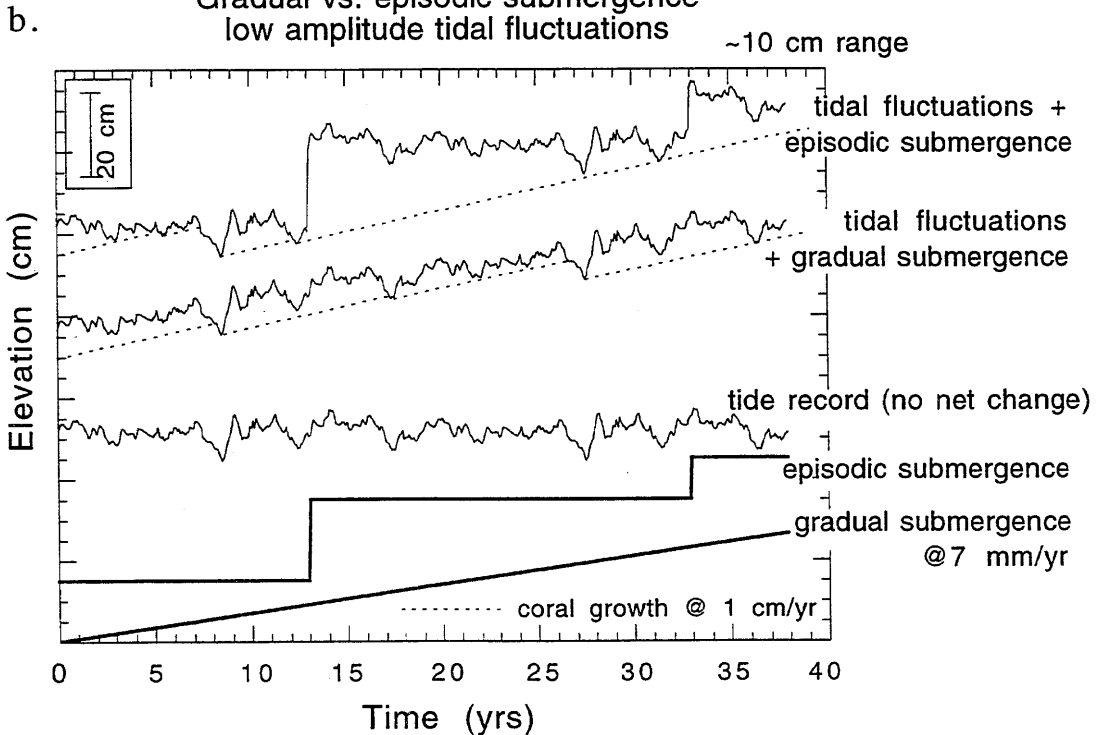
from Cocos. A submergence rate of 7 mm/yr is added to the tide record, first as a gradual submergence throughout the entire period, then as steps of 25 and 15 cm separated by periods of constant sea-level. The two resultant curves are shown in Figure 2.24a, the cumulative tidal-episodic curve above the tidal-gradual curve. The two curves are not noticeably different on first inspection. It is unlikely, in this case, that one could distinguish between gradual and episodic submergence from even the tide gauge record. It is even less likely that one could distinguish between the HLS records from two corals having grown under these conditions. If a hypothetical coral is allowed to grow at rates of 10 mm/yr, there are only two HLS clips for each record in thirty years. These occur at the same times, both periods of very extreme low tide, not unlike the 1995 low-tide from the Cocos record. The difference in HLS record is in the size of the emergence. In the gradual scenario, the two small emergences are of similar size. In the episodic scenario, the first emergence is fairly large, while the second is merely a clip, not a major emergence. Given these more realistic tidal conditions, it appears that it would be difficult to distinguish episodic from gradual submergence even with the tide record, let alone with an HLS record.

The range of tidal fluctuations in the previous scenario was about 50 cm, larger than the size of the postulated episodic emergence steps. Therefore, it is not unreasonable to expect that the signal from the step might be swamped by the tidal fluctuations. If the range of tidal fluctuations were less, the submergence step would probably be more noticeable. To examine that possibility, I made a similar plot of tidal record plus submergence, in which all elements are the same except that the amplitude of the tide record has been reduced to 20% of the original amplitude (Figure 2.24b). This amplitude is somewhat smaller than that observed in the Cocos record. When the tide record and submergence curves are added in this scenario, the episodic case is clearly distinguishable from the gradual case. The HLS record from corals growing under these conditions also

become much more distinguishable. In the gradual case, there are four small emergences, and they are fairly evenly spaced over time. In the episodic case, the clips are clustered early on, prior to the submergence, while after submergence there is a long period without HLS clips, while the coral attempts to grow up to the substantially higher water level.

These model suggest that distinguishing episodic from gradual submergence in HLS records may be possible in some cases, but is not always achievable. It depends strongly on the size of the submergence step relative to the size of the tidal range. If the size of the step is the same as or smaller than the range of tidal fluctuations, it will probably remain indistinguishable. If it is substantially larger, it may be possible to make the distinction, though probably not without some degree of uncertainty. The HLS record is not as clear as the tidal record. It is also very possible that what in fact occurs is somewhere between the end members presented here. In other words, a relatively long hiatus in HLS clips may be caused not by a submergence step event, but rather by an increase in submergence rate, or a slow-down in coral growth rate. A decline in growth rate should be distinguishable in a cross-sectional slab, but it is unlikely that corals will definitively reveal the difference between a submergence step and an increase in submergence rate.

Thus, unfortunately, one may never be able to distinguish gradual from episodic submergence with the coral HLS record, because submergence rate is only recorded within the limits imposed by the coral growth rate. This is unfortunate since knowing the details of the interseismic record on an annual scale could reveal a great deal about interseismic deformation patterns. The above discussion suggests that interpreting decade-long periods free of HLS clips as evidence of rapid submergence events rather than gradual subsidence is reasonable but still speculative. Even if one did make that assumption, the HLS record would still not fully illustrate the nature of the submergence event. Figures 2.23 and 2.24 illustrate episodic submergence as a step function, with the

submergence event interspersed with sea level stability. But an equally plausible scenario could involve a larger magnitude submergence event followed by rapid exponential relaxation which recovers almost all the deformation in a few years. This recovery was seen in the areas of coseismic subsidence of the 1964 Alaska earthquake and the 1946 Nankaido earthquake (Chapter 1). This might not be distinguishable in an HLS record. In a submerging environment, the HLS record is robust in determining average rate of subsidence on time-scales of decades, but less so in reflecting fine-scale changes on time-scales of years.

This study of living coral microatolls has demonstrated the effectiveness of the corals as natural tide gauges. Although there are limitations in the sensitivity of the coral gauge, especially in a subsiding environment, within these limitations, it can and has provided constraints on vertical displacement rates in the hanging wall. The data are not complete enough at this point to rigorously model interseismic strain accumulation over the interface as has been done with tide gauge and leveling data from Japan and Alaska that were distributed widely enough to open a broad window across the surface over the subduction interface. It is likely, however, that coral microatolls can provide similar data that will eventually permit robust quantitative modeling. With further sampling of corals at sites in and around the Mentawais, and along the Sumatran coast, one could conceivably get enough natural tide gauge records to constrain the along- and across-strike submergence variation and smooth out irregularities due to local effects that can arise from the use of point-source data. With reasonably dense coverage, those problems could be at least partially overcome.

It would be beneficial to ascertain the characteristics of interseismic deformation suggested here. For example, if uncertainties in rates were tightened by obtaining multiple HLS records from each of many sites, the gradient in rate across the islands could be

constrained. If the spatial distribution of submergence rates were well-defined, such that slip on different portions of interface were adequately modeled, it could shed light both on the modern deformation process and that of a projected future event. For example if the extent of fully and partially locked portions of the interface could be inferred from the interseismic patterns of displacement, and the amount of aseismic slip estimated, it could help define the likely limits of the rupture zone in a future earthquake.

2.4 Conclusions

Living corals from the Sumatran hanging wall were examined to test their efficacy as recorders of relative sea level variations. The corals contained annual records of sea level with elevation uncertainties on the order of ±4 cm within one coral and ±10 cm between corals.

By analyzing the stratigraphy of vertical cross-sectional slabs cut through coral heads, I produced detailed relative sea-level histories for seven corals at six sites in the outer-arc islands and on the Sumatran coast. The sea-level curves revealed that outer-arc islands have been submerging at average rates of 7±4 mm/yr over the last few decades of the interseismic period. Sea level on the mainland coast has been relatively stable in recent years.

A qualitative examination of the variation in submergence rate across the subduction zone indicates that it is broadly consistent with observations of interseismic deformation at other subduction zones and with elastic-dislocation and viscoelastic-coupling models of interseismic strain accumulation. The suggestion of a steep gradient in submergence rates across the outer-arc islands and indications of possible episodic submergence events imply that deformation processes other than simple aseismic elastic strain accumulation in the great earthquake cycle are responsible for some of the

submergence observed on the islands. Possible causes for the questionable gradient include aseismic slip on the shallowest portions of the interface, slip on subsidiary structures, and along-strike variations in submergence rate.

Data collected so far do not permit robust quantitative modeling of deformation. However, it appears that stratigraphic analysis of coral microatolls holds great promise for yielding a dense array of relative sea-level and vertical displacement records that could ultimately help define the nature of subduction-related deformation in the hanging wall of a large subduction zone.

Chapter III

U-series disequilibrium dating of fossil corals

3.1. Introduction

Living coral microatolls have been shown to be effective recorders of recent sea level fluctuations (Scoffin and Stoddard, 1978; Taylor et al., 1987; Woodroffe and McLean, 1990; Chapter 2 of this study). To extend this record of sea level into the past and use corals as paleoseismological recorders requires analyzing the sea level record of fossil microatolls. To effectively establish the timing of that sea level record and of paleoearthquakes in turn requires determining accurate and precise ages of the dead corals. ^{14}C has been used to date fossil corals, but long ocean residence times for carbon and differences between atmospheric and surface sea-water ^{14}C values means that ^{14}C coral ages may be overestimated by as much as a few hundred years (Edwards, 1988; Eisenhauer et al., 1993). ^{238}U-^{234}U-^{230}Th geochronology affords the necessary precision. U-Th dating can provide absolute ages, provided certain conditions are met.

In both 1994 and 1996, I collected samples and slabs from fossil corals as well as live corals in the Mentawai Islands to establish a paleoseismic history of the region (Figure 3.1). I dated most of the dead corals and some of the live corals with U-Th geochronological methods. The results of that work, the measured isotopic abundances and ratios and the calculated ages for the corals, are presented in this chapter. The paleoseismological implications of the dating results are presented in Chapter 4.

3.2. U-Th geochronology in corals

2a. ^{238}U-^{234}U-^{230}Th systematics

^{238}U-^{234}U-^{230}Th methods of dating are based on the radioactive decay of ^{238}U to ^{206}Pb through a series of intermediate daughters including ^{234}U and ^{230}Th, as follows:

$^{238}U ------>> \,^{234}U ------> \,^{230}Th ------->> \,^{206}Pb$
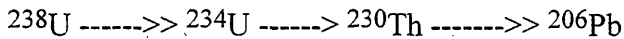
where the decay constants $\lambda_{238} = 1.551 \times 10^{-10}$ (Jaffey et al., 1971), $\lambda_{234} = 2.835 \times 10^{-6}$ (de Bievre et al., 1971 and Lounsbury and Durham, 1971), and $\lambda_{230} = 9.195 \times 10^{-6}$ yr^{-1} (Meadows, 1980). The double arrowheads indicate the presence of intermediate daughters that are not shown; the single arrowhead indicates direct decay between the two isotopes shown. The mean lives of the isotopes are 6.446×10^9, 3.527×10^5, and 1.088×10^5 yr for ^{238}U, ^{234}U, and ^{230}Th respectively. Given certain conditions and assumptions, measurements of the concentrations of these isotopes in corals yield the age of the coral.

Uranium occurs in significant concentrations in ocean water. Edwards (1988) found average concentrations of 3.2 ng/g in sea water from both the Atlantic and Pacific Oceans. The source of the uranium is eroded crustal material deposited in the ocean by rivers. ^{238}U in the source rock decays by alpha-decay. When the α-particle is emitted, it can damage the crystal lattice. The recoiled nucleus (^{234}Th that rapidly decays to ^{234}U) could be ejected into solution, or the remnant ^{234}U, which forms water-soluble uranyl ions (UO_2^{+2}), could be preferentially leached from the damaged sites during weathering (Faure, 1977; Edwards, 1988). Thus, the detritus, river water and ocean water are enriched in ^{234}U. The enrichment means the $^{234}U/^{238}U$ activity ratio of sea water is greater than one, the value at secular equilibrium. The enrichment of any material with respect to ^{234}U is generally described in terms of $\delta^{234}U$, which is ($[^{234}U/^{238}U]_{meas.} - 1) * 1000$. The $\delta^{234}U$ of sea water is between 140 and 150, and is fairly consistent throughout the world's oceans (Thurber, 1962; Koide and Goldberg, 1965; Miyake et al., 1966; Chen et al., 1986; Edwards, 1988). The residence time for uranium in the oceans is about 500,000 years, which is much less than the mean life of ^{238}U, and

Figure 3.1. Map of the Mentawai Islands - Sipora (Si), North Pagai (NP), South Pagai (P), and Sanding (Sd). Sites that I visited and at which I collected fossil coral samples for dating are labeled. Site names, which indicate the island, year, and site at which the samples were collected, correlate with sample names listed in Tables 1 and 2. Samples labeled "Pg04..." in the tables come from site P93-D.

Si94-B

Sipora

Si94-A

Mentawai Islands

○ 1993 Sites
◉ 1994 Sites
● 1996 Sites

10 km

N

NP96-B

NP96-A

North
Pagai

NP94-A/
NP96-C

P94-D

P94-C

P96-Q

P93-B

P96-B

South
Pagai

P94-H

P94-AB/P93-C

P96-P

P94-AA

P96-E

P94-Z/
P96-F

P96-O

P96-K

P94-Y/P96-H

P94-W

P96-R
P94-M

(P93-D)Pg04

P96-J

P96-L

P96-I

P94-X

P96-M

P94-U

P94-S

P96-N

Sd96-A

Sd96-C

Sanding
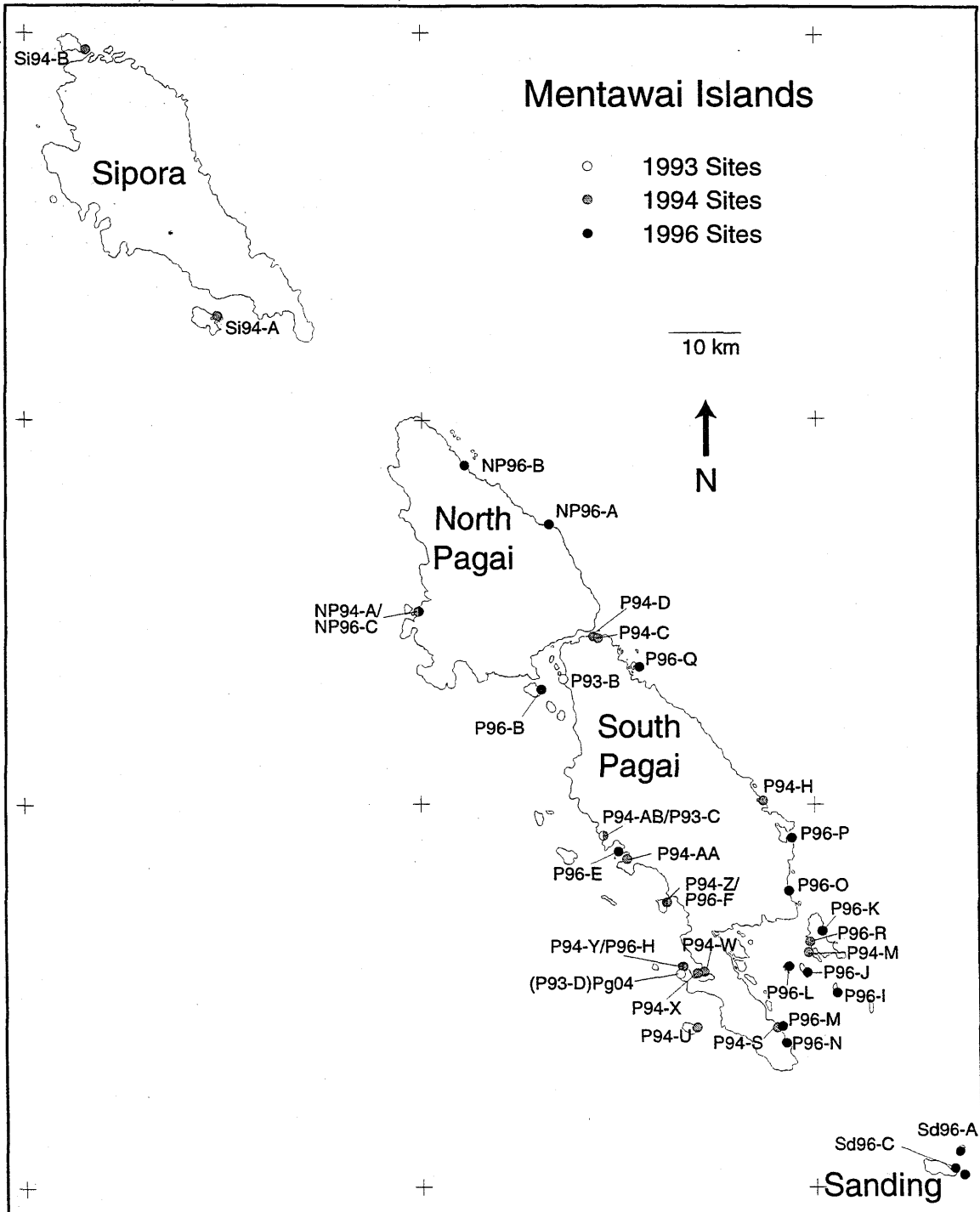
similar to the mean life of ^{234}U. The residence time of thorium is about 300 years (Faure, 1977).

Uranium in the ocean water is incorporated into authigenic minerals such as calcium carbonate and removed from the sea water. Thus corals, made of calcium carbonate, contain ocean-water-derived uranium in their skeletons. The incorporation process does not fractionate the uranium isotopes, so the ratio of $^{234}U/^{238}U$ in corals at the time of coral growth is the same as that in the water (Edwards, 1988; Edwards et al. 1987a, Gallup et al., 1994). Once the uranium is removed from the sea water and incorporated into the skeleton, the coral and the water are theoretically closed to further exchange of uranium. From the time of skeletal growth, the excess ^{234}U in the coral, which is unsupported by ^{238}U, decays to ^{230}Th, ultimately achieving secular equilibrium among all three nuclides. During the period in which the isotopes are still out of equilibrium, the concentrations of ^{238}U, ^{234}U and ^{230}Th can be used to determine the age of the coral skeleton.

The ^{230}Th age can be calculated by measuring the concentration of ^{230}Th, relative to ^{238}U and ^{234}U, assuming the system has remained closed to uranium and thorium. The decay equation for ^{234}U to ^{230}Th yields the age as long as the initial concentration of ^{230}Th in the coral is known. In general, this is assumed to be zero. Thorium is relatively insoluble in water, and most thorium that is introduced into the ocean is rapidly removed by adsorption of Th onto solid particles that are deposited as sediment. Thus, concentrations of Th in sea-water are very low. The concentration of ^{232}Th in most surface sea-waters is on the order of 0.05 - 0.1 pg/g and ^{230}Th concentration is about 1-3 x 10^{-6} pg/g (Chen et al., 1986; Edwards et al., 1987a; Andersson et al., 1994; Moran et al., 1995, 1997). Initial concentrations of ^{230}Th in clean coral, determined by measuring concentrations in living or very young coral or by multiplying sea water $^{230}Th/^{232}Th$ ratios by ^{232}Th abundance in very young coral, are likewise very low, generally less than

what would be produced by one or two years' worth of decay. As this is about the limit of analytical precision in dating, it is justifiable to assume that ^{230}Th/^{238}U in clean, living coral is zero (Edwards et al., 1987a; Edwards, 1988). Not all corals are clean, however, and contamination with initial thorium can occur. In these cases, the assumption of zero initial thorium is wrong and generates ^{230}Th ages that are older than the age of the coral. It is necessary to correct for the initial thorium contamination to obtain an accurate age.

The solution to the radioactive decay equation for ^{238}U and its daughters can be solved for the age of the coral, assuming the system is closed with respect to U and Th and the initial ^{230}Th content is zero. The resulting equations (Edwards, 1988; Edwards et al., 1987b, modified from Kaufman and Broecker, 1965) are as follows:

$$\left[\frac{^{230}\text{Th}}{^{238}\text{U}}\right] = 1 - e^{-\lambda 230 t} + \left(\frac{\delta^{234}\text{Umeas.}}{1000}\right)\left(\frac{\lambda 230}{\lambda 230 - \lambda 234}\right)(1 - e^{-(\lambda 230 - \lambda 234)t}) \tag{1}$$

and

$$\delta^{234}\text{U}(t) = (\delta^{234}\text{Umeas.})(e^{-(\lambda 234(t))}) \tag{2}$$

where (δ^{234}Umeas.) is the measured δ^{234}U, δ^{234}U(t) is the δ^{234}U at the time of coral formation, and the λ's are the decay constants for each isotope. $\left[\frac{^{230}\text{Th}}{^{238}\text{U}}\right]$ is the ^{230}Th/^{238}U activity ratio, and is calculated by multiplying the ratio of the decay constants $\lambda 230/\lambda 238$ by the measured atomic ratio of ^{230}Th/^{238}U.

These are two independent equations to calculate the coral age. Equation (2) depends on the initial δ^{234}U, which, in unaltered samples, should be equal to that of sea water. However, if Equation (1) is used to determine the age, Equation (2) can then be used to calculate the initial δ^{234}U. This provides a useful check on the assumption of

closed system behavior. If oceanic $\delta^{234}U$ has not changed significantly over time, as it appears it has not (Chen et al., 1986; Edwards, 1988; Stein et al., 1991), the calculated initial $\delta^{234}U$ should be equal to that of sea water if the system has indeed been closed. If the calculated initial value appears greatly different than the sea water value, it is an indication that ^{234}U has been added or removed since the deposition of the skeletal carbonate. Hence the assumption of a closed system is invalid, and the calculated ^{230}Th age is suspect.

With time, ^{238}U and ^{234}U return to secular equilibrium ($\delta^{234}U$ goes to zero), and Equation (1) reduces to $[^{230}Th/^{238}U] = 1-e^{-\lambda_{230}t}$. As t goes to infinity $[^{230}Th/^{238}U]$ asymptotically approaches one. Ultimately, as the age increases and the activity ratio nears one, analytical measurement errors make useful distinctions between ages impossible.

Until the 1980's, most U-Th measurements were done with alpha-spectrometry. The development of thermal ionization mass spectrometric (TIMS) methods of measuring nuclide abundances in various substances greatly improved analytical precision and increased the effective age range of U-Th as a geochronologic tool (Chen et al, 1986; Edwards et al, 1987a; Edwards, 1988). The effective age range for precise ^{230}Th dating is 0 to about 500,000 yrs. The ages of corals less than a few decades old may have uncertainties of ±1 or 2 years; ages of 100-200 years may have uncertainties of ±3 or 4 years; 8000 years, ± 50 years; and 120,000 years, ± 1,000 years (Table 3.1; Edwards et al., 1987a; Edwards, 1988).

3.2b. Previous work with corals

Dating corals with ^{230}Th methods began in earnest in the 1960's. Thurber and others (1965) measured U and Th isotopic abundances in corals and showed that ^{230}Th ages were equivalent to corrected ^{14}C ages but more precise. U and Th isotopic

measurements were made with alpha-counting techniques. The coral dating method was primarily used to date Quaternary sea level fluctuations.

Advances in mass spectrometric methods of measuring isotopic abundances led to significant increases in the precision of ^{230}Th ages (Chen et al, 1983; Chen and Wasserburg, 1984; Chen et al, 1986; Edwards et al, 1987a; Edwards, 1988). With the precision afforded by the new techniques, corals could be used to produce precise Quaternary sea level records and differentiate between sea-level highstands that previously had been impossible to distinguish. Many studies of Quaternary climatic history, especially of the Last Interglacial period (about 125 kA) have used TIMS U-series dating for geochronologic control (e.g. Edwards, 1987b; Stein et al., 1993; Muhs and Szabo, 1994; Gallup et al., 1994).

The newly acquired precision in coral dating meant that U-Th methods could be used to distinguish events on shorter time scales. For young corals (<200 yrs) this could be on the order of a few years (±5 yrs) (Edwards et al., 1987a), which is desirable for Quaternary paleoseismic applications, where recurrence intervals between events can be on the order of tens or hundreds of years. Edwards and others (1987c) presented the idea of using coral-dating as a geochronologic tool for paleoseismology in marine environments. Uplifted corals in Vanuatu were dated; the coincidence of coral death ages signified possible coseismic uplift as the cause of death. Since then, fossil corals dated with high-precision ^{230}Th ages have been used successfully to date and document paleoseismic events (Edwards et al., 1988; Taylor et al., 1990).

3.3. Laboratory methods

All laboratory work was performed at the Minnesota Isotope Laboratory at the University of Minnesota.

Table 3.1. ^{230}Th dates of Sumatran corals

Measured U and Th isotopic composition and calculated ages of corals from the Mentawai Islands, Sumatra (Figure 1). Sample names reflect the island where they were collected (NP-North Pagai; P (and Pg)-South Pagai; Si (and Spr) - Sipora; Sd - Sanding), the year they were collected (94, 96), the site they came from (different sites on each island are labeled with a different letter - see Figure 1), and the sample number. Multiple samples from the same coral head are presented together, the additional samples indented under the first. Samples with different names from the same came from different locations within the coral. For example, NP94-A-5A2.A is from the interior core of slab NP94-A-5, and NP94-A-5A1(1).A is from the exterior rim. Samples with the same name followed by (A) or (B) are multiple measurements from the same part of the coral. Some sites were visited and corals sampled in both 1994 and 1996 - these have different names but are from the same coral, e.g. P94-Z-4B.B and P96-F-1.B.

The genera in column 2 are: P-Porites; G-Goniastrea; F-Faviidae; C-Cyphastrea.

Errors follow the measured and calculated values in parentheses. Isotopic errors and the error in column 8, age BP (sample), are 2σ. The uncertainties in column 9, date of death (coral), include the 2σ analytical uncertainty and errors in counting of annual bands. Column 10, corrected date, errors include analytical and ring counting errors as well as the estimated uncertainty in the correction factor.

Calculated dates were corrected for contamination with initial thorium. The contaminant was assumed to have ^{230}Th/^{232}Th = 6.0 (+7.0/-6.0) x 10^{-6}. Isotopic concentrations and ratios were corrected by subtracting the component attributable to the contaminant; the ages were then recalculated with the corrected values.

Table 3.1 - U-Th analyses of Sumatran corals

sample name	genus	U238 (ppb)	Th232 (ppt)	230/232 x10-6	[230/238] x10E-5	d-234 initial	age BP (sample)	date of death (coral)	corrected date
NP94-A-5A1(1).A	P	2488 (4)	358 (27)	311	272	149.2 (1.3)	212 (7)	1792 (17)	1797 (18)
NP94-A-5A2.A	P	2486 (3)	2716 (130)	48.8	324	150.3 (1.4)	262 (7)	1772 (26)	1810 (51)
NP94-A-6.A	P	2632 (3)	2664 (13)	165	1013	148.0 (1.2)	919 (7)	1041 (7)	1076 (42)
NP94-A-7.A	P	2527 (3)	2666 (43)	184	1180	147.7 (1.2)	1081 (9)	872 (9)	909 (44)
NP94-A-8A1(2).B	P	2505 (7)	502 (12)	184	225	148.4 (2.4)	168 (3)	1836 (7)	1842 (11)
NP94-A-8A4(1).B	P	2492 (3)	624 (5)	123	187	147.1 (1.1)	133 (5)	1832 (5)	1841 (11)
NP94-A-9A1.B	G	2159 (2)	173 (13)	357	174	151.1 (1.2)	120 (6)	1834 (6)	1837 (7)
NP96-A-2.B	P	2485 (3)	5829 (81)	37.4	534	149.5 (1.4)	460 (27)	1505 (27)	1586 (99)
NP96-B-1.A	P	2796 (6)	239 (8)	534	278	147.3 (1.4)	218 (9)	1736 (9)	1739 (10)
NP96-B-2.A	P	2564 (3)	1590 (9)	125	473	144.7 (1.1)	404 (6)	1560 (6)	1581 (26)
NP96-B-4.A	P	3110 (5)	879 (3)	292	502	149.7 (1.5)	430 (3)	1523 (3)	1533 (12)
NP96-C-1.B	P	2586 (4)	884 (13)	110	229	145.3 (1.6)	171 (6)	1795 (6)	1807 (15)
NP96-C-2.A	P	2712 (11)	347 (17)	260	203	147.5 (2.9)	145 (11)	1820 (11)	1824 (12)
NP96-C-3.A	P	2420 (3)	3218 (20)	27.0	218	146.2 (1.4)	161 (5)	1798 (5)	1844 (54)
NP96-C-4.A	P	2400 (3)	1033 (4)	76.2	199	149.4 (1.2)	143 (3)	1814 (3)	1829 (18)
NP96-C-5.B	P	2660 (4)	912 (4)	109	226	150.8 (1.4)	168 (3)	1787 (3)	1799 (14)
P93-B-2	P	2434 (3)	115.2 (3.6)	6799	1957	150.3 (1.2)	1822 (17)	133 (17)	134 (17)
P93-C-2	P	2708 (3)	27781 (1675)	18.3	1141	149.0 (1.2)	1042 (37)	911 (37)	1267 (418)
P93-C-3	P	2619 (5)	17686 (963)	32.4	1332	149.8 (2.4)	1224 (30)	731 (30)	965 (276)
P93-C-7(A)	P	2290 (3)	37381 (2377)	12.3	1220	148.4 (1.2)	1118 (62)	832 (62)	1398 (665)
P93-C-7(B)	P	2366 (4)	12390 (1593)	20.1	639	146.8 (1.7)	564 (84)	1396 (84)	1578 (228)
P93-C-8(A)	P	2174 (2)	35279 (2497)	13.0	1278	149.5 (1.2)	1174 (64)	776 (64)	1339 (661)
P93-C-8(B)	P	2136 (5)	81147 (5461)	10.1	2327	151.7 (2.5)	2177 (220)	-222 (220)	1099 (1560)
P94-AA-1A.A	G	2218 (5)	84.3 (1.3)	9563	2210	149.7 (1.3)	2066 (14)	-103 (14)	-102 (15)
P94-AB-2A.C	P	2326 (5)	3711 (82)	52.4	510	144.5 (2.1)	440 (5)	1517 (5)	1572 (65)
P94-C-1.B	F	2250 (3)	981 (11)	2555	6770	149.7 (1.3)	6564 (59)	-4609 (59)	-4593 (62)
P94-C-3.B	P	2468 (3)	548 (4)	6112	8250	147.5 (1.3)	8078 (79)	-6114 (79)	-6105 (80)
P94-D-1.B	P	2681 (3)	1791 (9)	7.5	31	148.6 (1.2)	-16 (4)	1967 (4)	1990 (27)
P94-H-1A.A	P	2639 (2)	2631 (184)	41.1	250	148.5 (1.2)	192 (7)	1766 (7)	1807 (30)
P94-H-2.A	P	3492 (6)	638 (36)	186	206	146.8 (1.5)	151 (4)	1809 (6)	1817 (8)
P94-M-2.B	F	3437 (7)	8338 (80)	422	6230	151.8 (1.7)	6012 (43)	-4049 (43)	-3965 (112)
P94-M-3.A	F	3272 (6)	377 (29)	10444	7310	146.6 (1.4)	7131 (250)	-5175 (250)	-5169 (250)
P94-M-4.A	P	2257 (5)	99 (2)	638	171	146.9 (2.5)	117 (8)	1835 (8)	1836 (9)
P94-R-3.A	P	2292 (3)	320 (2)	92.1	78	148.3 (1.2)	29 (4)	1934 (4)	1939 (7)
P94-S-1.B	P	2141 (2)	4724 (333)	21.3	286	148.3 (1.3)	227 (9)	1731 (10)	1807 (90)
P94-S-3B.B	G	2077 (2)	553 (6)	113	183	148.5 (1.2)	128 (4)	1825 (4)	1834 (11)
P94-W-1.B	P	2496 (4)	2897 (139)	30.4	215	149.6 (1.7)	159 (5)	1794 (5)	1835 (47)
P94-X-1.A	G	1487 (1)	337 (17)	129.6	179	150.7 (1.1)	124 (8)	1830 (8)	1838 (12)
P94-X-3.B	F	2325 (3)	347 (13)	210	191	148.8 (1.2)	136 (3)	1829 (4)	1834 (7)
P94-X-4.A	G	2003 (2)	222 (4)	254	171	147.4 (1.1)	117 (4)	1836 (4)	1839 (6)
P94-Y-1A.A	G	2026 (2)	133 (2)	20742	8291	151.7 (1.2)	8093 (45)	-6142 (45)	-6139 (45)
P94-Y-3A.B	P	2381 (3)	1073 (12)	71.6	196	148.3 (1.4)	140 (3)	1815 (3)	1830 (18)
P94-Z-1A.A	P	2233 (3)	3880 (67)	70.5	745	149.7 (1.2)	662 (11)	1296 (11)	1356 (71)
P96-F-2.2.A	P	2583 (3)	3612 (15)	84.2	716	145.9 (1.3)	636 (6)	1322 (6)	1371 (57)
P96-F-3.B	P	2513 (3)	3614 (21)	82.0	717	149.8 (1.2)	635 (5)	1323 (5)	1373 (58)
P94-Z-2A.A	P	2714 (6)	1324 (47)	243	720	152.0 (1.4)	637 (10)	1328 (11)	1345 (23)
P94-Z-4B.B	G	2068 (2)	359 (48)	184	194	148.7 (1.2)	139 (6)	1818 (6)	1824 (9)
P96-F-1.B	G	1972 (2)	823 (14)	75.2	191	144.7 (1.2)	135 (4)	1817 (4)	1831 (17)

sample name	genus	U238 (ppb)	Th232 (ppt)	230/232 x10-6	[230/238] x10E-5	d-234 initial	age BP (sample)	date of death (coral)	corrected date
P96-B-2	P	2263 (4)	797 (29)	8.2	18	151.1 (2.0)	-29 (5)	1990 (5)	2003 (15)
P96-E-1.C	P	2606 (4)	5731 (33)	37.6	504	151.1 (1.3)	431 (5)	1532 (5)	1608 (89)
P96-E-2.C	P	2738 (4)	16127 (79)	18.0	645	150.8 (1.2)	566 (4)	1391 (4)	1595 (238)
P96-E-3.A	G	2703 (3)	170 (9)	1077	412	145.3 (1.2)	346 (3)	1606 (3)	1608 (4)
P96-H-1.A	P	2278 (15)	774 (6)	91	187	143.5 (1.3)	132 (3)	1824 (3)	1836 (14)
P96-I-1.A	P	2688 (4)	342 (16)	225	175	148.1 (1.3)	119 (15)	1835 (15)	1839 (16)
P96-J-1.A	P	2456 (3)	190 (7)	359	169	149.0 (1.2)	114 (10)	1839 (10)	1842 (11)
P96-J-2.C	P	2518 (4)	253 (8)	304	186	151.1 (1.2)	130 (4)	1831 (4)	1835 (6)
P96-K-1.B	P	2704 (4)	127 (3)	650	186	146.9 (1.3)	130 (3)	1830 (3)	1831 (3)
P96-K-4.A	P	2510 (6)	540 (40)	157	205	150.1 (2.2)	148 (12)	1810 (13)	1817 (16)
P96-K-5.A	P	2246 (5)	419 (7)	169	192	148.8 (2.1)	136 (6)	1821 (6)	1827 (10)
P96-L-1.1.C	P	2353 (2)	1019 (8)	133	350	149.1 (1.2)	286 (5)	1673 (5)	1688 (18)
P96-L-2.A	P	2296 (2)	542 (6)	258	371	150.7 (1.2)	305 (4)	1654 (4)	1662 (10)
P96-M-1.A	P	2644 (4)	4092 (40)	45.7	430	146.5 (1.3)	362 (6)	1603 (6)	1656 (63)
P96-N-1.B	P	2407 (6)	481 (103)	129.2	157	152.5 (2.3)	102 (32)	1860 (32)	1866 (33)
P96-N-2.A	P	2258 (3)	11010 (67)	13.3	395	150.7 (1.3)	328 (7)	1632 (7)	1800 (197)
P96-N-3.A	P	2299 (3)	9380 (47)	14.6	361	149.5 (1.3)	296 (4)	1662 (4)	1803 (165)
P96-N-4.B	P	2199 (2)	20827 (188)	10.5	605	151.0 (1.3)	527 (16)	1434 (16)	1761 (382)
P96-N-5.A	C	2342 (3)	3632 (15)	26.2	247	150.7 (1.1)	188 (3)	1765 (3)	1819 (63)
P96-O-1.A	P	3045 (4)	6434 (34)	454	5832	151.5 (1.3)	5612 (32)	-3658 (32)	-3583 (95)
P96-O-2.B	P	2557 (4)	15462 (135)	165	6082	149.9 (1.5)	5870 (36)	-3912 (36)	-3700 (259)
P96-P-1.B	P	3013 (4)	4075 (26)	32.4	266	151.4 (1.2)	206 (5)	1750 (5)	1831 (55)
P96-P-2.B	P	2482 (4)	123 (17)	776	234	151.0 (1.9)	175 (25)	1777 (25)	1778 (25)
P96-Q-1.A	G	2503 (4)	799 (9)	121	234	150.9 (1.4)	176 (9)	1789 (9)	1800 (16)
Pg04A-0.0.1(A)	P	2169 (2)	21112 (1336)	7.17	424	149.6 (1.7)	359 (20)	1591 (20)	1928 (393)
Pg04A-0.0.1(B)	P	2195 (2)	12479 (2735)	6.4	222	149.3 (1.2)	166 (36)	1789 (36)	1985 (232)
Pg04E-0.0.2(A)	P	2464 (2)	2745 (105)	29.6	200	149.0 (1.2)	147 (4)	1803 (4)	1842 (45)
Pg04E-0.0.2(B)	P	2157 (2)	1522 (185)	48.2	206	150.8 (1.2)	151 (11)	1802 (11)	1826 (31)
Pg04G-0.0.2(A)	P	2152 (2)	23087 (2067)	8.56	558	149.3 (1.2)	487 (29)	1463 (29)	1834 (434)
Pg04G-0.0.2(B)	P	2187 (3)	8124 (668)	13.6	308	148.9 (1.4)	248 (12)	1706 (12)	1834 (150)
Si94-A-1A.A	P	2597 (4)	607 (12)	212	301	149.9 (1.3)	240 (3)	1716 (4)	1724 (12)
Si94-A-2.A	P	2517 (3)	867 (6)	124.0	260	147.0 (1.2)	202 (6)	1759 (6)	1771 (15)
Si94-A-3.A	P	2513 (3)	849 (9)	113	233	148.1 (1.2)	176 (7)	1778 (7)	1790 (15)
Si94-A-5(1).A	P	2622 (3)	660 (5)	169	259	151.5 (1.2)	200 (4)	1759 (8)	1769 (12)
Si94-A-6A4.A	P	2613 (3)	164 (15)	556	212	150.8 (1.2)	155 (6)	1827 (7)	1829 (7)
Si94-A-6A3.A	P	2534 (3)	179 (9)	559	240	149.0 (1.5)	182 (5)	1822 (5)	1824 (5)
Si94-B-1.B	P	2526 (2)	4424 (431)	26.8	285	147.8 (1.4)	226 (25)	1728 (25)	1789 (75)
Spr9-0.0.3	P	2364 (3)	6774 (1407)	3.0	52	149.3 (1.2)	6 (5)	1948 (5)	2047 (116)
Sd96-A-1.1.B	P	2342 (4)	189 (4)	69.3	34	148.4 (1.5)	-14 (3)	1979 (3)	1982 (4)
Sd96-C-1.1.1.A(96-35)	P	2815 (4)	230 (3)	78.5	39	150.1 (1.2)	-9 (4)	1994 (4)	1997 (5)
Sd96-C-1.1.2.A(96-32)	P	2575 (5)	368 (7)	9.6	8	150.5 (1.7)	-38 (1)	1988 (1)	1993 (6)
Sd96-C-1.1.2.A(96-33)	P	2747 (5)	4537 (15)	11.7	118	150.5 (1.2)	65 (2)	1896 (2)	1953 (67)
Sd96-C-1.1.2.A(96-34)	P	2880 (4)	138 (1)	77.4	23	150.6 (1.2)	-25 (1)	1996 (1)	1997 (2)
Sd96-C-1.2.A	P	2667 (5)	234 (4)	118	63	150.7 (1.3)	13 (2)	1937 (2)	1940 (4)
Sd96-C-1.3.A	P	2428 (3)	185 (2)	9.5	4.4	150.2 (1.2)	-42 (1)	1992 (1)	1994 (3)
Sd96-C-2.B	P	2409 (5)	84 (12)	73.5	16	147.0 (2.3)	-31 (3)	1986 (3)	1987 (4)

3.3a. Sample preparation

Coral samples were collected in the field as either 10 cm thick slabs or large hand samples. I sliced these samples into thin (4-10 mm) slabs, parallel to the growth direction. I then x-rayed the thin slabs to reveal the annual growth bands.

To get samples for dating, I used a hammer and small chisel to break out a piece from the thin slabs, preferably from a single annual band, from the cleanest part of the coral. I sampled as close to the outside as possible given cleanliness restrictions, so as to minimize the age uncertainties from ring counting, since in general I was interested in finding the age of the outermost ring. Areas with a sugary or powdery texture that looked as if they might have experienced recrystallization and possible diagenesis, which would yield inaccurate ages, were avoided. Most of the sampled corals were very young, less than 500 years, so the chances of alteration were small. XRD examination of a few samples showed virtually pure aragonite, with no secondary calcite (J. Hsieh, written comm.). The samples had little or no interstitial cementation.

I broke the sampled piece into small chunks about 1-3 mm thick. I examined the pieces under a microscope and removed any pieces with visible detritus and any especially dark and discolored parts. Some samples were filthy throughout, but the cleanest, whitest portions were selected. I put the selected pieces in a vial, rinsed them in distilled super clean water, and put the vial in an ultrasonic bath for three sequences of ultrasonication and rinsing. Some samples were also cleaned with a handheld ultrasonicator that removed more tightly bound detritus from the outermost layers. After ultrasonicating, I placed the samples in a low-heat oven to dry thoroughly.

3.3b. Chemical procedures

The samples were prepared with methods similar to those described by Chen and Wasserburg (1981), Chen and others (1986), Edwards (1988), Gallup and others (1994),

and Gallup (1997). I weighed the rinsed, dried samples, then covered them with water and slowly dissolved them in 7N nitric acid. Most samples weighed between 1 and 3 grams. I then spiked the acid-sample solution with U and Th spikes. The U-spike was a double ^{233}U-^{236}U spike with $^{233}U/^{236}U\sim1$, and a ^{233}U concentration of about 9.3 pmol/g, and was added such that $^{238}U/^{233}U$ ratio was 10-20, usually. The Th spike was a single ^{229}Th spike, with a concentration of about 0.2 pmol/g. I usually added about 0.5-1 g of spike for a gram of sample. The concentration of the uranium spike was periodically calculated by measuring mixtures of spike and gravimetric uranium standard (NBL 112a). The ^{229}Th spike was mixed with a gravimetric standard of Ames Th to determine concentration.

After spiking, I dried the spiked solution, then added about 25-40 drops of perchloric acid to assure the spike and sample were in equilibrium/in the same oxidation state, and dried the solution again. Once the sample was fully dry, I dissolved it in 2N HCl and added 2-6 mg iron in a chloride solution, which made the solution bright yellow. I then added concentrated NH_4OH to the solution until the color changed to clear and the iron, with the U and Th, began to precipitate. The mixture was centrifuged and the supernate discarded. I rinsed the precipitate with pH 8 superclean water twice, and centrifuged after each rinse, discarding the supernate after each centrifugation. I dissolved the precipitate in 14N HNO_3 and dried it down, repeating this sequence three times.

The elution scheme to remove the U and Th from the iron mixture was patterned after the methods of Edwards (1988) and Gallup (1997). For the first step, I prepared a 750-800 µl column filled with anion exchange resin, which had been cleaned in bulk by rinsing with a sequence of HNO_3, HCl, and water. I prepared the resin for the sample by running three column volumes (cv) of 7N HNO_3 through it. I dissolved the sample in 1 cv of 7N HNO_3 and added this to the resin. The sample was then rinsed with 1 cv of 7N HNO_3 to separate and remove the iron. The Th fraction was eluted into a clean vial with

3 cv of 6N HCl, 1 cv at a time. The U fraction was then eluted with 4 successive column volumes of 1N HBr or H_2O. The U and Th fractions were then dried and dissolved in 14N HNO_3 three times.

To clean the fractions, I prepared a 175 µl resin column in the same way as above. The Th fraction was dissolved in 1 cv of 7N HNO_3, added to the column, rinsed with 1 cv of 7N HNO_3 and withdrawn with 4 cv 6N HCl. The resin was then flushed with water and equilibrated again with 3 cv of 7N HNO_3. The U fraction, dissolved in 1 cv of 7N HNO_3, was added, rinsed with 1 cv of 7N HNO_3 and removed with 4 cv of 1N HBr or H_2O. I dried and redissolved the cleaned fractions in 14N HNO_3 three times in preparation for loading onto filaments.

3.3c. Loading

The samples were dissolved in 0.1N HNO_3 and loaded with pre-cleaned polyethylene syringe tubing onto zone-refined rhenium filaments. I loaded about 1/5 of the U fraction onto the evaporation side of a parallel double filament. About two-thirds of the Th fraction was loaded onto a single filament, and either topped with or sandwiched between layers of colloidal graphite after the method of Chen and Wasserburg (1981).

3.3d. Mass spectrometric methods

The samples were analyzed on the Minnesota Isotope Laboratory's Finnegan-MAT 262-RPQ thermal ionization mass spectrometer. Both uranium and thorium were measured using the electron multiplier in pulse counting mode. The uranium sample was run with the evaporation filament at about 0.8-1.0 A of current and the ionization filament at about 4 A and a temperature of around 1700-1800°C. Data were gathered in peak-jumping mode - by sequentially measuring masses 233, 233.5, 234, 234.4, 235 235.5, and 236. Mass 238 was not measured directly because the signal from ^{238}U was

too large for the ion counter. Rather, mass 235 was measured. Ratios and concentrations involving ^{238}U were ultimately calculated from the measured 235 values assuming a natural $^{238}U/^{235}U$ ratio of 137.88 (Ivanovich and Harmon, 1992). Each mass was measured for four seconds; the ^{234}U peak was measured four times in succession for a total of 16 seconds. Under typical conditions, a ^{235}U beam of 200,000 counts per second (cps) was maintained, and about 150 to 200 scans of this mass spectrum was sufficient to yield 2σ counting statistics of 1‰ on ^{234}U. An exponential fractionation correction was applied to all ratios using the measured ^{233}U-^{236}U ratio in each scan.

Thorium data were collected with filament currents at about 4 amps. The temperature associated with the current varied considerably between samples and within a single run, depending on the amount of graphite, the degree to which the graphite had bonded with the filament, the thickness of the filament, etc. Usually analyses began with temperatures in the 1600°-1700° range and ended with the filament burning through at about 2000°. The peak-jumping sequence for thorium runs was ^{229}Th (4 seconds)-^{230}Th (16 s) -^{230}Th (16 s) -^{232}Th (4 s). Thorium runs continued until the sample was gone and/or the filament burned through. Because most of the samples were young (< 500 yrs) counting statistics for ^{230}Th generally yielded uncertainties nearer 1 % than 1‰. Ratios were corrected for an observed multiplier mass bias of 0.8 ‰/amu.

3.3e. Calculations and corrections

The measured isotopic ratios were used to calculate the concentrations of ^{234}U, ^{238}U, ^{230}Th, and ^{232}Th, which were in turn used with equations (1) and (2) to determine the age of the sample and its current and initial $\delta^{234}U$ values. All raw data were fully propagated through corrections for: 1) spike impurities, 2) abundance sensitivity, 3) dark noise, and 4) filament and analytical blanks.

For ^{234}U, the measurement positions of masses 233.5 and 234.4 were used to correct for the tail of the ^{238}U peak at mass 234. This correction, in 234/235 ratio, was typically about 5 ‰. Mass 235.5 was measured to correct the 236 peak for tail effects as well. Spike corrections were made for the contribution of ^{234}U and ^{235}U from the ^{233}U-^{236}U spike. Given typical spike/sample ratios of 1/3-1, this amounted to a correction of 1-4% for 234 and 1-3% for 235. The corrected ^{234}U/^{238}U was calculated from the ^{234}U/^{235}U ratio assuming a natural ^{238}U/^{235}U ratio of 137.88. Likewise, ^{238}U concentrations were calculated from the corrected ^{235}U/^{233}U ratios. The ^{238}U concentration was further corrected for analytical blanks. Blanks were measured periodically during the course of the study. The blank correction was usually very small, about 0.005 ‰. The largest blank measured, 0.2 pmol, generated blank corrections in ^{238}U concentration of 0.02 ‰.

For thorium, similar corrections were applied to measured data. ^{230}Th was corrected for contributions of ^{230}Th from the ^{229}Th spike. The relative magnitude of this correction varied considerably, being much more significant in younger samples. In my oldest samples, about 8000 years old, the spike correction was about 0.2 ‰; in 200 year old samples, about 1%; and in an 8 year old sample, about 6%.

The thorium data were also corrected for tail contributions from ^{232}Th and ^{229}Th. In a typical sample this correction was insignificant, less than 1 ‰, but for very young, somewhat dirty samples, it was as much as 8 %. The abundance sensitivity measurements at 1 amu and 2 amu were either made directly on high ^{232}Th samples, or estimated from measurements of the ^{238}U tail at masses 237 and 236. Corrections for dark noise on the SEM were generally about 1% or less, as typical ^{230}Th beams were 10 to 500 cps and darknoise was < .08 cps. However, in very young samples, where ^{230}Th count rates were <5 cps, darknoise corrections could be as much as a few percent. Finally, corrections for analytical blank were again highly dependent on the age of the sample. 230 blanks were

usually about 0.01 fmol. For 8000 year-old samples, this generated a correction of about 0.2 ‰; for 200 year old samples, about 5 ‰; for an eight year old sample, 3 %.

For ^{232}Th, I corrected the raw data for filament and analytical blanks. Filament blanks were estimated by running filaments loaded with only a small amount of graphite through 1600° to 2000° while monitoring masses 229, 230 and 232. Filaments with anomalously high 232 count rates were discarded. The importance of the filament blank correction depended strongly on the degree of ^{232}Th contamination in the sample. The correction was negligible in dirty samples with high ^{232}Th concentration, but were as high as 3% for clean samples with low ^{232}Th concentrations. Chemistry blanks for ^{232}Th were generally about 0.05 pmol. Corrections for analytical blank in ^{232}Th in most cases were about 1%.

3.4. Results and Discussion

3.4a. Isotopic measurements

The results of the mass spectrometric analysis of all sampled corals are presented in Table 3.1. Uranium concentrations of the analyzed coral sample (column 3) range between 1500 and 3500 ppb, which is consistent with uranium concentrations in corals determined in other studies (e.g. Edwards et al., 1987b; Muhs and Szabo, 1994; Stein et al., 1993; Eisenhauer et al. 1993). Most are between 2000 and 3000 ppb. The lower concentrations are found primarily in *Goniastrea* sp. corals. ^{232}Th concentrations (column 4) are highly variable, ranging from 84 to over 80,000 pg/g. Because thorium is not present in sea water in high concentrations, the presence of significant amounts of ^{232}Th in the corals indicates contamination from detrital sources. ^{232}Th concentration and the effects of thorium contamination will be discussed later.

The initial $\delta^{234}U$ values were calculated using equation (2) and the ^{230}Th age (column 7). Because most of these corals are very young, the measured $\delta^{234}U$ values are usually about the same as the calculated initial values. These range from 143.5 to 152.5, with a mean value of 149.1 ± 3.8 (2σ). These values are consistent with measured $\delta^{234}U$ values for living coral and open ocean water (Edwards, 1988; Edwards et al., 1988; Chen et al., 1991; Eisenhauer et al., 1993;) and support the assumption that the system has remained closed with respect to uranium since deposition of the coral skeleton.

The eighth column of the table shows the ^{230}Th ages (BP) of the sampled pieces, with only analytical uncertainties (2σ). The ninth column contains the dates of the outermost part of the coral, determined by counting annual rings out from the sampled piece to the edge and subtracting the years represented by these rings from the analytical age of the sampled piece. The uncertainties include both the analytical error for the sample and a ring counting error. Ring counting errors were dependent on the clarity of the annual growth bands in the x-radiographs of cross-sectional slabs through the corals. I calculated the difference between my best estimate of the number of rings from sample to outer edge and the maximum and minimum number of intervening rings I thought possible. I used the larger of these differences as the ring counting uncertainty. In most cases, the date in the ninth column corresponds to the date of death of the coral. A few of the corals dated were still living, and in these cases the age and date shown in the eighth and ninth columns are the age and date of the outermost, living ring. The last column in Table 3.1 contains the dates of coral death (or the most recent ring growth) that have been corrected for initial thorium contamination. The nature of the correction is discussed later.

3.4b. Correcting for contamination with initial thorium

The concentration of Th in sea water is low (Chen et al., 1986; Andersson et al., 1994; Moran et al., 1995, 1997), and because corals effectively exclude Th in their

skeletons, there should be very little Th in pristine living corals (Edwards et al., 1987a; Edwards, 1988). This permits one to assume that ^{230}Th is negligible such that equation (1) can be solved for the coral age. If one assumes that there is no initial thorium nor any diagenetic effects in the sample, then all ^{230}Th present in a fossil coral must be a decay product of the ^{234}U and thus can be used to calculate the age of the coral. If the assumption of zero initial ^{230}Th is incorrect, if there is indeed thorium in the living coral in appreciable quantities, then the age calculation for fossil corals will yield a ^{230}Th age that is falsely old. Only if one knows how much ^{230}Th was originally in the coral can the age equation be solved for the correct age.

The assumption of zero initial ^{230}Th is subject to a check. ^{230}Th and ^{232}Th behave chemically similarly and presumably are incorporated into the coral skeleton in the same ratio in which they exist in sea water (^{230}Th/^{232}Th ~ 1-50 x 10^{-6}). The half-life of ^{232}Th is long, about 1.40 x 10^{10} yrs, and is essentially stable on time scales relevant to this dating method. If corals contain ^{232}Th in significant amounts, it indicates that the assumption of zero initial ^{230}Th is incorrect and that some quantity of thorium from other sources has been introduced into the coral skeleton during growth. The source of this initial thorium could be detrital material that is incorporated into the skeleton, or it could be that the water in which the coral grew had an abnormally high thorium concentration.

The first coral samples from this study were collected in summer 1993, and analyzed in October 1993. These dated samples had been collected from the outermost ring of a hand sample, without particular regard to the color and "dirtiness" of the coral. They had been cleaned in an ultrasonic bath before chemical preparation. However, this had failed to remove most of the discoloration. When analyzed, the samples showed very high ^{232}Th concentrations, as high as 35000 pg/g (P93-C-7(A), P93-C-8(A), Pg04A-0.0.1(A), Pg04E-0.0.2(A), and Pg04G-0.0.2(A) in Table 3.1). This indicated that there was a source of contamination that had introduced anomalous, excess thorium into the

skeleton. It implied that the uncorrected dates were inaccurate. The calculated age of Pg04A-0.0.1(A), 359±20 yrs BP bore out that suspicion since the sample was taken from the interior of a live coral that was probably not big enough to be 400 years old, given that annual bands are about 1±0.5 cm thick.

My first attempt to decipher the effects of the thorium contamination involved trying to find cleaner pieces of coral to sample. If the contaminant were detrital in origin, and were only present in the interstices of the coral skeleton rather than within the calcium carbonate structure itself, possibly it could be physically removed. I selected new samples for dating from several of the same hand sample specimens that had had such high thorium concentrations. Instead of merely sampling the outermost piece of the coral, I selected the cleanest-looking, whitest piece I could find in each. As the slabs were generally darkest at the outside and whitest deep in the interior, the new dating samples were usually far from the edge. However, the age of the outermost layer could be determined from counting growth bands out from the interior sample. Having selected the whitest part of the coral, I then cleaned the slab with a hand-held ultrasonicator in a water bath. The ultrasonicator was capable of removing a large amount of debris from the interstices of the skeleton and the samples were noticeably cleaner. I then prepared the samples for dating following normal procedures.

In the second round of analyses (shown in Table 3.1 with the (B) ending), almost all the corals had substantially lower ^{232}Th concentrations than in the original runs, with the exception of P93-C-8(B) which was much higher than in the first run, and indeed was substantially higher than any other sample. The ^{232}Th concentration in the other samples however decreased to one-half to one-third of the original values. As expected, the calculated ages decreased significantly, indeed well out of the range of the analytical uncertainty of the uncorrected ages. Furthermore, the cleaning improved the precision in several cases. In general, dirty, brown samples with high ^{232}Th concentrations have

relatively large analytical uncertainties. They don't load as easily or run as well, the ionization efficiency decreases, and high ^{232}Th concentrations with consequently low ^{229}Th $/^{232}$Th and ^{230}Th $/^{232}$Th values require that the counting rate for ^{229}Th and ^{230}Th must stay very low while measuring. This leads to greater imprecision.

The treatment of the 1993 samples and consequent improved results indicated that analyzing clean samples was of paramount importance in obtaining accurate and precise results. During the 1994 and 1996 field seasons, I was very careful to select the cleanest specimens I could find in the field. The correlation between white color and high ^{230}Th/^{232}Th was very strong. It was generally easy to estimate in the field how contaminated the sample would be. There was also a correlation with species. *Porites* sp. tended to be much dirtier and much more contaminated than other larger-pore corals such as *Goniastrea*. In some cases, such as at site P96-E, where the two *Porites* corals, which were excellent samples morphologically, were filthy, I sampled a *Goniastrea* along with the *Porites* to better constrain the age of death of the corals, assuming that all had died simultaneously. Indeed the two *Porites* samples (P96-E-1 - 1608±89, P96-E-2 - 1595±238) and the *Goniastrea* sample (P96-E-3 - 1608±4), yield replicate corrected ages, but the *Goniastrea* sample yields a much more precise age because it was so much cleaner than the Porites samples. Thus, the emergence event that killed both the *Goniastrea* and *Porites* corals can be dated to ±4 years (corrected) using the *Goniastrea* date. By selecting clean field samples and then using the cleanest parts of those for dating and ultrasonically cleaning them further, I could reduce the contamination contributed by detrital material. In general, the ^{232}Th concentrations for later samples were substantially lower than the earlier ones.

Improving the selection of samples and choosing the cleanest possible corals makes a great difference, but it does not completely remove the problem of contamination. First, it is not always possible to find clean samples. The corals that were

appropriate for studying tectonic uplift occurred in the inter-tidal zone, near the shore of islands composed of old trench sediments and not far out to sea. In general, corals that are near shore tend to have higher ^{232}Th concentrations than do those in the open ocean (Andersson et al., 1994). Presumably, they are more likely to be contaminated by terrestrial material that is brought in by rivers and settles out as soon as it reaches the ocean. Furthermore, wave and tide action can stir up sediment from the sea floor and deposit it on coral heads. Although most well-preserved corals in the Mentawais occurred in bays and calm-water environments, they were often at the mouths of rivers that could have been a source of detritus. The Pagais and Sipora are composed of extremely unresistant, easily weathered rock, and the rivers draining them have a high silt content (Verstappen, 1973). Faced with the option of collecting dirty samples or no samples, I chose to take dirty samples, knowing I would have a problem with contamination. Secondly, the ultrasonic cleaning reduces the ^{232}Th concentration and presumably the amount of detrital material in the coral, but it doesn't remove all of the contaminant. The 1993 results implied that the contaminant was primarily detrital and at least partially if not primarily present as particulate matter in the skeletal interstices, since it could be removed with ultrasonic cleaning. Nevertheless, there is some fraction, inaccessible to ultrasonic cleaning, present in some form and incorporated in such a way that it cannot be removed physically. Thus, the problem requires an additional solution. One option, that I did not pursue, would be to chemically treat the samples to remove the remainder of the contaminant chemically after removing whatever I could mechanically with ultrasonication. Various chemical treatments have been attempted by other workers to remove the effects of initial thorium contamination in carbonates such as leaching of the contaminant or contaminated fraction (e.g. Ku and Liang, 1984; Schwarz and Latham, 1989). However, these have had only moderate success.

In the absence of any definitive method to remove the contaminant from the sample, and given that I often had no choice but to sample dirty corals, I have tried to remove the effects of the contamination by correcting for it in the age calculations. The idea of correcting for the presence of initial ^{230}Th is not new, and has often been done to account for excess thorium and/or stratigraphic inconsistencies (e.g. Stein et al., 1991 and Eisenhauer et al., 1993).

Simply, the correction subtracts the ^{230}Th that was present initially, as contaminant, using the measured ^{232}Th concentrations and assuming an initial $^{230}Th/^{232}Th$ ratio. Initially, I assumed the same $^{230}Th/^{232}Th$ ratio that has been used by other workers making similar corrections (e.g. Stein et al., 1991 and Eisenhauer et al., 1993). I assumed that the source of the contamination was detritus, incorporated at the time of original coral growth, that it had $^{232}Th/^{238}U=3.8$, the composition of average crustal material (Eisenhauer et al., 1993), and that the U and Th were in secular equilibrium. This yields a $^{230}Th/^{232}Th$ ratio of 4.4×10^{-6} for the contaminant. I used this ratio, with an arbitrarily assigned uncertainty of ±50%, to subtract the initial ^{230}Th due to contamination. I also used the assumed values to correct the ^{238}U and ^{234}U concentrations. In doing this, I assumed the contaminant had been incorporated at the start of coral growth, and not at a later time. Using the corrected uranium and thorium concentrations, I recalculated the ages.

Making a correction in this fashion is only valid for young samples. The ^{230}Th that was initially present also decays away. In young samples, this effect is negligible, but in older samples it can be significant, and would require a more complex formula to account for the decay of the initial ^{230}Th.

The accuracy of the corrected dates depends on the validity of the assumptions about the contaminant. One possibility for testing this is to measure the isotopic composition of the contaminant. However, that requires identifying and being able to

isolate the contaminant, which I did not do. Another possibility is to check the assumptions by testing the consistency of multiple measurements, and/or testing the correction with samples of known age. In fact, data from living samples corrected with $^{230}Th/^{230}Th$ (initial) = 4.4 ppm did not yield accurate ages. This suggested to me that the composition of initial thorium in the samples may encompass a wider range than that value allows for. Therefore, I decided to try to constrain the range of values appropriate for my samples.

To do this, I selected all the living corals whose age I knew to within the ring-counting error (usually $\leq \pm 5$ years) and the corals for which I had performed multiple analyses. Though I did not know the age of the corals with multiple analyses, I did know that the two dated samples from the same coral should have the same age. Using the ^{238}U, ^{232}Th and ^{230}Th concentrations, for each coral I calculated a corrected $[^{230}Th/^{238}U]$ activity ratio for a suite of assumed $^{230}Th/^{232}Th$ ratios for the initial thorium component. I plotted the corrected values for two samples of the same coral on the same plot of $^{230}Th/^{232}Th$ (initial) vs. $[^{230}Th/^{238}U]_{corr.}$, an example of which is shown in Figure 3.2. The values for each of the two analyses plotted on separate lines. Since the corals were the same age, the intersection of the two lines should give the best estimates of $[^{230}Th/^{238}U]$ activity and $^{230}Th/^{232}Th$ (initial) appropriate for that coral. I made similar plots for all duplicate corals. Sometimes the two samples were not from the same growth band and thus were not the same age. However, knowing the age difference from counting the growth bands between the two samples, I could find the appropriate $^{230}Th/^{232}Th$ (initial) value, which is simply the value at which the two lines are separated by a $[^{230}Th/^{238}U]$ difference equivalent to the age difference (e.g. Figure 3.3). For two corals, I had three separate analyses. For samples from living corals, I calculated the $[^{230}Th/^{238}U]$ for the known ring-counting age of the sample and determined the $^{230}Th/^{232}Th$ (initial) value that would be consistent with that activity ratio.

Figure 3.2. An example of using one coral that was sampled and analyzed twice to estimate the initial ^{230}Th/^{232}Th ratio in the coral. Two pieces from the same growth ring in this coral were analyzed separately. A series of [^{230}Th/^{238}U] activity ratios, corrected for given ^{230}Th/^{232}Th values, was calculated using the measured concentrations of ^{230}Th, ^{232}Th and ^{238}U for each of the two samples. These points, which are linearly distributed, are plotted with a line through them. The calculated uncertainties, based on the 2σ analytical uncertainty of the concentrations, are also shown. The intersection of the two lines should be the initial ^{230}Th/^{232}Th ratio in the coral (column 2 in Table 3.2) and the corrected [^{230}Th/^{238}U] activity ratio (column 4 in Table 3.2). The box indicates the area in which the uncertainties on the plotted points overlap. This area of overlap is the uncertainty on the calculated initial ^{230}Th/^{232}Th ratio.

Sample P93-C-8

$230/232 = 7.98 \ +2.82/-2.60 \ \times 10^{-6}$,

$230/238 = 0.00481 \ +.00340/-.00368$

$^{230}Th/^{232}Th \ (initial)(x \ 10^{-6})$

$[^{230}Th/^{238}U]$
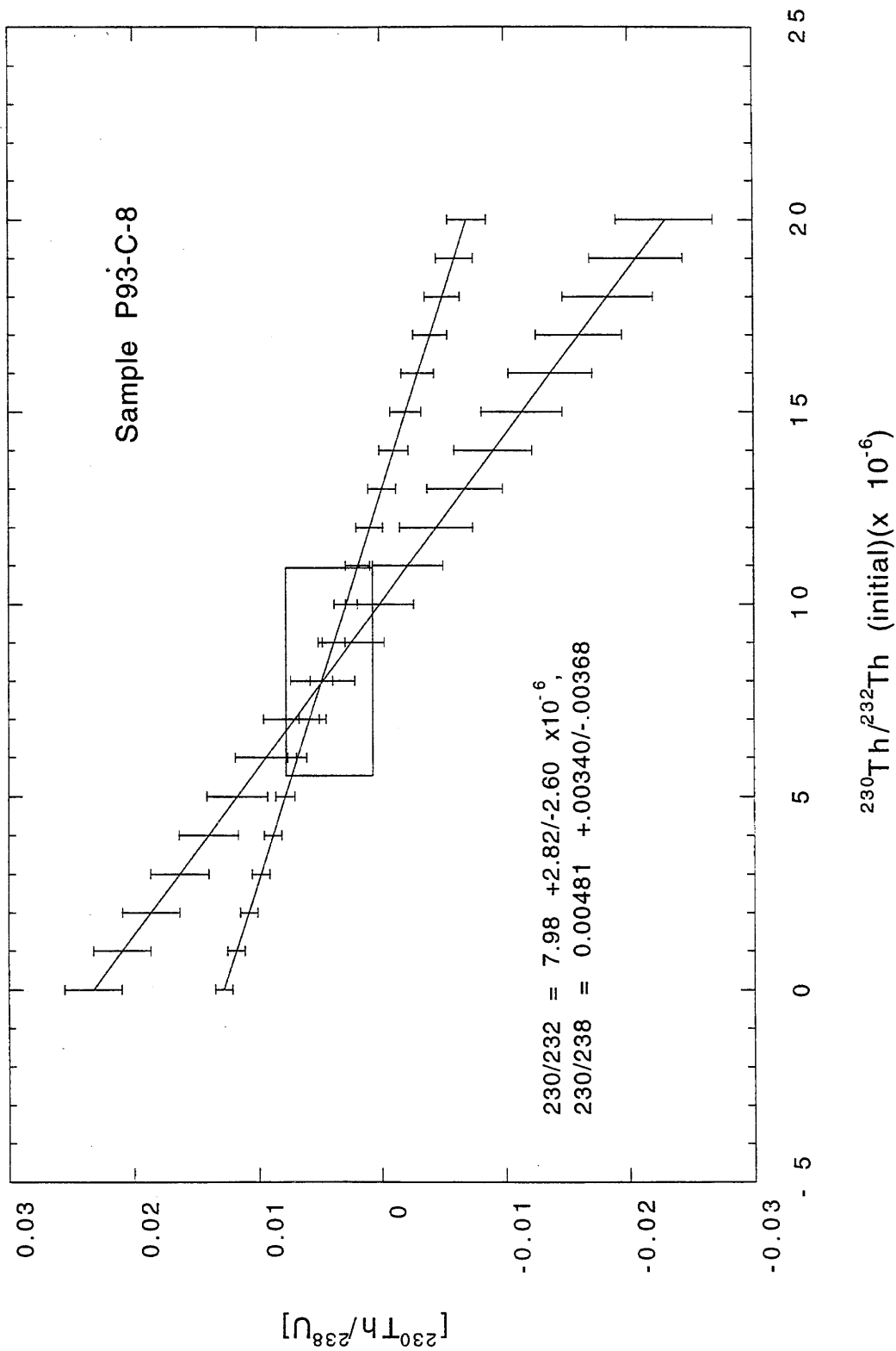
Figure 3.3.

An example of multiple samples from a single coral similar to that in Figure 1. However, in this coral, the two samples were from different parts of the coral. Rather than the value at the intersection of the two lines, the value at the point where the lines are separated by a $[^{230}Th/^{238}U]$ activity ratio equivalent to the age difference between the two samples (determined from ring counting) should be the initial $^{230}Th/^{232}Th$ ratio for the contaminant. The small box shows the size of the uncertainty based on analytical uncertainty alone; the large box represents the error based on analytical uncertainty and ring counting uncertainty.

Sample NP94-A-5

age difference from ring counting = 15±15 yrs

230Th/232Th = 6.33 +5.46/-5.05 x 10^{-6}

[230Th/238U] = .00282 +.00028/-.00023
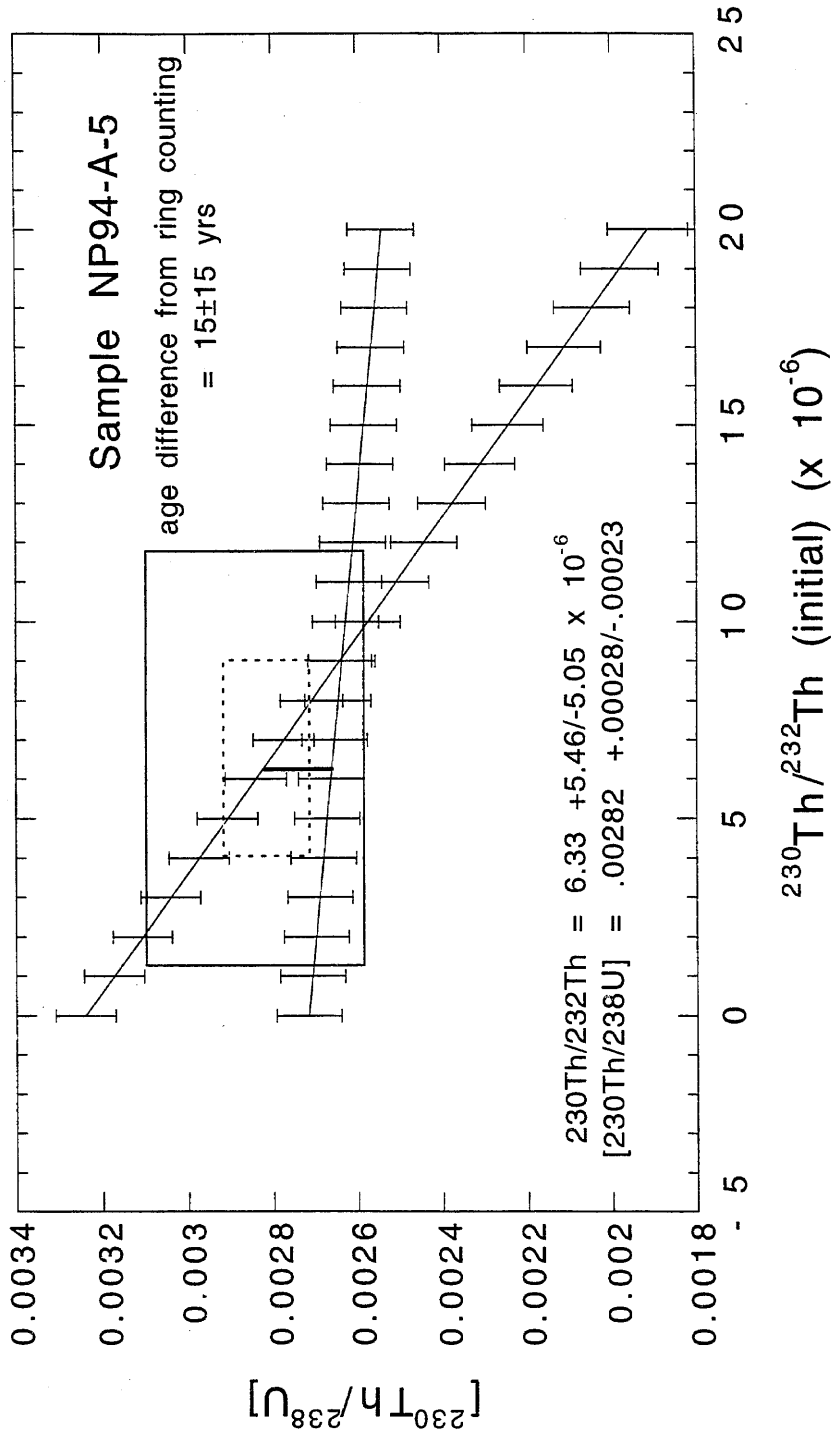
I determined the uncertainties associated with ^{230}Th/^{232}Th (initial) values, by including the full range of possible values. Each of the lines on the plot had error bars derived from the analytical uncertainties of the isotopic concentrations. The uncertainty for ^{230}Th/^{232}Th (initial) encompasses the entire range over which the error bars for the two lines overlap. When there was an age difference between the two samples, or for samples from living corals, the ring counting errors were also incorporated. Samples that were very similar generated large uncertainties and were not very useful for constraining ^{230}Th/^{232}Th values.

I calculated the ^{230}Th/^{232}Th (initial) values for all possible samples (Table 3.2). They ranged from 0 to 13 x 10^{-6}, with the average around 6 or 7, depending how it was weighted. The two lines for one sample, Pg04e-0.0.2, actually intersected at ^{230}Th/^{232}Th = -2.3 x 10^{-6}, but since negative values aren't possible I assigned it a value of zero. Sd96-A-1, a sample from a live coral whose age was determined by counting growth bands, had a value of 37.1 x 10^{-6}. This ratio was so different from any of the others, that it was discarded as an outlier in determining an average value that might be applied to other samples. However, unless it is simply a mistake, it does give an indication of possible, if rare, materials with very high ^{230}Th/^{232}Th ratios that could conceivably contaminate corals.

The ^{230}Th/^{232}Th (initial) values determined for these numerous samples suggest that the composition of the contaminant is not simply that of average crustal material, but may differ significantly from it. The wide range of values further suggests that the nature of the contaminant may vary from place to place in the islands, or it may vary over time. Nevertheless, there is no clear correlation between site and ^{230}Th/^{232}Th ratio, nor between ^{230}Th/^{232}Th ratio and [^{230}Th/^{238}U] activity ratio. Samples P93-C-7, P93-C-8, and P94-AB-2 are all from the same site, indeed they are from different parts of the same coral head, and the ^{230}Th/^{232}Th values are clustered round 8 x 10^{-6}. However, other sites

such as NP94-A and P94-Z/P96-F, each with two sampled corals, show no similarity in the values determined from the two corals. Living coral ^{230}Th/^{232}Th values range from 0.9 to 10.5 (or 37.1, if Sd96-A-1 is included), which is virtually the entire range of values observed. Indeed that variability occurs within a single coral, Sd96-C-1. Given that the assumptions of average crustal material do not seem adequate and that there is no clear pattern to the observed ^{230}Th/^{232}Th values, it seems prudent to apply a broad range of possible ratios when correcting the ages of samples without multiple samples or known ages. To that end, I chose a value of 6.0 (+7.0/-6.0) x 10^{-6} to apply as a correction factor to remove the effects of initial thorium contamination. This uncertainty accounts for all the calculated values of double or known samples except the one outlier.

I applied the correction in the same way as I had originally and as others have, only using the new ^{230}Th/^{232}Th value. The original ^{230}Th/^{232}Th correction value I had used was derived from the assumption both that the contaminant was average crustal material with ^{232}Th/^{238}U=3.8, and that it was in secular equilibrium. Obviously, if the new factor is applicable, then at least one of those assumptions is incorrect. If the contaminating material is in secular equilibrium, then for a ^{230}Th/^{232}Th value of 6.0 x 10^{-6}, ^{232}Th/^{238}U=2.8. In practice however, this value doesn't change the corrected age very much, usually less than 1 ‰, and in the worst case by 3 ‰. In either case, the change in age due to uncertainty over the appropriate ^{232}Th/^{238}U value is tiny compared to the analytical errors and the errors due to uncertainty in the ^{230}Th/^{232}Th correction factor.

3.4c. Ages

Most of the corals are less than 500 years old. Almost forty samples died in the first half of the nineteenth century. There are seven mid-Holocene corals, dating from about 6100 to 3500 BCE. There are also twelve samples from living corals, although the

Table 3.2. ^{230}Th/^{232}Th values for initial thorium contaminant.

Corals that had multiple analyses or samples whose ages were known from ring counting were used to determine the ^{230}Th/^{232}Th ratio of the material contaminating the dated corals. The presence of the contaminant was identified by high ^{232}Th concentrations in samples. The table presents the estimated initial ^{230}Th/^{232}Th ratio in the coral (column 2) and the [^{230}Th/^{238}U] activity ratio (column 4) for twelve corals which were sampled at least twice, and eight samples of known age. The asterisk indicates values that were so poorly constrained as to be useless. Multiple samples whose original analyses were similar did not offer useful constraints, as the area of their intersection, including error bars, was almost total. An average value estimated from these calculations of 6.0 (+7.0/-6.0) x 10^{-6} was used to correct the dates of all sampled corals (column 10, Table 3.1).

Table 3.2. ^{230}Th/^{232}Th values for the initial thorium contaminant

Sample(s)	$^{230}Th/^{232}Th$ init. x 10^{-6}	error x 10^{-6}	$[^{230}Th/^{238}U]$ act. x 10^{-5}	error x 10^{-5}
NP94-A-5	6.3	(+5.5/-5.1)	282	(+279/-234)
NP94-A-8	12.3	(+23.3/-21.1)	*	*
P93-C-7	8.7	(+3.0/-2.5)	346	(+192/-192)
P93-C-7/P94-AB-2	7.6	(+1.5/-0.6)	428	(÷15/-44)
P93-C-8	8.0	(+2.8/-2.6)	481	(+340/-368)
P94-H-1&2	13.0	(+4.9/-4.5)	*	*
P94-Z-1/P96-F-2&3	12.8	(+9.5/-6.1)	605	(+57/-84)
P94-Z-4/P96-F-1	1.0	(+8.5/-8.3)	188	(+18/-15)
P96-F-2&3	5.1	(±40+)	671	*
P96-L-1&2	0.5	(+14.2/-14.4)	348	(+46/-32)
Pg04e-0.0.2 (-2.26)	0.0	(+6.4/-5.9)	216	(+37/-39)
Pg04g-0.0.2	5.8	(+1.8/-1.3)	176	(+45/-59)
Pg04a-0.0.1	8.1	(+11.2/-5.9)	55	(+57/-42)
P96-B-2	3.1	(+3.3/-2.4	11	(÷2/-2)
Sd96-C-1.1.1(96-35)	4.0	(+10.9/-10.8)	37	(÷4/-4)
Sd96-C-1.1.2(96-32)	9.6	(+1.9/-1.9)	0	(+0.5/-0.5)
Sd96-C-1.1.2(96-33)	10.5	(+0.3/-.3)	12	(+1/-1)
Sd96-C-1.1.2(96-34)	0.9	(+5.3/-5.2)	22	(+1/-1)
Sd96-C-1.3(96-31)	9.5	(+2.5/-2.6)	0	(+0.5/-0.5)
Spr9-0.0.3	2.8	(+1.1/-0.7)	3.7	(+1.8/-1.8)
Sd96-A-1.1.b	37.1	(÷8.3/-8.5)	16	(÷3/-3)

*range of possible values too high to constrain value

dated piece itself was not usually alive. The uncertainties in most of the uncorrected dates are less than 5%, although a few are over 20%. In general, the dates of the older corals have better precision, with most of the mid-Holocene dates having uncertainties of less than 1% (e.g. ±45 years uncertainty on an 8100 yr old coral - sample P95-Y-1a.a, Table 3.1). The uncorrected dates of the living corals are much less precise - most of the samples with uncertainties of 10-20% are living corals. This is not surprising. The uncertainty of the date rests primarily on the uncertainty in ^{230}Th measurements. Considering that for very young samples, there has been such little time for ingrowth of ^{230}Th, the age precision is limited by the abundance of that isotope.

Replicates were done on several samples. These are listed together in Table 3.1. For some replicates, I ran two halves of the sample separately on the mass spectrometer to ensure that the dates could be replicated. The data for these samples in the table are an average of the results of the two runs. In most cases where I dated the same coral twice, different growth rings were sampled. Therefore, the ages should differ by the number of rings between the two samples. For example, NP94-A-8A1(2).B and NP94-A-8a4(1).B are from the same slab of coral but were separated by 39 ± 4 rings. The ages of the samples differ by 35 ± 6 years and agree within the offset in the annual growth bands. When the age of death is calculated for these two samples, they are well within error of one another (1836 ± 7 and 1832 ± 5). In the case of sample Sd96-C-1, a living coral from which samples from numerous locations were dated, the uncorrected "date of death" (actually, the collection date, or the age of the outer living ring) was not the same for all the samples (see Sd96-C-1.1.1.A(96-35), Sd96-C-1.1.2.A(96-32), Sd96-C-1.1.2.A(96-33), Sd96-C-1.1.2.A(96-34), and Sd96-C-1.3.A). However, once corrected for initial ^{230}Th, the dates were the same within the uncertainties. Furthermore, the dates are accurate, since the slab was collected from living coral in 1996. For a few corals that were not slabbed, I dated an inner and an outer piece of the same coral head. However, I have

no ring information to compare the two dates and test the precision. I had dated the two pieces of these samples in order to get an estimate of the growth rate of the coral. Coral head P94-H-1.A and P94-H-2.A were outer and inner parts of a coral head respectively. The uncorrected dates for these two samples are inverted from their stratigraphic relative ages. However, P94-H-1.A has a fairly high ^{232}Th concentration, significantly greater than that of P94-H-2.A. When the correction is applied to the two samples, the inversion disappears, within the uncertainties.

For the samples that had multiple analyses that I used to calculate the appropriate initial 230Th/232Th, those individually calculated correction factors, listed in Table 3.2, could be used to correct the date of death. Table 3.3 lists these samples, their uncorrected date of death, the death date corrected using the general correction factor of 6.0 (+7.0/- 6.0) x 10^{-6}, and the death date calculated using the individually determined correction factor from Table 3.2. In most cases, the individual correction improves the precision in the death date.

The corrections for initial ^{230}Th, dependent on the ^{232}Th concentration, range from 1 to 1764 years, with over half of the corrected dates less than 20 years different from the uncorrected dates (Tables 3.1 and 3.3). The correction introduces a much greater uncertainty into the age calculations, especially for samples with low ^{230}Th/^{232}Th ratios. Only 24 of the 92 samples have uncertainties in their corrected ages of less than 5%, while for some of the living corals the uncertainty on the corrected ages is near 200%. This large uncertainty in corrected ages derives primarily from the fact that the appropriate correction factor, the initial ^{230}Th/^{232}Th ratio of the contaminant, can only be poorly constrained. I assigned it a large uncertainty to ensure that it encompassed most of the possible contaminants. The effect of the correction on the age uncertainty is most pronounced in those corals with low ^{230}Th/^{232}Th ratios. For example, when the correction was applied to sample P94-AA-1A.A, which had a ^{232}Th concentration of

Table 3.3

Table of corrected dates for those samples whose initial $^{230}Th/^{232}Th$ ratio was calculated independently. Column 1 shows the sample name; column 2 has the original uncorrected date of death; column 3 shows the date of death corrected with the average correction factor used for all other samples (6.0 (+7.0/-6.0) x 10^{-6}); column 4 has the death date corrected using the initial $^{230}Th/^{232}Th$ ratio calculated independently from multiple samples of a coral (those ratios appear in Table 3.2). Uncertainties in the date of death appear in each column in parentheses following the date .

Table 3.3 - Age corrections

sample name	uncorrected death date	average correction	specific correction
NP94-A-5A1(1).A	1792 (17)	1797 (18)	1797 (17)
NP94-A-5A2.A	1772 (26)	1810 (51)	1812 (43)
NP94-A-8A1(2).B	1836 (7)	1842 (11)	1850 (16)
NP94-A-8A4(1).B	1832 (5)	1841 (11)	1850 (18)
P93-C-7(A)	832 (62)	1398 (665)	1550 (155)
P93-C-7(B)	1396 (84)	1578 (228)	1626 (95)
P93-C-8(A)	776 (64)	1339 (661)	1527 (271)
P93-C-8(B)	-222 (220)	1099 (1560)	1542 (656)
P94-AB-2A.C	1517 (5)	1572 (65)	1587 (15)
P94-H-1A.A	1766 (7)	1807 (30)	1841 (29)
P94-H-2.A	1809 (6)	1817 (8)	1823 (8)
P96-F-2.2.A	1322 (6)	1371 (57)	1364 (42)
P96-F-3.B	1323 (5)	1373 (58)	1366 (43)
P94-Z-4B.B	1818 (6)	1824 (9)	1819 (11)
P96-F-1.B	1817 (4)	1831 (17)	1819 (13)

about 84 pg/g and $^{230}Th/^{232}Th = 9563 \times 10^{-6}$, the ratio of calculated initial ^{230}Th to total ^{230}Th was 0.6‰. The age decreased by 1.5 years, and the uncertainty increased by only one year, or from 6.8‰ to 6.9‰. The ratio of estimated initial to total ^{230}Th in the dirtiest sample that did not have an individually calculated correction factor, P94-C-2, was 33%. It decreased in age by 356 years, and the uncertainties in this age increased by 381 years, or from 3.4% to 57%. With such large uncertainties, the dates become nearly useless for the purposes of paleoseismology. Clearly, if the contamination is too great, the corals cannot be used for more than very rough age estimates, such as distinguishing mid- from late Holocene events.

3.5. Conclusion

I dated 81 samples from 63 corals using U-series disequilibrium dating methods. All but 11 samples were from fully-emerged, dead corals. I dated the fossil coral samples as a means of dating the hypothesized emergence events and associated earthquakes that presumably were responsible for killing the corals. I dated the living corals to verify that I was getting good results and to constrain the nature of contamination that was affecting the results.

^{238}U concentrations between 2 and 4 ng/g were typical of corals elsewhere. Measured $\delta^{234}U$ values were within the range of modern coral and sea water values for almost all corals, as were the calculated initial $\delta^{234}U$ values. Many corals had high ^{232}Th concentrations suggesting they had been contaminated with Th-bearing materials, most probably terrigenous detritus. Corals with high ^{232}Th concentrations probably have a high abundance of unsupported ^{230}Th as well and yield falsely old ages. Attempts to remove the contaminant physically helped but did not solve the problem. I used multiple samples from one coral and individual samples from corals of known age to try to constrain the

$^{230}Th/^{232}Th$ ratio in the contaminant. I found that correcting the ages for contamination with initial thorium with ratios of 6.0 (+7.0/-6.0) x 10^{-6} would be appropriate for most corals. The corrections produced more accurate ^{230}Th ages for corals of known age, and presumably for the others as well, but also generated large uncertainties in the corrected ages. The results emphasize the importance of collecting the cleanest possible samples. The correction seems to improve the accuracy of most coral ages, but it is only an estimated correction and may not apply to every coral. Dates from corals with very high concentrations of ^{232}Th will always be somewhat suspect even after correction.

Chapter IV
Documenting Late Holocene earthquakes at the Sumatran subduction zone using emerged coral microatolls

4.1 Introduction

4.2 Results

> *4.2a. Field Methods*

> *4.2b. Field Observations*

> *4.2c. Dates of emergence*

> *4.2d. Early 19th-century emergence events*

> *4.2e. Other Paleoseismic events*

4.3 Discussion

> *4.3a. Fossil corals as paleoseismic and paleogeodetic recorders*

> *4.3b. Mid-Holocene microatolls and Holocene relative sea-level stability*

> *4.3c. 1833 coseismic emergence event*

> *4.3d. Earlier paleoseismic records*

> *4.3e. Composite HLS records through multiple earthquake cycles*

> *4.3f. Recurrence intervals*

> *4.3g. Coseismic slip estimates*

> *4.3h. Segmentation and clustering*

> *4.3i. Long-term vertical motion and implications for subduction zone deformation*

4.4 Conclusions

4.1 Introduction

Newcomb and McCann's (1987) historical record of earthquake activity in western Sumatra includes a number of events inferred to have occurred on the subduction interface beneath the Pagai and Sipora Islands (Chapter 1; Figure 4.1). The largest of these, Mw = 8.7, occurred in 1833. Based on shaking and tsunami extent, Newcomb and McCann believe this event ruptured the plate interface between the Batu Islands in the north and Enggano Island in the south, and from the trench to the west coast of Sumatra. Given the magnitude of this earthquake, the inferred rupture zone, and the proximity of the Mentawai island chain to the subduction trench, one would expect that the islands had experienced significant vertical displacements during the event. Newcomb and McCann estimated slip on the fault plane in the event to have been between about 4.5 and 7 m. Slip of that magnitude on a shallow interface might be expected to yield vertical displacements at the surface of about 1 m. Thus, based on the historical record, it is likely there would be, in the Pagai and Sipora Islands, evidence for uplifts from the 1833 earthquake on the order of one meter. Historical records contained evidence of other, less well-documented earthquakes in the years prior to 1833, in 1797, 1770, 1756, and 1681, that were felt in wide areas of Sumatra and the Mentawai Islands. These too might have produced measurable displacements on the islands.

As illustrated in Chapter 2, changes in low water levels, defined by a coral's highest level of survival (HLS), are permanently recorded in the skeletons of living microatolls. If the microatolls are preserved after death, the records of HLS fluctuations that they experienced during their lifetime may remain contained within the fossil skeleton, so that, even after death, the record of former relative sea level fluctuations can be unraveled.

The successful use of living corals to document ongoing modern submergence in the Pagai and Sipora Islands argues that they may work well to document pre-modern vertical displacements, both sudden and gradual, as well. The study of living corals indicated that sea-level changes of a few centimeters or more could be ascertained from the microatoll record, and the uncertainties from ring counting were usually less than ±5 years in a 50 year record. The living coral study supported observations from other sites that corals respond to changes in HLS greater than 5-10 cm quickly, although the response to small changes might be delayed a few years (Taylor et al., 1987).

U-Th geochronometry applied to young, clean corals can provide Holocene ages with uncertainties of a few years or decades. Although contamination in dirty corals can greatly reduce that precision, in general the ^{230}Th ages are more precise than radiocarbon ages. Given the absolute age of a coral from U-Th geochronometry and a well-preserved fossil coral, the HLS record for clean, dead corals may be almost as precise as that of live corals. These uncertainties are smaller than are generally obtainable at subaerial paleoseismic sites where usually only coseismic displacements can be measured and radiocarbon ages are determined from detrital charcoal contained in faulted sediments. Thus, fossil corals could provide excellent constraints on the nature of paleoseismic and paleogeodetic activity on the tectonically and seismically active Sumatran margin. If the Pagai Islands experienced significant coseismic displacement during the 1833 and earlier earthquakes, these events should, if they involved more than a few centimeters of vertical displacement, be recognizable in the morphology and stratigraphy of microatolls from that era.

Coseismic uplifts would cause the microatoll to emerge above water, either partially or fully. If it emerged fully, the whole coral would die; if only partially, only the part below HLS would continue to grow and it would develop the "hat"-like shape of partial emergence depicted in Figures 1.14 and 1.16 of Chapter 1. Unlike submergences,

Figure 4.1. Sumatra and the Mentawai Island chain. Shaded areas represent the rupture zones of two $M_w \sim 8.5$ earthquakes in 1833 and 1861 inferred from Newcomb and McCann's (1987) analysis of historical records of felt intensity and tsunami extent. The plate convergence rate is from GPS studies by Tregoning and others (1994).

95° E · · · · · · · · 100° E

Simeulue

Banyak

1861

Nias

Pini

Batu

0°

Siberut

67 ± 7 mm/yr

Sipora

Indian and Australian
Plates

N. Pagai   Sikakap

S. Pagai

Sanding

1833

5° S

Enggano

Southeast-
Asian Plate

SUMATRA

Great Sumatran Fault

Padang

Mentawai Fault

Bengkulu

Malaysia

Borneo

Java
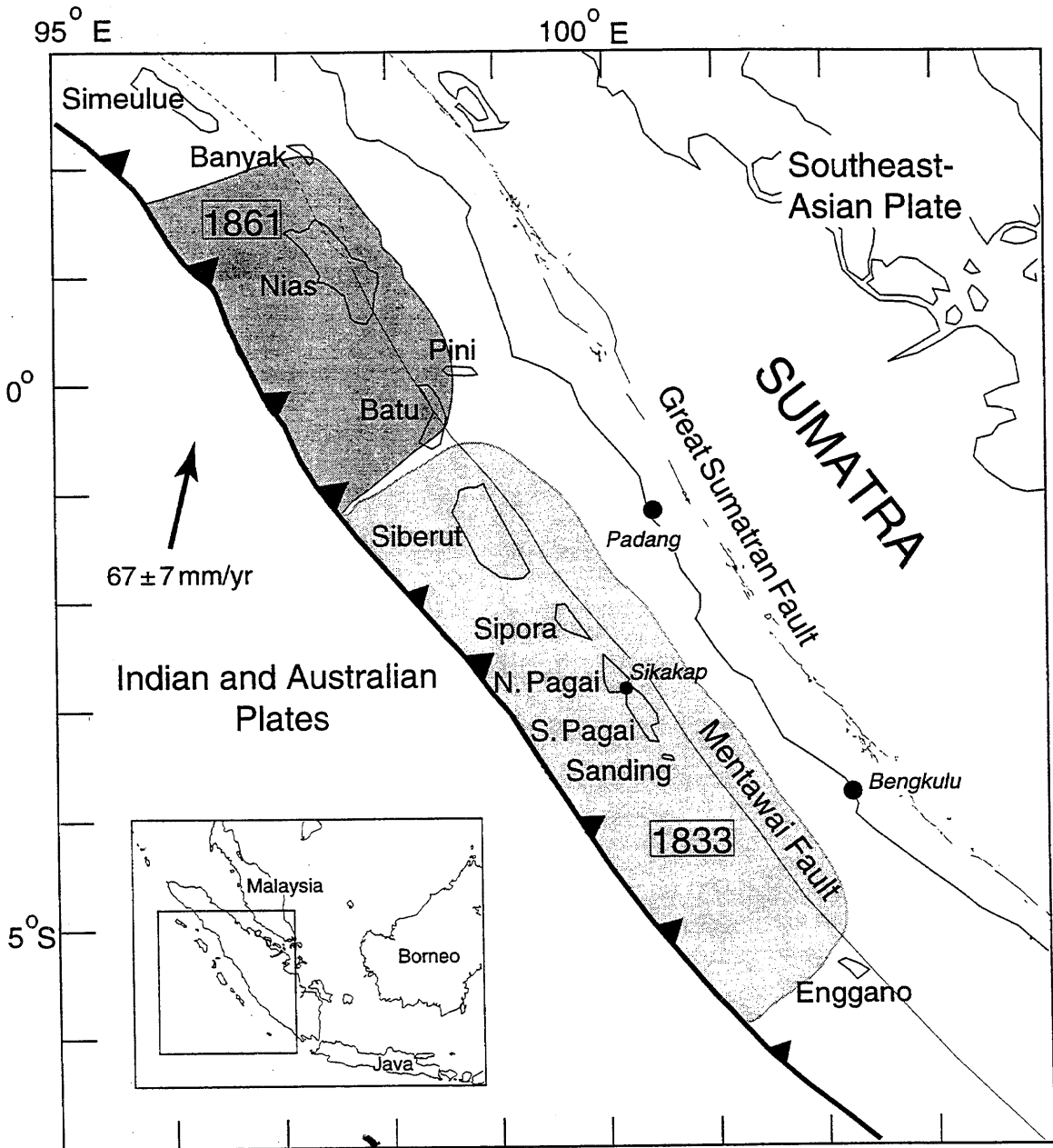
sudden emergences are usually readily distinguishable from gradual emergence. The morphology of a coral killed in a coseismic uplift event of more than a few cm should be distinctive. The largest emergence recorded in the living corals occurred in 1994 or 1995. About 5 cm, it was reflected in the stratigraphy of all slabs and the morphology of all observed living corals. In most cases, the emergence was recorded virtually immediately in the corals. There was little or no downstepping or sloping between the higher HLS and the lower. The exposed portion was smooth and essentially uniform in age - the emergence was recorded as an "instantaneous event." Given the coral response to an emergence of about 5 cm, it is likely that in most cases, a larger sudden emergence would be recorded at least as rapidly. Thus, in suddenly emerged corals, one might expect to find a smooth emerged edge, the outer rind of the emerged portion composed of one, or maybe two, annual bands, reflecting the rapidity with which the exposure kills the coral. In this way, large sudden emergences should be recognizable in the field from the morphology of the head. They would be distinct from heads with downstepping edges associated with gradual emergence and oceanographic fluctuations. The details of the emergence, especially the temporal details, would still require stratigraphic analysis of cross-sectional slabs.

One can infer the magnitude of the emergence from the change in HLS elevation before and after the event. Thus, the amount of any displacement sustained in the 1833 and earlier earthquakes should be constrained by the HLS histories of microatolls living at those times. The coseismic vertical displacements, derived from the HLS histories of coeval corals throughout the region, can further help constrain the size of the earthquake and the extent of the rupture zone. The age of the coral, determined from U-Th geochronology, yields the date of the earthquake so that a complete paleoseismological record of the past event may be obtained. With an array of such HLS histories through time, spanning multiple paleoseismic events, one could produce a sawtooth sea level

curve representing the long-term record of vertical deformation through several earthquake cycles, e.g. Figure 4.2. Such a record provides information on earthquake recurrence and magnitude, as well as insight into the deformational processes of loading and unloading at a subduction zone.

The use of coral microatolls to date and characterize paleoseismic events is not new. As discussed in Chapter 1, Taylor and others (1980; 1985; 1987) demonstrated that microatolls could be used to document the magnitude and extent of uplift associated with earthquakes in Vanuatu by studying partially emerged living microatolls, whose partial emergences coincided in time with known earthquakes. Edwards and others (1987c; 1988) and Taylor and others (1990) applied those methods to emerged corals in the same region. They inferred a similar cause of emergence death for several fully emerged microatolls. They determined the ^{230}Th ages for these corals, effectively establishing the date of the earthquake in which they were presumed to have died. The presence of multiple suddenly-emerged coral heads with the same age of death at a single site supported the argument that a coseismic uplift event was responsible for the death.

In this chapter, I present the results of a paleoseismic and paleogeodetic study of the Sumatran subduction zone using fossil microatolls from the Mentawais. I apply the methods of Chapter 2 to dead, emerged corals that I dated with U-Th geochronometry (Chapter 3). The ages of those corals yield the time frame for which the HLS curves apply. The live coral study illustrated the accuracy and precision of the HLS histories derivable from microatolls. Presumably, the precision for live corals - of known age, in situ, with minimal erosion, weathering and alteration - provides an estimate of the greatest precision for dead corals. I use the HLS histories derived from the stratigraphic analysis of slabbed coral heads and the dates of emergence to generate a record of paleodeformation - slow interseismic deformation punctuated by earthquakes. The results presented here are by no means complete, but they do illustrate the feasibility of

Figure 4.2. Hypothetical sea level curve that might, in principle, be derived from living and dead coral microatolls. The corals a record of yearly sea level fluctuations over their lifetime, and U-Th geochronometry can yield the absolute ages of the corals. By combining highest level of survival (HLS) records from corals that lived and died at different times, a long-term record through multiple earthquake cycles could be determined.
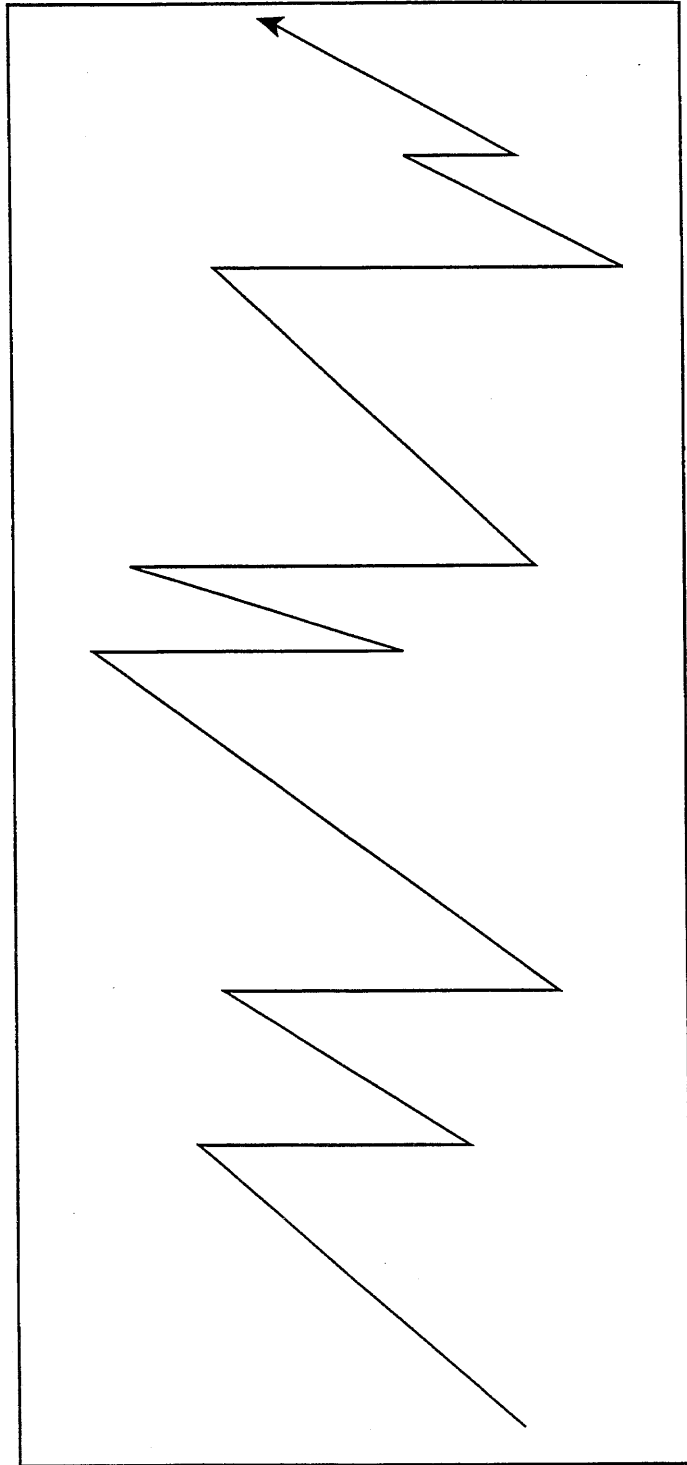
Sea Level

Time

using dead corals as a paleoseismic and paleogeodetic tool and reveal some of the history of past vertical deformation and paleoearthquakes that have affected the region.

4.2 Results

4.2a. Field methods

Field methods employed to study the dead corals were much the same as those used to study living coral (Chapter 2). At each site, I made a reconnaissance to determine the general nature and morphology of the fossil corals. In 1994, I measured the elevations of corals and their multiple HLS surfaces relative to water level and usually also to the HLS of living coral at the same site. In 1996, I included fossil corals in the detailed surveys of microatolls and HLS elevations carried out with the total station.

In collecting corals for sampling, I used criteria for measuring and sampling that were similar to those used for live corals; I sought complete, untilted corals that seemed representative of all or a significant fraction of those observed in reconnaissance. When collecting slabs or hand samples for dating, I searched for clean white pieces to minimize the problem of contamination in the dating process. Where it was not possible to find clean samples, I usually collected a contaminated sample anyway if the coral was important because of its morphology. In several instances, I measured and sampled or slabbed a dirty *Porites* head for its sea level record, and collected a small piece of a neighboring clean *Goniastrea* or other large-pored coral without a good morphology to constrain the date, assuming, based on field relations, that the two corals were contemporaneous.

I could not sample and date every coral, but strove to compile an ample and representative collection of samples to characterize each site. Thus, I wished to collect

two or three samples for each generation of coral head at a site, a representative slab for each generation, and elevation data and morphological descriptions for numerous others. Since multiple generations were not easily distinguishable in the field, I usually sampled several dead corals from each site, but it was only when the corals were dated that I could tell if they represented different generations. Consolidated basal reef material that formed a substrate upon which microatolls often grew was mid-Holocene in age. However, there were no similar constraints on microatolls, for which I obtained both late and mid-Holocene ages. I certainly did not see the clearly demarked terraces at different elevations to differentiate between generations that have been observed elsewhere, e.g. Huon Peninsula, Timor or New Zealand (Bloom et al., 1974; Chappell, 1974; Ota et al., 1993; Pandolfi et al., 1994; Jouannic et al., 1988; Ota et al., 1991).

Because I could not group corals by age from macroscopic properties, I had to date virtually all the dead corals I sampled. The laboratory methods for selecting and dating samples are discussed in Chapter 3.

4.2b. General field observations

Emerged fossil microatolls were ubiquitous in the bays of the Pagai and Sipora Islands. Although many coral heads were out of place, tilted, broken or highly eroded, many sites also contained well-preserved microatolls with few signs of erosion and displaying their original morphology. They often occurred in the same bays as living corals. They sat upon either dead, eroded reef flat composed of cemented fragments of coral, or on a sandy substrate. Dead corals were usually nearer shore than the living corals and were usually higher, their tops usually about half a meter higher than the tops of the living rings in modern microatolls. They were generally exposed above water at low to medium tides, even in Jan.-Feb. 1996, when the lowest tides were well above the tops of

the living microatolls. Often fossil corals were partially buried by or recently exhumed from the beach berm, testimony to the ongoing subsidence of the islands and consequent landward migration of the berm. At a few sites, coconut palms grew rooted on or among fossil corals.

There were variations in the elevations of the fossil corals, but these were rarely more than half a meter, except in a few cases. In general, the fossil microatolls were confined within a narrow elevation range, their bases still within the intertidal zone. Excursions into the jungle behind the storm berms rarely revealed the presence of microatolls. Although these excursions were not extensive, no microatolls or reef corals were found exposed at substantially higher elevations than those of the microatolls in the intertidal zone of the bays. Where microatolls were found, they were in or slightly above the modern intertidal zone, often buried in peat or rooted in swamps. Thus there was no evidence for a vertical progression of fossil corals like the exposed reef terraces in New Guinea and elsewhere that testify to ongoing permanent uplift (Chappell, 1974). The elevations of the tops of all emerged fossil corals in the Mentawais were generally within a meter of each other.

The morphology of uneroded, untilted fossil microatolls was broadly similar throughout the islands. Most were relatively steep-sided, or smoothly sloped down and out, and many had the cup-like morphology indicative of a submergence history during their lifetime. In some cases, there were multiple HLS flats, down-stepping from an exterior raised rim toward a lower interior flat. In others, there was only one outer ring above the central flat. Thus, the predominant morphology of the fossil corals was similar to that of the live corals. Of the hundreds of fossil corals observed, only a handful had an outer, lower rim suggesting an emergence prior to death. Of these, many occurred as outer flanges on the edge of a coral that otherwise had the morphological signature of submergence. There was little evidence in most microatolls of sea-level stability or

emergence dominating the pre-death interval, although some showed signs of slower submergence or longer periods of stability.

These observations suggested that the fossil corals had died by emergence following several decades of submergence. The steep sides and absence of down-and-out stairstepping implied the emergence was sudden and precipitated death rapidly. The cup-like morphology and high walls testified to a pre-emergence history of submergence, much like what is occurring presently in these islands. The fact that elevation differences between fossil corals were slight suggested that there had been little net vertical while these corals lived. In light of these observations and the tectonic environment of the island, it seemed reasonable to suspect that the sudden emergences were a result of coseismic uplifts, and that these uplifts counteracted the preseismic submergence.

There was no clear indication of the relative ages of emerged microatolls based on their elevations, so it was not clear from field observations alone if the emerged corals represented a single emergence event, or multiple events. To determine if the emergences were caused by tectonic uplift, I collected samples from the uplifted corals for dating and stratigraphic analysis. The paleoseismological studies of Edwards and others (1987c; 1988) and Taylor and others (1990) showed that the occurrence of multiple microatolls of the same age and having similar HLS signatures could, in tectonically active environments, be used to document coseismic uplift events, if oceanographic causes for the HLS change could be rejected. The 1833 earthquake could serve as a good test. If multiple corals were found to have died suddenly from emergence in 1833, it is probable that they died as a result of coseismic uplift in that event. If that event left its mark, then earlier, undocumented or less well-documented, earthquakes could have as well. The occurrence of older sudden emergence events could, by inference, be used to document the timing and size of earlier, prehistoric earthquakes.

4.2c. Dates of emergence

I analyzed 81 samples from 63 emerged fossil coral heads from various sites around the islands with U-Th geochronometric methods. The dates are shown in Table 4.1; the site locations appear in Figure 4.3. The ^{230}Th ages of about half the samples are from the early part of the 19th century, with the rest distributed throughout the preceding centuries and millennia.

Figure 4.4 shows the distribution of dates of death of late Holocene corals. Black dots represent the uncorrected dates. Grey dots represent the dates corrected for initial thorium contamination. The uncertainties are those of the corrected ages. Each point represents a dated sample, so microatolls with multiple analyses are represented more than once. The dominance of late-18th and early 19th century dates is clear in both the corrected and uncorrected data but is much more pronounced in the corrected data. The uncertainties increase substantially when the correction is applied (Chapter 3). In a few cases, the uncertainties are greater than several decades, which greatly diminishes the value of the analyses in distinguishing paleoseismic or paleogeodetic events.

Since about forty samples died in 1800±50, it is worth examining the distribution of dates in that period more carefully. The likelihood of many of them having been killed in the 1833 earthquake is high. However, the distribution is broad enough that some of them may represent other paleoseismic events in that period. In the uncorrected suite of dates, about 38 samples from 33 coral heads died between 1750 and 1860 (Figure 4.5a). The samples do not cluster clearly into multiple, distinct episodes of mortality. However, about two-thirds of the corals did die between 1820 and 1840. The older ages are almost evenly distributed between 1750 and 1810, with only slight weighting toward the younger end of that period.

Applying the correction for thorium contamination pulls more of the deaths closer to 1830 and creates a small secondary grouping more focused around 1800-1805 (Figure 4.5b). The existence of a great earthquake in 1833 being known, many of the 19th century coral data fall into place. Although the ranges of only 11 uncorrected dates, from 10 corals, encompass 1833, the corrected dates of 37 samples from 33 corals allow an 1833 death date (Figure 4.5b). There are eight (corrected) coral ages that yield death dates earlier than 1833, but none necessarily yield younger dates. Part of the reason for the plethora of 1833 candidates in the corrected version is probably that the correction increases the uncertainties associated with the ages so much. However, the correction also brings the mean age of many corals closer to 1833.

To reduce somewhat the effect of increased uncertainty on enhancing the pool of 1833 candidates, I plotted only those samples with ^{232}Th concentrations <1000 pg/g (Figure 4.6). Low ^{232}Th concentration indicates minimal contamination and hence minimal "over-aging" of the samples. The corrections on low ^{232}Th samples change the dates only slightly (usually < 10 yrs) and increase the uncertainty only a few percent. Using only clean samples, there are still 21 samples (19 corals) that could have emerged during the 1833 earthquake. Furthermore, the steepening of the curve and the increased clustering around "1833" compared to the uncorrected ages are still most evident.

The plots of corrected dates and clean, corrected dates still indicate several coral deaths that occurred around the turn of the 19th century but appear not to have been part of the "1833" event. The secondary "cluster" of dates around 1800 is still not well-defined; the error bars are large, and it is unclear if those earlier deaths are related to each other and represent a unique emergence or death event or events, or if they are simply random coral deaths unrelated to each other or to large scale tectonic or oceanographic events. Newcomb and McCann (1987) reported an earthquake in 1797 that generated

Table 4.1. [230]Th dates of death of emerged fossil corals in North Pagai, South Pagai and Sipora Islands. An interior piece from each coral head was sampled and dated with U-Th geochronometry. The uncorrected date of coral death is calculated by subtracting the number of annual growth bands between the interior sample and the outermost band of the coral head. Uncertainties on the ages are a combination of the 2σ analytical uncertainties on the U-Th sample age and the ring counting uncertainties, which are estimated based on ring clarity. The corrected ages have been corrected for contamination with initial thorium (Chapter 3). The correction is applied to the measured age of the sample; the date of death is calculated from that. Uncertainties in the corrected dates of death include 2σ analytical uncertainties, ring counting uncertainties, and uncertainties in the correction factor.

Table 4.2. Preseismic submergence and coseismic emergence in 1833

Sample	Distance from trench #	Preseismic submergence rate (HLS only) cm/yr	Preseismic submergence rate (HLS plus minimum) cm/yr	Minimum coseismic emergence (cm)	Coral height (cm) (minimum)	Last 2 decades preseismic submergence rate (and year beginning)
P96-J-2	112.7 (122.6)	0.48	0.49	20	40	.81(1816)
P96-K-4	118.2 (128.2)	0.45	0.52	5	33	.60 (1812)
P96-H-1	99.6 (109.4)	0.66	0.60	10	126	1.12 (1815)
P96-F-1	103.7 (113.4)	0.83	0.81	17	65	1.13 (1819)
NP94-A-9	105.3 (112.1)	1.05	1.12	33	37	1.18 (1816)
NP94-A-8	105.3 (112.1)	.84	.72	13	70	1.41 (1818)
Si94-A-6	115.5 (117.3)	NA	-0.04	27	97	-.04 (1810)
*		0.71*	0.84*	70*		1.21 (1789)

*Si94-A-6 experienced 2 emergence events, one in about 1804 (1810) in which it was partially emerged and a second in 1827 (1833) in which it emerged the rest of the way. The first row of values refers to the 1827 (1833) event and the period prior to it and following 1804. The second row of values, with asterisk, refers to the 1804 (1810) event and period prior to it. The pre-1833 rate based on HLS is not available because all the rings have been eroded and HLS is not well-defined.
Distances are measured orthogonally from each site to the trench itself. Distances in parentheses are measured from the sites to a line best fit to approximate the strike of the trench.

Figure 4.3. Map of sites on North and South Pagai, Sipora and Sanding visited during July 1994 and January 1996. My colleagues and I collected samples at the named sites; sites at which we measured coral elevations but did not collect samples for U-Th analysis appear as unlabeled dots. Sites where we performed detailed surveys with a "total station" surveying instrument are labeled in italic print; sites where we collected large living or dead slabs for coral stratigraphic analysis are labeled in bold print. Two sites, P96-J and NP94-A/NP96-C, were both survey and slab sites.

Pagai and Sipora Islands
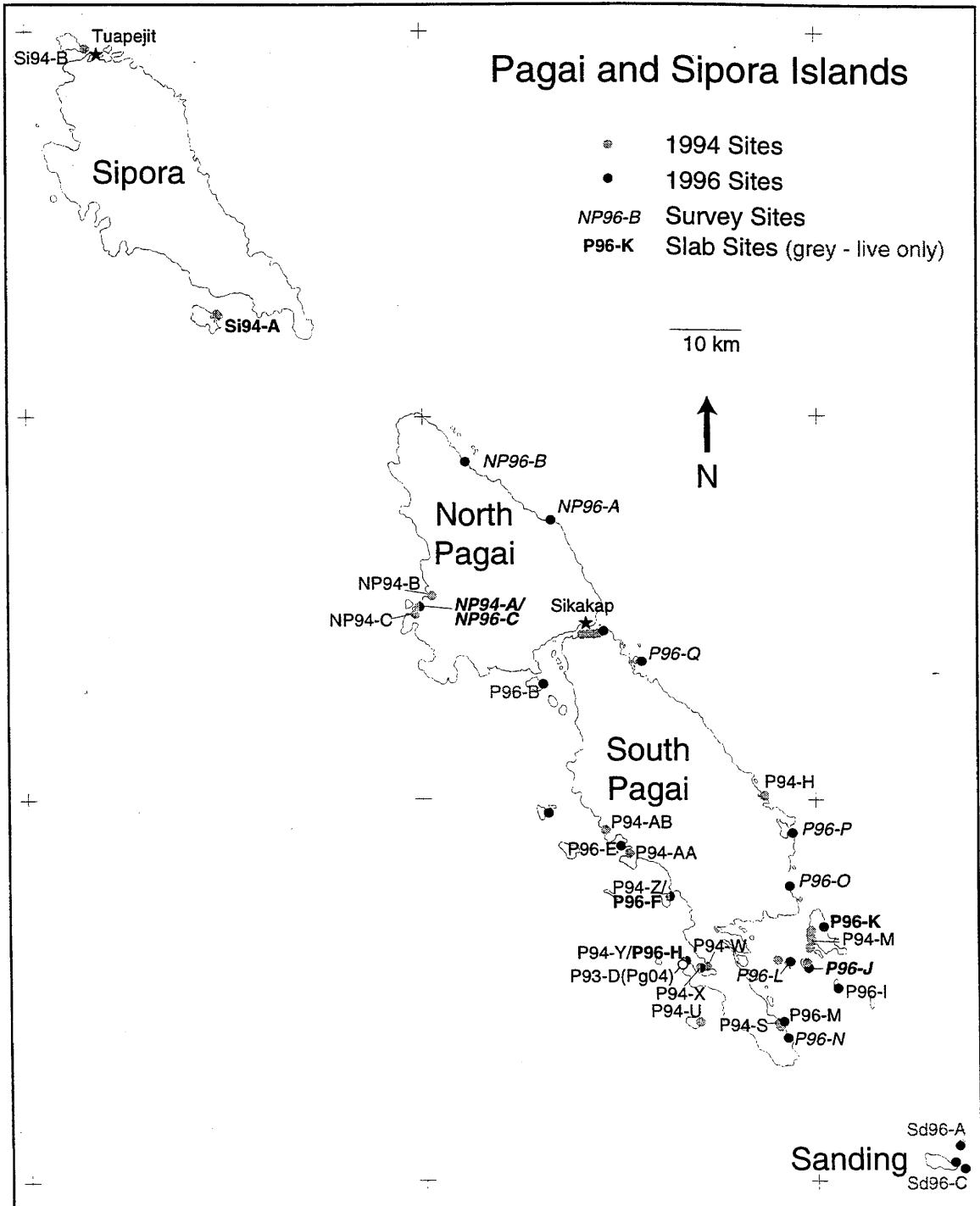
Figure 4.4. Distribution of dates of coral emergence deaths in the last ~2000 years. I determined the dates of emergence by dating an interior piece of the coral and counting the annual bands from there to the outer surface. The uncertainties in the uncorrected ages (black dots) are a combination of the U-Th analytical uncertainty and the ring counting uncertainty. The uncertainties for the corrected dates (grey dots) (corrected for contamination by initial thorium) include the uncertainty in the correction factor.

All Late Holocene Deaths

Figure 4.5. Uncorrected (a) and corrected (b) dates of coral deaths between the mid-18th and mid-19th centuries.

a.

1750-1860 coral deaths - uncorrected
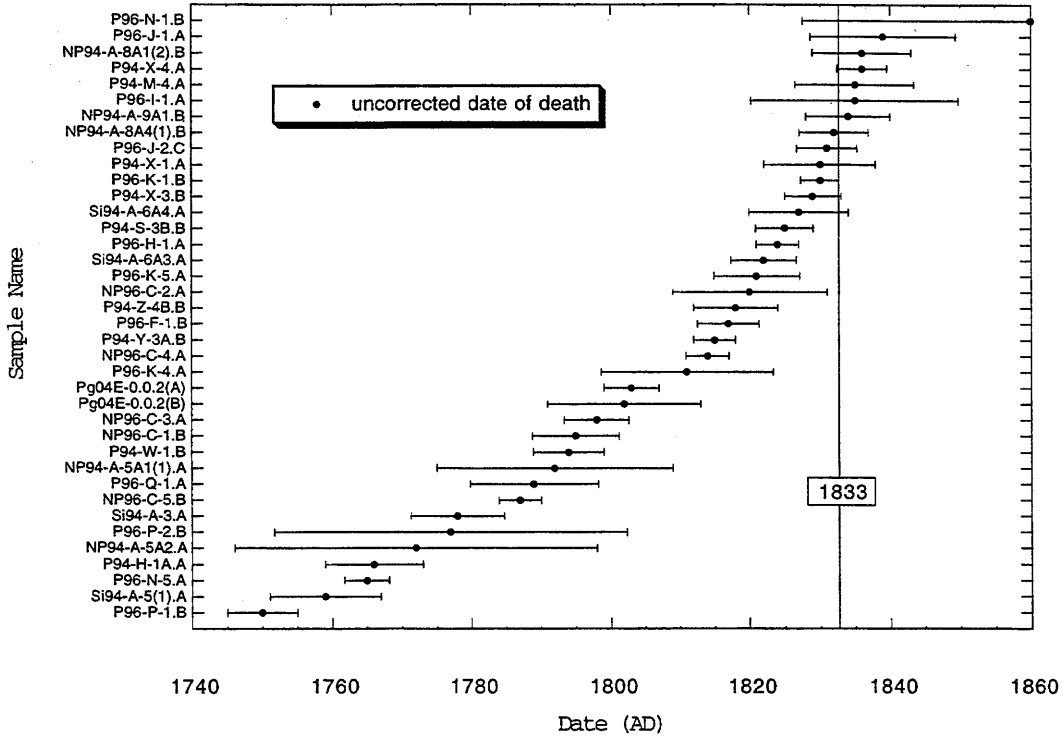
b.

1760-1850 coral deaths - corrected
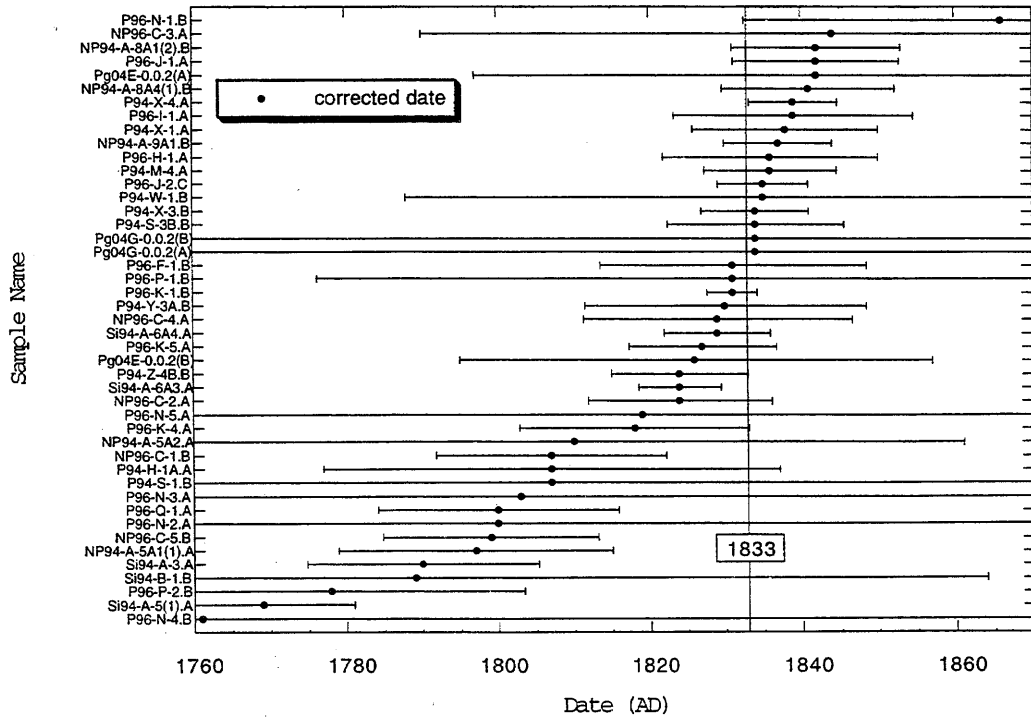
Figure 4.6. Dates of coral deaths from samples with relatively low ^{232}Th concentrations. The ^{232}Th concentration is a measure of the degree of contamination of the sample. The correction factor for contamination is not well-constrained, so the corrected dates of highly contaminated corals have high uncertainties. By using only clean corals, the age uncertainties are minimized and any clustering of events around certain dates is almost certainly real and not a function of high age uncertainties. The clean samples show that the clustering around 1833 implied in the plot of all dates (Figure 4.5) is significant. It further suggests, since there are clean corals that do not fall into the 1833 realm, that the pre-1833 "event(s)" revealed in Figure 4.5 probably also occurred.

a.

1730-1860 coral deaths - uncorrected
clean samples only

b.

1750-1860 coral deaths - corrected
clean samples only
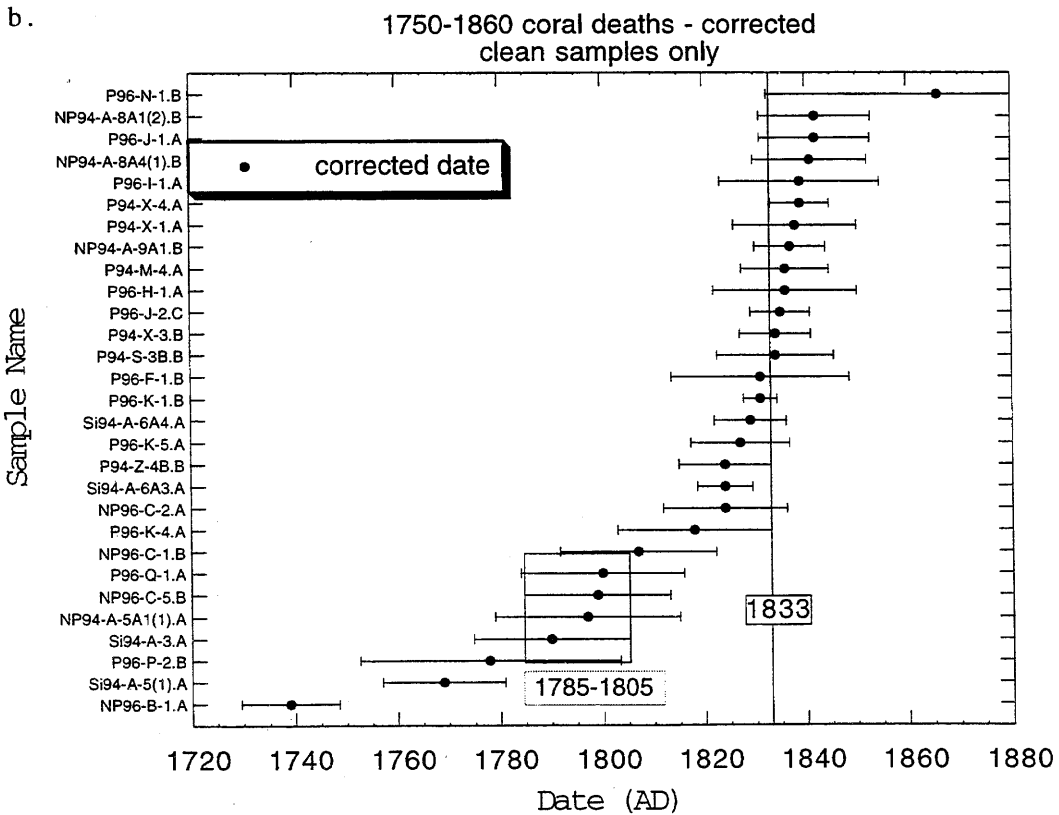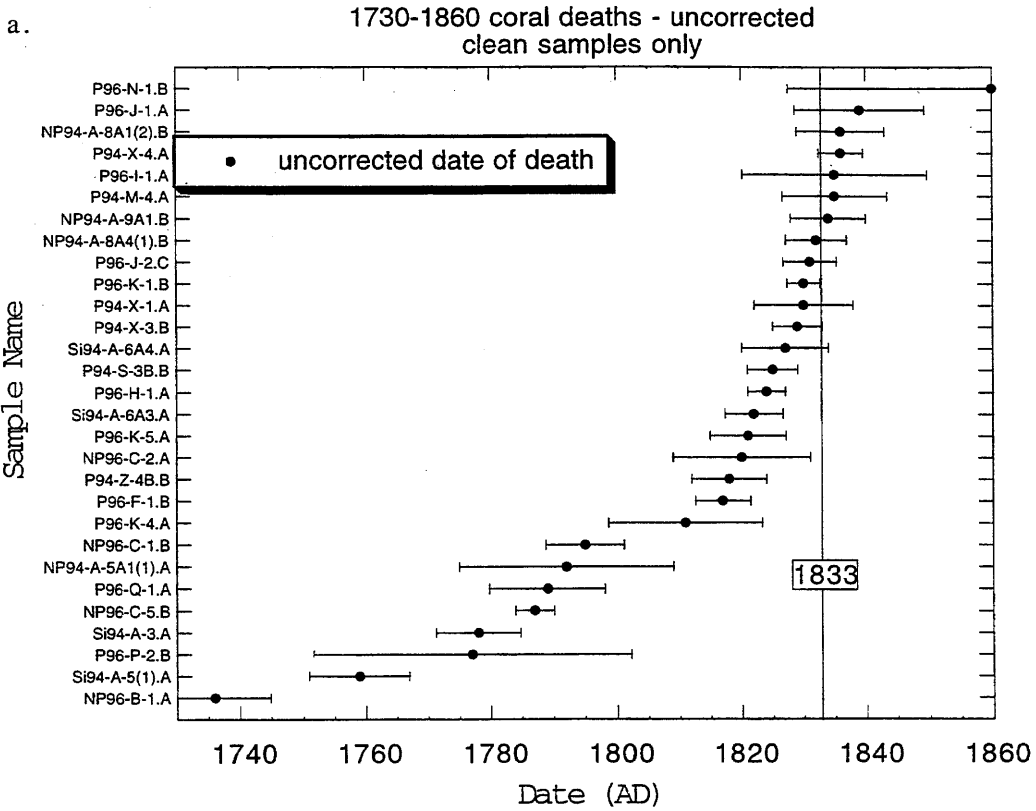
tsunamis in the Batu Islands and on the coast of Sumatra, northeast of Sipora. It is possible that this event is represented by some of the corals in the early cluster.

There is ample evidence in the ages of emerged corals from sites throughout the Pagais and Sipora of the existence of a death event between 1820 and 1845. The coincidence of this cluster of coral deaths with 1833, the year of the Mw 8.7 earthquake, suggests strongly that the corals in the islands died from exposure shortly after emergence during that event. The twenty-plus sampled corals that died around that time then should have recorded the vertical displacements associated with the event. The size of the emergence needed to lift them out of the subtidal zone and kill them is a measure of the coseismic uplift. The HLS record retained in their fossil skeleton is a measure of their preseismic displacement history.

4.2d. Early 19th-century emergence events

The results in Chapter 2 showed the value of slab stratigraphic analysis for obtaining detailed histories of HLS. Gross morphology in live corals was consistent with the general picture of modern submergence but did not constrain the details. Absolute elevations of HLS were the same at any given site, usually within ± 10 cm, although ranges as high as 25 and even 45 cm were observed. The same strengths and weaknesses should apply in analyzing fossil corals. Slab stratigraphy should provide more well-constrained and detailed records of HLS fluctuations, while the gross morphology may provide a general picture of relative sea-level changes on a similar or slightly poorer scale as the living corals. Emergences and submergences of more than a few cm should appear recorded in the slab stratigraphy within a few years of the event. Morphology might indicate "emergence" or "submergence" but not the timing or details of the event.

At most of these sites I observed numerous fossil microatolls exposed above the subtidal zone. Although at several of these sites, only 1833 corals were found, at others, sampling of multiple corals revealed the existence of other generations of coral in the same vicinity and at or near the same elevation. These offered a glimpse of the pre-1833 paleogeodetic and paleoseismic history of the site.

Most of the samples from corals that died in 1833 were hand samples. However, I collected slabs from seven corals whose ages are consistent with an 1833 death. The rest of the 1833 corals were only hand-sampled. The slabs come from sites on or near all three large islands, one from Sipora, two from North Pagai, and four from South Pagai (Figure 4.3). The slabs were collected, x-rayed, and analyzed in the same manner as were the slabs from live corals (Chapter 2).

I use the results of the stratigraphic analysis of the slabs in conjunction with morphological analyses of both slabbed and unslabbed corals from each site to try to constrain the emergence history of the site. At some sites in 1996, precise surveys were carried out, illustrating the relative elevations and gross morphological characteristics of the emerged corals. At sites where no survey was conducted, I measured elevations relative to water level and to HLS of live corals with a meter stick. Elevation data are less well-constrained at those sites.

In the following discussions, I will assume 1833 as the date of death for corals inferred to have died in that event. Discussion of the HLS history and dates of older rings and HLS impingements recorded in those corals will be referenced to an 1833 death. In discussing older corals and possible older emergence events recorded by them, I shall use the dates of death corrected for initial thorium contamination.

1833 slab records

Site Si94-A

Si94-A was one of only three sites visited on Sipora. It was on the small island Siruamata at the southern tip of Sipora (Figure 4.3). Several corals at this site attest to two large emergence events that occurred in rapid succession in the early 1800's (Figure 4.7). The latter probably occurred during the 1833 giant earthquake, but there is clear evidence here of an earlier event near the turn of the century. This site was not included in the 1996 surveys, but sketches and elevation measurements provide similar data. Elevation data were measured relative to HLS of living coral in 1994.

Slab Si94-A-6

Slab Si94-A-6 was taken from Coral 1. This microatoll was one of only a handful observed in the Mentawais that had a lower outer rim. The rim is indicative of a sustained partial emergence prior to final emergence. The coral head was 320 cm in diameter at the base and rose about 1 m above the sandy that partly buried its base. The outer rim was 20-25 cm high and 25-35 cm wide with a small horn on top of the outer edge; on the side of the coral from which the slab was taken, the horn was solitary, whereas on the opposite side, it was more complex. From the outer rim, the coral rose about 70 cm to a raised rim around a lower interior flat. The raised rim was double, the outer part rounded on top and the inner part having its own small set of horns on top (Figure 4.7d). The coral was well-preserved; it was located near the storm berm and may have been only recently exhumed from burial and protection under the sand.

The slab from this coral was the most intact of all slabs collected in 1994 and 1996 and possessed the least ambiguous annual banding (Figure 4.8a). I determined its age from U-Th dating of two samples from two separate rings. I counted the rings between the sample and the outermost ring to determine the age of death of the coral. The two dated samples yield consistent ages for the death. The outermost sample had a

corrected date of 1797 ± 7, which yielded a date of 1829 ± 7 for the death of the coral. The inner sample had a corrected date of 1770 ± 5, which yielded a death date of 1824 ± 7. There are 22 rings between the two samples, with very little ambiguity. The average date of death yielded by the two samples is 1827 ± 4. This is slightly younger than 1833, suggesting either that it emerged prior to 1833 or that the ages are inaccurate. In this discussion, I assume the final emergence occurred in 1833.

The coral head was large, so the saw did not reach the inner of the two raised rims, but did include part of the flat just inside and below the outer raised rim (Figures 4.7 and 4.8a). The slab cross section displays a history of submergence punctuated by two large emergence events. The oldest annual band sampled grew in about 1764. Growth from this time to about 1789 was unimpeded except for a brief HLS impingement in 1778. In 1789, an emergence of 8 to 10 cm occurred. Further submergence soon followed, as no HLS impingements occurred between 1789 and 1810. The coral had not again reached HLS when, in 1810, HLS dropped at least 70 cm, and the entire outer living band except the bottom 25 cm died. This is the only slab from a coral that records the elevation of the bottom of such a large emergence step, though it is the earlier coseismic step. Unfortunately, because the coral was not at HLS prior to emergence, the measured elevation difference, 70 cm, is still only a minimum. Nevertheless, it may be nearly exact. Double rims, like that on this coral head, were often observed in live corals, with both the inner and outer rims alive. Therefore, although, the inner rim was not sampled, it may have been a contemporary of the outer rim. The inner rim had a small flat at the top, suggesting it was at HLS a few years prior to emergence. Therefore, the top of the outer rim may also have been near HLS a few years prior to emergence although it is not explicitly recorded in the sample.

Lateral growth of the lowest 25 cm of the head continued after 1810, producing the lower outer flange. Post-emergence growth occurred at a reduced rate evidenced by

Figure 4.7a. Pace and compass map of site Si94-A, on Siruamata Island at the southeast corner of Sipora Island. Coral heads here record two large emergence events occurring against a backdrop of gradual submergence.

b. Cross-sectional sketches of several corals from Si94-A. The low outer rims on Corals 1 and 3 show that they had experienced a large (>70 cm) emergence prior to their final emergence. Analysis of a slab from Coral 1 reveals that the first emergence was sudden and probably occurred in about 1804. The final emergence occurred in about 1827 and was at least 27 cm in magnitude. The other two coral heads at this site, which do not have lower outer rims, appear to have died earlier than 1833. Their substrates are slightly higher than those of Corals 1 and 3.

c. Photo of emerged Coral 2. This coral died in 1790±15.

d. Photograph of coral head Si94-A-6, during the cutting of the slab. The coral has a doubled raised rim. The two parts are about the same elevation and may be the same age. Many live corals were observed with similar double rings that were both living. The interior rim has two small horns flanking a small flat, which indicates the coral reached HLS. The outer rim is rounded and does not have the horns. The slab only included the outer rim and a piece of the flat surface between the two rims.

a.

b.

c.

d.
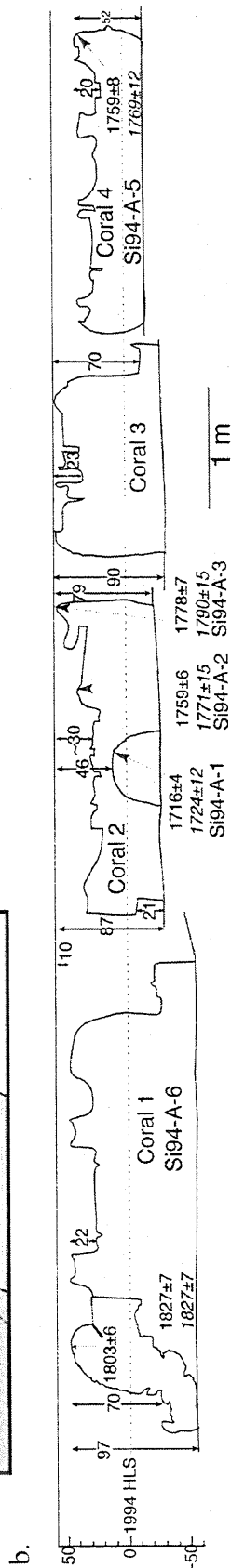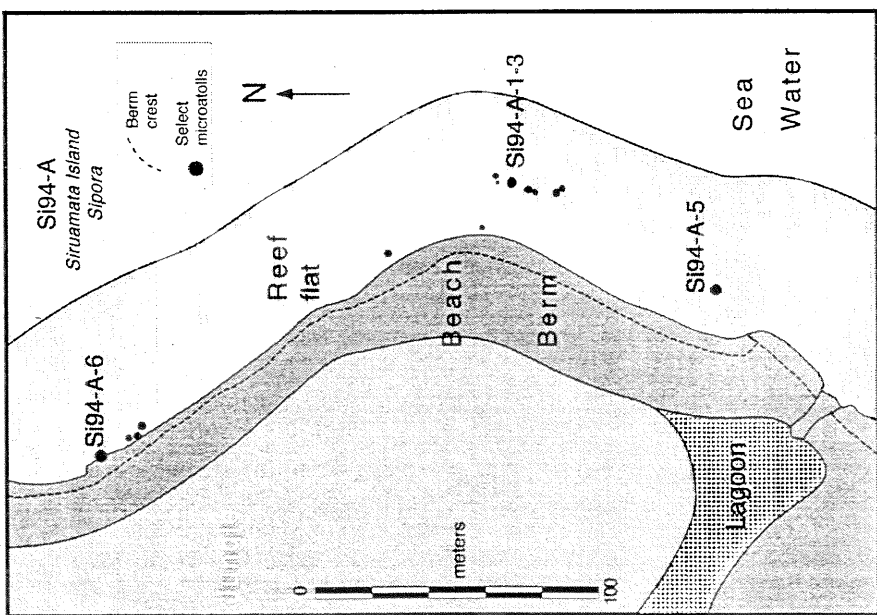
Figure 4.8. Tracings of x-radiographs of vertical cross-section slabs from coral heads. Outline of the slab, annual rings and old HLS surface are indicated. The methods for preparing and analyzing these slabs are presented in Chapter 2.

Figure 4.8a. Si94-A-6 - The outer portion of this coral head reveals a complex history of submergence and emergence. Final emergence probably occurred in 1833. This slab shows an early history of submergence with a couple of HLS clips or small emergence episodes. This coral experienced a large (>70 cm) emergence about 25 years prior to its final emergence.

Si94-A-6
P. Siruamata, Sipora

1769 ± 4 — Date from U-Th analysis and ring counting

1771 ± 5 — Date from U-Th analysis corrected for initial Th-230 contamination and ring counting

[1779 ± 3] — Date from ring counting, assuming final emergence and death occurred during 1833 earthquake

— Location of dated sample

10 cm

Emergence (≈ 9 cm)
1783 ± 6
1786 ± 7
[1789 ± 2]

1772 ± 6
1776 ± 7
[1779 ± 2]

1768 ± 5
1770 ± 5
[1779 ± 3]

Inner sample gives dates 5 yrs younger from rings only

1795 ± 6
1797 ± 7
[1801 + 0/-3]

32 +3/-0 rings

Emergence (≈ 70 cm)
1804 ± 6
1806 + 0/-3
[1810 + 0/-3]

eroded surface

Final emergence and death (≥27 cm)
1827 ± 7
1829 ± 7
[1833]

Figure 4.8b. NP96-A-9 - a complete slab through a small *Goniastrea* microatoll. The coral may not have been at HLS at the time of its final emergence. The flat surface in the center of the coral may approximately represent an old HLS surface. However, the surface is eroded, so HLS is not indicated. The magnitude of the emergence recorded by this coral is about 33 cm, the vertical distance from the top to the bottom of the outermost ring. Coseismic emergence could have been greater since the coral head rose above HLS completely.

NP94-A-9
P. Silabusabeu,
North Pagai

1830 ± 6
1833 ± 7
[1829 ± 1]

HLS
1819 ± 6
1822 ± 7
[1818 ± 1]

Final emergence and death
1834 ± 6
1837 ± 7
[1833]

erosional surface

10 cm

[1830]

[1825]

[1830]

[1825]

[1819]

[1815]

HLS
1820 ± 6
1823 ± 7
[1819]

1830 ± 6   Date from U-Th analysis and ring counting

1834 ± 7   Date from U-Th analysis, corrected for initial
            Th-230 contamination, and ring counting

[1829 ± 1] Date from ring counting, assuming final emergence
            and death occurred during 1833 earthquake

            Location of dated sample
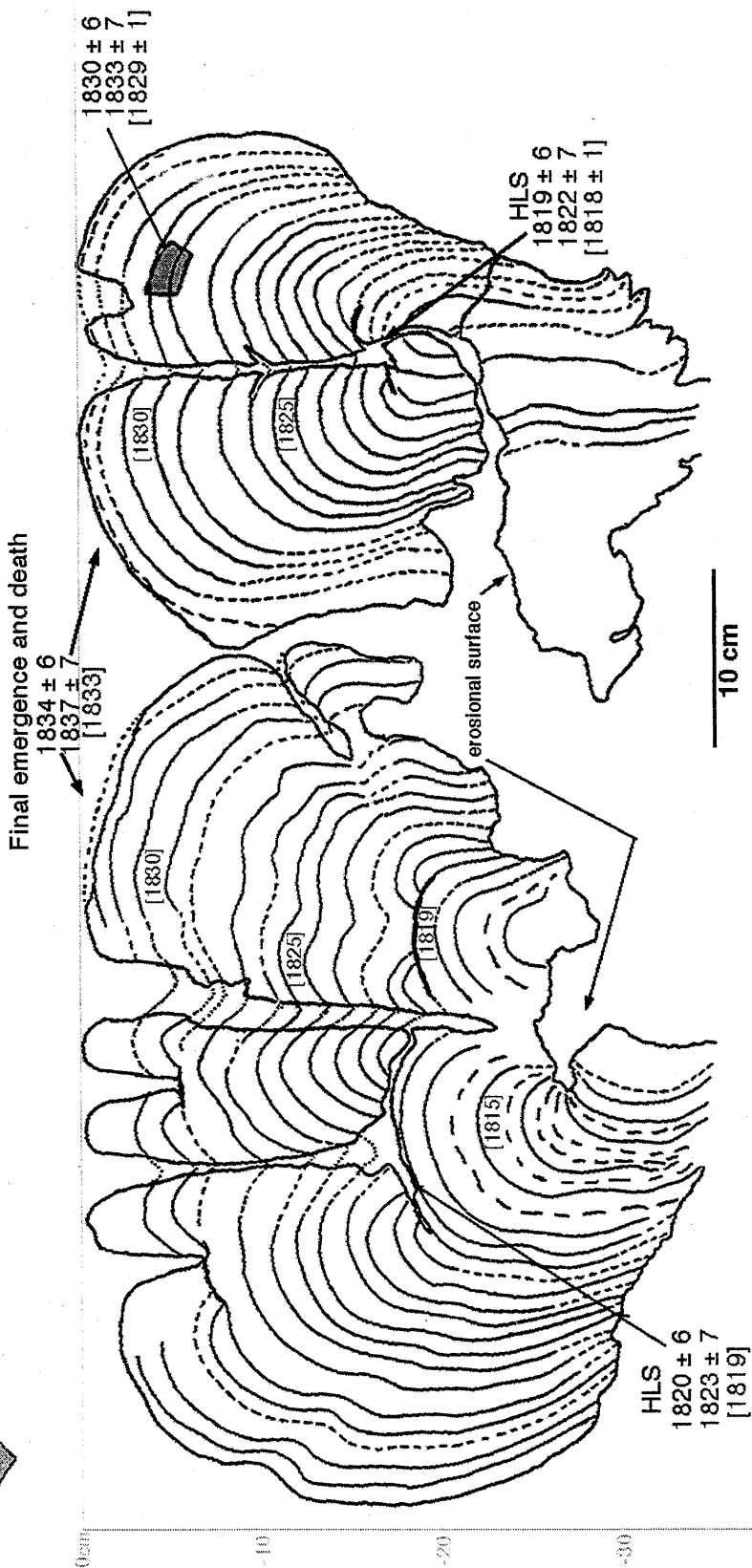
Figure 4.8c. NP96-A-8 - about half of a large *Porites* head near NP94-A-9. The interior was at or below HLS until the late 1700's when it emerged partially above HLS. There appears to have been an increase in substrate level at the same time or just afterwards that may reflect burial by sand. Later submergence allowed the development of the outer ring. Several HLS clips occurred during its lengthy period of submergence. Because the bottom part of the outermost ring is missing, the magnitude of the final emergence can only be constrained to be at least 13 cm, although the full height of the coral is much greater.

NP94-A-8
P. Silabusabeu, North Pagai

1817 ± 4 Date from U-Th analysis and ring counting

1824±11 Date from U-Th analysis corrected for initial Th-230 contamination and ring counting

[1821 ± 4] Date from ring counting, assuming final emergence and death occurred during 1833 earthquake

Location of dated sample

10 cm

Figure 4.8d. P96-F-1 - outer rim and part of the central flat of a *Goniastrea* coral. The central pieces are not directly connected to the outer rim, along this cross-section, so ring and age interpretations for interior section and correlation with the outside are speculative. A period of HLS stability represented by the central flat was followed by about 30 cm of submergence, punctuated by at least one episode of HLS impingement. The magnitude of final coseismic emergence was at least 20 cm.

Photographs show the top of the coral before slabbing (lower right) and during slabbing (upper right). The slab after sawing is also shown, with the relative position of the composite pieces and the location of the former HLS surfaces depicted. The shape in the drawing of the x-rayed slab is not exactly like that in the photo of the slab. The thin slab used for x-ray was cut from the interior of the larger slab. The shape of the slab changes because of morphological variations perpendicular to the cut face of the slab.
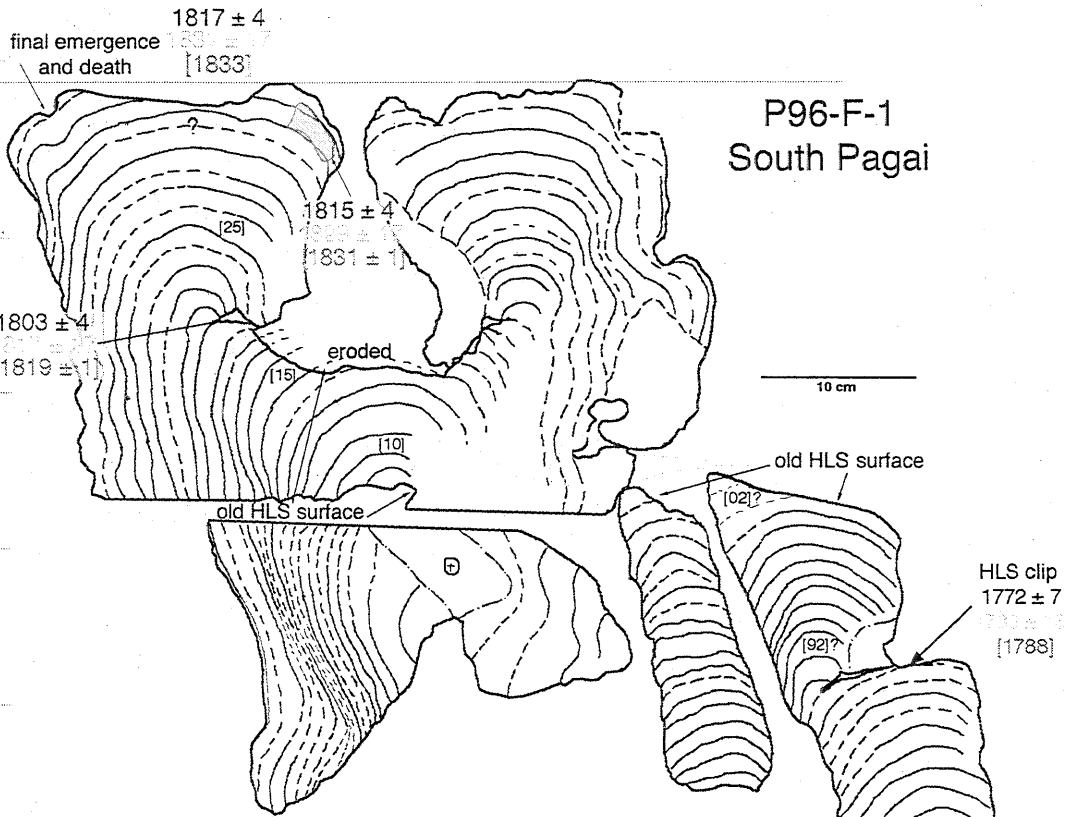
P96-F-1
South Pagai

1817 ± 4
final emergence
and death
[1833]

1815 ± 4
[1831 ± 1]

1803 ± 4
[1819 ± 1]
eroded
[25]
[15]
[10]

10 cm

old HLS surface
[02]?

old HLS surface
[92]?

HLS clip
1772 ± 7
[1788]

[80]?

1817 ± 4   Date from U-Th analysis and ring counting

            Date from U-Th analysis corrected for initial
            Th-230 contamination and ring counting

[1833]   Date from ring counting, assuming final emergence
            and death occurred during 1833 earthquake

            Location of dated sample

            Old HLS surface estimated from photograph (not x-ray)

approximate
location
of slab
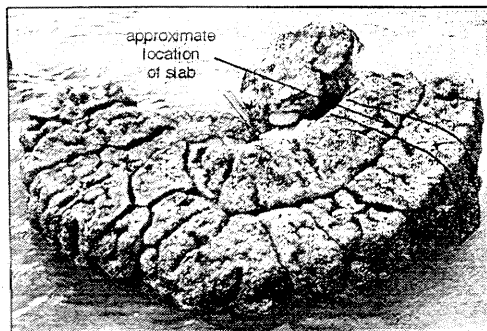
Figure 4.8e. P96-H-1 - slab from 120 cm-high *Porites* microatoll. Two HLS flats record periods of sea-level stability in an environment dominated by submergence. The minimum coseismic emergence recorded in this coral is only 10 cm because the bottom of the outer ring is missing, in the plane of the cross-section. The lack of a post-1833 lower outer rim allows the possibility that emergence was greater than 120 cm.

282

P96-H-1
Teluk Tiop, South Pagai

1806 ± 4   Date from U-Th analysis and ring counting
1818 ± 14 Date from U-Th analysis, corrected for initial
           Th-230 contamination, and ring counting
[1815 ± 2] Date from ring counting, assuming final emergence
           and death occurred during 1833 earthquake
           Location of dated sample

1782 ± 5
1794 ± 15
[1791 ± 3]

1806 ± 4
1818 ± 14
[1815 ± 2]

1818 ± 3
1830 ± 14
[1827 ± 1]

final emergence
1824 ± 3
1836 ± 14
[1833]

10 cm

Figure 4.8f. P96-J-2 - outer rims and portion of the interior of a *Porites* microatoll from one of the many islands southeast of the South Pagai peninsula. Two flats, a central flat and a flat near the top of the outer rim suggest two episodes of HLS impingement during a period of overall submergence. The horns at the top of the rim suggest that submergence occurred about 3-4 years before final emergence. The final emergence was at least 22 cm.

P96-J-2
Siatanusa Island, South Pagai

final emergence
1831 ± 4
1835 ± 6
[1833]

1820 ± 4
1824 ± 6
[1822 ± 1]

1814 ± 4
1818 ± 6
[1816 ± 1]

1814 ± 4   Date from U-Th analysis and ring counting

1818 ± 6   Date from U-Th analysis corrected for initial
Th-230 contamination and ring counting

[1816 ± 1] Date from ring counting, assuming final emergence
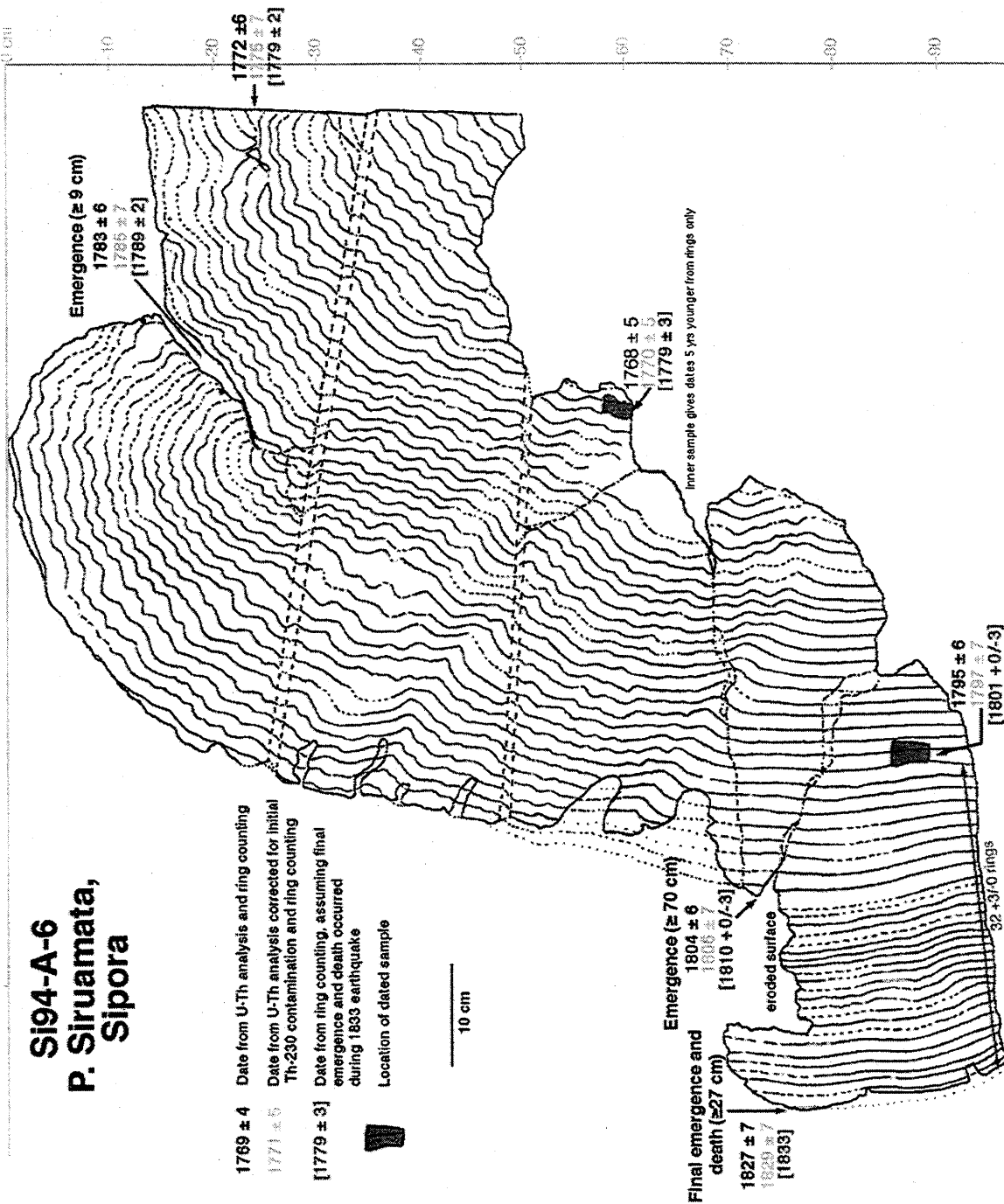and death occurred during 1833 earthquake

Location of dated sample

10 cm
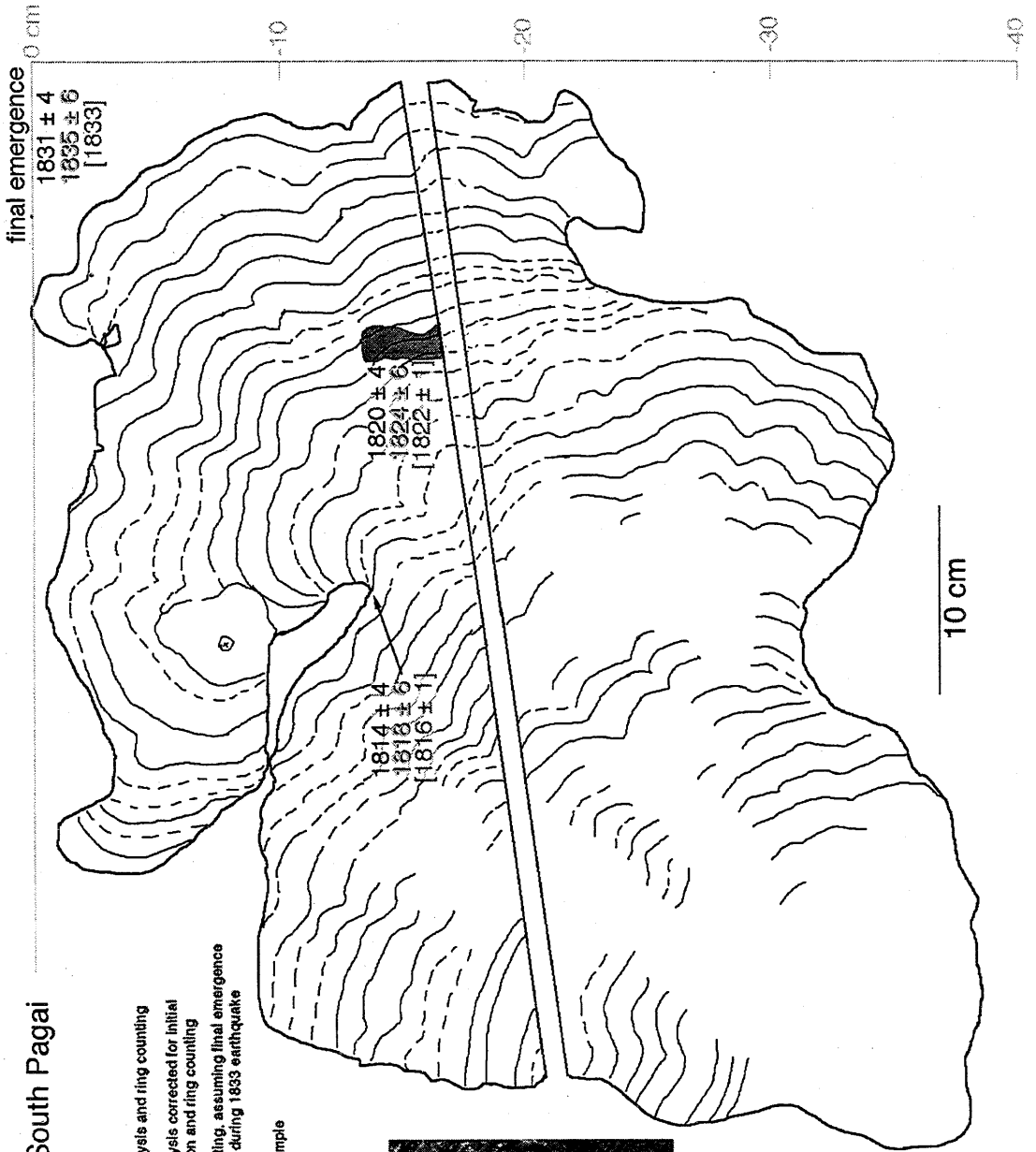
Figure 4.8g. P96-K-4 - outer rim and portion of the interior flat of a *Porites* microatoll. Only one early interaction of the coral with HLS is recorded in the short record this slab provides. Submergence dominates the history of this head, prior to its death by emergence. Minimum final emergence was 27 cm.

P96- K- 4
Taitanopo Island, South Pagai

1802 ± 12 Date from U-Th analysis and ring counting

1809 ± 15 Date from U-Th analysis corrected for initial
Th-230 contamination and ring counting

[1824 ± 2] Date from ring counting, assuming final emergence
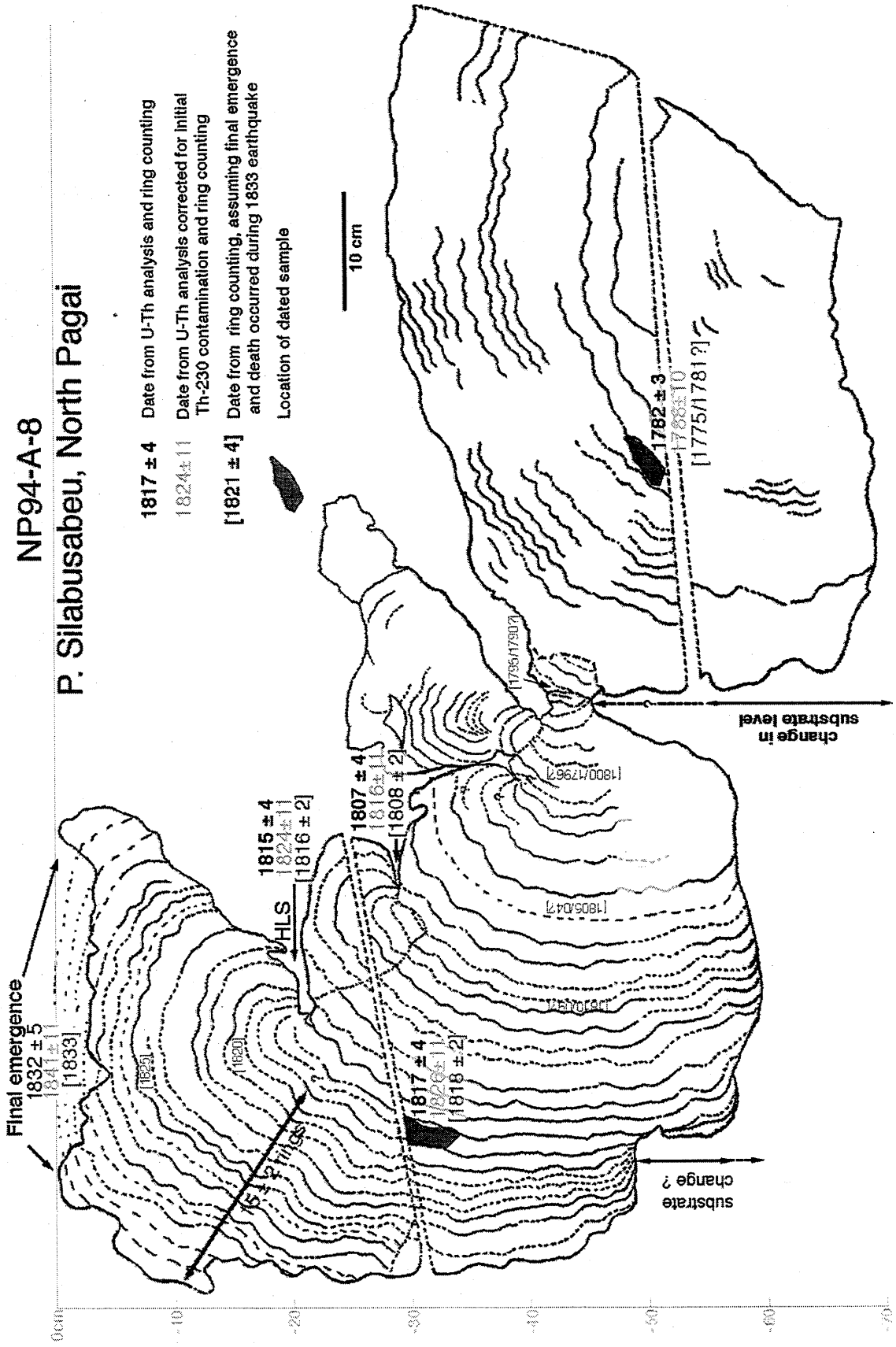and death occurred during 1833 earthquake

Location of dated sample

Final emergence
1810 + 12
1817 ± 15
[1833]

1802 ± 12
1809 ± 15
[1825 ± 2]

1790 ± 12
1797 ± 15
[1813 ± 1]
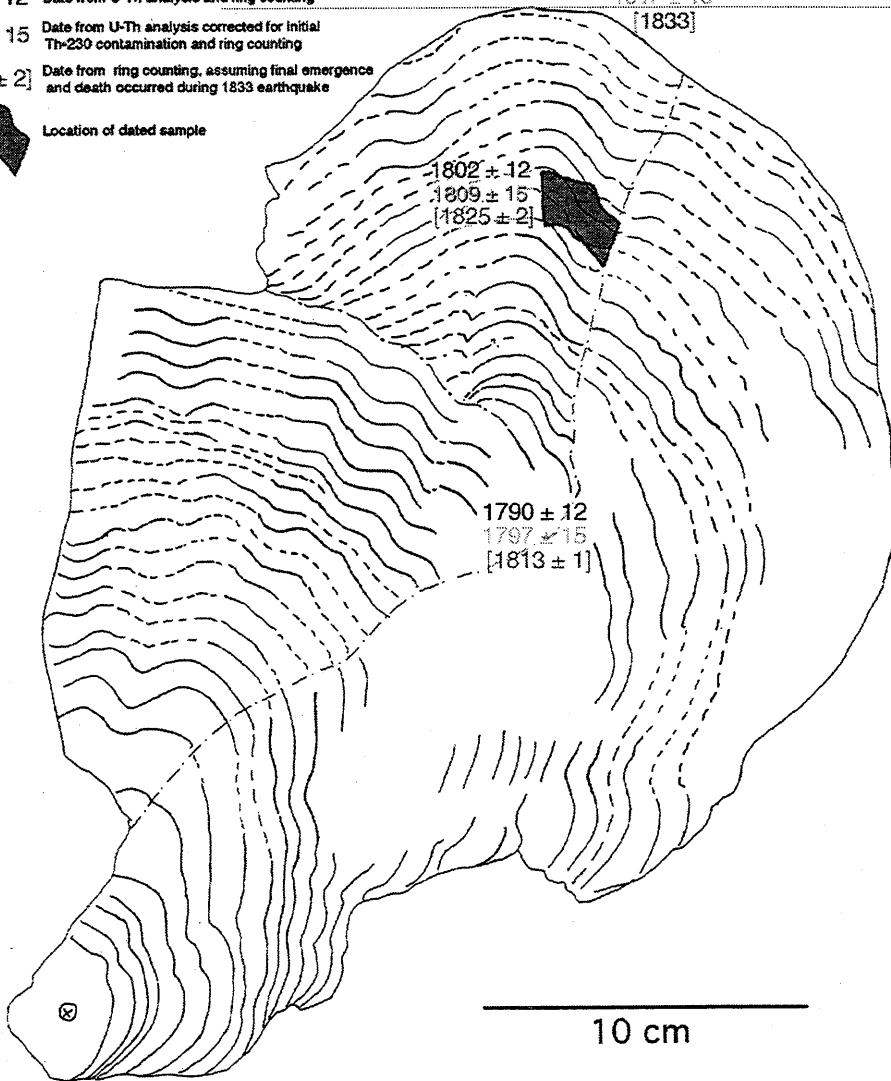
10 cm

the narrow growth bands from 1810 to about 1824. The average thickness of these rings is about half that of the pre-1810 bands. Perhaps the shallow water over the reef flat following the emergence led to warmer water temperatures or poorer circulation of nutrients during low tide. Either or both of these effects could have created a more harsh environment for the microatoll which inhibited growth.

Erosion has removed the top of the lower rim so it is unclear exactly how the coral responded to HLS in the decade or two following the emergence. On the side of the coral opposite the slab, the outer rim has an almost flat top, with two or three small raised rims, stepping up to the outside. This side was not examined stratigraphically. However, its shape, and measurements of the elevations of the small rims, suggest HLS was nearly stable within a few centimeters in the decades between 1810 and the coral's death in 1833, or there may have been slight submergence following the 1810 coseismic emergence, but at most about 8 cm over the 23 years. The slight emergence suggested by the decrease in elevation of the outermost several growth bands on the flange in this slab is probably due to erosion, not HLS impingement, since the rings are truncated and do not taper. About 30 years after the 70+ cm emergence, a second emergence lifted the rest of the coral head above its HLS and killed it. This emergence, which was probably from the 1833 event, was at least 27 cm, the height of the outer rim above the substrate. In fact, because the outermost ring is not complete all the way to the substrate, technically this emergence can only be constrained to be at least 10 cm. It seems likely that the entire coral and its substrate emerged, but a sample with complete rings all the way to the bottom would be necessary to precisely determine that.

A graph depicting relative HLS history derived from this coral appears in Figure 4.9. I plotted the history relative to an 1833 final death date. Elevation is measured relative to the top of the head, which is presumably either the HLS just prior to emergence or some unknown distance below HLS if the coral was not at HLS. The

coseismic emergence is the last leg of the curve, with the downward arrow illustrating that this is only a minimum estimate of the emergence. Since the coral was completely emerged, the curve ends here, and there is no record of the post-1833 HLS history.

The morphological and stratigraphic signature of HLS in Si94-A-6 indicates that it died as a result of a sudden emergence about 25 years after another emergence of at least 70 cm. The proximity of its date of death to 1833 suggests that the emergence was precipitated by coseismic uplift in the giant earthquake of that year. If uplift caused Si94-A-6 to emerge fully and die, other corals living at the site at that time should also have been uplifted. Thus, other corals of similar age should reveal similar HLS records. The degree to which these records are similar or dissimilar constrains the precision of the coral instrument. Corals of different age at the site may likewise reveal the existence of other emergence events.

Si94-A-6 and other corals from site Si94-A

Of the four corals examined at Si94, two had a lower outer rim, indicative of partial emergence (Figure 4.7b). The other two did not. The rims on both Coral 1 and Coral 3, are about 25 cm wide and 70 cm below the highest part of the coral. Stratigraphic analysis of the slab, Si94-A-6, indicated that the HLS of Coral 1 dropped at least 70 cm about 23 years before its final emergence. I did not slab or date Coral 3, but its morphology suggests that it was a contemporary of Coral 1 and experienced a similar HLS history. Furthermore, the absolute elevations of the two corals are with 10 cm of each other, consistent with the corals being contemporaries. Like Coral 1, Coral 3 appears to have been slightly below HLS just before that emergence, so the amount of emergence is a minimum. However, it too had two small horns, 5 cm above a small flat on a raised interior rim that was the same elevation as the outermost raised rim. If the two rims of equal elevation were coeval, it suggests that the corals were at or near HLS about 5 years

Figure 4.9. Plots of HLS elevation versus time for the seven corals that died from emergence in about 1833. Dots mark the elevations of HLS surfaces or "clips". Arrows indicate lowest limit for HLS in years in which the rings were unimpeded by HLS. Instead, their upward growth was limited by their natural growth rate. Thus, HLS must have been somewhere above the tops of the rings. Downward-pointing arrows at the end of each curve indicate that the measured total coseismic uplift is greater than or equal to the vertical extent of the youngest annual band, since the coral head emerged completely.

The horizontal axis is time measured relative to an 1833 death date for the corals. The curve based on the uncorrected or corrected date of death would have the same form but would be shifted forward or backward the appropriate number of years.
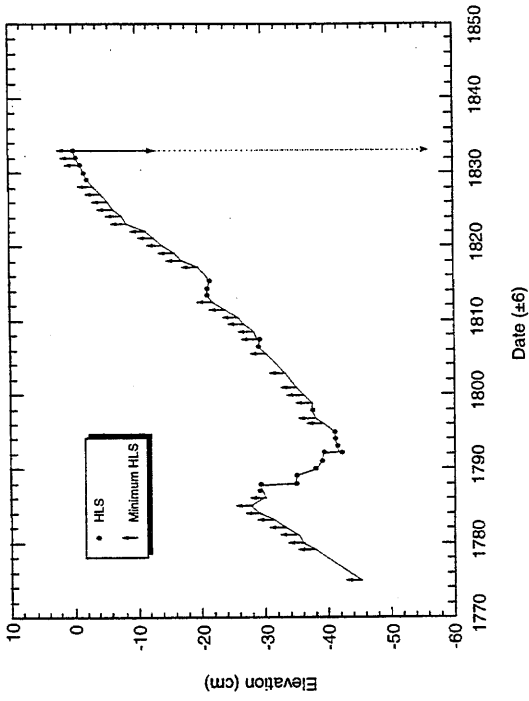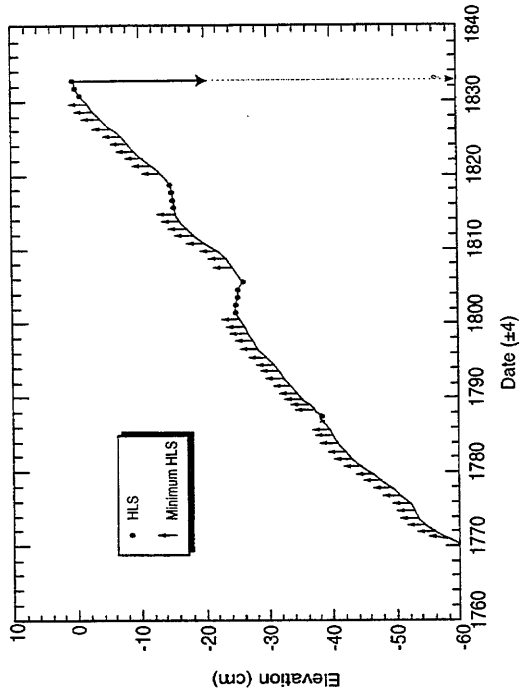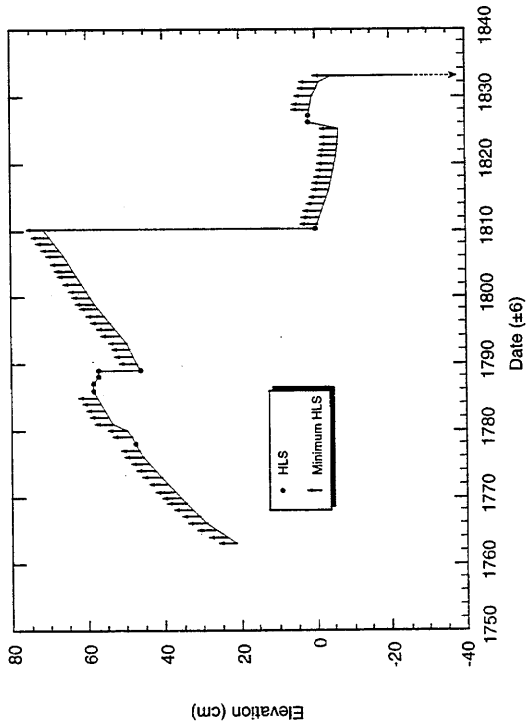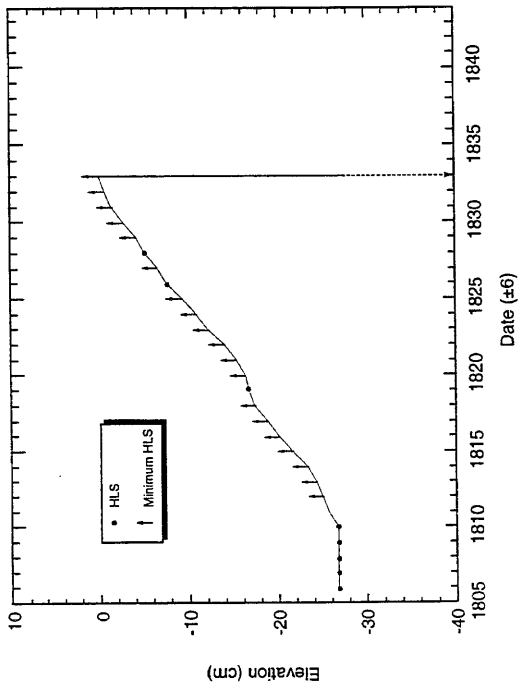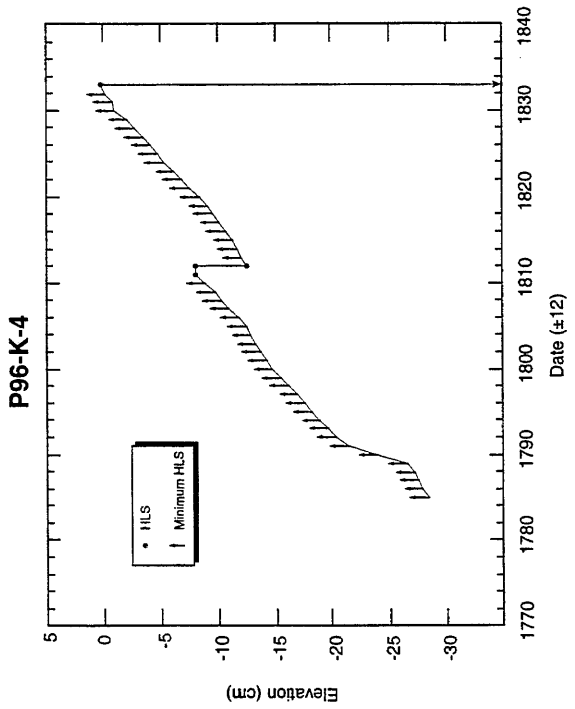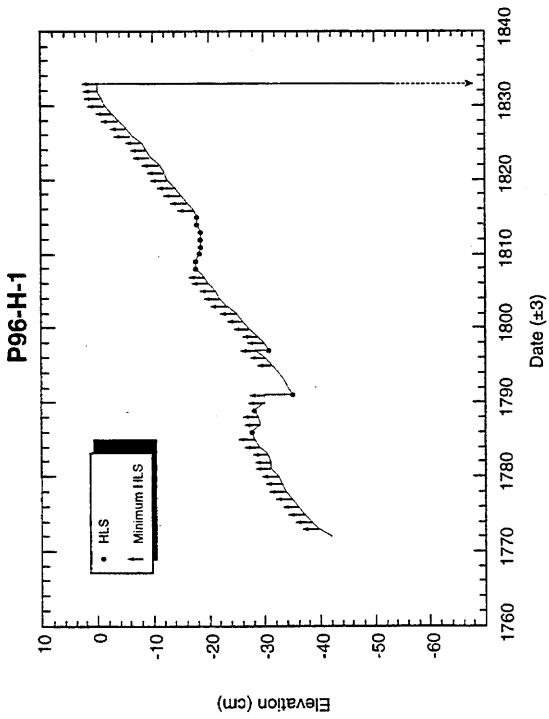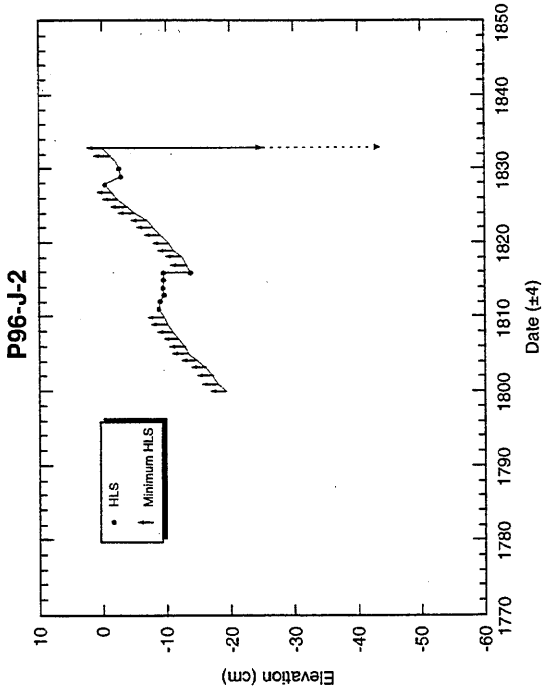
before the emergence. Again, like Coral 1, the low outer rim of Coral 3 is within a few centimeters of being flat, with maybe a slight (2 cm) lip at the outside, indicating that sea level was relatively stable for several years following the partial emergence. The short post-seismic period was then followed by another emergence that brought the coral completely out of the water.

Although the morphologies of Corals 1 and 3 suggest they may have been near HLS just before the 1810 emergence and although both have HLS steps of about 70 cm, the absolute elevation of the top of Coral 1 is about 14 cm lower than Coral 3. This elevation difference does not mean that the corals cannot be contemporaries. The study of living corals revealed that elevations of contemporaneous HLS may differ from coral head to coral head by ±10 cm or more.

The tops of Corals 2 and 4 at this site are within 20 cm of the tops of Coral 1 and 3. They have no lower ring, suggesting they experienced a different HLS history from the other two corals. Their substrates are higher than those of the ringed corals, and their bases sit at approximately the same elevation as the top of the outer lower rings in Corals 1 and 3. U-Th analysis of Corals 2 and 4 indicate that they died in 1790 ± 15 and 1769 ±12, respectively. The uncertainties on the dates permit them to be contemporaries in death of each other, but not of Corals 1 and 3. They could not have died in 1833, if their ^{230}Th ages are correct. However, their lives must have overlapped with those of Corals 1 and 3, since they died a few decades prior to Coral 1. Thus, the HLS records of Corals 2 and 4 should be consistent with those of Coral 1 and maybe Coral 3.

Coral 2, about 80 cm tall and steep-sided, was broken in half (Figure 4.7c.). One side was relatively intact, the other eroded. The intact side showed the development of an outer rim, above and overhanging a central flat. The "flat" itself, is not flat but has a step up to a higher level about halfway across. The core of the coral was a hemispherical mound, partially detached from the flat around it, suggesting an emergence had occurred

before the hemisphere had first reached HLS. Submergence and coral growth, up to and at HLS, following that emergence, resulted in development of the stepped central section, and further submergence permitted development of the outer, raised rim. The morphology of the outer rim suggests the coral was at or near HLS just prior to emergence. The top of this coral is about 10 cm higher than the top of Coral 1.

I dated three different pieces from Coral 2. The outermost edge of the coral has an age of 1790±15; a subdued riser within the central flat has a date of 1771±15; and the outer edge of the central hemisphere has a date of 1724±12.

The morphology of Coral 2 suggests it could have emerged fully and died during the emergence event that caused the 70-cm step in Coral 1. The base of Coral 2 is nearly at the elevation of the top of Coral 1's outer rim, so the partial emergence in Coral 1 would register as a total emergence of Coral 2. However, the uncertainties on the ^{230}Th ages just barely do not permit an 1810 date of death. If the ages are correct, then, the coral must have died during an earlier emergence event. Since the record from Si94-A-6 goes back to 1764, this event should be recorded in Coral 1 also. Two HLS impingements appear in Si94-A-6 before the 1820 event - a 10 cm emergence in 1789 and an HLS clip in 1778. The 1789 emergence is constrained to be 10 cm because the coral was at HLS before and after; only the bottom of the 1778 event is defined.

The 1789 date is consistent with the age of death of Coral 2. However, the 10-cm emergence step seems too small to have killed the entire coral, which is 80 cm tall. A 10-cm emergence could have killed Coral 2 if at least the bottom 70 cm of the head were already dead prior to the final emergence. This seems unlikely, given the steep sides of the coral, which suggest a common age for the entire outer edge of the coral. However, steep-sided corals were sampled that had incomplete outer growth rings. In the absence of a slab sample from the base of the coral, this possibility cannot be ruled out. The bottom parts of the coral might have died during or after the emergence, but from some other

cause besides emergence above HLS, since they would still be below HLS. A possible cause might be burial of the lower reaches by sand, although 70 cm is a lot of sand.

The 1779 date is another possibility for emergence, and the size of the emergence step is not constrained. There is only an HLS clip at that time in Si94-A-6; HLS before the clip is not defined. The clip could just reflect the bottom of a substantial HLS drop, although it seems slightly fortuitous that is should barely clip the surface of the coral. Indeed, if the HLS clip allows an unconstrained emergence since the coral was growing an unknown distance below HLS prior to it, so do all the years of growth without any clips at all, since large emergence events could occur and never be recorded by a coral as long as it stayed below HLS. The top of Coral 2 is only 10 cm above the top of Coral 1. Assuming the absolute elevations of HLS in the two corals were within about 20 cm of each other, Coral 1's HLS should have been no more than 30 cm above the current top of the head at the time of Coral 2's final emergence. An emergence that brought Coral 1's HLS from 10 to 30 cm above the top of the coral to the level of the HLS clip would be about 33 to 53 cm, since the clip is about 23 cm below the top of the coral. A 33-53-cm emergence in Coral 2 seems more likely to have killed the coral outright than the 10 cm emergence of 1789, although it still requires that the bottom 25-45 cm were already dead at the time of emergence, or died from some other cause during it.

Coral 4 was one of a population of corals, at the southern end of the reef flat, whose tops were at a lower elevation than those of Corals 1, 2 and 3, and corals near them in the northern and central parts of the reef. The southern corals were closer to half a meter tall, while the northern corals were nearer one meter high. Coral 4 was a wide, low coral with several raised rings indicative of submergence prior to final emergence. The date of the outermost part of its raised rim was 1769±12. If the age and uncertainties are correct, it could have died in 1778, but not 1789 or 1810. It was 52 cm high, and the lower half of the coral was undercut, suggesting the growth rings may not have been

complete to the bottom. It appears to have been at HLS just prior to emergence, based on the morphology of the outer ring. However, the absolute elevation of its HLS is 15 to 20 cm below that of Coral 2, and thus 35 to 40 cm below the HLS postulated for Coral 1 in 1778. A 15 to 20 cm elevation difference between HLS in Corals 4 and 2 seems possible, given the observed variation in HLS elevation in living corals, but 35 to 40 cm is probably too great a difference. Thus, if Coral 4 died in 1778 and all the corals were at or below HLS at the time, the absolute elevation of HLS in Coral 1 was probably not 20 cm above Coral 2, but at about the same elevation, 15 to 20 cm above Coral 4. So, the 1778 emergence could have been no more than about 25 cm. Final HLS in Coral 4 would have been about 25 cm above the base of the coral. Again, in this case, the lower rings of the coral must either already have been dead prior to emergence, or they died during or just after the emergence from a cause other than the emergence itself.

The prospect that Coral 4 emerged earlier than Coral 2 did is possible, and supported by the morphological and elevation differences between the southern and central coral populations. Any earlier emergence event that might have killed Coral 4 must have occurred after 1757, based on the ^{230}Th age of the outer rim. If the emergence were sufficient to raise the entire coral out of the water, it would be greater than 50 cm. This emergence should be recorded also in the younger corals. Sample Si94-A-6 has rings back only to 1764, so no record of 1757-1764 is available for that coral, but, given the rate of coral growth, probably HLS in 1757 could not have been lower than a few cm below the height of the 1764 rings. This would again result in post-emergence HLS still being well above the bottom of the dead Coral 4. If HLS dropped more than a few cm below Coral 1's 1764 ring, it would have to have rebounded rapidly in the seven years between 1757 and 1764.

There is no clear record of an emergence between 1757 and final emergence in Coral 2 either, although one would expect it, if Coral 4 emerged in that period. The step

up in the central "flat" of Coral 2 suggests submergence occurred in 1771. The outer edge of the central hemisphere may represent an emergence, but since the date of a sample from that part of the coral was 1724±12, it seems too early to be the emergence event recorded by Coral 4. Although Coral 2 was not slabbed, it was split open and its interior revealed. There is no clear record in that coral of the emergence that killed Coral 4, unless it was the final emergence. This would constrain the event to having occurred between 1775 and 1781, making the 1778 scenario more likely.

The four corals of Si94-A illustrate the possibilities and the pitfalls inherent in using fossil microatolls to document past relative sea level changes. The HLS record derived from the slab, Si94-A-6, from Coral 1 is very robust. Three emergence events of about 10 cm, 70 cm, and >25 cm are extremely well-documented. The time between the event is also constrained to within a couple of years, since this slab has such clear growth rings. Submergence preceded the earlier events, as evidenced by both the slab stratigraphy and the morphology of the coral head, which has a cup shape. Insofar as the ^{230}Th age is accurate, the slab HLS record establishes a history of emergence and submergence in fossil corals with the size and absolute ages of events constrained as well as they can be in living corals.

The robustness of the slab record is not matched by the morphological record of HLS displayed in corals that were sampled but not slabbed. Several apparent discrepancies appear between the corals, based on their age and morphological characteristics. Morphologically, Corals 2 and 3 appear consistent with the record from the slab of Coral 1. However, the ^{230}Th age of Coral 2 is not consistent. Thus, either the age is wrong, or if it is right, Coral 2 documents another emergence event that caused the death of Coral 2, but shows up barely, if at all, in Coral 1, and requires that other factors besides exposure above HLS be responsible for the death of Coral 2. It may be that the ^{230}Th age of Coral 2's emergence, only a few years younger than the 1810 emergence in

Coral 1, is, in fact, inaccurate, and the coral is of the same age as Coral 1. It would make the HLS morphology of those corals more consistent. Such an age error could be due to insufficient correction for initial thorium contamination. A larger correction factor applied to corals at this site could bring Coral 2's emergence date to 1810, as well as bringing the age of death of Coral 1 closer to 1833, if that is indeed when Coral 1 died. A correction using an initial $^{230}Th/^{232}Th$ ratio of 22 x 10^{-6} would bring Coral 1's death date to 1833, and Coral 2's death date to 1821.

Coral 4 is harder to reconcile with the records of the other corals in the area, even without age uncertainties, because the emergence that killed it, if it occurred independently of the emergence that killed Coral 2, does not appear to be recorded in the other corals at all. Whether the apparent disparity between Coral 4's HLS history and that of the other corals is a function of incomplete rings, dating errors, errors in elevation measurements, HLS variability, posthumous shifting of one or more of the corals, variations in coral growth rate, or other factors is not immediately evident.

This analysis indicates that while slab HLS histories are robust and can allow distinction between emergence events of more than a few cm only a couple of decades or less apart, errors in ^{230}Th ages or contamination correction and morphological and elevation variations can introduce a significant degree of ambiguity in correlating between corals at one site. As the study of live corals indicated, slab stratigraphic analysis far outweighs morphological analysis alone in constraining the details of HLS history. It is likely that slabs taken from Corals 2, 3, and 4 would permit accurate and consistent correlations between corals where morphology alone will not. Finding cleaner corals and constraining the correction factor for ^{230}Th ages would also help clarify the site-wide HLS history. The degree of consistency and variability between corals at one site illustrated here for site Si94-A can be used to inform the analysis of coral records at other sites.

Site NP94-A/NP96-C

I visited site NP94-A/NP96-C in both 1994 and 1996. It is located on the west side of North Pagai, about two-thirds of the way down the coast from the northern tip of the island, in a bay just across from a small island (Figure 4.3). I surveyed profiles across the tops of sixteen emerged coral head here (Figure 4.10). There are a multitude of different morphologies and elevations represented. Fortunately, there is good age control here, with seven of the corals surveyed in 1996 dated, as well as three others dated but not surveyed from 1994.

There are at least two, and possibly three, distinct groups of corals distinguished by elevation. Relative to water level on the afternoon of 12 February 1996, one group was largely exposed above water and one group was distinctly below. Dead corals D1, D2, D6, D7 and D8 belong to the high group, while corals D9, D12, D13, D14, D15, D16 and NP94-A-9 are from the low group. Corals D3, D4 and D5 could belong to the high group or might better be placed in a group of intermediate elevation, along with D10, which otherwise would be in the low group. The tops of the intermediate group sat approximately at water level. Corals D11 and NP94-A-6 were also low but were highly eroded, and therefore their low elevation is not significant.

ne elevation differences between the two groups should be significant on the ʋ determined from studying live corals. Modern mean HLS in different corals at a site was usually the same to within ± 10 cm. Here, the elevation difference between the high and low populations (excluding highly eroded corals) is as much as 55 cm. The clustering of coral ages roughly matches the grouping by elevation. The two high corals, D1 (source of sample NP96-C-5) and D7 (sample NP96-C-1), died in 1799±14 and 1807±15. Medium high D10 (sample NP94-A-5) also died in the late 1700's. The low corals D9

Figure 4.10. Map (a) and cross-sectional profiles (b) of dead coral microatolls at site NP96-C (also NP94-A). The locations and elevations of coral NP94-A-9 and NP94-A-6 were not surveyed in 1996; they are approximately located from field notes and a pace-and-compass map made in 1994. Corals surveyed in 1996 are labeled by their survey number, distinguished further between living and dead. Dead coral head 9 was the source of NP94-A-8

The profiles (b) show at least two populations of coral microatoll - one high and with complex morphology, the other lower, smaller and with much simpler morphology. Several corals from the lower population appear to have died in the 1833 emergence event. The higher corals may have died earlier, near the end of the 18th century. The morphology of both populations suggests they experienced preseismic submergence.

c. Photograph of emerged coral D1. This coral died in 1799 ± 14. The sample came from the outermost raised rim.

NP96-C

Legend:
- ◐6 dead coral head *with profile line*
- **9**● live coral head *with profile line*
- • beach survey point *high tide line*
- ✶ total station
- ☐ beach
- ☐ sea

b.

c.

raised outer rim

eroded flat
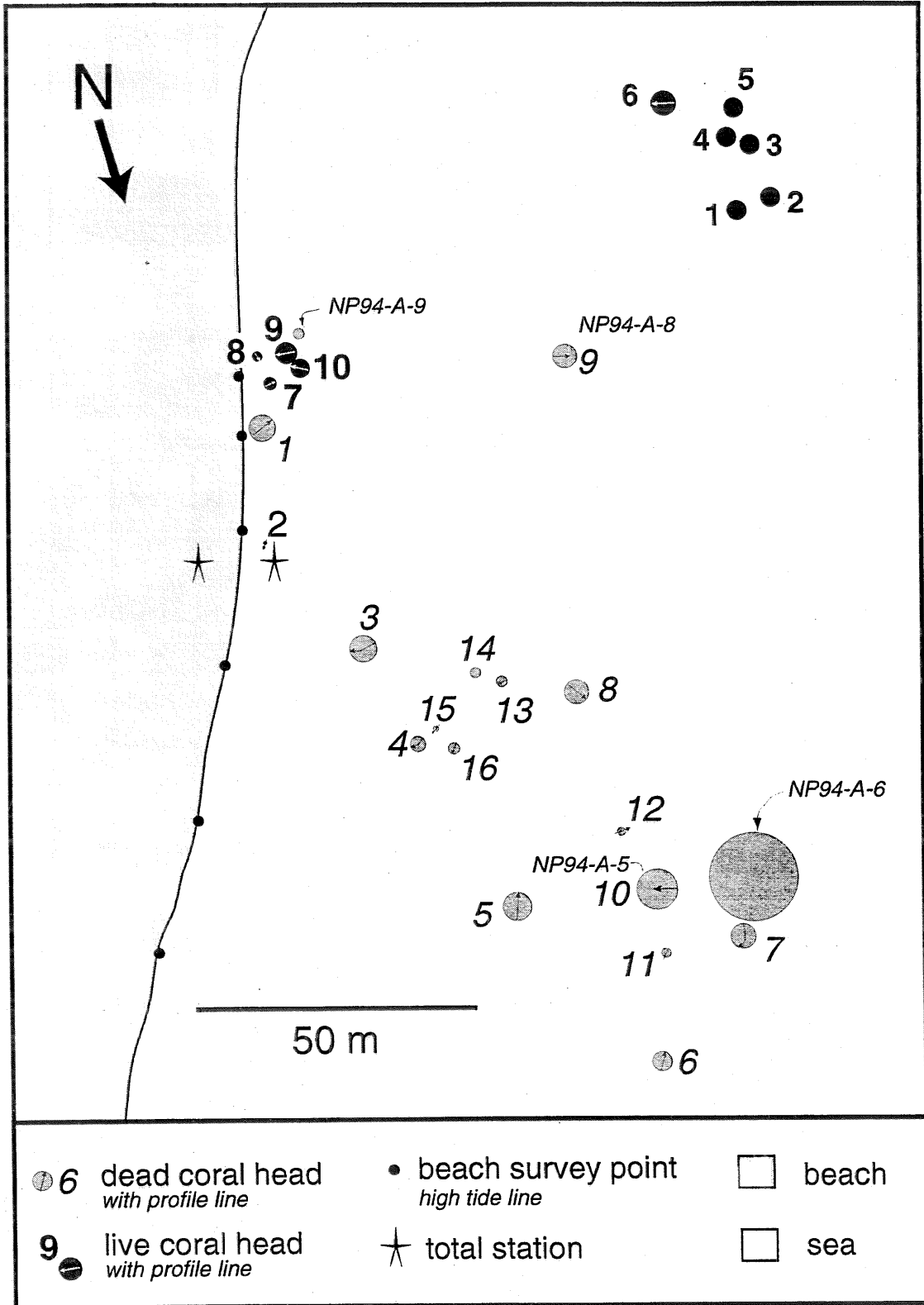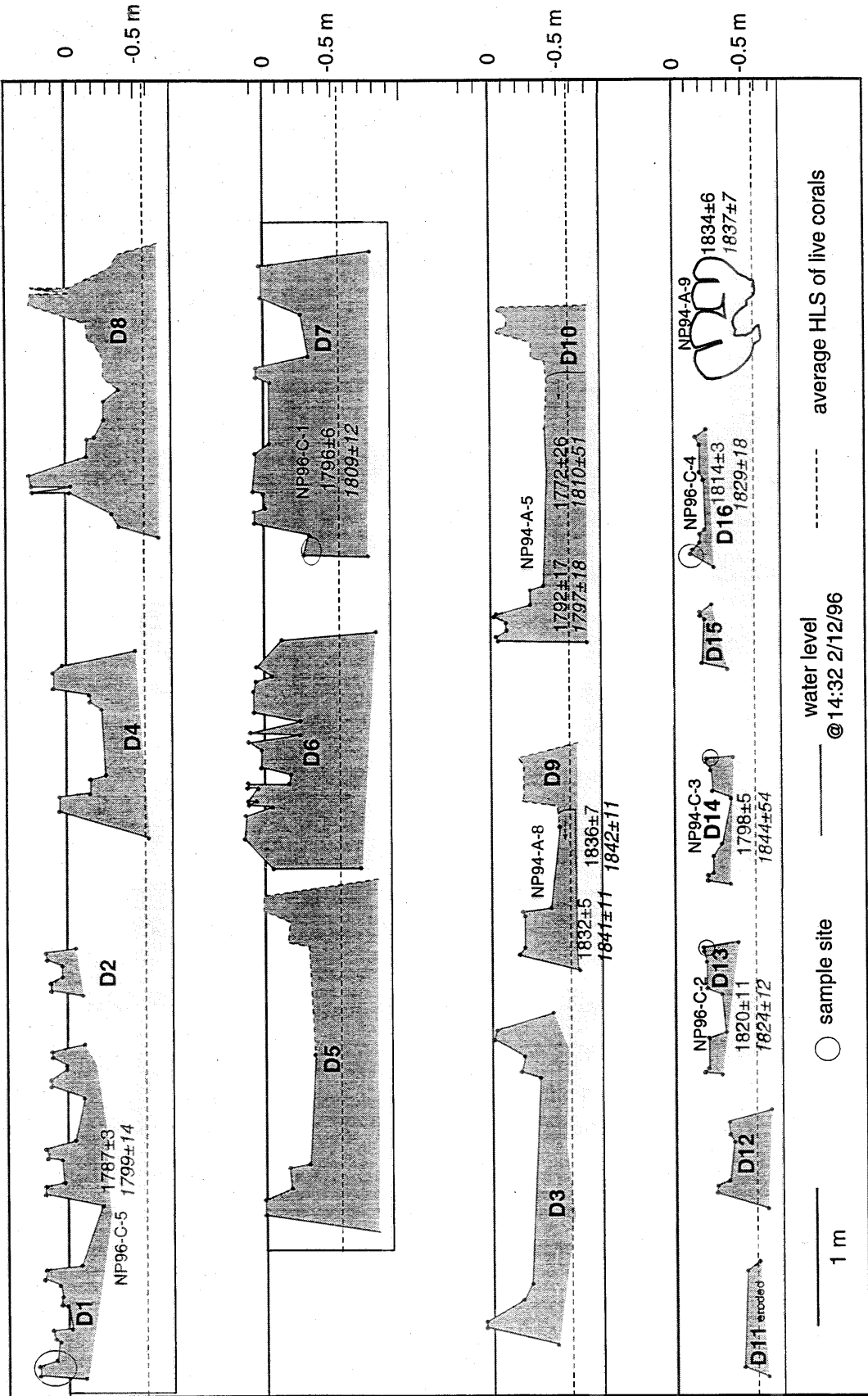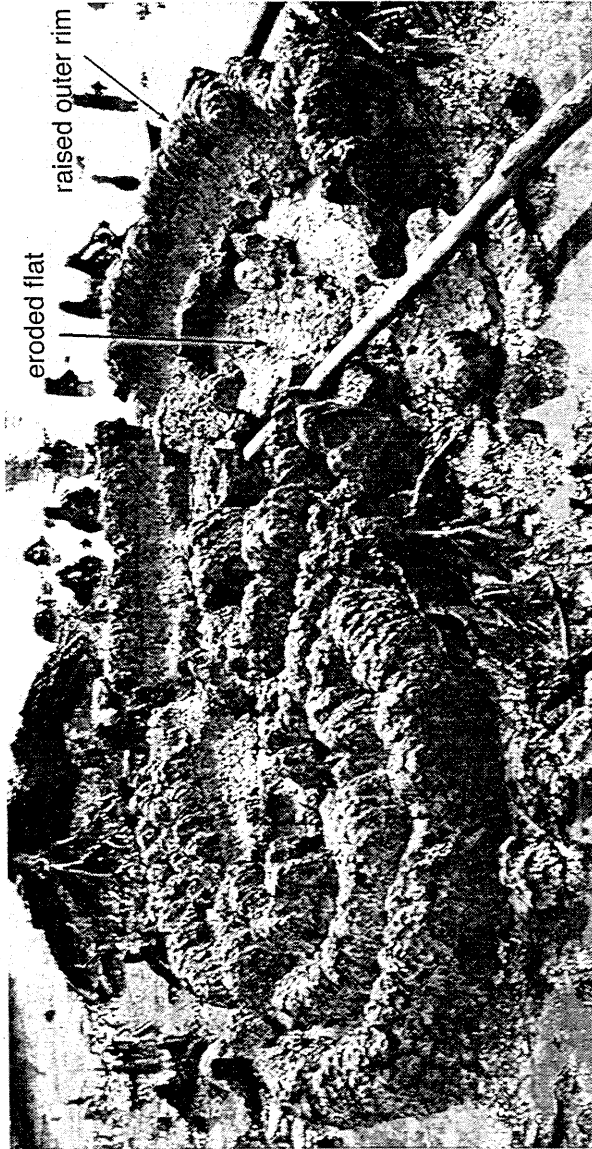
(sample NP94-A-8), D13 (sample NP96-C-2), D14 (sample NP96-C-3), D16 (sample NP96-C-4), and NP94-A-9 are all possible 1833 fatalities (Table 4.1; Figure 4.10b). (D14 could be late 1700's, but the large uncertainty leaves it in doubt.) The elevation differences are probably not due to faulting or folding within the bay, since no simple pattern of deformation would generate the observed distribution of high and low corals, and there is no indication of faulting in the reef flat. Furthermore, the individual coral heads do not exhibit noticeable tilt in any direction. Finally, the apparent correlation of older ages with higher elevations, and 1833 ages with lower elevations, suggests that the two populations represent different generations, and the elevation differences result from different growth histories, not posthumous erosion or displacement.

NP94-A-9 and NP94-A-8

Two slabs, NP94-A-9 and NP94-A-8, were collected from corals at this site, both apparent 1833 casualties. The first, NP94-A-9, came from a small *Goniastrea retiformis* coral (Figure 4.11). Its corrected ^{230}Th date of death is 1837 ± 7. Its location relative to other microatolls at the site appears in the surveyed map of the site (Figure 4.10a). It was located very near shore and at the southern edge of the collection of emerged microatolls, near the transition to the living community. The coral head was about 40 cm in diameter and slightly tilted to the south such that its height above the sandy substrate was 21 cm on the northern side and 14 cm on the southern. The top of the coral was slightly higher than that of other neighboring corals, mostly *Porites*, which may be only because HLS for *Goniastrea* is somewhat higher relative to lowest low tide than *Porites* HLS. Sand buried the bottom of the coral. The sample is a complete cross-sectional slab through the center of the coral.

Figure 4.8b is a tracing of the x-radiograph of the slab, which broke into several pieces along holes in the skeleton. This coral, like many *Goniastrea* and some *Porites*,

grew in lobes, separated from each other by long vertical voids through most of the skeleton, joined only at the base. Elevations of rings and HLS flats are measured in, and relative to the top of, the left-hand lobe, although some impingements are visible only in the right-hand lobe.

The rounded top and relatively intact annual rings at the top of the coral indicate that this microatoll was still below HLS when the final emergence event occurred. The slightly thinned top ring near the head's center may indicate exposure at HLS, but the outer appearance of the microatoll suggests this ring was removed by slight erosion. Slight HLS impingements appear to have occurred in 1828 and 1826, and a substantial impingement produced a small flat surface in 1819. Prior to that, there is evidence in the left lobe, of an old HLS flat about 26 cm from the top. The flat is eroded, but the way the rings curve down toward the eroded flat surface indicates that it was an old death surface, and that the younger rings had to grow up and over it from the side after death rather than continue growing straight upward, as they would with no impingement. How much time the flat represents is unclear because of the erosion, but it appears to have lasted at least a couple of years, maybe from 1806 to 1810. The right lobe also has an eroded flat surface about 22 cm from the top, which may correlate with the oldest HLS surface recorded in the left lobe. However, the rings below that surface are hard to recognize in the x-radiograph and the dates represented by the flat are uncertain.

The coral appears to have suddenly and completely emerged, resulting in death, in 1833. Because the emergence of this coral was total, the height from the lowest to highest occurrence of the outermost ring is a minimum measure of the magnitude of final emergence. It is plausible that the HLS dropped only to a point just below the bottom of the outer ring. In that case, although the coral was not fully emerged, all of the upper living part was, and the entire coral died as a result. In this case, the minimum magnitude of emergence was about 29 cm.

Figure 4.11. Photograph of the NP94-A-9 microatoll before slabbing.

approximate location
of slab cut
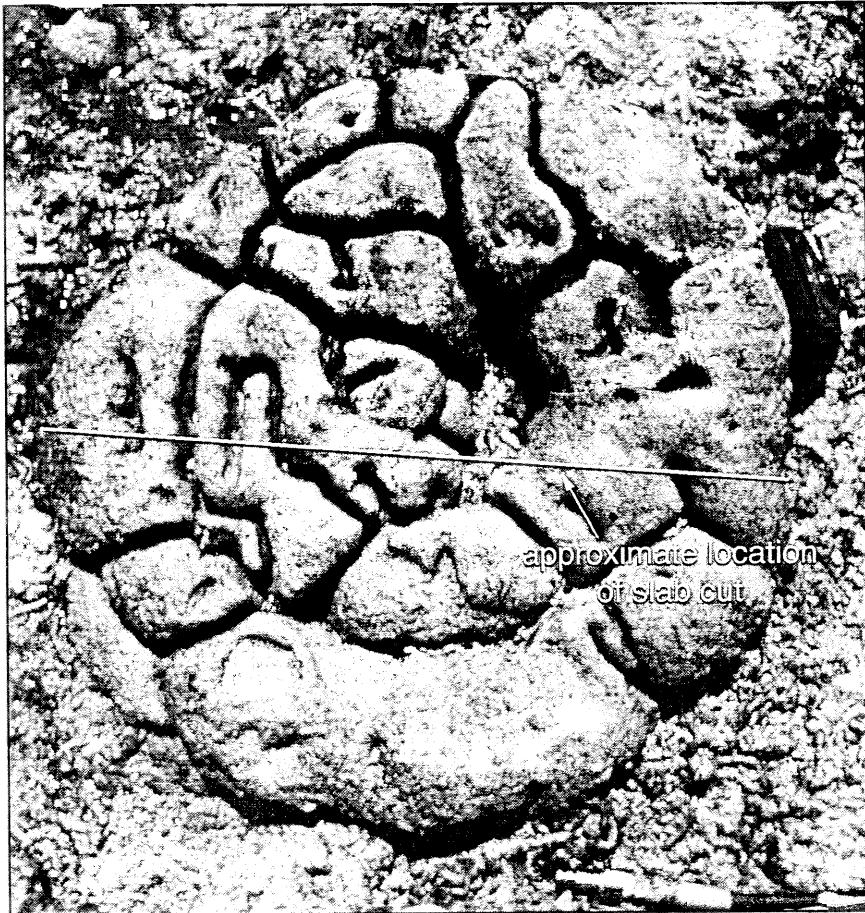
Slab NP94-A-8 was cut from Coral D9, about 50 m northwest of NP94-A-9 and at the southern limit of the dead coral community (Figure 4.10a). The microatoll was an untilted *Porites* sp. coral, 165 cm in diameter, with three distinct former HLS flats (Figure 4.12). The vertical slab was cut radially, slightly beyond the center of the head. Two pieces from this sample, one from the interior of the central flat and one from the raised outer rim, were dated. The corrected ^{230}Th dates of death were 1841 ± 11 for the exterior piece, and 1842 ± 11 for the interior piece. There are about 40±3 rings between the two samples.

The slab shows the three flat surfaces and evidence of multiple HLS impingements (Figure 4.8c). Though the rings at the center of the microatoll are difficult to discern, it appears that the coral grew hemispherically below HLS for 30 to 50 years before first reaching HLS. This first interaction with HLS occurred in the context of an emergence. The time over which the emergence occurred is unclear, because the rings near the top of the central hemisphere are truncated and may be slightly eroded. The oldest ring exposed at the surface has a date between 1783 and 1789. This may reflect the first year of HLS impingement and emergence. In that case, the emergence continued over the course of a few years, ending in about 1792 when HLS was 14 cm below the top of the hemisphere. If the older rings are exposed because of slight erosion, the emergence may have been more sudden, occurring in about 1792 and causing HLS to drop to 14 cm below the top of the hemisphere. A third option is that the emergence was sudden and occurred between 1783 and 1789, but the coral took several years to reflect the full magnitude of the emergence in its rings, giving HLS the appearance of have dropped gradually. In general, however, the hemispherical core surrounded by the raised outer rim indicates that the coral had been growing below HLS until a relatively sudden emergence in about 1792 dropped HLS from somewhere above the top of the hemisphere to about 14

cm below it. This holds true regardless of the details of how the emergence occurred over the span of a few years.

At the same time as or shortly after the emergence, there was also a change in elevation of the coral's base, perhaps from burial by sand. The change in substrate depth may have been related to whatever caused the emergence. The effect of increasing substrate level and decreasing sea level was to reduce the living part of the coral so that only a narrow band of corallites remained alive. The bridge may not always have been so tenuous; it seems possible, if not likely, that some erosion of the underside of the bridge has occurred since the coral was alive; the original substrate change may have been only 10 cm since the outer rim grew down to an elevation well below the present bottom of the bridge.

After the 1790's emergence, the rim again grew up and out in the wake of a rising HLS, with small impingements in about 1798 and 1808. The second of the three HLS surfaces was produced when the coral reached HLS again in about 1813, where it remained for about 3 years. The broad flat between the two horns at the top of the outermost rim suggests that the coral reached HLS again just before final emergence in 1833. It may have been at HLS in 1832 or just slightly below; erosion has erased the inner edges of the horns. Emergence was sufficient again to raise the living portions of this coral completely above HLS, causing the head to die. Unfortunately, the outermost ring either did not grow on, or has since been removed from, the edge of the coral below about 13 cm from the top, although it is possible that the living band extended farther down elsewhere on the perimeter. Thus, 13 cm is the minimum amount of emergence recorded by this coral.

The HLS curves illustrating the growth histories derived from these two slabs appear in Figure 4.9. Four episodes of HLS impingement are recorded in NP94-A-8 in about 50 years. That in the 1790's was longer-lived than the others and involved an

Figure 4.12. Photo of NP94-A-8 just prior to removal of the sampled slab. The central flat surface consists of a central dome and a younger rim. The younger rim is surmounted by a still younger raised rim. The small horns atop the raised rim and intervening flat suggest that the coral head was near HLS just before final emergence. The base of the coral and the sandy substrate are under water.

emergence of about 14 cm, whereas the others were primarily HLS clips. After the HLS impingement that may be associated with the development of the now-eroded flat, NP94-A reveals three short-lived HLS clips in about 20 years. The last of these corresponds temporally to an episode of impingement in NP94-A-8; the earliest slightly postdates an impingement in NP94-A-8. The NP94-A-9 curve is similar in shape to that of NP94-A-8, but has fewer HLS clips, which are shorter-lived. The impingements did not occur at the same times in the two samples, although they usually occurred within a few years of each other.

Other NP94-A/NP96-C corals

The two slabs from this site reveal a history of submergence prior to final emergence and death, probably in 1833. Final emergence was sudden and, based on the slab of NP94-A-9, was at least 29 cm. The morphological characteristics of the other corals that died in about 1833 are consistent with the HLS history of the two slabs. Those that are uneroded possess a raised outer rim surrounding a central flat, the signature of rising water level. Some of these rims are 20 cm high, similar to the height of the rim in NP94-A-8 and the elevation of the top of NP94-A-9 above an eroded flat surface. The similarity of the stratigraphic and morphological signatures of all the 1833-age emerged microatolls, the number of the corals of this age, the suddenness and size of the emergence, and the coincidence in time with a known earthquake all suggest that the cause of the emergence and death was coseismic uplift in the 1833 earthquake, following several decades of submergence.

In addition to the final emergence event in 1833, the stratigraphic record of NP94-A-8 also reveals the occurrence of an earlier emergence in the late 1780's or early 1790's. Because the coral head never reached HLS prior to that emergence, the true size of the emergence is not known from the slab. The minimum size of the earlier emergence is thus

about 14 cm, the elevation difference between the top of the central hemisphere and the bridge from hemisphere to rim.

The 1790's event recorded in NP94-A-8 probably correlates with the emergence that killed some or all of the group of corals with higher elevations. Two high corals (D1 and D7) and one intermediate-depth coral (D10) died around the turn of the 19th century, in 1799 ± 14, 1809 ± 12, and 1797 ± 18, respectively. Given the overlap in ages, the two generations of coral must have experienced the same sea level conditions and should therefore have similar HLS histories. Unfortunately, I have no slab from the older generation. A slab was collected from head D10, but the rings were too ambiguous to yield a clear HLS history. Nevertheless, these corals do provide some morphological constraints on the history of HLS in the 18th century.

Although more irregular in form and usually slightly more eroded than the younger corals, the older corals have a submergence-related morphology. Raised outer rims record submergence of as much as 30 to 40 cm in the decades before final emergence. The steep-sides of all the corals suggest final emergence was sudden. Coral D7, in contrast with the other corals, has a lower, outer flange that appears on one side of the coral profile but not on the other (Figure 4.10b). The sample that was collected from the flange yielded an 1809 ± 12 death date. The outer flange suggests an emergence prior to final emergence, but without a slab, the details of that emergence are not available. The hand sample includes only part of the flange, not the older riser. However, the nature of the rings in the sample suggest the flange was not an erosional remnant but rather a constructional feature. The uncertainties on the age of the sample do not allow for this coral's final emergence to have been in 1833. On the other hand, they don't allow for a 1792 emergence either, so the uncertainties may be underestimated. The morphological similarity and the coral's elevation indicate it is a contemporary of the other late 18th-century corals. The flange does not appear in other 1790's corals, although the undated

microatoll D8 has a sloping lower outer rim. The nature of a possible emergence prior to final emergence of D7 remains unexplained.

If the high corals died in the late 1700's, they must have emerged completely, so that all living corallites were moved above HLS. The flange in D7 is 50 cm above the substrate; the top of the coral is 82 cm above. The top of D1, which died in 1799 ± 14, is about 30 cm above the substrate. The other high corals that may, based on their similar heights, be contemporaries of D1 and D7, reach as high as 93 cm above the substrate. These elevations suggest the emergence may have been more than half a meter, if the entire substrate emerged above water in the event. However, the height of the corals need not be indicative of the minimum amount of emergence, as was suggested by corals at Si94-A. Although the steep sides suggest that the outer surface of the dead corals was approximately the same age, in the absence of a sample through the base of the coral, one cannot know for sure that the outermost ring at the top is complete all the way to the substrate. In both NP94-A slabs, the bottom of the outermost ring or rings were missing from the record. Water level was near the top of the 1790's corals when I examined them, so even the morphological details of the bottom reaches of the coral are not well-constrained.

If, because the rings may not be complete, one need not consider the base of the coral to be a constraint on the size of emergence, then the unsampled 1790's corals offer no information about the post-emergence HLS elevation. However, they do constrain the elevation of HLS prior to the emergence. The outer rims of the corals are nearly flat, suggesting they were growing at HLS before they emerged. In some corals, there are small horns at the edges of the flat rim, indicating the likelihood of a slight upgrowth over that HLS; nevertheless, the flat of the rim defines HLS within a couple of years of final emergence. The elevation of D1's pre-emergence HLS is about 20 cm above an arbitrary datum, keyed to water level in 1996; D10' HLS is almost exactly at the datum. The top of

D7 is about 8 cm above the datum; the top of the flange is about 30 cm below the datum. Other, undated corals from the high population are about 5 to 25 cm above the datum. A reasonable estimate of average HLS prior to the 1790's emergence is 10 to 15 cm above the datum.

If the 1790's corals themselves do not constrain the elevation of the post-emergence HLS, the slab from NP94-A-8 may. The emergence of the 1790's that killed the population of high corals must have affected this coral since it was alive then. Moreover, it does record an emergence at that time. As mentioned above, the coral was not at HLS before the emergence but it was afterwards. So, while the 1790's corals may record only the elevation of the pre-emergence HLS, NP94-A-8 records the elevation of the post-emergence HLS. From the slab, the lowest post-emergence HLS elevation recorded is 42 cm below the top of the coral, or about 60 cm below the 1996 datum. By taking the difference between the HLS elevations derived from the 1790's corals and the 1833 coral, one can obtain an estimate of the full amount of the emergence in the 1790's. The estimated emergence, then, was about 70 cm. If the flange on Coral D7 represents the pre-emergence HLS, then the emergence would be closer to 40 cm.

If the other corals that died in 1833 were alive in the 1790's, they too should have recorded this emergence. There is no clear evidence of the emergence in any of them. Corals NP94-A-9, D13, D14, D15, and D16 all sit above the level of the post emergence HLS. If the sea floor now is their substrate, then all these corals would have emerged fully in a 70 cm emergence event. Thus, they must either not have been alive at the time, of the emergence or their substrates are now buried under several tens of centimeters of sand. NP94-A-9 suggests both of these may be true. The oldest ring one can confidently count has a date of about 1806. If unimpeded growth rates remained approximately constant throughout the coral's life, it probably began growth after 1790. In addition, the base of this coral was buried in sand; its substrate was about 20 cm below the top of the

sand in 1994. The substrate below many of the others may also be buried. The base of corals D12 and D13 are exposed below the level of the post-emergence HLS. They do not show any signs of an outer rim of post emergence growth. However, these corals have not been dated, so they may not be 1833-age corals. Even if they are, they are small enough that they could have begun growth after the emergence. Most of the small corals that died in 1833 probably began to grow after the 1790's emergence. D9 (NP94-A-8) is then the only representative of 1833 that experienced both the 1790 and 1833 emergence. This is consistent with its being significantly larger than the other corals of its age.

In this analysis, I have assumed that the height of the 1790's corals and the elevation of the substrate below them do not place a constraint on the magnitude of uplift, even though the corals emerged completely. If this assumption is true, it requires that the lower part of the coral have been killed by something other than emergence. The bases of the both D7 and D10 are below the elevation of the postulated post-emergence HLS. If the rings were continuous down to the substrate prior to emergence, they would have remained below HLS after a 70 cm emergence, and a low ring of outer growth should have developed at an elevation 70 cm below their pre-emergence level. This was not observed. Therefore, either the rings were not continuous to the substrate or the lower part of the coral died during the emergence event from a cause other than exposure above HLS, since it was not above HLS.

Another possible explanation for why the bottom of the tall corals did not continue to grow after the event is that they were, after all, raised completely above HLS, but the absolute elevation of HLS of the high corals and D9 (NP94-A-8) was not the same. It is about 90 cm from the pre-emergence HLS to the substrate below the corals. If the entire coral emerged, 90 cm would be the minimum emergence, about 20 cm more than what was calculated above. A 90 cm emergence would have moved the HLS of the high 1790's corals to about 80 cm below the reference datum. If the emergence were 90

cm, coral D9 (NP94-A-8) should also have been raised another 20 cm. If the absolute elevations of the pre-emergence HLS's were the same elevation, post-emergence HLS in NP94-A-8 would have been 80 cm below the datum, also, or about 34 cm below the top of the central hemisphere. NP94-A-8 shows no HLS impingement at that elevation. However, if the absolute elevation of D9's HLS were 20 cm above that of D7, or 30 cm above the datum, then its post-emergence HLS would be only 60 cm below the datum, consistent with what is observed. Although the absolute elevation of HLS in live corals usually differs by less than 20 cm, 25 cm and even 45 cm were observed between mean HLS's in two live corals in the same bay (Chapter 2). Thus, if D7's HLS were 20 cm lower on an absolute scale than D9's, the emergence that was large enough to be fatal to D7, would still have permitted the bottom of D9 to survive.

The most likely explanations for the distribution of microatolls at this site are either 1) that there was a 70 cm emergence in 1790 that fully killed a number of large corals, whose lower 20 cm or more were already dead before the emergence or died during the emergence from something other than exposure above HLS, and that also partially killed one microatoll whose lower reaches remained alive; or 2) that there was a 90 cm emergence that killed the large corals but did not fully kill the other coral, whose absolute HLS elevation was about 20 cm lower than that of the large heads. The former may be more likely, since in most live corals the range of HLS elevations is less than 20 cm.

Although it seems unlikely at first glance that essentially all the large corals would have incomplete or dead lower rings, it is certainly possible. Burial by sand commonly kills the corallites near the base of a coral (Scoffin and Stoddart, 1978). Sand could easily have been distributed across a broad expanse of the site sometime prior to or during the 1790's emergence and buried the bottoms of all the corals, causing their death. Tsunamis can deposit large amounts of sand over coastal areas just after a large earthquake

(Atwater, 1987; Atwater and Yamaguchi, 1991). If the 1790's emergence was caused by coseismic uplift associated with a subduction zone earthquake, there may well have been tsunamis capable of depositing sand over the reef at this site. The fact that NP94-A-8 is located more than 50 m from the other corals is consistent with that explanation; the sand may have covered the whole northern part of the bay, while leaving the southern part less affected. The NP94-A-8 slab records a probable change of substrate depth near the time of the emergence, which may have been to sand build-up that was not quite enough to kill all the corallites. The sand that buried the bases of the tall corals must have been removed since then, as the substrate below the tall corals is now exposed.

Such an explanation, involving death of the lower parts of the microatolls before or during an emergence that caused the death of the upper parts by exposure, implies that while steep sides on a coral may indicate sudden emergence as the cause of death, they do not necessarily indicate that the whole outer edge of such a coral is the same age or that post-emergence HLS was necessarily below the bottom of the coral. The presence of multiple steep-sided corals with their tops half a meter above the substrate may suggest a sudden emergence of similar magnitude, but, in fact, the height of the corals does not provide even a minimum constraint on the size of the emergence. However, a complete slab that samples the full height of the coral, can help constrain the maximum elevation of post-emergence HLS.

P96-F

Site P96-F (also P94-Z) is located on an island off the central west coast of South Pagai (Figure 4.3). This is one of the few sites with two widely separated generations of fossil coral, 1833-vintage and 14th century. P96-F-1 came from a *Goniastrea retiformis* microatoll (P94-Z-4, a hand sample, was also from this head) (Figure 4.8d). Tilted about 5° seaward, with half its rim broken off, the microatoll stood about 60-65 cm above the

substrate and had a 180 cm diameter. It had a wide (45 cm) outer rim, with a deep void between the inner and outer halves. The corrected ^{230}Th date of its death is 1831 ± 17.

The slab from this coral also records a history of submergence punctuated by brief periods of stability or emergence (Figure 4.8d). The interior pieces of the slab are detached from the outer. Matching rings across isolated pieces is an uncertain process, so age estimations for the early history of this slab are speculative. I tried to match rings based on relative location (assuming that rings usually continued across the void between pieces at about the same elevation) and on the thickness and appearance of the rings, keeping in mind that rings can change thickness and appearance over short distances. The coral reached HLS four times during the lifetime of the slabbed portion. The last HLS impingement occurred in 1831, just prior to final emergence. An older HLS flat appears about 15 to 18 cm below the top. This flat is eroded, so the age of first impingement is not certain, and the original elevation of the HLS flat can only be estimated within a couple of centimeters. I estimate that it reached HLS in about 1815 and grew constrained below that elevation through 1819. Another flat, defined in part by the tops of the smaller detached pieces to the right and below the outer rim, was the central HLS flat surface of the microatoll. Both the detachment of the flat's pieces, and the unfortunate fact that the saw cut through the HLS surface in the large, outer fragment of the slab, renders the age and elevation estimates on the flat tenuous. From the last countable ring in the outer rim, I estimate that the flat represents about 5 years of relative HLS stability, from 1801 to 1806. The innermost fragment of the coral has a small HLS impingement of about 2 years duration, about 15 years and 13 cm below the top of the fragment. If the date of 1803 is applied to the top of the fragment, the HLS impingement occurred in 1788.

The HLS curve for this coral appears in Figure 4.9. The HLS impingements occur periodically every 10 to 15 years. The regularity of the impingements may be an

indication that the average submergence rate remained nearly constant through the time recorded by the slab.

There was no evidence at this site of a significant emergence event in the late 1700's or early 1800's. I found no corals that died at that time, nor is there any evidence of such emergence in P96-F-1. There is an HLS impingement estimated in about 1788, but it was just a clip. There is evidence of significant emergence event in the 14th century, recorded in two emerged corals at the site. This event will be discussed later

P96-H/P94-Y

P96-H (also P94-Y) was at the seaward edge of a deep embayment, Teluk Tiop, on the western side of South Pagai, about 10 km south of P96-F (Figure 4.3). During low tide in July 1994, a 30 m wide reef was exposed at this site, with *Porites* microatolls exposed above water just offshore; in 1996, the basal reef was under water, but a few microatolls were partially exposed above water at low tide. A sample, P94-Y-1a.a, from the basal reef yielded an early Holocene age of 8093 ± 45 years BP. Two microatolls, P96-H-1 and P94-Y-3, are probably 1833 casualties. Sample P96-H-1 came from a large *Porites* microatoll, 235 cm in diameter, and 126 cm high, from the substrate to the top of the outer rim. The rim was two-tiered, with the higher outer rim about 20-30 cm above the central flat. The outer edge of the coral sloped down and out from the top at about 50-60 degrees; near the base of the coral, this slope steepened to near vertical. Because the microatoll was so large and largely under water even at low tide, I could not cut a slab all the way to the substrate, but truncated it a bit more than halfway down the side of the coral.

The slab shows a record of submergence punctuated by a few small emergences or periods of stability (Figure 4.8e). Most of the central core is missing from the sample, since I could not saw to the center of a 235 cm coral and still retrieve the sample.

However, the innermost part of the sample comes from the inner flat of the coral. The rings of the innermost piece of the central flat, which is separated from the rest, are not easily matched with the larger outer piece, so the absolute age of the interior piece is uncertain. However, it appears that upward growth was first impeded in about 1786 to 1789. Based on the shape of the rings, it appears that an emergence of about 6-8 cm occurred in 1791 and was immediately followed by upward growth. Here, the record continues in the main part of the slab, and the stratigraphic analysis is less speculative. The coral again reached HLS in about 1809 and grew laterally at this elevation until it emerged slightly in 1815. This was the last recorded emergence before the final emergence. The coral may have reached HLS immediately before final emergence since the outermost ring does not continue over the top of the head. Indeed, although the coral was over a meter high, the absence of a significant outermost ring means that a rigorous estimate of minimum emergence yields only about 10 cm. The HLS clips occur more irregularly in this record than in the records of some other corals, and there is a longer period of HLS stability recorded in this coral around 1810 than is observed in other corals (Figure 4.9).

Another steep-sided *Porites* microatoll (P94-Y-3) at this site was sampled but not slabbed. This coral died in 1830 ± 18, and its morphology was similar to that of P96-H-1. It was about 2 m in diameter, 53 cm tall, with a 40 cm-wide raised outer rim, about 25 cm above a second, interior rim. The interior rim was a couple of centimeters above the central "flat," which was bowl-shaped rather than strictly flat. The bowl shape may indicate gradual submergence or, perhaps more likely, bioerosion and hollowing of an originally flat surface (Scoffin and Stoddart, 1978). If it is result of gradual submergence, it records 8 cm of vertical motion for 40 cm of horizontal growth, a ratio of 0.2 and much less than the vertical to horizontal ratio recorded by the rims, about 30 cm over 50-60 cm horizontal, or about 0.5.

P96-J

Sample P96-J-2 was collected from the east coast of Siatanusa Island, one of the small islands east of the South Pagai peninsula (Figure 4.3). The coral sat on a highly eroded emerged reef with only a few small microatolls located very near the storm berm. Most of these were only about 40-60 cm in diameter and a similar height. Their rims were subdued, suggesting that they had experienced minimal preseismic submergence. Two fossil corals from this site were dated. They yielded dates of death of 1842±11 and 1831±3. The latter microatoll, P96-J-2, was the largest fossil microatoll observed at this site, about 110 cm in diameter, and had a somewhat more robust rim than the other, more eroded dead corals (Figure 4.8f).

The slab through P96-J-2 indicates that a period of unimpeded upward growth below HLS was followed by several years of growth near HLS under conditions of relatively stable sea level from about 1811 to 1816 (Figure 4.8f). In 1816, HLS dropped about 5 cm and immediately rose again, permitting further upward growth. HLS rose above its 1811-1815 height, since upward growth continued past the old central flat after about 1821. The coral again reached HLS in about 1829. After a year or two at this elevation, HLS rose, and the coral was released to grow upward again, producing the small horns on top of the rim. In 1833, however, the entire coral emerged above HLS and died. The vertical distance from the top of the outermost ring to its lowest extent, 22 cm, is a minimum measure of the emergence at that time. The HLS curve appears in Figure 4.9. Like, P96-H-1, it experienced sustained growth at one elevation for several years after 1810 before growing upward again.

P96-K

Site P96-K was on the east side of the large island of Taitanopo, six km north of P96-J (Figure 4.3). Numerous living and dead microatolls exist in several bays around this site. Three of the dead corals from this site, K-1, K-4 and K-5, were dated, yielding ages near 1833. P96-K-4, however, could also belong to an older population, having yielded a death date of 1818 ± 15. There is a slab from this coral. The morphologies and elevations of both living and dead corals varied noticeably throughout the area. Although most of the dead corals were several tens of centimeters higher than the living corals, P96-K-4 was at about the same level as most of the living corals, which may indicate either that it was no longer in growth position or that it emerged only slightly when it died and the corals that grew afterward started growth at a similar elevation. If the age is older than 1833, then the latter is possible. If it died in 1833, the, given the difference in elevation between this and the other 1833 corals (P96-K-5 was only about 30 m from K-4, and its top was about 40 cm higher than K-4's), I suspect the former. The head was small, about 50-60, with a dimple in the center down to an old HLS surface.

Because the coral was small, the P96-K-4 slab records only a short HLS history, with a single submergence event (Figure 4.8g). The coral grew unimpeded until it reached HLS at about 1811. Shortly thereafter, HLS dropped, the coral emerging about 3 cm. Further unimpeded upward growth followed until it emerged fully in 1833 and died. The minimum amount of emergence was about 27 cm (Figure 4.9).

Preseismic and coseismic HLS records

The HLS curves derived from stratigraphic analysis of all seven 1833 slabs appear together in Figure 4.13. The figure includes the plots based on an age of death relative to measured ^{230}Th ages (Figure 4.13a), corrected ^{230}Th ages (Figure 4.13b) and assumed 1833 death date (Figure 4.13c). The plots reveal that the shapes and slopes of the curves

Figure 4.13. Plots of HLS elevations vs. time for all seven coral slabs that died around 1833. Points show HLS clips seen in the annual growth-band patterns; the lines pass through minimum HLS elevations.

a. Relative HLS elevations based on uncorrected coral-death dates. The average submergence rates based on HLS clips only appear next to the curves. These rates and the rates derived from elevations of HLS minima are listed in Table 4.2.

b. Relative HLS elevations based on corrected coral death dates.

c. Relative HLS elevations versus time, if each coral emerged during the giant earthquake of 1833.

d. Relative HLS elevations of modern corals from five sites around South Pagai and Sanding Islands versus time. Sites P96-J and P96-K have samples from both the 1833 and modern eras. The submergence rates for these sites are very similar in both periods. The average submergence rates for the Pagais and Sipora based on all the corals from the various sites together are also very similar in the preseismic early 1800's and the interseismic late 1900's.

a.

b.

c. Preseismic and Coseismic HLS Histories
Assuming corals emerged in 1833

d. Modern Submergence Rates
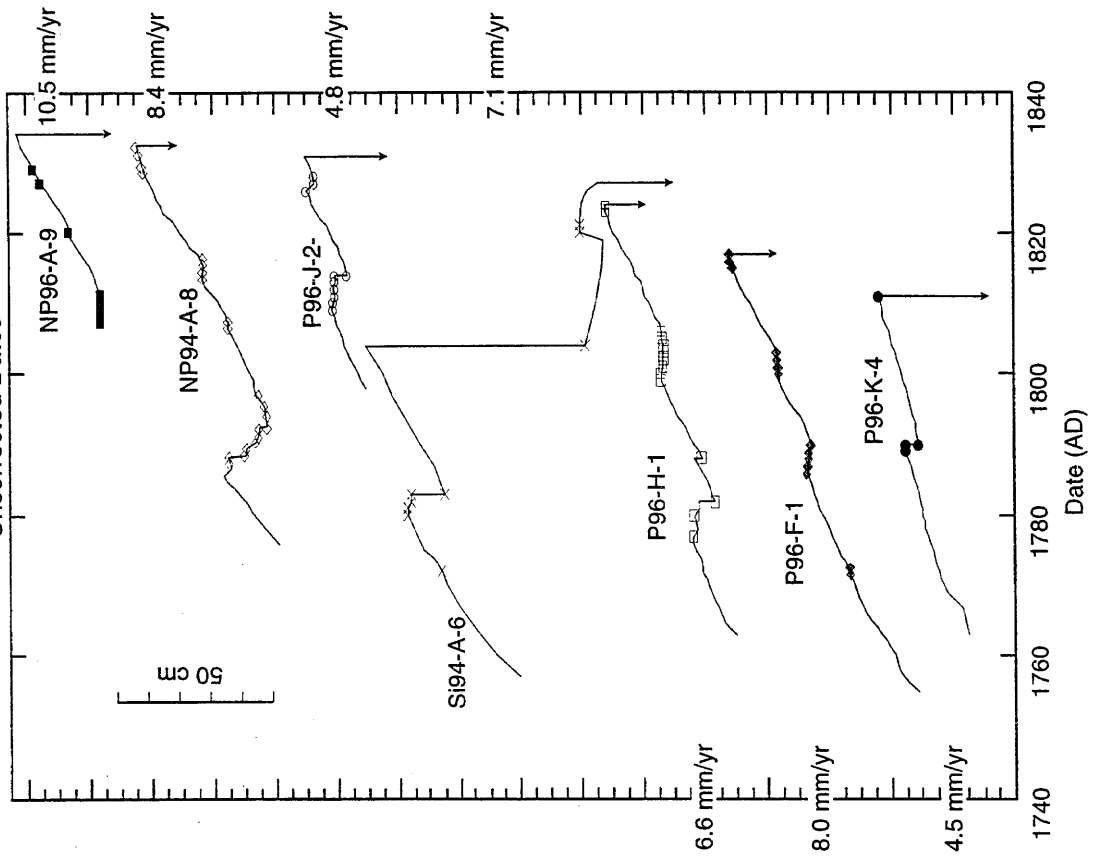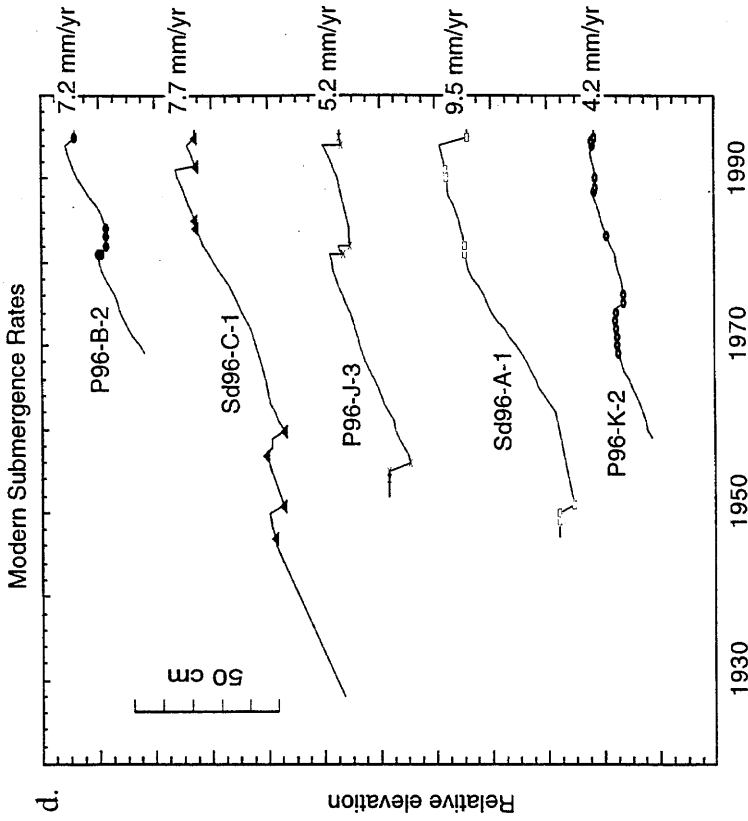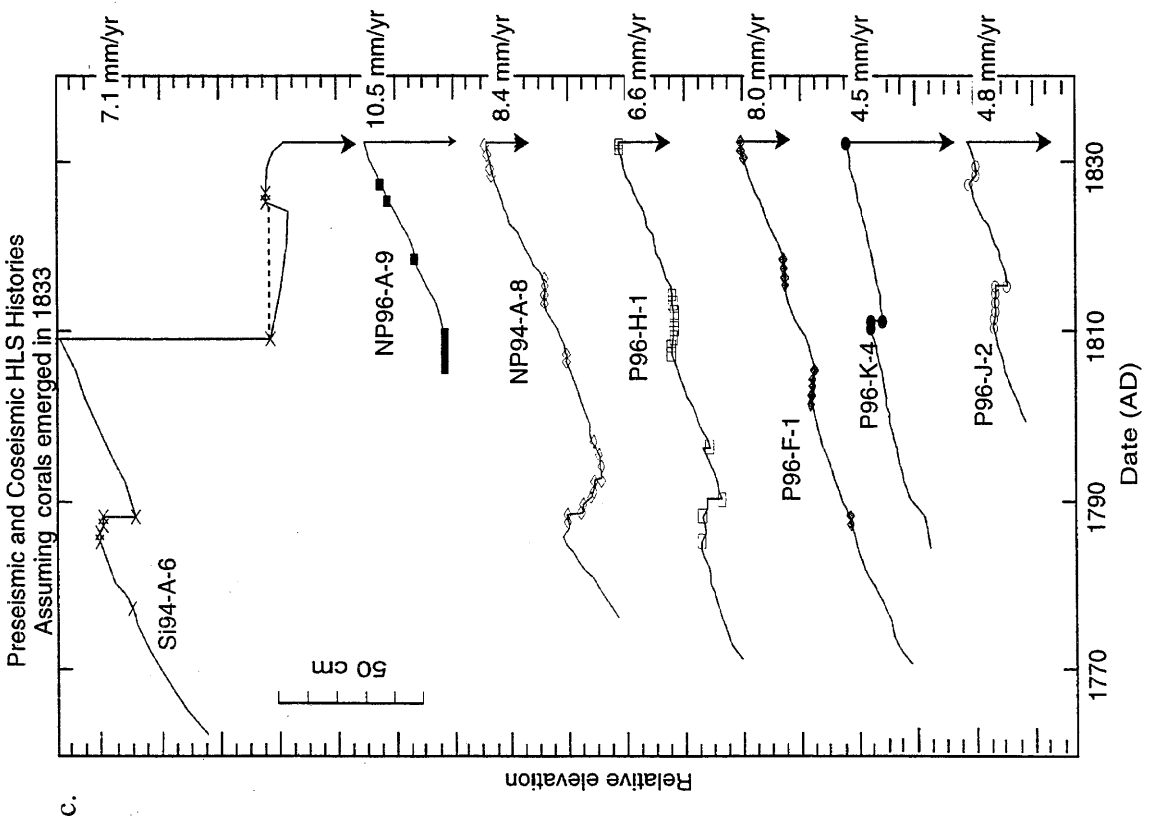
representing the preseismic period are similar, with the exception of Si94-A-6 (Figure 4.13a). The times at which HLS clips, and certainly final emergence, occurred vary substantially in the plot based on uncorrected ages, and few clips occur at the same time in all or most corals. The curves coincide more closely in the plot based on corrected ages, again with the exception of Si94-A-6 and also of P96-K-4 which remains substantially older than the others, even after the correction. This is to be expected, since we already know the corrected ages of death cluster more closely than the uncorrected ages.

When the curves are plotted assuming an 1833 death date, the variation between samples drastically declines (Figure 4.13c). Most samples experienced HLS clips around 1830, just prior to the emergence event. Most also experienced a period of stability between about 1810 and 1815. Prior to that, the variation is greater (the uncertainty in the ages due to ring counting is also greater), but most corals show at least one more HLS clip around the turn of the century or slightly before. Besides Si94-A-6, corals NP94-A-9 and P96-K-4 seem to differ the most from the general pattern described by the other corals. The shape of the curves for NP94-A-8, P96-H-1, P96-F-1 and P96-J-2 are very similar. Even Si94-A-6, though its post-1810 history is very different, displays an HLS pattern similar to the others prior to that emergence event. These results support the contention that all the corals died in a single, widespread emergence event caused by uplift in the 1833 earthquake.

The degree to which the differences between the HLS curves might be due to inherent variability in coral HLS levels and sensitivity, such as different response times to similar changes in water level, can be gauged by comparing the HLS-curve variability between these dead microatolls and that between live microatolls (Figures 4.13c and 4.13d). Although the variability in the dead curves plotted with uncorrected ages may be larger than that in the live corals, the plot with final emergence normalized to 1833 does

not seem more variable than the plot of live coral HLS's. This suggests that much of the variation between the 1833 curves is a function of HLS variability, or errors in ring identification, rather than substantial difference in relative sea level between sites during the preseismic period. Assuming the 1833 emergence for all the corals, the precision afforded by the stratigraphic analysis of fossil corals is similar to that of living corals.

Another way to check if the observed differences are a function of HLS variability or different relative sea-level histories would be to see if variation in HLS histories between sites is much greater than that between corals at one site. Presumably, corals of the same generation at any given site have experienced the same sea level history. Any variation in the plots of HLS history between such corals is probably noise and does not represent differential vertical motion. Intersite variability that exceeds the intrasite/interhead variability may represent a physically significant signal. The only site with two 1833 slabs is NP94-A. NP94-A-8 differs from NP94-A-9 by at least as much as it differs from corals at other sites, except Si94-A-6, so there is no evidence of a radically different history between any of the sites other than Si94-A.

In saying the sea-level history between most of the sites does not differ much, I mean that the major events have been similar. In other words, all the sites on the Pagais record a lifetime of submergence with a few short-lived episodes of HLS impingement or minor emergence. These episodes of impingement have been recorded in nearly the same years in different corals. With the exception of NP94-A-8 and Si94-A-6, most of the slabbed corals probably experienced only one large emergence event, which was sufficient to lift their living portions completely above HLS and kill them. This does not mean that they did not submerge at different rates or that the amount of coseismic uplift was the same at all sites.

Preseismic submergence rates for the Pagai sites, determined by taking the slope of best-fit line through just HLS points, indicate that all the sites had been submerging at

average rates of between 5 and 10 mm/yr prior to final emergence (Figure 4.13a; Table 4.2). NP94-A-9's and P96-K-4's rates may actually be higher, since the corals were not at HLS before they emerged. Submergence rates calculated using only measured HLS are nearly identical to those using minimum HLS values. Sites P96-J and P96-K, the only sites on the east side of the islands and the farthest south, had the lowest average submergence rates - 4-5 mm/yr.

A comparison of the estimated submergence rates of NP94-A-8 and NP94-A-9 can provide a sense of the uncertainties that should be applied to these rates. Living at the same site, within a few tens of meters of each other, the two corals should have experienced the same sea-level fluctuations during their lifetimes. The average rates derived from the curves vary by a few mm/yr - NP94-A-9 indicates submergence at rates of 10 mm/yr and NP94-A-8's record suggests rates of about 8 mm/yr. However, NP94-A-8's rate is based on a longer record. If the rates are calculated for only period in which both corals lived, the disparity decreases. The growth rate of NP94-A-9 after the development of a small flat in about 1819 was 12 mm/yr. The growth rate for NP94-A-8 increases to 14 mm/yr after the development of a small flat between 1813 and 1815. The rate discrepancy between the two corals is similar, but reversed if the earlier history of NP94-A-8 is not included.

The submergence rates recorded by both NP94-A corals increased by a few mm/yr in the last 15-20 years before emergence. It is possible that the rates at all the sites changed. If the average submergence rates from the time of penultimate HLS clip, which in all the corals occurred between 1812 and 1819, to the final emergence are calculated, it is clear that the submergence rates for all sites increased in the decade or two immediately before the 1833 earthquake (Table 4.2).

The pre-1833 record from Si94-A-6 is markedly different than all the others because of the large (>70 cm) emergence it experienced about 25 years before the 1833

Table 4.2. Preseismic submergence rates and magnitude of coseismic emergence derived from coral HLS records of seven slabbed microatolls from six sites in the Sipora and Pagai Islands. All seven corals probably died as a result of emergence in the 1833 giant earthquake. Table indicates distance from each site to the subduction trench; the preseismic submergence rate calculated from the slope of the best fit line through HLS-elevation points; the preseismic submergence rate calculated from the slope of the best fit line through the minimum HLS-elevation points; minimum coseismic emergence determined from the slabs; height above the substrate of the emerged corals; and the preseismic submergence rates calculated from HLS points for the last two decades prior to emergence in 1833.

Table 4.1 - 230Th dates of death of Sumatran corals

sample name	date of death (error)	corrected date (error)	sample name	date of death (error)	corrected date (error)
P94-Y-1A.A	-6142 (45)	-6139 (45)	NP96-C-5.B	1787 (3)	1799 (14)
P94-C-3.B	-6114 (79)	-6105 (80)	P96-N-2.A	1632 (7)	1800 (197)
P94-M-3.A	-5175 (250)	-5169 (250)	P96-Q-1.A	1789 (9)	1800 (16)
P94-C-1.B	-4609 (59)	-4593 (62)	P96-N-3.A	1662 (4)	1803 (165)
P94-M-2.B	-4049 (43)	-3965 (112)	NP96-C-1.B	1795 (6)	1807 (15)
P96-O-2.B	-3912 (36)	-3700 (259)	P94-H-1A.A	1766 (7)	1807 (30)
P96-O-1.A	-3658 (32)	-3583 (95)	P94-H-2.A $	1809 (6)	1817 (8)
P94-AA-1A.A	-103 (14)	-102 (15)	P94-S-1.B	1731 (10)	1807 (90)
P93-B-2	133 (17)	134 (17)	P96-K-4.A	1810 (13)	1817 (16)
NP94-A-6.A	1041 (7)	1076 (42)	P96-N-5.A	1765 (3)	1819 (63)
NP94-A-7.A $	872 (9)	909 (44)	P94-Z-4B.B	1818 (6)	1824 (9)
P93-C-2	911 (37)	1267 (418)	P96-F-1.B #	1817 (4)	1831 (17)
P93-C-3 $	731 (30)	965 (276)	NP96-C-2.A	1820 (11)	1824 (12)
P94-Z-2A.A	1328 (11)	1345 (23)	Si94-A-6A4.A	1824 (5)	1825 (5)
P94-Z-1A.A	1296 (11)	1356 (71)	Si94-A-6A3.A $	1822 (5)	1824 (5)
P96-F-2.2.A #	1322 (6)	1371 (57)	Pg04E-0.0.2(B)	1802 (11)	1826 (31)
P96-F-3.B #	1323 (5)	1373 (58)	Pg04E-0.0.2(A) *	1803 (4)	1842 (45)
NP96-B-4.A	1523 (3)	1533 (12)	P96-K-5.A	1821 (6)	1827 (10)
P94-AB-2A.C	1517 (5)	1572 (65)	NP96-C-4.A	1814 (3)	1829 (18)
P93-C-7(B) #	1396 (84)	1578 (228)	P94-Y-3A.B	1815 (3)	1830 (18)
P93-C-7(A) #,*	832 (62)	1398 (665)	P96-P-1.B	1750 (5)	1831 (55)
P93-C-8(A) $	776 (64)	1339 (661)	P96-K-1.B	1830 (3)	1831 (3)
P93-C-8(B) $,*	-222 (220)	1099 (1560)	Pg04G-0.0.2(B)	1706 (12)	1834 (150)
NP96-B-2.A	1560 (6)	1581 (26)	Pg04G-0.0.2(A) *	1463 (29)	1834 (434)
NP96-A-2.B	1505 (27)	1586 (99)	P94-X-3.B	1829 (4)	1834 (7)
P96-E-2.C	1391 (4)	1595 (238)	P94-S-3B.B	1825 (4)	1834 (11)
P96-E-1.C	1532 (5)	1608 (89)	P94-W-1.B	1794 (5)	1835 (47)
P96-E-3.A	1606 (3)	1608 (4)	P96-J-2.C	1831 (4)	1835 (6)
P96-M-1.A	1603 (6)	1656 (63)	P96-H-1.A	1824 (3)	1836 (14)
P96-L-1.1.C	1673 (5)	1688 (18)	P94-M-4.A	1835 (8)	1836 (9)
P96-L-2.A $	1654 (4)	1662 (10)	NP94-A-9A1.B	1834 (6)	1837 (7)
NP96-B-1.A	1736 (9)	1739 (10)	P94-X-1.A	1830 (8)	1838 (12)
P96-N-4.B	1434 (16)	1761 (382)	P96-I-1.A	1835 (15)	1839 (16)
Si94-A-5(1).A	1759 (8)	1769 (12)	P94-X-4.A	1836 (4)	1839 (6)
P96-P-2.B	1777 (25)	1778 (25)	NP94-A-8A4(1).B	1832 (5)	1841 (11)
Si94-B-1.B	1728 (25)	1789 (75)	NP94-A-8A1(2).B $	1836 (7)	1842 (11)
Si94-A-3.A	1778 (7)	1790 (15)	P96-J-1.A	1839 (10)	1842 (11)
Si94-A-2.A $	1759 (6)	1771 (15)	NP96-C-3.A	1798 (5)	1844 (54)
Si94-A-1A.A $	1716 (4)	1724 (12)	P96-N-1.B	1860 (32)	1866 (33)
NP94-A-5A1(1).A	1792 (17)	1797 (18)	Sd96-C-2.B	1986 (3)	1987 (4)
NP94-A-5A2.A $	1772 (26)	1810 (51)			

$ sample is from the interior of the same coral the above-listed sample comes from; first sample is usually from outer raised rim, second sample from interior flat

\#   analysis is from same region of slab as above-listed sample (e.g. both from outer rim), but from a different hand sample collected in a different year

*   repeat analysis of same sample as the above-listed sample

emergence. Prior to the earlier emergence event, the record is similar to the others. The submergence rate in that period is 7.1 mm/yr based on HLS's only and 8.4 mm/yr using minimum values. These are well within the range of preseismic rates established at other sites. The rate between the two events is hard to determine precisely because the tops of the rings are eroded. However, the maximum elevation of the outer rim is about the same as or slightly higher than the "1810" ring, implying a negligible change or a low submergence rate (< 1 mm/yr). This stands in contrast to the HLS history recorded by NP94-A-8. This site too may have experienced a 70 cm emergence a few decades before final emergence, but unlike Si94-A, it underwent submergence at rapid rates from the time of the early emergence until final emergence.

Unfortunately, from the slabs collected so far, there is still no good measure of the total coseismic step in 1833. Thus, whereas the tallest coral sampled was 126 cm high and apparently killed suddenly, the largest documented estimate of coseismic emergence from these slabs is 29 cm, which ironically comes from one of the smallest corals.

Although there is no rigorous estimate of the size of the coseismic step, I suspect that it was substantially larger at most sites than 29 cm. The tops of the 1833 corals were at the same approximate elevation, but the level of the substrate varied widely. Yet every 1833 coral observed had fully emerged during the event. Though most of the slabbed coral heads had outer rings that truncated above the substrate, it is likely that some of the steep-sided microatolls that were observed but not slabbed had complete rings down to the substrate. It seems more plausible that the coseismic emergence was significantly greater than the height of most of the corals, so that none were left with remnant living flanges, than that the corals were all lifted to a point just below the lowest part of their living ring. A coseismic step that was of the same size or less than the elevation range of the bases of the 1833 corals would probably leave a few corals alive at the base. That we

observed none suggests that the uplift pushed the entire population well out of the water. The possible size of the coseismic step will be discussed further later.

Other sites with 1833 or late 19th century corals

Numerous other sites throughout the Pagai Islands had fossil corals that died around 1833. I did not slab these, but recorded morphological descriptions and relative elevation measurements. All had the morphological signature of sudden emergence following decades of submergence. These corals probably died during the 1833 earthquake. Their occurrence throughout the Pagai Islands helps constrain the geographic extent of the coseismic uplift. There is also evidence of other late 18th-early 19th century events. Two corals from sites P96-P and P96-Q, on northern South Pagai, probably died in that period.

1833 Coral elevations and modern HLS

Almost all the 1833 corals stood above water during low tides. I compared the elevation of tops of those corals, which should be at or near 1833 HLS, and HLS of living corals (Figure 4.14). In 1994, the average elevation of the top of the outermost rim of dated 1833 corals was 48 cm higher than modern HLS in living corals. A similar comparison of corals sampled in 1996 shows that 1833-generation corals were 50 ± 28 cm (or 51 ± 22 cm excluding P96-K-4, which I suspect of being slightly out of place and lower than its original position) above living corals. If submergence continues at its current rates, the HLS of living corals should be at the level of the 1833 corals within 50 to 100 years if growth continues at rates similar to modern rates, and no major emergence events occur.

Figure 4.14. Comparison of the elevations of the tops of 1833-aged corals (presumably at or near preseismic 1833 HLS) and modern HLS.

a. Elevations for all living and dead samples collected in 1994. The elevations were measured relative to water level and corrected for tidal fluctuations using a tide gauge record from Sikakap harbor, between North and South Pagai (Figure 4.1).

b-e. Comparison of elevations at four sites on North and South Pagai in 1996. These elevations were measured with a surveying instrument. Their precision is >±1 mm, but they cannot be compared from site to site. Dated corals at P96-P and P96-Q may have died in a 1790's emergence event rather than in 1833.

f. Plot of the average difference between the living and 1833 elevations at several of the 1996 sites together.

a. All Sites - 1994

b. P96-N

c. NP96-C/NP94-A

d. P96-P

e. P96-Q

f. 1996 vs 1833 HLS by site
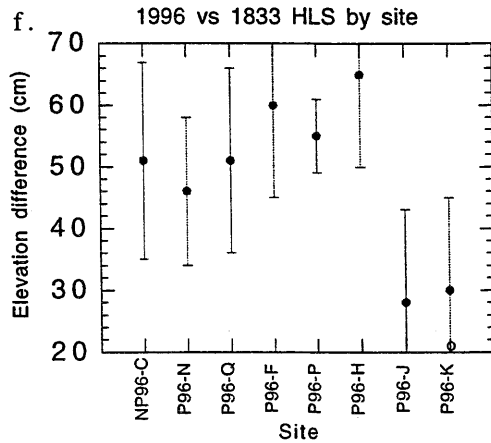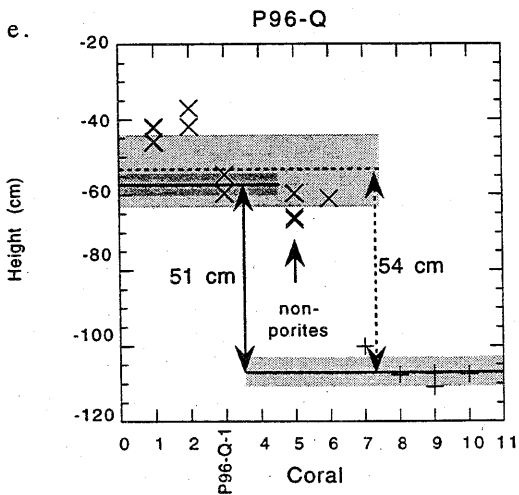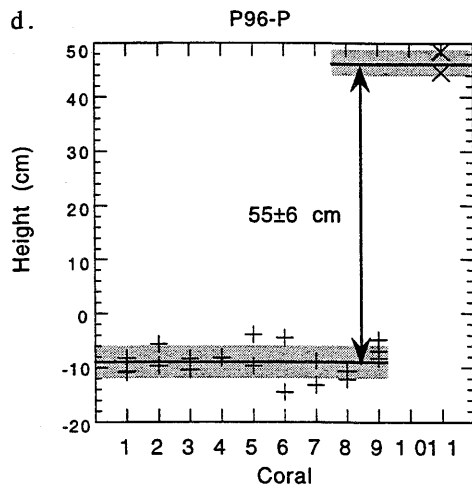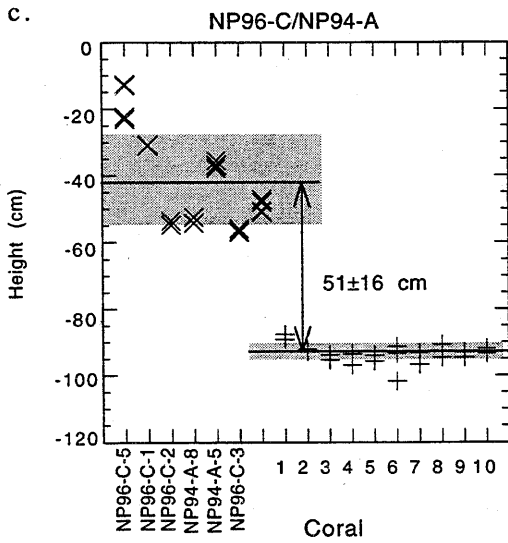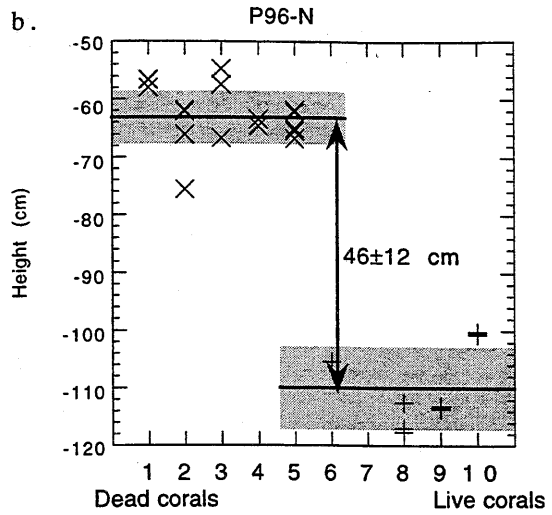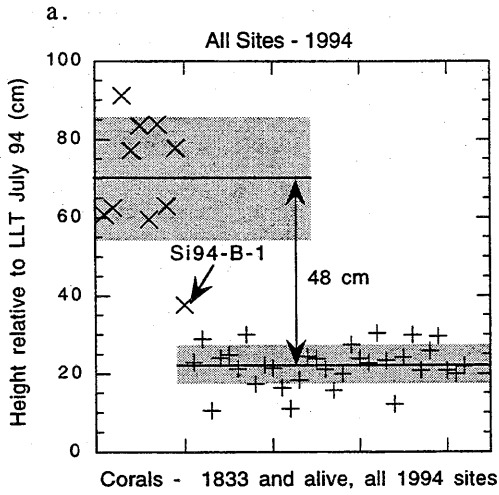
4.2e. Other emergence events

Late Holocene

The plot of late Holocene deaths clearly indicates the possibility of clusters of deaths, earlier than the 1830's, that might also represent paleoseismic events (Figure 4.4). Events in 1810 and about 1790 have already been documented at sites on Sipora and North Pagai and possibly South Pagai as well. Older "events" are not as clear, because they are represented by fewer corals, and in many cases by only one. Obviously, the more samples with the same age, the more likely their date of death represents the occurrence of a paleoseismic event. Clusters of late Holocene coral deaths appear in the early to mid-1600's and the 1300's. However, several of the 1300 dates come from the same coral head, so the cluster may not be that significant. The large errors on some older corals make it difficult to determine if other dates really do cluster.

There is evidence, in the form of at least one dated, emerged microatoll, for sudden emergence events in about 100 BC, 130 AD, 1100, 1360, 1530, 1600, 1680, besides 1790, 1810 and 1833. The first three are represented by one coral only. Two corals from a single site (P94-Z/P96-F) died around 1345-1375. Some events are hard to distinguish from others. The dates of several samples are uncertain enough that the different emerged corals could have died in multiple events or a single event.

<u>16th to 18th century events</u>

Several corals from numerous sites died in the 16th through 18th centuries. How many separate events these represent is unclear. The constraints on the ages of some of the corals indicate that not all the corals could have died in a single event. The errors on

most of the other corals of this general age are too large to determine precisely the time of death or exactly how many events occurred.

NP96-B

NP96-B was on the northeast side of North Pagai, about 15 km from the northern tip of the island (Figure 4.3). It contained numerous emerged microatolls rooted on a broad reef flat (Figure 4.15). Some of the corals were partially buried in sand, but others appeared to have been recently exhumed. The ages of microatolls at this site suggest the occurrence of two or three emergence events in the 18th and 16th centuries. The morphologies of the different microatolls are also highly variable, supporting the idea that they represent multiple generations of growth and emergence.

The youngest coral sampled at this site, NP96-B-1, died in 1739±10. This microatoll (D1) was slightly lower than most of the others and farther out from shore. Another, undated coral, D8, had a similar elevation and occurred farther from shore than the others; it might have been a contemporary of D1. These corals had a cup-like morphology, with central hollows about 15 cm below the tops of the rims. Their wide rims, 50 to 60 cm wide, suggest that they experienced a relatively long period of HLS stability prior to emergence. Small horns on top of the rims of both indicate that a slight short-lived submergence occurred between the period of stability and final emergence. Their elevations are about 40 cm above living HLS, so they should be near the elevation of microatolls from 1833. The outer edges of D1 step down and out suggesting emergence may not have occurred in a single, sudden event. The outer flange of D1 appeared to be a constructional, rather than erosional, feature. D8, by contrast has much steeper sides and no outer flange. These variations may indicate that the two corals are not contemporaries. Clarifying that would require more detailed sampling and dating of

Figure 4.15. Map (a) and cross-sectional profiles (b) of dead coral microatolls at site NP96-B. This site has at least two generations of microatoll present, based on U-Th ages. Coral heads D1 and D8 are lower than the rest of the dead corals; D1 died in the mid-18th century. Most of the higher corals have either sloping sides or a lower, outer flange that is indicative of emergence prior to the final emergence that killed the coral.
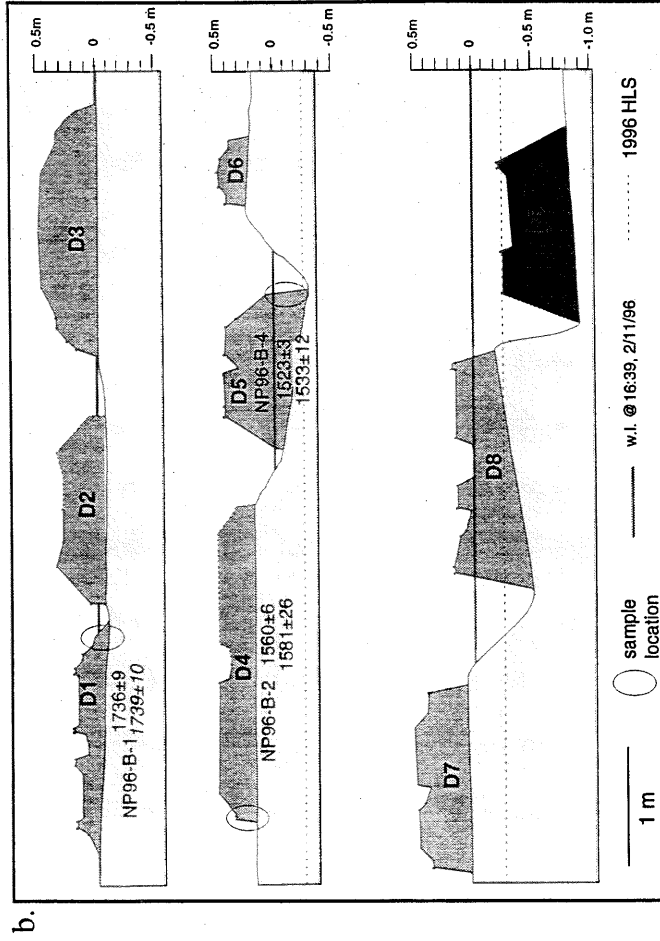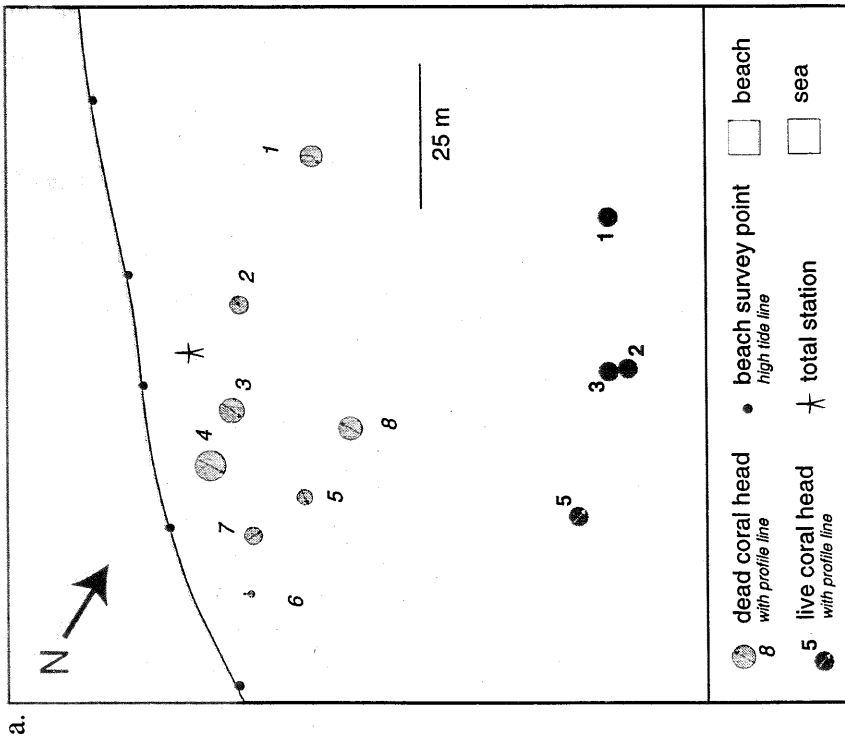
both corals. NP96-B-1 is too old to have died in the 1790's emergence event that affected site NP94-A/NP96-C on the opposite side of North Pagai and must represent a different event.

NP96-B-2 (d. 1581±26) came from Coral D4. This coral was about 30 cm higher than the 18th-century coral D1. It also had a broad flat outer rim, and its edges sloped down to a small, lower flange at the outer edge of the coral. No other microatoll here displayed a similar morphology, the closest being D1, which is clearly younger. The elevation of head D4 was similar to that of most of the other corals besides D1 and D8. The radius of this coral was about 140 cm, suggesting it lived about 140±70 years, based on an estimated 1±0.5 cm/yr growth rate.

Sample NP96-B-4, came from head D5, which also died in the 16th century (d. 1533±12), but it may not have been from the same generation as NP96-B-2 because their ages miss overlapping by 12 years. It came from a tall (~70 cm), partially buried microatoll with a central depression and sides that sloped downward from the top of the coral to about 40 cm below the top. Although the sloping sides may indicate that the coral experienced gradual emergence prior to a sudden and complete emergence, it is more likely that the coral grew with sloped sides, so the outer edge is a growth surface. In that case, the coral probably emerged suddenly. If coral D5 and D4 overlapped in time, the emergence of D5 should appear in D4. Given its radius and estimated life span, D4 should have been alive when D5 emerged. There is no clear evidence of that emergence in D5. The relationship between these two corals and their HLS histories cannot be resolved by gross morphology alone. Slab stratigraphic analysis could clarify the situation, differentiating between the events, or indicating that there was only one event and the apparent age differences between the corals is not real. In the absence of slabs, we know only that there is a likelihood of two emergence events having occurred in the 16th century, one early and one late.

P96-E

The errors on the ages of two *Porites* coral heads from this site, P96-E-1 and P96-E-2, are very high. However, as discussed in Chapter 3, a much better constrained date from a *Goniastrea retiformis* coral (P96-E-3) at the same site yields a death age of 1608±4. These three corals all grew within 10 m of each other. P96-E-1 and P96-E-2 were microatolls; P96-E-3, was lower than the microatolls and was still below HLS when it died. Given the proximity of three corals, and the absence of any other noticeably different population of corals at the site, I suspect the three corals died in the same emergence event. If that is so, then the age uncertainties of P96-E-3 can be used to constrain the time of the event. If the emergence occurred in 1608±4, then it indicates that the corals at P96-E must have emerged in a different event than the event at NP96-B.

P96-E-3 has the well-constrained age, but the two microatolls constrain the relative sea level history. Both of these *Porites* corals were slabbed with the chain saw. P96-E-1, partially buried by the beach berm, was 155 cm in diameter, with an 11 cm high outer rim; its top was 45 cm above the sand. The raised rim was eroded and sloped down to the outside. The top of the coral was 76 cm above modern HLS. E-2 had a similar morphology although it was somewhat more steep-sided, slightly larger and about 5 cm higher than E-1, and a few meters farther offshore. It was 180 cm in diameter, rising 84 cm above the substrate, and had a raised outer rim.

The slab drawings and HLS curves derived from the stratigraphy of these two slabs appear in Figure 4.16. The record from E-2 is only 18 years long, from the first interaction of the coral with HLS found in the sample (Figure 4.16a). That interaction, which followed at least twenty years of unimpeded growth, occurred in 1576 (corrected ^{230}Th age), after which HLS stepped up a couple of centimeters. In 1578, the coral was constrained to grow at a relatively stable HLS for about three years. That stability was

Figure 4.16. Drawings from x-radiographs of slabs P96-E-1 and P96-E-2, from coral heads that were killed by emergence in the early 17th century. They came from a bay on the west side of South Pagai (Figure 4.3). Both corals reveal a history of submergence and rapid growth prior to final emergence. The minimum emergence for P96-E-1 is about 60 cm; for P96-E-2, it is about 40 cm. These are the only two slabs of this age.

a.

1391 ± 4
1593 ± 238

P96-E-2
South Pagai

1381 ± 4
1583 ± 238

1384 ± 4
1586 ± 238

1377 ± 4
1579 ± 238

1590

1582

1575

1570

1565

b.

P96-E-1
South Pagai

1530 ± 6
1607 ± 89

1600

1517 ± 5
1593 ± 89

1519 ± 5
1595 ± 89

1511 ± 6
1587 ± 89

1605

1590

1585

1580

1500 ± 7
1576 ± 89

10 cm

1570
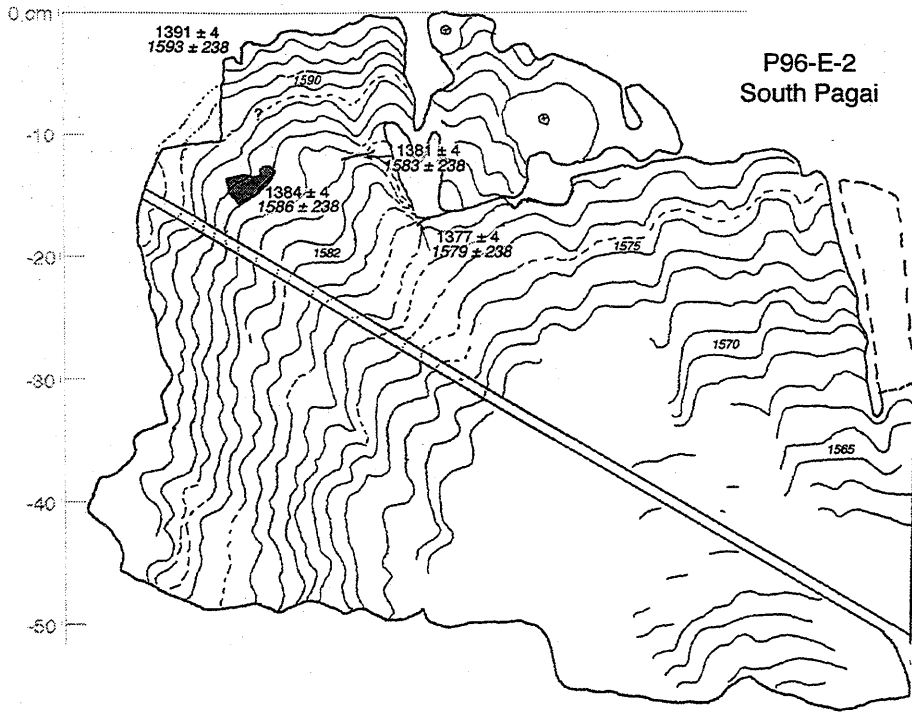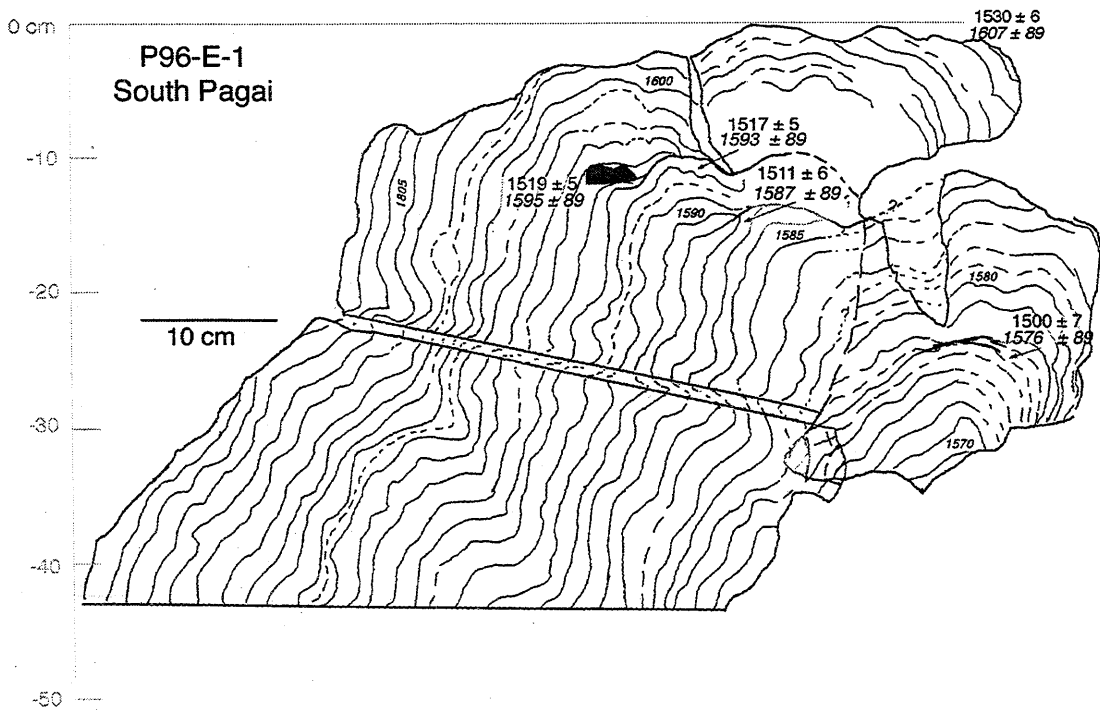
1500 ± 7 Date from U-Th analysis and ring counting

1576 ± 89 Date from U-Th analysis, corrected for intiial
thorium contamination, and ring counting

Location of dated sample

followed by submergence that outpaced coral growth. The top was slightly eroded, so it is unclear if the coral was at HLS when it emerged. The final emergence, which killed the entire coral, was at least 40 cm, determined from the slab, while 84 cm would account for emergence of the whole vertical-side coral.

P96-E-1 (Figure 4.16b) has a 35-year record, 30 from the first HLS clip in about 1576 (uncertainties in absolute age are ±89 years; in relative ages ± 1-3 years). An emergence of six centimeters occurred in 1585. This emergence was not observed in P96-E-2. It seems to have occurred before E-2 ever reached HLS and so was not recorded there. The small emergence was followed by stability for several years and then submergence after 1589. The coral reached HLS again between about 1600 and 1604. One HLS clip between the beginning of submergence and 1604, in 1593, may indicate that the submergence was gradual, at a rate just above the coral growth rate. However, the total submergence was only about 16 cm. It could have occurred suddenly, the intervening clip having been caused by a very low tide year. 16 cm is within the range of normal oceanographic fluctuations (Chapter 2). The coral was at or near HLS for about four years before it emerged. The outer rim of the coral is eroded, so the exact HLS elevation and time of first impingement is uncertain. The presence of the rim, however, indicates at least a few years of HLS stability. Minimum emergence was 60 cm.

The HLS curves for these two corals appear in Figure 4.17, which shows HLS elevation versus time, relative to a 1608 death date. The preseismic submergence rates for these corals, calculated from the HLS elevations only, are 8.4 mm/yr for E-1 and 8.7 mm/yr for E-2. Using both the HLS elevations and the minima together, the rates are 8.4 and 11.8 mm/yr, respectively. The greater rate of E-2 is at least partially due to the fact that E-1 includes a longer pre-subsidence record than does E-2. The submergence rate of E-1 for just the last twenty years is 9.2 mm/yr. The rest of the discrepancy may be caused by errors in ring identification and counting, erosion, or other undetermined factors. The

average preseismic submergence rate for this site of 8 to 10 mm/yr is slightly higher than average rates before the 1833 event. However, it is similar to the 1833-era rates from the last two decades preseismic.

The uncertainties on the corrected age of sample NP96-B-2 yields a youngest possible date of death of 1607. Thus, it is possible that that coral head (D4 at site NP96-B) died in the same event as the P96-E corals.

NP96-A and P94-AB

Corals from these two sites may have died in the 16th or 17th centuries; their ages are poorly constrained. Site NP96-A was located about 13 km southeast of NP96-B (Figure 4.3). There was an array of elevations represented with no clear distinction between different populations (Figure 4.18) - many of the corals at this site (D2, D4, D5, D6) had a cup-shape indicative of preseismic submergence; the two other surveyed dead corals (D1 and D7) had outer flanges that suggested a possible preseismic partial emergence event prior to final emergence. D3 was irregular, with very low relief across the top of the head and may have been eroded; it shows hints of both a subdued interior hollow and an outer flange on one side.

Coral head D7 (NP96-A-2), with a lower flange and the only dated coral from the site, had a corrected ^{230}Th age death date of 1586±99. It too could have died in 1608. Its morphology, however, is dissimilar to that of the microatolls at P96-E. Those corals were tall and steep-sided, with well-developed central hollows, suggesting rapid submergence prior to final emergence, which was sudden. NP96-A-2, by contrast, was broad and flat. It did have central hollows and multiple raised rims indicative of submergence, but probably at a lower rate than that indicated by the P96-E morphologies. NP96-A-2 also had an outwardly down-stepping outer edge suggestive of periodic small emergences prior to final emergence. In this, it is more like NP96-B-2 than like the P96-E corals.

Figure 4.17. HLS histories from slabs P96-E-2 and E-1. These corals experienced submergence at rapid rates prior to their final emergence in the early 17th century. The submergence rates before this event were about 30% faster than the preseismic rates recorded by corals that died in 1833. Large black dots indicate elevations of HLS impingements; small black dots indicate the tops of annual bands or minimum HLS elevations; the grey dots indicate incomplete rings that may have been clipped by HLS but are slightly eroded.

a. **P96-E-2**

Submergence rates
HLS only - 12.2 mm/yr
HLS and minima - 12.5 mm/yr

b. **P96-E-1**

Submergence rates
HLS only - 8.2 mm/yr
HLS and minima - 7.9 mm/yr
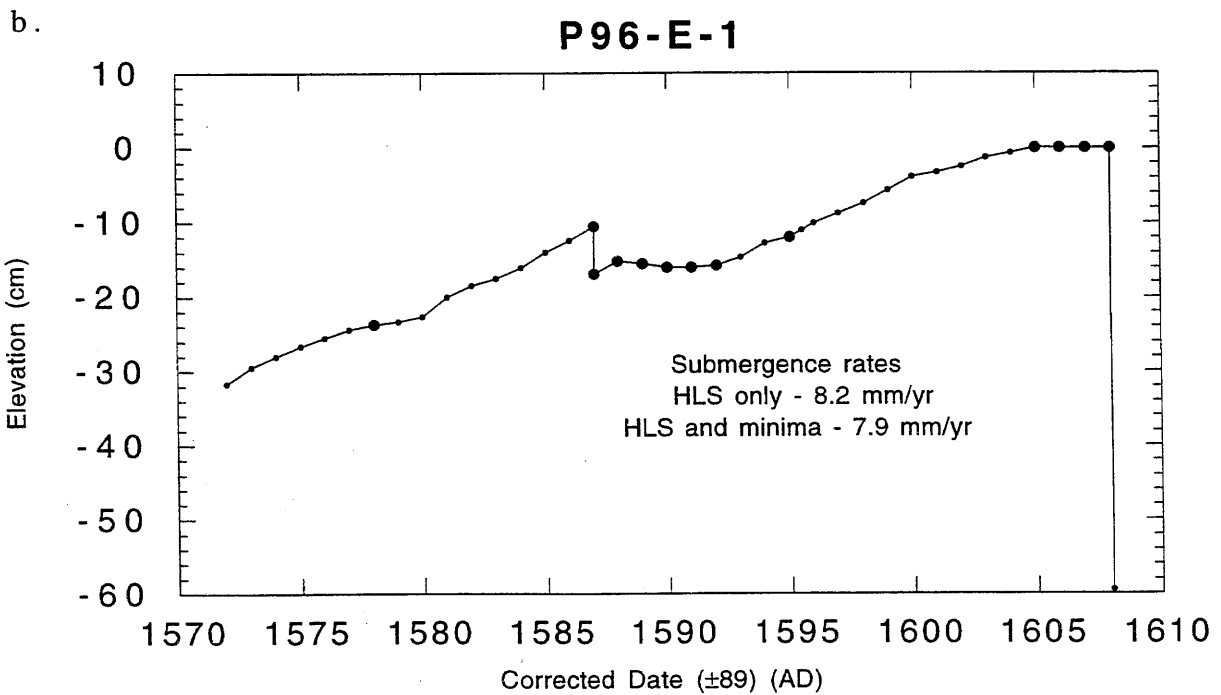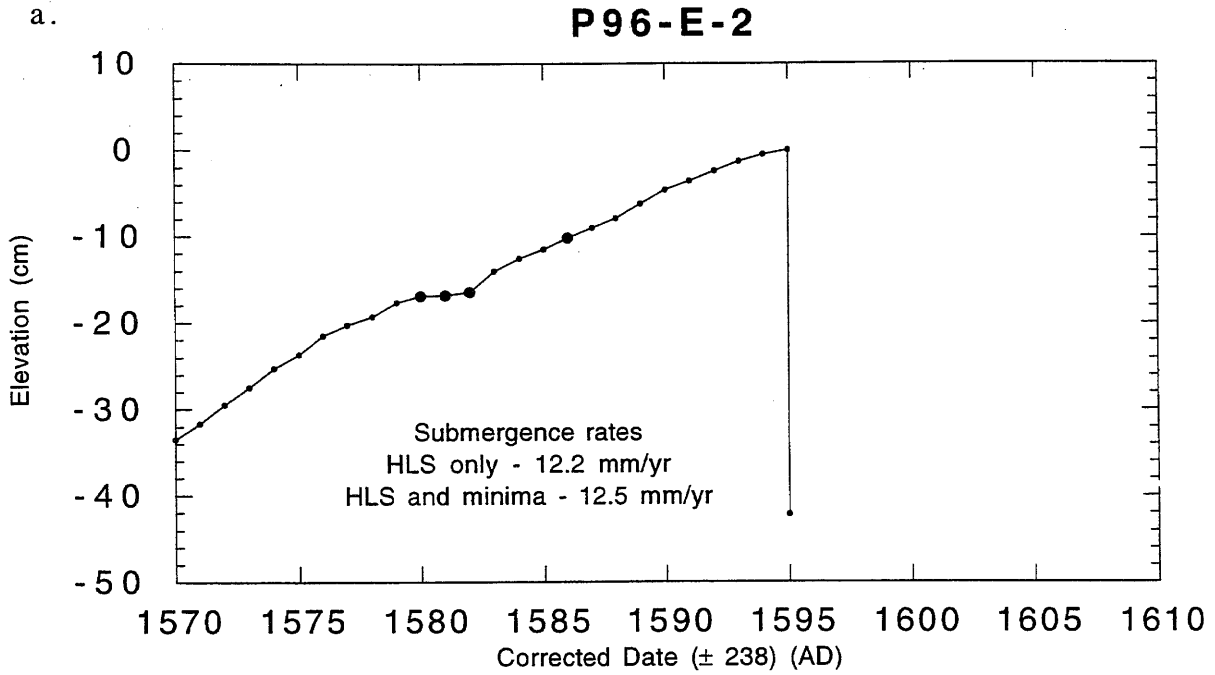
Figure 4.18. Map (a) and cross-sectional profiles (b) of corals at site NP96-A. In the bottom, right corner is a photograph of coral head D7, the only coral from this site that was dated. It died in 1586 ± 99. The age is poorly constrained, but it may have died in an early 17th century event that was also recorded in corals from P96-E, on the west side of South Pagai.

NP96-A

a.

| | dead coral head with profile line | | beach survey point at water level near low tide | | beach |
| 3 | live coral head | ★ | total station | | sea |

b.

0.5 m

water level at 14:42; 2/10/96

1996 HLS
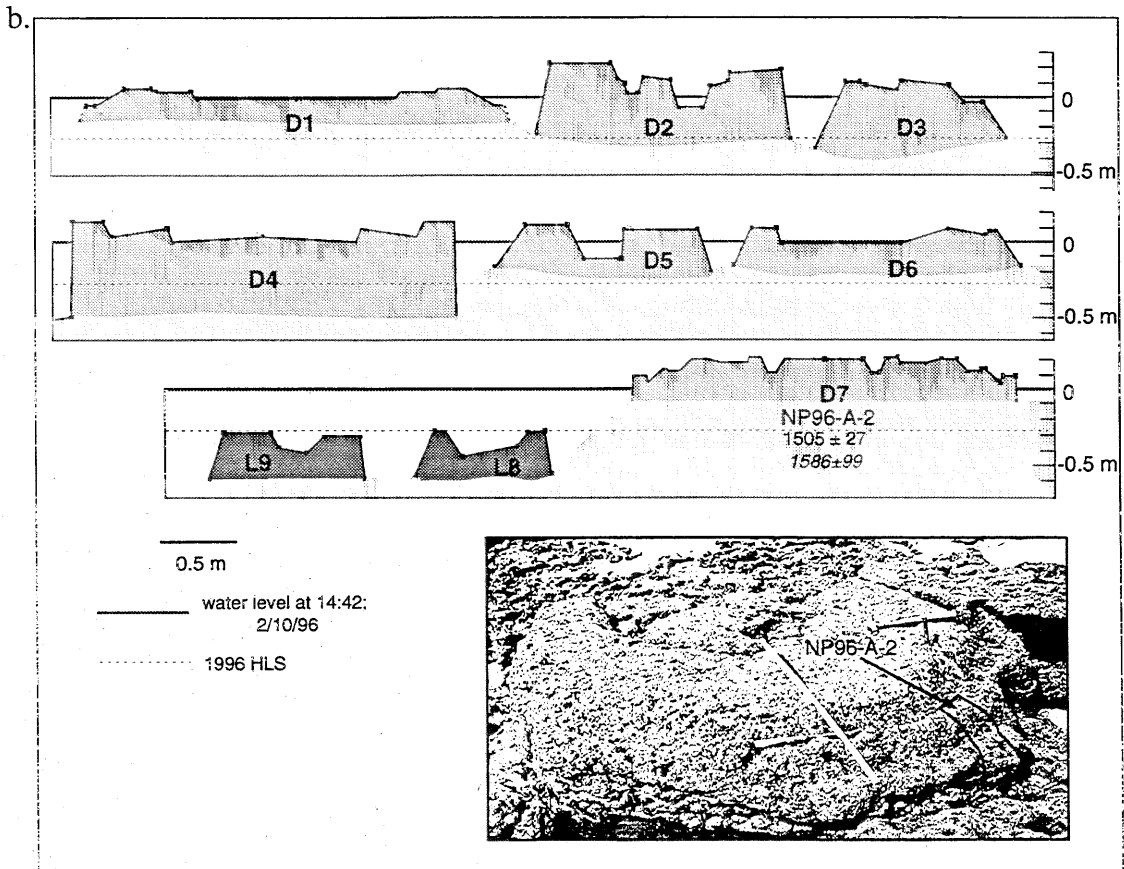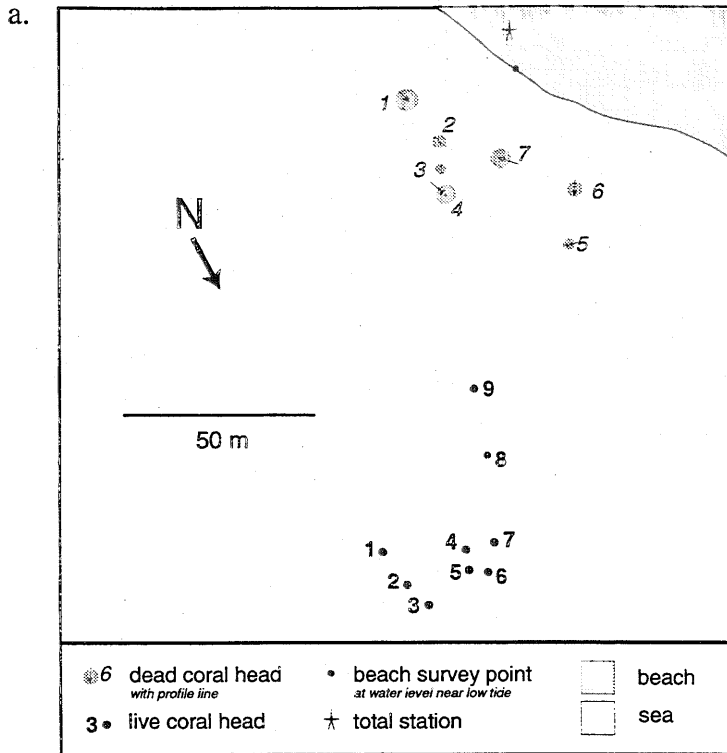
Site P94-AB was about 10 km northwest of P96-E and had numerous microatolls perched on top of a reef substrate of cemented coral fragments. Sample P94-AB-2 (d. 1572±65) (and its poorly constrained companions P93-C-7 and P93-C-8, exterior and interior samples respectively) came from a large, tilted *Porites* microatoll. The coral had a well-defined outer rim surrounding a depressed central flat. The uncertainties of the corals age allow it to be of the same generation as NP96-B-4 or the corals from P96-E.

P96-M and P96-L

Two other sites, in the South Pagai archipelago, with 17th century corals were P96-M and P96-L. The corals at these sites had ^{230}Th ages in the mid- or late 17th century. P96-M-1's date of death, 1656±63, is uncertain enough that it could be of the same age as the P96-E corals. It was one of several corals at this site on the west side of a small island just off the east coast of the South Pagai Peninsula. Most of the microatolls here were highly eroded and/or overturned. Across from this island and a few hundred meters north on the South Pagai peninsula, I observed a reef flat with numerous large microatolls over turned and out of place (Figure 1.19 in Chapter 1). Those were probably deposited by a tsunami, given their size; the same tsunami may have overturned many of the microatolls at site P96-M, even though it is on the more protected west side of the small island. The coral from which sample M-1 came was also somewhat eroded; the sample is from what appeared to be the youngest part of the coral. The microatoll was about 130 cm in radius, with a 40 cm-wide raised rim. The rim was about 11 ± 5 cm above a lower, inner rim, that itself rose 5 cm above the central flat. The outside edge of the coral was undercut.

P96-L was about 10 km north of P96-M, on a small island (Figure 4.3). Two large emerged microatolls were present at this site, and both were somewhat eroded and broken. A sample, P96-L-1, taken from the outer edge of one coral yielded a date of

death of 1688±18. The sample came from a piece of the outer rim, which had broken off and separated from the central core of the coral. The central core, composed of the inner flat with an interior raised rim, about halfway in from the edge, was about 2 m in diameter and rose about 30 cm above the sand. The interior rim rose 12 cm above the central flat. The detached rim, which appeared to have dropped directly below its original growth position, without being noticeably shifted or overturned, was about half a meter wide and about 30 cm thick. The other microatoll had a similar morphology to the first, and it too was broken into several pieces. Although the corals were not intact, the broad, flat central section, the outer rim, and the relatively low height to diameter ratio, suggest they experienced submergence at moderate average rates prior to final emergence. The submergence rate may have increased during the corals last decades, permitting the development of a raised outer rim. Its late 17th century age does not permit coral P96-L-1 to have been a contemporary of the corals at P96-E and other late 16th and early 17th century corals.

14th century event

Two corals, both from site P94-Z/P96-F, had corrected ^{230}Th dates of death of about 1345-1375 AD. This was the only site with corals of this age. There were several elevations of microatoll at this site. However, the suspicion that each elevation represented a different generation proved false. Sample P94-Z-1 (also P96-F-2 and 3) came from a coral that was 94 cm tall, 125±9 cm above living HLS, 54 cm above P94-Z-2 and 62 cm above P94-Z-4 (aka P96-F-1; d. 1831±17) (Figure 4.19). However, both P94-Z-1 and P94-Z-2 died in the mid-14th century while P94-Z-4/P96-F-1 died in about 1833.

The elevations would suggest that P94-Z-2 and P94-Z-4 were the contemporaries, rather than Z-2 and Z-1. The great (54 cm) difference in elevations of Z-1 and Z-2 must

Figure 4.19. Coral from site P94-Z/P96-F. The plot at the top shows the ages and relative elevations of different generations of coral at this site. The photographs below are of each of the three sampled microatolls. The P94-Z-1/P96-F-2&3 and P94-Z-2 are the same age but are morphologically dissimilar and their elevations differ by 54 cm. P94-Z-4/P96-F-1 was slabbed. The tracing of that slab appears in Figure 4.8d.
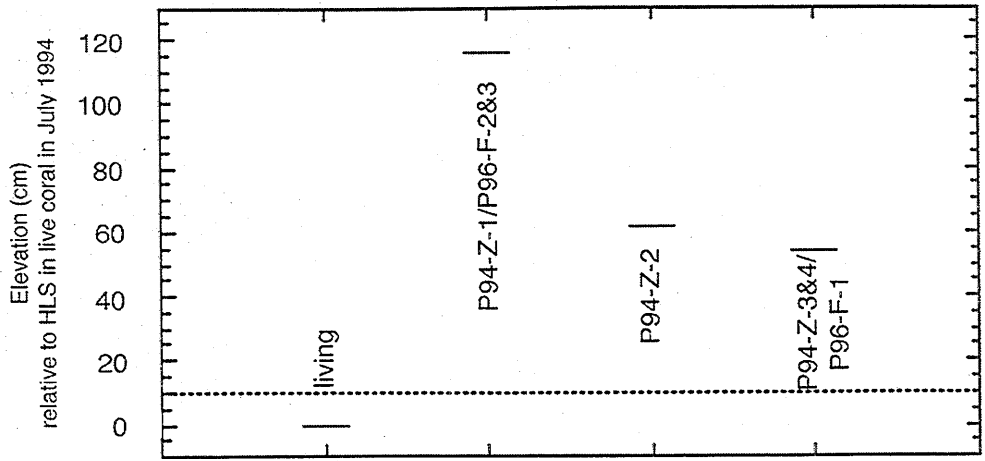
P94-Z-1/P96-F-2&3

P94-Z-3&4/P96-F-1

P94-Z-2

mean either that one or both of the corals have shifted and are out of place, or that the HLS of the two corals during growth was very different. Given that the variation in HLS in live corals was generally not more than about 20 cm, and that many microatolls at this site, including P94-Z-2, were tilted, I suspect the former explanation. Thus, the relative elevation measurements between corals of the older generation here are questionable. Since P94-Z-1 did not appear to be tilted, it is more likely that it is in place and P94-Z-2 is out of place. The elevation of P94-Z-1 is thus a better estimate of the original elevation of HLS.

11th century event

NP94-A-6 (exterior piece; NP94-A-7 is interior piece), which died in 1076±42, was the largest fossil microatoll observed in the Mentawais. The coral was 7.9 m in diameter and probably represented 400±200 years of growth. The rim was eroded almost to the level of the interior. The top of the coral was about 40 cm lower than NP94-A-5, a 1790's fatality (d. 1797±18), 25 cm lower than NP94-A-8, an 1833 fatality (1841±11), and 25 cm above living HLS (Figure 4.10b). Given that the rim has been eroded somewhat, this coral in its uneroded state was probably originally within a couple of tens of centimeters of the elevation of the 18th and 19th century corals.

103 BC event

P94-AA-1, a *Goniastrea retiformis* coral that died in 103±14 BC (102±15 BC corrected) came from a site on the west coast of South Pagai at which several microatolls occurred. The uneroded raised outer rim of this coral was 48 cm above currently living HLS, and the coral appeared to have died suddenly. Another emerged but undated coral nearby showed evidence of two emergence events (Figure 1.16 in Chapter 1). A rounded dome surrounded by a 20 cm wide flange, 17 cm below the top, indicated a partial

emergence 20 or so years before the final emergence. The rounded top of this *Porites* microatoll was 4 cm below the top of P94-AA-1. If the two corals were the same generation, one would expect to see the partial emergence affecting both corals. P94-AA-1 has no outer flange so probably the two corals were not contemporaries. If not, the fact that the HLS's are the same elevation suggests little net vertical deformation at the site over the lifetime of both corals.

Mid-Holocene

Seven samples yielded ^{230}Th dates that were mid-Holocene, between 3500 and 6200 BC (Table 4.1; Figure 4.20). In addition, two samples, collected from the east coast of Sipora during a reconnaissance in 1993 and dated with ^{14}C methods, had mid-Holocene ages (K. Sieh, personal. comm.). The radiocarbon dates, corrected by 400 years to account for residence time in the ocean, are 4075±55 and 4216±60 BC. Of the nine mid-Holocene corals, six were from microatolls, and three were samples from consolidated basal reef platforms composed of a cemented mass of coral fragments. Like most emerged microatolls in the islands, the tall, steep-sides of the mid-Holocene microatolls suggest that they died from sudden emergence. Likewise, their cup-like morphology indicates that they experienced submergence prior to the emergence. Given their morphological similarity to 1833 and other late Holocene emerged microatolls, I suspect they died from exposure after uplift during mid-Holocene earthquakes. The samples from P96-O were two of a group of eight to ten elevated dead coral heads that may all have died at once in a single event (Figure 4.3).

All of the microatolls were located within or slightly above the intertidal zone. The elevations of the corals from P94-C were related to lowest low tide (LLT) of July

Figure 4.20. Mid-Holocene U-Th and ^{14}C dates of coral emergence and death for nine samples. The sample name indicates the site at which it was collected (e.g. P96-O-1.A was sample 1.A collected from site P96-O ; see Figure 4.3 for site locations). Six corals, marked with "m.a.," were microatolls; the other three came from eroded or fragmented coral heads embedded in a basal reef flat that often formed the substrate upon which younger microatolls grew. The dates are shown both uncorrected and corrected for initial thorium contamination (Chapter 3); the error bars are the 2σ-uncertainty on the corrected dates. The two P96-O microatolls, were from a cluster of eight *Porites* sp. coral heads at about the same elevation. The two P94-C microatolls from were different families - P94-C-1 was a *Faviid?* and was located well back from the shore in a muddy lagoon; P94-C-3 was a *Porites* sp. and was located on the reef flat in the intertidal zone.

Mid-Holocene coral deaths

Legend:
- U-Th date of death (coral)
- U-Th corrected date
- C-14 Date (corrected)

Date (AD)

Sample Name

Sample names: P96-O-1.A, P96-O-2.B, P94-M-2.B, Si93-B, Si93-J, P94-C-1.B, P94-M-3.A, P94-C-3.B, P94-Y-1A.A
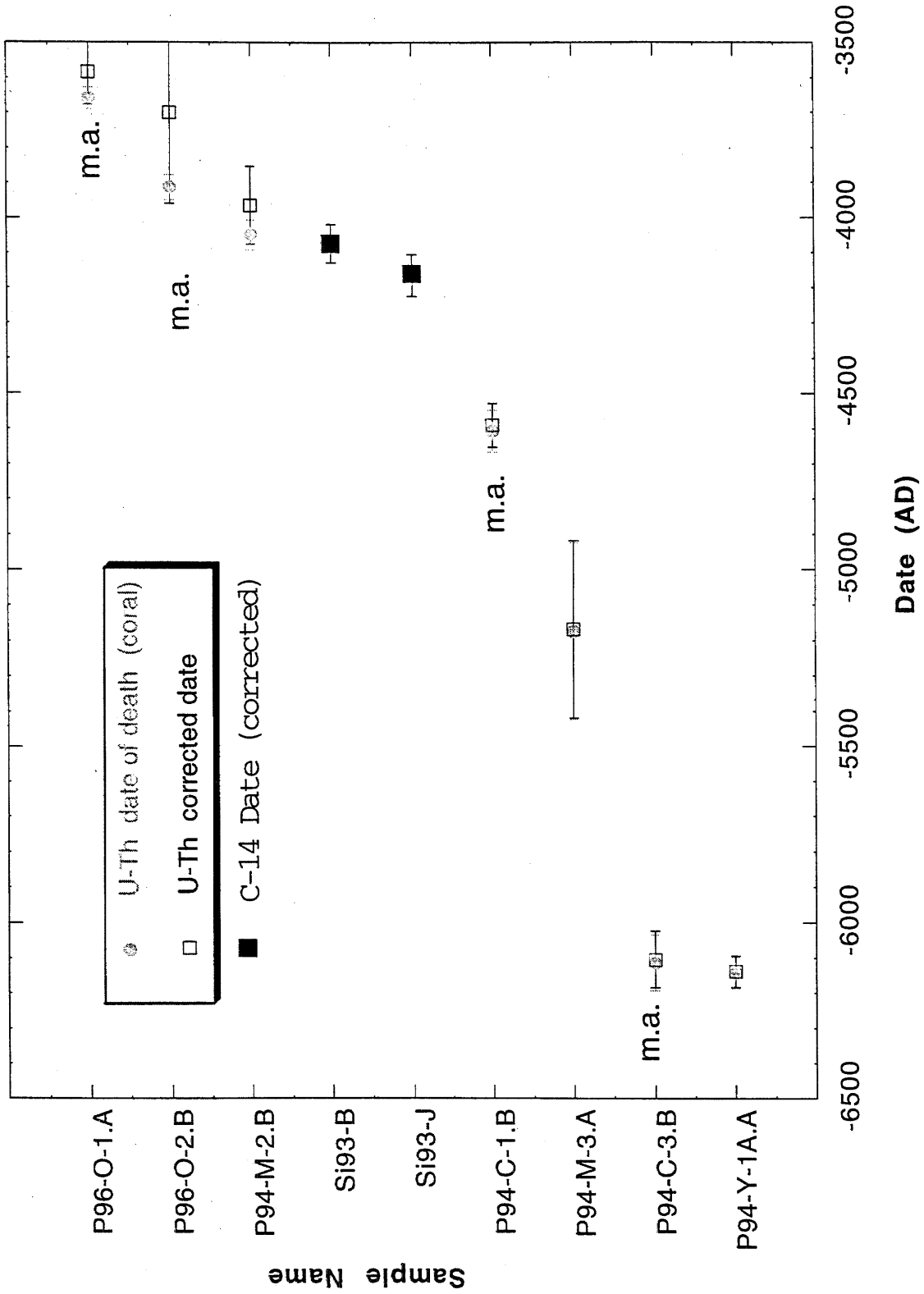
1994 by way of the tide gauge installed at Sikakap (Chapter 2). P94-C-1 was 134 cm above LLT, while the slightly eroded P94-C-3 was 109 cm above LLT. These microatolls were about 50-70 cm above most late Holocene (ca. 1833) corals. The elevations of the 1996 samples at P96-O were not measured relative to LLT because of a failure of the tide gauge. However, field observations revealed them to be about 50-80 cm above 1833 samples in the area (central east coast of South Pagai)(Figure 4.21). Though these elevations are very roughly estimated, I estimate P96-O-1 and P96-O-2 to be about 140 and 120 cm above LLT of July 1994. Live corals were about 20 cm above LLT of July 1994 (Chapter 2). Mean sea level was about 60 cm above LLT (Figure 2.13, Chapter 2).

4.3 Discussion

4.3a. Fossil corals as paleoseismic and paleogeodetic recorders

In Chapter 2, I showed how coral microatolls can be used to generate records of sea-level fluctuations . Stratigraphic and morphological analysis of live corals from the Mentawai Islands yielded records, up to 50 years long, of annual sea-level changes with uncertainties of a few years and a few centimeters. In this chapter, I have used these analytical methods to obtain past sea level records and paleoseismological records from fossil corals dated with U-Th geochronometry.

In principle, fossil corals can provide a sea-level record with essentially the same precision afforded by live microatolls. U-Th dating methods applied to corals a few hundred years old can yield uncertainties of only a few years (Edwards, 1988; this study), which is the same magnitude of uncertainty inherent in ring counting alone in a 50-year record. Sea level records obtained from clean, uncontaminated fossil corals could therefore be nearly as precise as those from living corals. Unfortunately, in the Mentawais, many of the emerged fossil corals are dirty and highly contaminated.

Uncertainties in these U-Th dates are significantly larger than those of clean corals, both because mass spectrometric analysis of dirty corals tends to generate larger analytical errors, and because the correction applied to remove the effects of the contamination is so poorly constrained. Thus, while in principle age precision in the coral-derived sea level histories of fossil corals need not be much worse than in live corals, in practice it may be. As long as the correction factor for contamination remains poorly known, the key to achieving age-precise paleoseismic and paleogeodetic records lies in the ability to find clean samples.

The other contributing factor to paleogeodetic uncertainty is in elevation. Elevation data for fossil corals are slightly less well-constrained than those for live corals but are often *nearly* as precise. Fossil corals are more likely to be eroded than live corals. However, I found many microatolls that had retained much of their constructional surficial relief. Erosion in these cases was probably only a couple of centimeters at most. Furthermore, it generally affected only the outermost part of the coral. The annual rings and HLS record from the coral interior were as pristine and precisely located as in living corals.

Absolute elevations are probably not as well-constrained because fossil corals may have been moved out of position by storms, tsunamis or shaking from later earthquakes, while living corals are by definition *in situ*. However, the sea level records derived from stratigraphic analysis of coral slabs record relative sea level changes, not absolute elevations. The relative elevations are recorded internally in the coral head and are not affected by absolute elevation changes or tilting that may have befallen the coral after emergence. Elevation comparisons between different generations of coral *are* affected by such movement so correlations over time without a direct coral connection are more tenuous. To fully constrain sea level histories through multiple paleoseismic events and multiple coral generations, one *would need coral records that overlap in time, such*

Figure 4.21. Surveyed map and cross-sectional profiles of emerged mid-Holocene microatolls from site P96-O on the east coast of South Pagai. These corals were noticeably higher than most other, younger, emerged corals. Their higher elevation is primarily due to their having lived when regional mean sea level was higher than it is now. These emerged heads suggest the islands might have been submerging at a very low rate over the past 6000 years.

P96-O
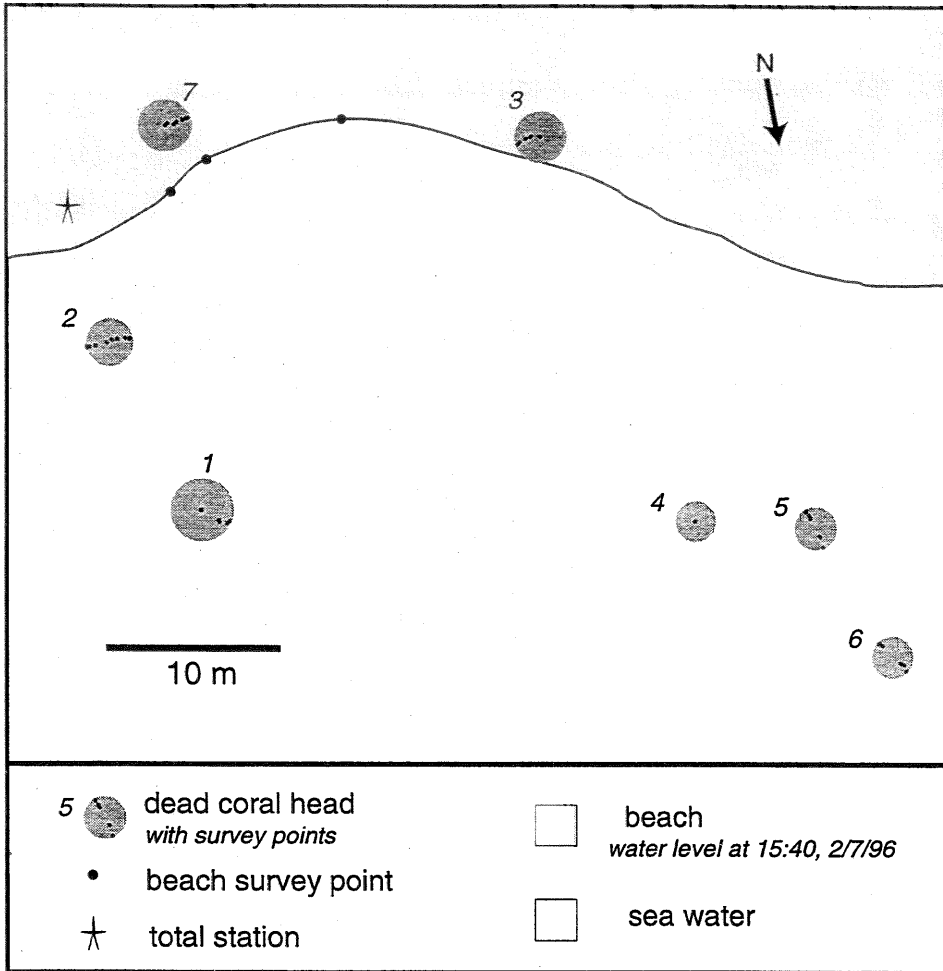
5 — dead coral head *with survey points*

• — beach survey point

✶ — total station

□ — beach *water level at 15:40, 2/7/96*

□ — sea water

P96-O-1
3912 BC ± 36
3700 BC ± 259

P96-O-2
3658 BC ± 32
3583 BC ± 95

○ approximate sample site

——— water level @ 15:40, 2/7/96

- - - approximate elevation of 1833-aged samples on southeast S. Pagai

2 m

10 m
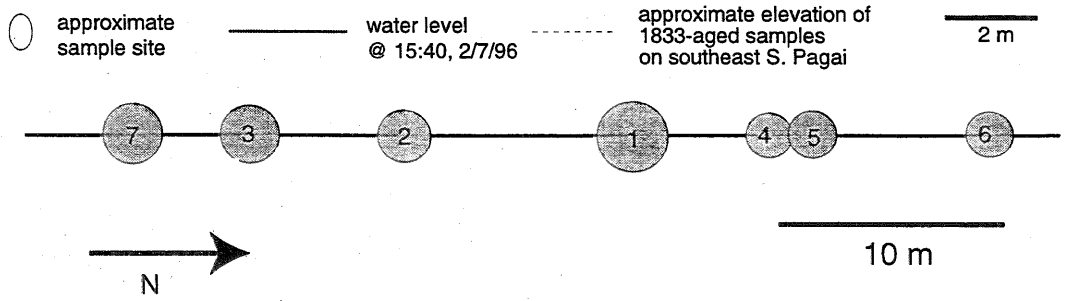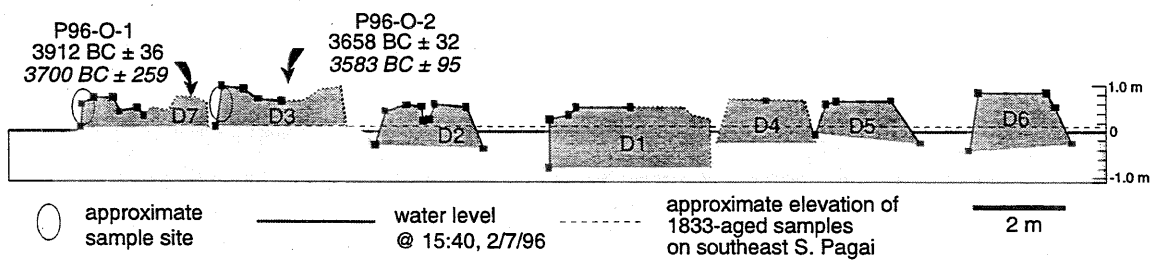
that the final emergence recorded in one coral is an early partial emergence in another whose final emergence is the first event recorded in a third coral and so on. Enough overlap to provide a complete record through time until the present would obviate the need for absolute elevation measurements beyond that of the living coral.

HLS records from site NP94-A/NP96-C overlapped in this fashion. The 1790's emergence that killed many corals at the site raised NP94-A-8 only partially out of the water so that the HLS record that began in the older corals continued after their death in the partially emerged NP94-A-8. If another coral had been found that emerged only partially in 1833, the record could have continued further. Combination of the HLS records from the 1790's corals and NP94-A-8 yielded an estimate of the magnitude of emergence in the 1790's. This estimate still depended on the assumption that the corals were in place, since neither generation of coral recorded the entire 1790's emergence in its morphology. The estimate of the emergence depended on the measurement of the relative elevations of the corals in their 1990's positions. Thus, if they had shifted relative to each other in the decades since 1833, that estimate would be inaccurate. However, the orientation of the corals strongly suggested that they were in growth position, so I suspect the estimates are sound. In principle, the correlations of events, e.g. the final event of Coral 1 with the partial event of Coral 2, could be made with very tightly constrained ages and/or distinctive stratigraphic characteristics such as, for example, four narrow rings followed by one thick ring, and two more thin rings.

The results from this study suggest that this method of analysis can yield very tightly constrained records of past paleoseismic and paleogeodetic events. At sites with multiple, overlapping generations of coral, it was possible to make distinctions between past emergence events that occurred only a few years apart. Although this was most clearly demonstrated in corals from the early 19th century, for which at least some historical records are available, there is no reason similar precision cannot be obtained for

older events. The interior of older corals is no less well-preserved than in younger corals, so, as long as corals that are in place and relatively uneroded occur, the older corals should yield records just as precise. The limiting factor is primarily the degree of preservation of the older corals. A huge proportion of the sampled corals in this study died in 1833 or just prior, primarily because the 19th century corals are better preserved than older corals that have spent centuries in the intertidal zone, worked on by waves, storms and tsunamis. Younger corals will probably always be better represented than older corals, especially given the location of almost all observed emerged corals in the intertidal zone, where they are subjected to wave and storm action, but that is to be expected. However, the presence of well-preserved microatolls as much as 8, 000 years old indicates robust paleoseismological records could be obtained throughout much of the Holocene.

4.3b. Mid-Holocene microatolls and Holocene relative sea-level stability

I found no fossil microatolls more than a meter above the modern intertidal zone in the Mentawai Islands. The six mid-Holocene microatolls, as old as 8,100 years, were all less than a meter above younger fossil microatolls and less than a meter and a half above their living counterparts. These observations are consistent with published data indicating the presence of Holocene reef material only a couple of meters above modern sea level in Sipora (Verstappen, 1973). They indicate that the Pagai and Sipora Islands, while currently subsiding, have remained nearly stable relative to sea level over the last 6-8,000 years.

However, eustatic sea level during that period has not been constant. In an effort to clarify the nature and amount of long term deformation better, I compared the elevations of the mid-Holocene microatolls to elevations predicted from glacio-isostatic

models of Holocene sea-level history. W.R. Peltier and his colleagues modeled relative sea-level changes over the past 20,000 years for several locations around the Mentawais (Chapter 1; Figure 4.22a; Peltier et al., written communication). The curves of relative sea-level versus time reflect glacio-eustatic changes in sea level, sea-level change resulting from climate changes and the earth's isostatic response to unloading of the ice and loading with meltwater (Peltier and Tushingham, 1991; Mitrovica and Peltier, 1991). The curves reflect estimates of the elevation of former mean sea level (MSL) relative to modern MSL.

I used these curves to estimate the elevation of relative MSL at the times each of the dated microatolls lived (Figure 4.22b). I assume the difference between MSL and low-low tide (LLT) has remained approximately the same throughout the Holocene, and therefore I can use the long-term change in MSL to represent the change in LLT or HLS. Using the estimated mid-Holocene elevations, I calculated the resultant elevation change that each site has experienced since the life of the coral, and the rate of vertical motion that has occurred since then (Figure 4.23).

The microatolls from the two sites on Sipora and the two from site P96-O indicate that these sites have been submerging since about 6000 years ago at a rate of about 0.16-0.28 mm/yr. Site P94-C, on the northeast corner of South Pagai, yields ambiguous results, different than those of the sites to the north and south. P94-C-1 shows essentially no net change over the 6600 years since it grew. At the same time, the older sample, 8100 year old P94-C-3, suggests almost six meters of uplift since it died. The younger sample is not grossly incompatible with the results for Sipora and P96-O given the uncertainties in estimating relative elevations and in the estimated sea level curve. However, P94-C-3 is substantially different. Several explanations are possible - 1) the samples are in fact out of place and their current relative elevations do not represent their original relative elevations, 2) the predicted sea level curve is grossly incorrect, 3) site P94-C has

experienced substantial differential vertical motion relative to the other sites in Sipora, or 4) the nature of vertical motion has changed significantly since 8100 years ago. The last option arises because the samples from P94-C are older than the others, C-1 by about 400-1000 years, and P94-C-3 by about 2000-2600 years. If the Pagais and Sipora experienced rapid uplift until maybe 7000 years ago, more moderate uplift until 6000 years ago, then submergence at an average rate of 0.2 mm/yr, the P94-C samples might still show signs of net uplift or no net vertical motion. Without further sampling and measurement of absolute elevations, the question will probably not be solved. At any rate, however, the mid-Holocene microatolls are testament to the fact that net vertical motion during the late Holocene has occurred only at sub-mm/yr rates - essentially all interseismic displacement is recovered coseismically (or in aseismic slip events) and the deformation of the hanging wall of the Sumatran subduction zone in this area is nearly elastic on that time scale. This contrasts with places like the Huon Peninsula where coral reef terraces 5-10,000 years old occur as much as 20 m above modern sea level, indicating uplift rates of 2-4 mm/yr (Ota et al., 1993).

4.3c. 1833 coseismic emergence event

Newcomb and McCann (1987) compiled historical records of the seismic history of the Sunda Arc (around Sumatra and Java) over the past 300 years. Their sources included historical records of felt intensities from the late 1600's to about 1900 and early instrumental records from about 1900 to the 1970's. The record derived from coral microatolls correlates with this historical record to some extent.

The 1833 earthquake, felt throughout much of Sumatra and as far away as Java and Singapore, was recorded by corals throughout the Pagais and Sipora. No 1833 corals have been found north of the Batus, although several corals that died in 1861, the year of

Figure 4.22a. Predicted sea-level curves for the past 15,000 years relative to modern mean sea level (Peltier, written communication, 1995). The models predict past sea-levels at four sites near the Mentawais resulting from the viscoelastic response of the earth to redistribution of water between ice sheets and oceans.

Figure 4.22b. A sea-level curve averaged from the modeled curves in Figure 4.22a that may approximately represent past sea levels near the Pagais. The date of death of each mid-Holocene coral is marked along the curve. The curve and the U-Th provide an estimate of the elevation that the corals would have been at when they were alive, relative to modern mean sea level.

a.

Sea Level Models

Legend:
- Site 1 (0 S, 98 E)
- Site 2 (0 S, 99.5 E)
- Site 3 (4 S, 102.3 E)
- Site 4 (5 S, 102 E)

b.
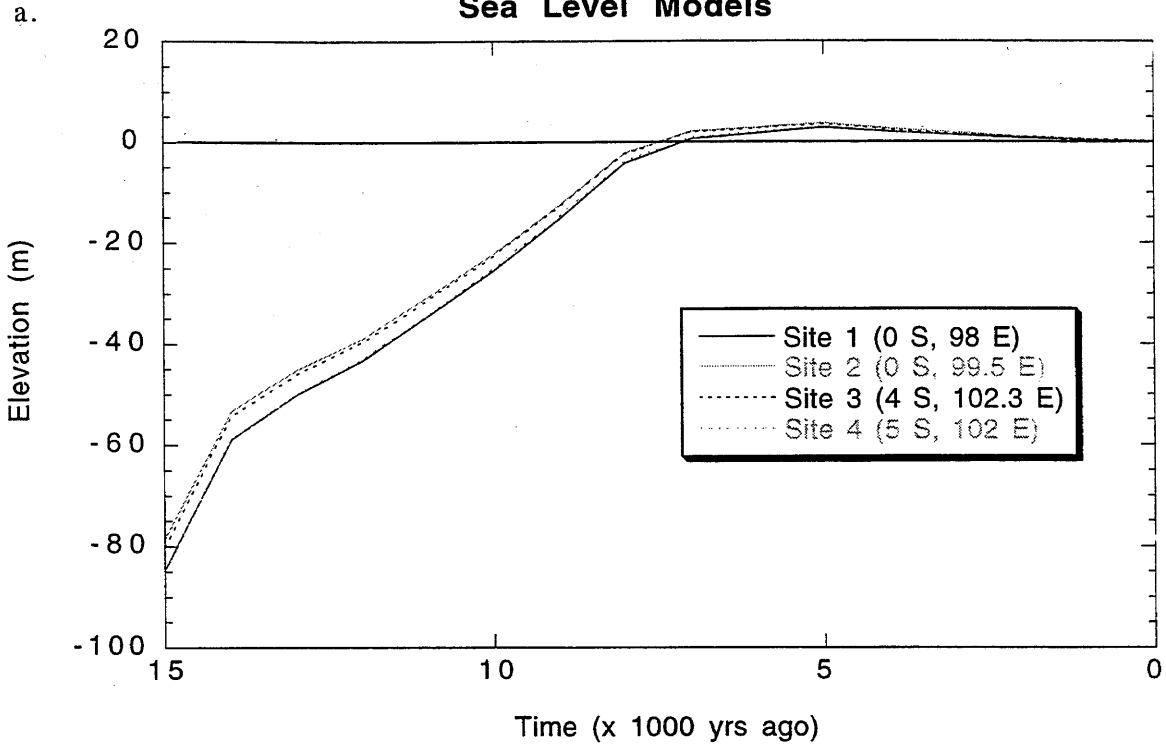
Mid-Holocene Sea Level Predictions

P96-O-2 (m.a.) 5696 ya

P96-O-1 (m.a.) 5579 ya

P94-C-1 (m.a.) 6589 ya

Sipora site #1 6091 ya

Sipora site #2 6212 ya

P94-C-3 (m.a.) 8101 ya

Sample	Date	Original Elevation
P96-O-1:	-3583 -->	+2.3 m
P96-O-2:	-3700 -->	+2.2 m
P94-C-1:	-4593 -->	+1.1 m
P94-C-3:	-6105 -->	-5.2 m
Si Site 1:	-4075 -->	+1.7 m
Si Site 2:	-4216 -->	+1.6 m
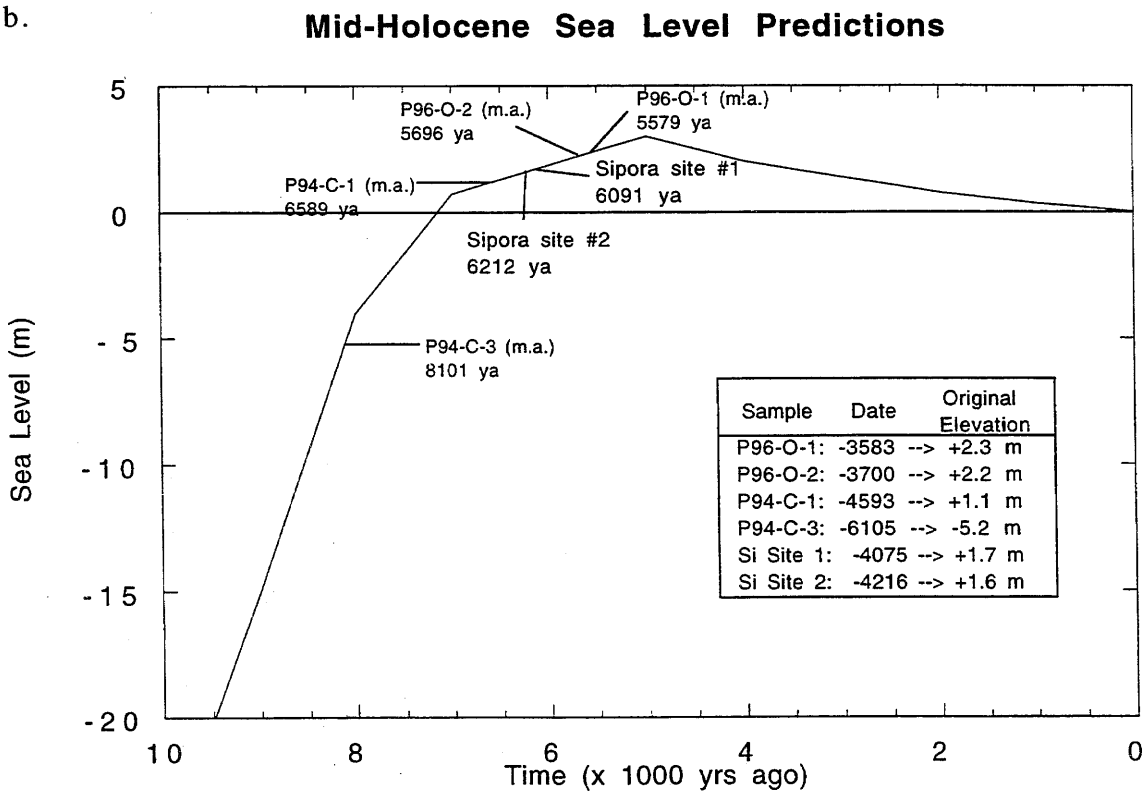
Figure 4.23. Map of the Pagais and Sipora with estimated average rates of vertical motion over the last several thousand years. The rates were calculated from the age of the samples and the approximate elevation difference between the corals' current elevations and their modeled elevations at the time they were alive (Figure 4.22b). All corals but the oldest (8055±80 BP) indicate the islands have been subsiding at sub-mm/yr rates since the mid-Holocene.

Pagai and Sipora Islands

● Sites with
mid-Holocene microatolls

⎯⎯⎯ 10 km

↑
N
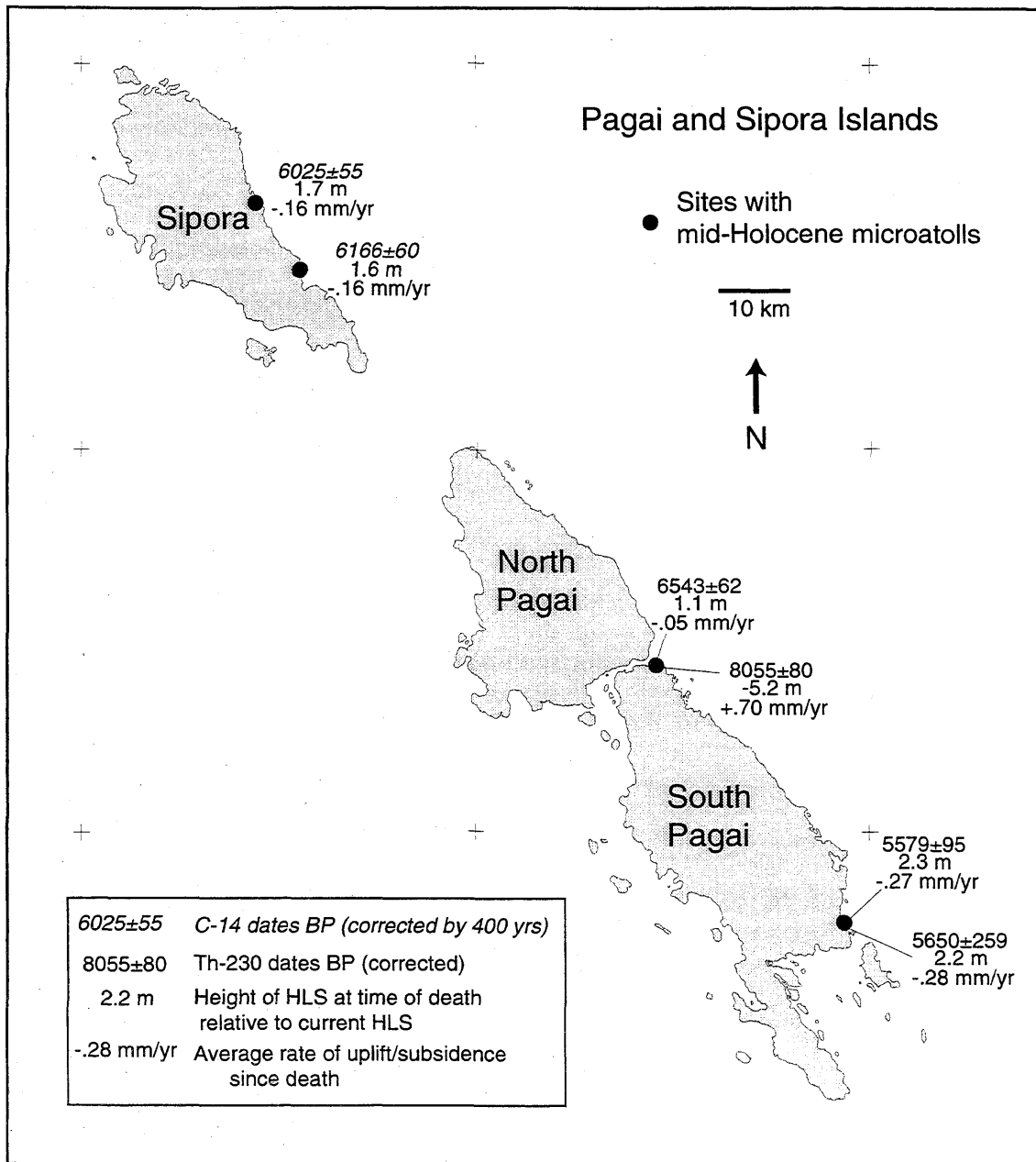
Sipora

6025±55
1.7 m
-.16 mm/yr

6166±60
1.6 m
-.16 mm/yr

North
Pagai

6543±62
1.1 m
-.05 mm/yr

8055±80
-5.2 m
+.70 mm/yr

South
Pagai

5579±95
2.3 m
-.27 mm/yr

5650±259
2.2 m
-.28 mm/yr

6025±55	*C-14 dates BP (corrected by 400 yrs)*
8055±80	Th-230 dates BP (corrected)
2.2 m	Height of HLS at time of death relative to current HLS
-.28 mm/yr	Average rate of uplift/subsidence since death

a historically recorded great earthquake in northern Sumatra, have been found (Sieh et al., 1994; Zachariasen et al., 1995).

The geographic distribution of corals that may have died in 1833 appears in Figure 4.24. They occur over the length and breadth of the Pagais and Sipora. 1833 samples predominate in southern South Pagai, but this is probably a function of the fact that there were more corals collected from that region. Only the more tightly constrained dates are labeled on the map; sites that had samples with poorly constrained 1833 ages are indicated but unlabeled. Newcomb and McCann (1987) estimated that rupture on a 600-km long segment of the plate interface, from the latitude of Enggano to the Batu Islands, induced the 1833 earthquake. The broad distribution of corals that died around 1833 provides evidence of coseismic displacements over 200 of the estimated 600 km, in the central portion of the suggested segment.

Preseismic HLS history

Stratigraphic analysis of slabs from seven coral heads from six sites in the Pagais and Sipora indicates that the corals died as a result of sudden uplift around 1833. Numerous other fossil microatolls rooted in the intertidal zone at locations throughout the islands also died in about 1833. The coincidence of this widespread 19th century emergence event with an historically recorded earthquake in 1833, suggests that coseismic uplift in the earthquake caused the emergence.

The stratigraphy of all the slabbed corals is consistent with preseismic submergence occurring at all sites on North and South Pagai. Average rates of submergence over the 40 to 50 years of the preseismic period were about 5 to 10 mm/yr in North Pagai and Sipora. Rates were lowest in southern South Pagai - 5 mm/yr at sites P96-J and P96-K. Other, unslabbed corals from southern South Pagai had more subdued

raised rims than corals farther north, supporting the contention that the south was submerging more slowly than the north prior to 1833.

The HLS history of southern Sipora, documented by slab Si94-A-6, indicates submergence at very low or negligible rates in the pre-1833 period. This preseismic period was also the postseismic period following a 70-cm emergence in 1810. The response to that emergence probably affected the nature of the preseismic displacement history at the site.

There is some indication that submergence rates increased in the last two decades prior to the emergence event. Records from all sites are consistent with an increase in that time of as much as 20 to 50% over the average rates for the whole period. On the other hand, the increase, if any, is not great, and argues against a substantial change in the nature of subduction and strain accumulation just prior to the earthquake. Savage and Thatcher (1992) found evidence in Japan that the immediate preseismic deformation rate outpaced the average interseismic rate estimated from the modern post-seismic record. However, since they have data from only the second half of one earthquake cycle and the first half of another rather than a complete cycle, they argue that there may be differences in average interseismic deformation rate between earthquake cycles rather than differences between the interseismic and preseismic rates within an earthquake cycle. Obtaining the earlier interseismic record before the 1833 event could clarify whether the increase in rate just before the event is unique to the preseismic period, or if fluctuations in rate of this magnitude occur throughout the interseismic period.

1833 coseismic uplift

Slabbed corals provide minimum estimates of the magnitude of coseismic emergence. All of the living portions of the corals emerged fully in the event, so there is no HLS record of the full emergence in any coral. The minimum estimates of uplift are

Figure 4.24. Map of sites with corals that died in or near 1833. The dates of death of the emerged microatolls, both uncorrected (italic) and corrected (plain), are shown along with their locations. Sites with corals that may have died in 1833 but whose age uncertainties are very high are shown with dots but the dates are omitted. The geographical distribution of these events suggests that at least the whole of the Pagais and Sipora experienced substantial uplift.

Pagai and Sipora Islands
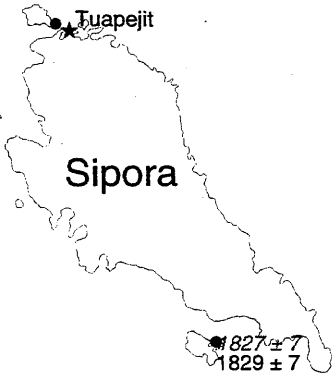
- Sites with corals that may have died in 1833 earthquake

U-Th dates of emerged microatolls:

1827 ± 7 italic - uncorrected dates
1829 ± 7 plain text - corrected for initial thorium contamination

Tuapejit

Sipora

1827 ± 7
1829 ± 7

10 km

N

North Pagai

1820 ± 11   *1832 ± 5*
1824 ± 12   1841 ± 11

1814 ± 3   *1834 ±6*
1829 ± 18   1837 ± 7

Sikakap

South Pagai

1766 ± 7
1807 ± 30

1750 ± 5
1831 ± 55

1830 ± 3   *1821 ± 6*
1831 ± 3   1827 ± 10

1818 ± 6
1824 ± 9

1815 ± 3
1830 ± 18

1794 ± 5
1835 ± 47

1811 ± 12
1818 ± 15

1824 ± 3
1836 ± 14

1835 ± 8
1836 ± 9

1839 ± 10
1842 ± 11

1836 ± 4
1839 ± 6

1830 ± 4
1834 ± 6

1829 ± 4
1834 ± 7

1830 ± 8
1838 ± 12

1825 ± 4
1834 ± 11

1835 ± 15
1839 ± 16

1860 ± 32
1866 ± 33
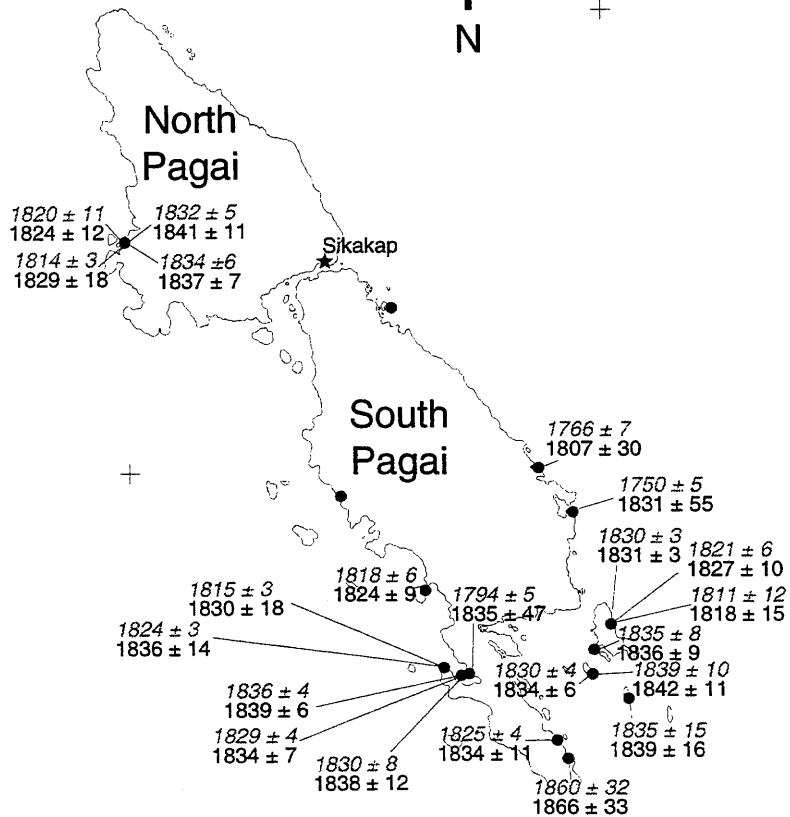
Sanding

the elevation differences between the top and bottom of the living growth band at the time of emergence. The highest minimum estimate obtained was 29 cm. However, the fact that all sampled 1833 corals, some over a meter tall, emerged fully during that event suggests that the true magnitude of coseismic uplift was greater than 29 cm and closer to a meter or more.

The HLS records from seven 1833-vintage microatolls appeared in Figure 4.9. I combined these records with the HLS records from living corals (Chapter 2) to provide a better estimate of the coseismic uplift. By plotting both together, I obtain a partial record of the vertical displacements recorded by the corals from 1833 to the present, a part of the sawtooth curve envisioned in Figure 4.2 (Figure 4.25). The record is still incomplete - the postseismic and early interseismic periods have not been documented in any corals. However, if one assumes that the modern submergence rate has been constant since the earthquake and projects it back in time to the event, one can estimate the coseismic step in 1833.

I collected both modern and 1833 slabs at only two sites, P96-J and P96-K, and they are, unfortunately, small slabs. The two sites are from neighboring islands in the southeast South Pagai archipelago. Analysis of these slabs revealed that the sites were experiencing some of the lower rates of submergence in the outer arc islands for the modern period, about 4 mm/yr (Chapter 2). The preseismic 19th century submergence rates are similarly low (Table 4.2). Plotting the modern and 19th century records together illustrates the observed and projected rates of deformation in this area during an earthquake cycle (Figure 4.25a and b). The vertical relationship between the 19th-century and modern HLS records is defined by the measured elevation difference between the top of the 1833 corals and the modern HLS in live corals (Figure 4.14). Clearly any postseismic shifting of the 1833 corals would make these elevation relations incorrect. Indeed, at P96-K, I used the elevation difference between live HLS and the *other* 1833

corals, not the slabbed sample, since the slabbed coral was so much lower than the average that I suspected it was out of place. The estimated magnitudes of coseismic uplift at sites P96-J and P96-K are about 113 cm and 99 cm, respectively.

All the other sites with slabs have only either 1833 or living slabs, not both, so a direct comparison of the two is not possible. However, Figures 4.25c-f show the 1833 HLS curves from various sites with an estimated modern HLS curve based on the measured submergence rates from the sites nearby. In most cases I used 7±2 mm/yr; elsewhere, near sites with slightly higher modern rates, I used 7.5±2.5 mm/yr. Using these average interseismic submergence rates, I can estimate a coseismic step for 1833 at the other sites. These vary from about 160 to 190 cm in the Pagais. Since the uncertainty on the interseismic rates is about 2-2.5 mm/yr for the 164 years since the event, the uncertainties on the estimated coseismic steps are about ±30-40 cm.

The 1833 coseismic step estimated from the Si94-A-6 slab and a 7 mm/yr interseismic submergence rate is 89 ±34 cm. This is between 50% and 75% of the estimated slip at the other sites. However, this site underwent at least 70 cm of uplift only about 25 years earlier. If the earlier was caused by the same source, it would not be unreasonable that slip in 1833 was less pronounced here. Uplift in the two events combined is about 160 cm, similar to the estimated uplift at the other sites. On the other hand, site NP94-A/NP96-C experienced a prior uplift event of about 70 cm in the 1790's, yet estimated 1833 coseismic uplift there is also about 160 cm. If the source of the 1790's event were different, maybe slip on a backthrust, then perhaps slip on the interface in over the 1790-1833 interval did not vary greatly between North Pagai and Sipora.

The assumption of a constant rate of submergence since the event may be wrong. The outside lip on sample Si94-A-6 suggests that site experienced sea-level stability, or submergence at low rates, after the "1810" event, while tide gauge and leveling data from before and after earthquakes in Japan, Alaska and Jalisco suggest those areas experienced

Figure 4.25. Modern and 19th-century HLS curves for sites with slabbed corals that died in 1833. Sites P96-J (a) and P96-K (b) had both living and dead slabs, so records of both are shown. At the other sites (c-f), no live slabs were collected, so they are shown with a modern submergence rate averaged from live corals at sites nearby in the Pagais (Chapter 2). These estimated modern rates are extrapolated linearly back to 1833 to provide a simple estimate of the coseismic uplift in 1833 at each site. A viscoelastic response to the 1833 deformation could yield higher rates early in the post-1833 period. In that case, the linear extrapolations would underestimate the 1833 coseismic uplift.

b. P96-K
99 ± 16 cm

d. P96-F/P94-Z
169±33 cm

f. SI94-A-6
70 ± 2 cm
88±33 cm

a. P96-J
113 ± 16 cm

c. NP94-A/NP96-C
NP94-A-8
NP94-A-9
163 ±41 cm

e. P96-H-1
188±41 cm
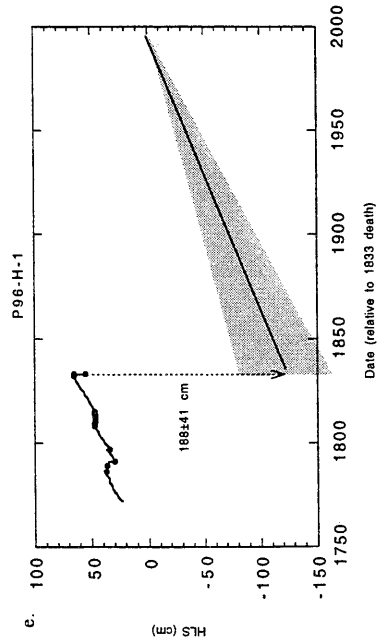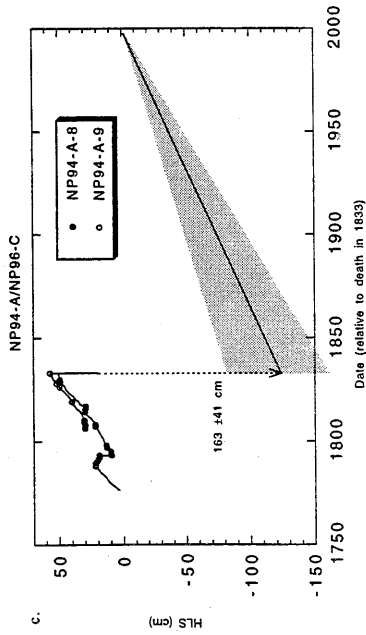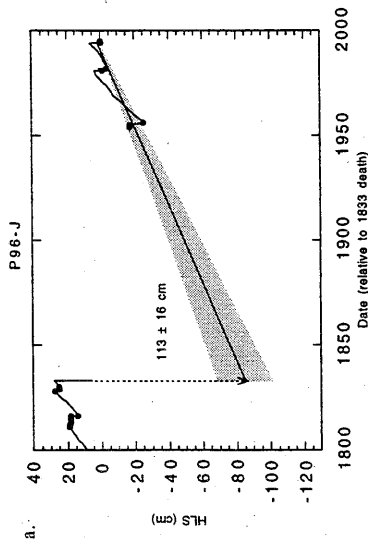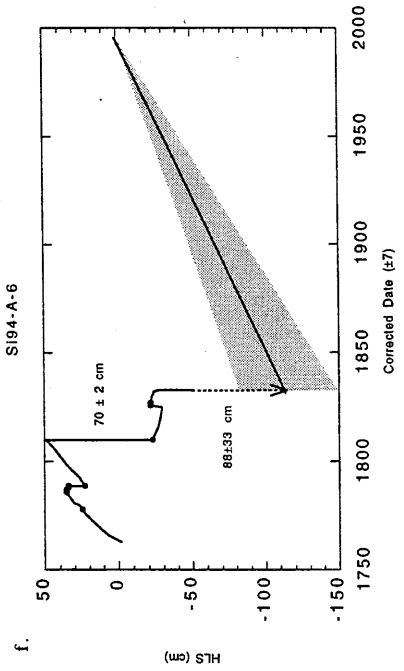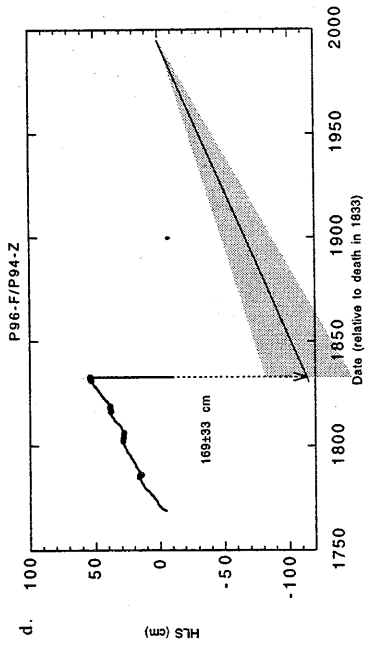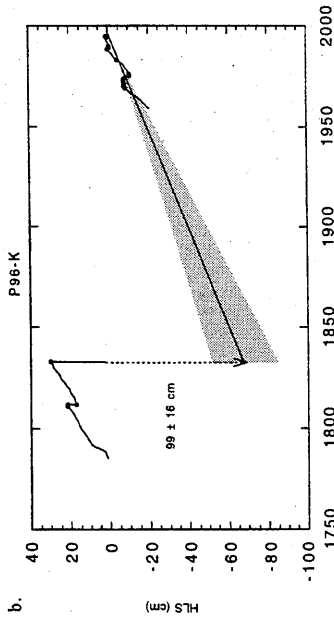
a transient postseismic displacement rate greatly exceeding the average interseismic rate (Thatcher and Rundle, 1984; Savage and Plafker, 1991; Savage and Thatcher, 1992; T. Melbourne, pers. comm., 1997). However, in the absence of any record for this period, a linear extrapolation of the modern interseismic rate will suffice for a first estimate. This estimate will be too high if a period of stability followed the 1833 event, before the establishment of the recent interseismic submergence rate. It would be too low if initial postseismic rates were higher than modern rates. Savage and Thatcher (1992) find the contribution of the transient postseismic deformation phase to be about one fourth of the total interseismic deformation through an earthquake cycle. If a similar postseismic phase occurred here too, the coseismic uplifts might be 30-40 cm higher than a linear extrapolation of the modern submergence rates yields. To fully constrain the paleoseismic and paleogeodetic history, obviously a coral record of the complete cycle is required.

Plotting all the pre- and coseismic records from the 19th century slabs together, excluding Si94-A-6, which clearly had a different history, assuming final emergence in 1833, and averaging their values, provides an estimate of the average deformational history of the Pagais over the last 200 years (Figure 4.26). It suggests an average coseismic emergence of about 160 cm.

4.3d. Earlier paleoseismic records

In addition to the geographically widespread emergence in 1833, several sites also had corals that died in earlier emergence events, shortly before 1833. Corals at site Si94-A in southern Sipora revealed the occurrence of sudden emergence of at least 70 cm in about 1810. It is likely that this represented an earlier coseismic event, possibly smaller than 1833.

There is no evidence for an 1810 event elsewhere in the islands, but corals from site NP94-A on North Pagai suggested the occurrence of an emergence event in the early

1790's. The estimated magnitude of this emergence event is 40 to 70 cm. There is no unambiguous evidence of this event having occurred at other sites, although emerged corals at sites along the east coast of South Pagai have similar ages . An emergence in 1789 was recorded in Si94-A-6, but it was only 10 cm. If this was the same event as the 1790's event at NP94-A, the magnitude of the emergence decreased from 40-70 cm to about 10 cm between the two sites.

Newcomb and McCann's (1987) catalogue of historical earthquakes includes an earthquake in 1797, probably near the Pagais. This event generated tsunamis in the Batu Islands and on the west coast of Sumatra just north of Padang, across from Sipora (Figure 4.1). It may be the 1790's event recorded at NP94-A. However, the stratigraphic analysis of NP94-A-8 indicates that there are probably more than 36 annual growth bands between the 1790's HLS and the outer, 1833, edge. Therefore, the event at NP94-A-8 is likely not the historically recorded event. That, in turn, means that the 1797 earthquake may not have caused a significant emergence in the Pagai and Sipora Islands. There is no evidence of a 1797 emergence in slab Si94-A-6, which was growing unimpeded by HLS in that year. Conversely, the 70-cm emergence event that is well-documented in Si94-A-6 does not appear in the historical record.

The 16th and 17th century dates of corals from sites throughout the Mentawais suggest the occurrence of multiple emergence events in that period. The youngest coral from this period died in 1739 ± 10 at site NP96-B. One coral from site P96-L clearly emerged in the late 17th century. The age constraints on both these death dates are tight, and no other well-constrained ages correlate with them. The younger coral may have died from a cause other than emergence or it may represent a paleoseismic event. The proximity and morphological similarity of a microatoll 2 meters from the P96-L coral, suggest both corals died at once. Thus, it is likely an emergence event was responsible for both their deaths and affected at least that whole site.

379

Figure 4.26. HLS curve for the Pagais from pre-1833 to the present, averaged from the HLS curves from each of the six slabs in Figure 4.25. A linear extrapolation of the modern interseismic submergence rate back to 1833 suggests an average coseismic uplift of 161 cm for the Pagais.

Average HLS history for Pagai Islands
1833 and modern
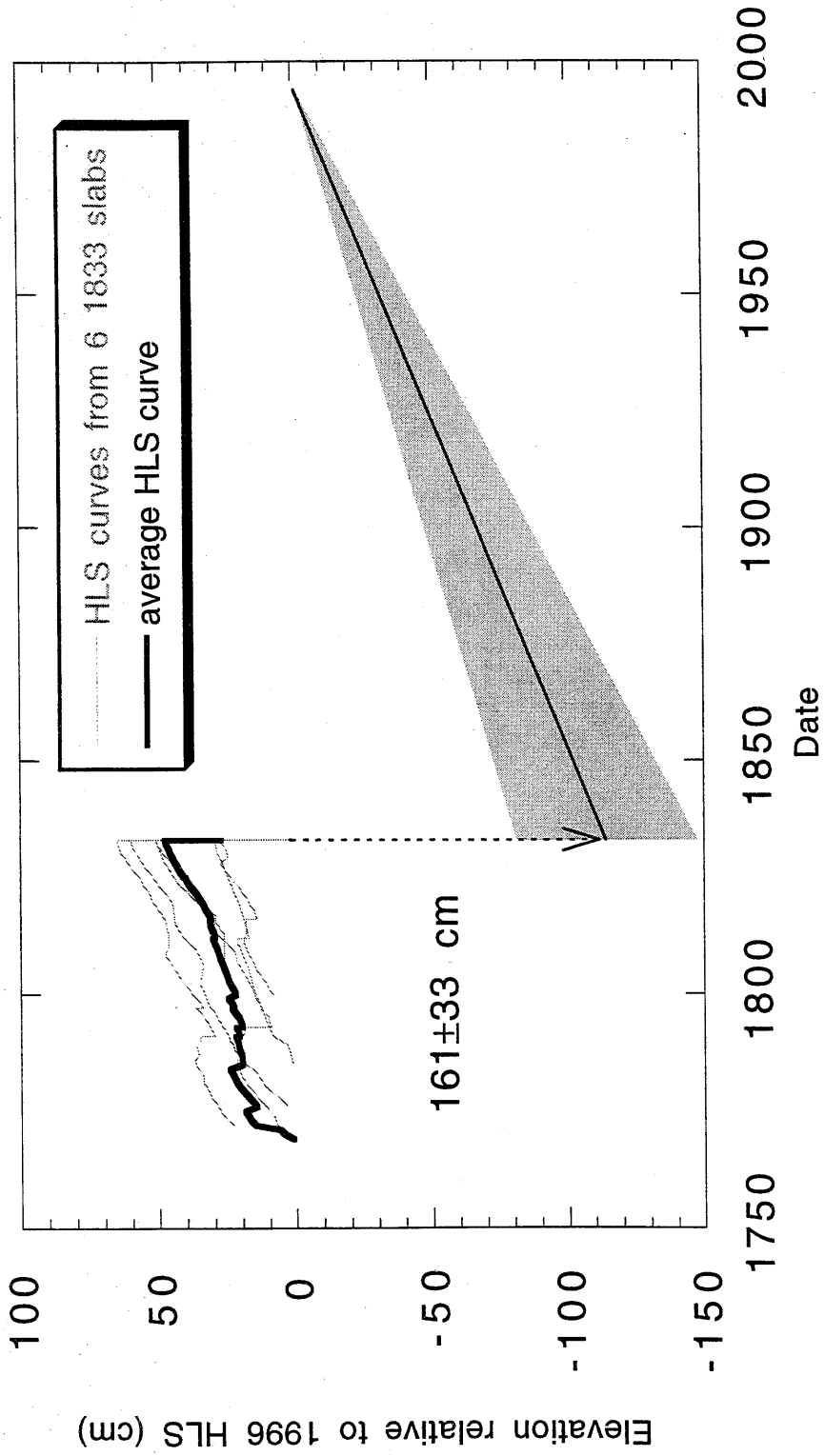
There is ample evidence for a substantial emergence event in the early 1600's. The date is well-constrained, although those constraints depend on the assumption that the non-microatoll P96-E-3 was the same age as the two other P96-E microatolls that record a large emergence. Although the ages of other late 15th to early 16th century corals are not well-constrained, there are several corals from various sites that could be contemporaries of the P96-E corals. The sites that have corals that might have died in a 1608 emergence event appear in Figure 4.27. They span the length and breadth of South Pagai and include the east side of North Pagai. I collected no corals of this age in Sipora, but sampling was sparse there. If all the early 17th-century corals did emerge in a single event, their size and geographic distribution indicate the event may have been a large subduction zone earthquake similar to the 1833 event.

Finally, one coral at site NP96-B has a tightly-constrained date of death in 1533 ± 12. If this represents an emergence death, then it indicates that three distinct emergence events between the mid-18th and mid-16th centuries were recorded in corals at a single site. The size of the corals, which probably represent over a hundred years of growth each, suggests that the emergences should overlap; in other words, the younger corals should have recorded the HLS change associated with the emergence events that killed the older corals. Evidence for such earlier emergences is not evident in the gross morphology of the coral heads, but might appear if cross-sectional slabs were collected and analyzed.

4.3e. Composite HLS records through multiple earthquake cycles

I collected and analyzed only two slabs older than 1833, both from site P96-E and emergent in about 1608. If the 1608 event was a subduction zone event similar to the 1833 event, the HLS records from these two microatolls can, with the 1833 and modern corals, yield a partial HLS record that illuminates the nature of vertical displacements

over 400 years and at least 2 earthquake cycles. Linear extrapolations of modern and preseismic submergence rates provide a first, tentative estimate of the HLS record for South Pagai for this period (Figure 4.28a). This record is a composite of HLS records from the ca. 1608 slabs at site P96-E, the 1833 slab, P96-F-1, and modern submergence rates. Dates of death for corals from several locations in North and South Pagai suggested that the 1608 P96-E event may also have caused emergence at those sites, so this composite HLS record may approximately describe the 17th-century vertical displacements throughout North and South Pagai.

The composite record suggests that submergence at high rates, 8 to 12 mm/yr preceded coseismic uplift of almost 2 m. This was followed by interseismic submergence that almost, but not quite, recouped all the coseismic uplift before another uplift event of 170 cm occurred in 1833. Submergence has dominated since then. This record is incomplete, in spite of the slab histories. Coral dates suggest that other emergence events occurred in the periods between 1608 and 1833 and before 1608. These are not included. However, since they are not represented by many corals, they may have been limited in their geographic extent. If other events had occurred in the intervening periods, then presumably the estimated magnitude of coseismic emergence would have been divided between the events with each having a smaller coseismic step.

A longer composite record can be produced by including the record from the corals at P94-Z/P96-F that died in the mid- to late 14th century. Only elevation measurements of these corals are available since no slabs were collected, so this HLS record is more tenuous. The elevation difference between the tops of the two apparently coeval 14th century corals is about 54 ± 9 cm. However, since the lower coral was tilted, it may have been out of place. Nevertheless, including these corals extends the vertical deformation record back to the 14th century (Figure 4.28b). The estimated coseismic step from the 14th century event is about 290 cm if the higher elevation is used and the coral

Figure 4.27. Map of sites containing corals that might have died in an early 17th-century emergence event.

Pagai/Sipora Islands
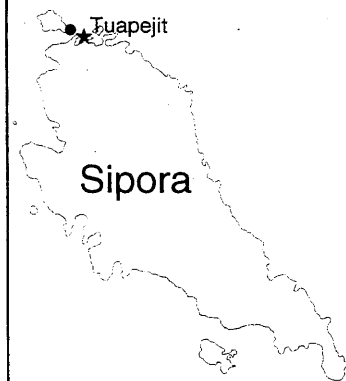
●   Sites with corals that may
have died in 16th-17th century earthquakes

U-Th dates of emerged microatolls:
1517 ± 5   italic - uncorrected dates
1572 ± 65   plain text - corrected for initial
thorium contamination

Tuapejit

Sipora

10 km

↑
N

North
Pagai

1560 ± 6
1581 ± 26

1505 ± 27
1586 ± 991

Sikakap

South
Pagai

1517 ± 5
1572 ± 65

1606 ± 3
1608 ± 4

1532 ± 5
1608 ± 89

1391 ± 4
1595 ± 238

1603 ± 6
1656 ± 63
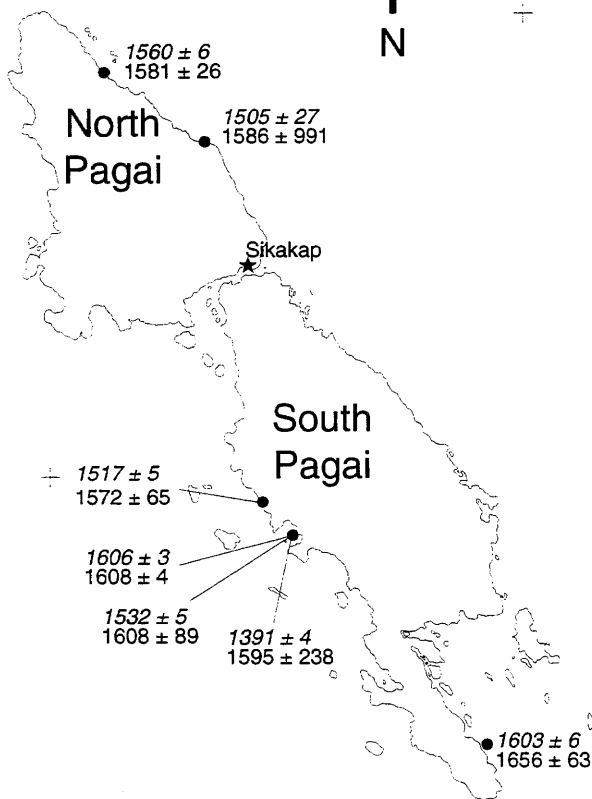
Sanding

Figure 4.28. Two speculative HLS elevation histories from corals on South Pagai Island.

a. A 400-year history based upon HLS records from slabs from corals that died in sudden emergence events in 1833 and 1608, and from living corals. The preseismic submergence rate in the 16th century is slightly higher than that in the 19th century or than the present rate. The estimated coseismic steps for the a833 and 1608 events are 175 and 181 cm.

b. A 600-yr record, which includes measurements of relative elevation of 14th century corals at site P96-F (P94-Z).

Western South Pagai Late Holocene HLS history based on data from P96-E and P96-F

a.
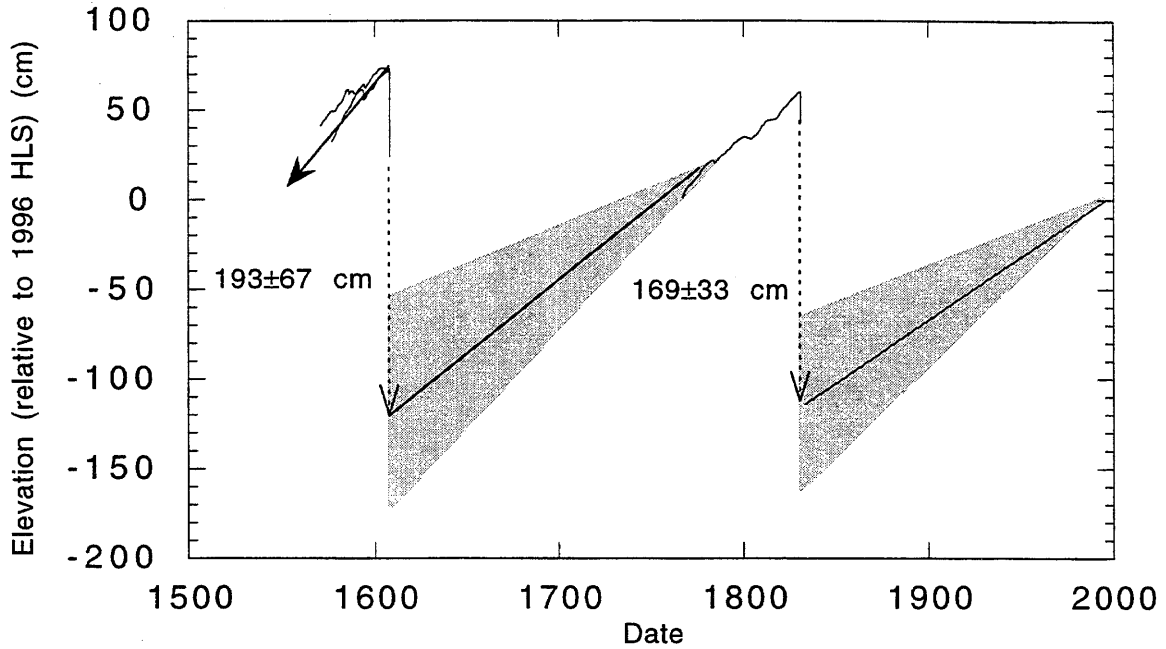
b.
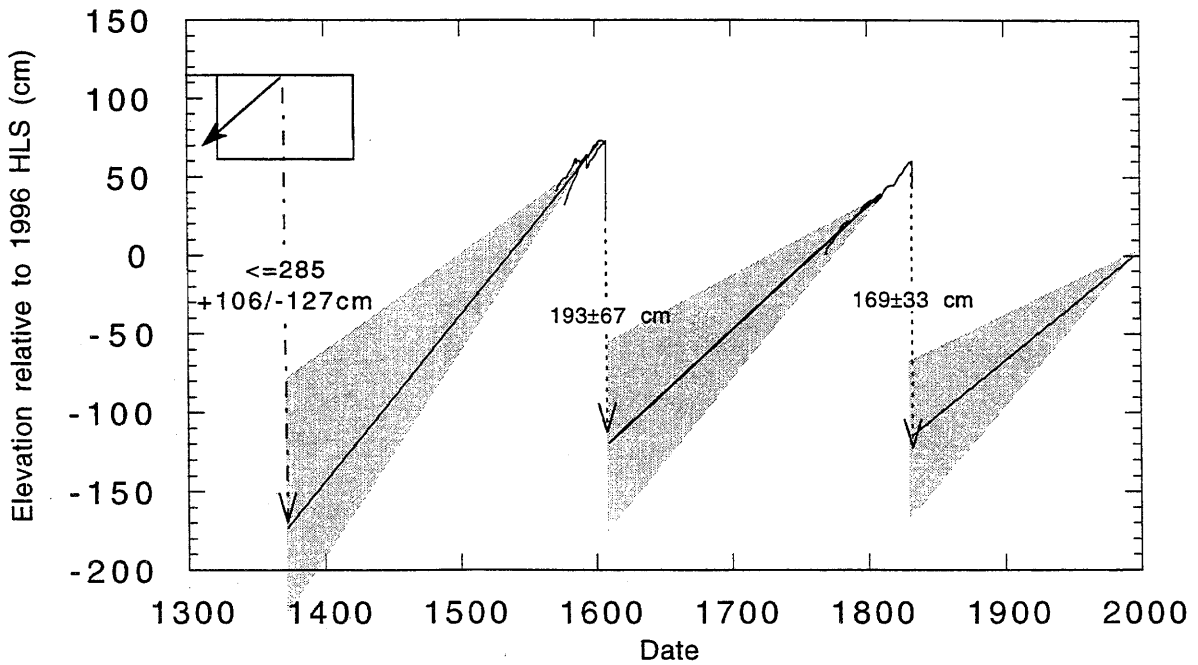
emerged in 1370. The uncertainty on this estimate is high. The elevations are poorly constrained. The uncertainty on the age of death is about ±50 years; the estimated coseismic step will increase or decrease commensurately if the age of death is earlier or later than 1370. Finally, the pre-1608 submergence rate used to extrapolate back through the interseismic period comes from the last twenty years of growth in the P96-E microatolls. The 1833 corals suggested that preseismic submergence rates in the two decades prior to final emergence might be higher than the longer timescale interseismic rates. This appears to be true also in Japan, where displacement rates prior to the 1946 Nankaido earthquake were greater than recent interseismic rates (Thatcher, 1984; Thatcher and Rundle, 1984). The 290 cm estimate, then, is probably an upper bound on the coseismic emergence in the 14th century event.

4.3f. Recurrence intervals

It has been 164 years since the great 1833 earthquake, which was accompanied by uplift throughout the Pagais and Sipora. The events prior to that earthquake in Sipora and North Pagai were 25-40 years earlier but more geographically limited than the 1833 event. Corals from sites around North and South Pagai indicate the possibility of emergence occurring across both these islands in the early 17th century. Other events after that occurred but over a more limited geographic area. The record from South Pagai suggests large uplift events occurred also in about 1370. The extent of that event is unknown, but it may have produced well over a meter of uplift, and thus could have had a wide effect. The 1833, 1608 and 1370 events yield an average recurrence interval of about 230 years. Sporadic representation of still older events suggests either that the interval between events was longer in the past or that the events have simply not yet appeared in the collected samples. The former may be true; the latter almost certainly is. The great bulk of sampled corals died in the 19th century. Representation of earlier

generations decreases with age. This is probably not because fewer corals died then but rather because fewer have been preserved. Thus, recurrence intervals based on older generations of coral may *appear* longer than those based on ones that are more recent even if recurrence has stayed the same over time; the more recent events probably yield a more accurate estimate.

Given the 230-yr recurrence interval suggested by recently dead South Pagai corals, one might expect another large event to occur on the Sumatran subduction zone within the next 50-100 years. On the other hand, the records at North Pagai and Sipora make it clear that significant events can occur within much shorter time frames than 230 years, so a large (>50 cm uplift) event is conceivable at any time.

4.3g. Coseismic slip estimates

The upper limit to the average slip rate across the subduction interface is the plate convergence rate of 67 ± 7 mm/yr (Tregoning et al., 1994). Over an average 230 year interval, this rate yields about 14 to 17 m of accumulated slip, if the subduction interface is fully locked throughout the interseismic period. A more appropriate estimate of slip per event would use an average slip rate lower than the 67 mm/yr plate rate, since the Great Sumatran Fault, 250 km inland from the trench, is carrying 10 to 30 mm/yr of the boundary-parallel component of slip (Sieh et al., 1991; Sieh and Natawidjaja, in prep.). Removing a 20 ± 10 mm/yr trench-parallel component yields a better estimate of the slip rate across the subduction interface, about 56 +13/-17 mm/yr. With this rate, slip accumulation on the interface during a 230-year interseismic period would be between 9 and 16 m.

Nine to 16 m of slip on a 12°-dipping plane has a vertical component of about 2.5 ± 0.7 m. Although the hanging wall of the subduction zone is not a rigid block, this provides a rough estimate of the average magnitude of coseismic vertical displacement

that might be observed at the surface. It is consistent with the vertical coseismic step estimated from coral HLS records from the Pagais and Sipora.

An elastic dislocation model of slip on a 12°-dipping plane, with 13 m of slip occurring on the interface from the trench to 170 km down-dip appears in Figure 4.29. The estimated coseismic vertical displacements at the sites that had 1833 slabs are also shown, projected onto an axis orthogonal to the trench. Although the displacements are only estimated from minimum measures of emergence recorded in the coral slabs, there appears to be a gradient across the islands, with higher uplifts occurring nearer the trench. The gradient is partly a function of the relative elevations of the 1833 coral and partly a function of the linearly extrapolated interseismic submergence rates. Sites P96-J and P96-K, farther from the trench than the other sites, had lower interseismic rates of submergence than the more trench-proximal sites. Therefore, the gradient in estimated coseismic uplift will reflect the gradient in interseismic submergence rates.

The down dip extent of the rupture plane in the model is similar to what was used to model interseismic locking in Chapter 2. The up-dip extent is unconstrained. I have assumed the interface failed up to the surface. However, it has been suggested that the upper 10 km of the subduction interface may not undergo brittle failure (Byrne et al., 1988; Marone and Scholz, 1988). The model implies the zone of maximum coseismic uplift is west of the Mentawais and the zone of maximum subsidence is east of them, over the fore-arc basin. Moving the up-dip terminus of the rupture zone down-dip, to 10-km depth, enhances the peak of uplift to the west of the islands, and may increase the gradient across the islands. It does not greatly affect the average size of the uplift in the islands. The 1833 uplifts estimated from the coral records in the Mentawai Islands are consistent with values of slip on the interface suggested by plate convergence rates, slip on the great Sumatran Fault, and a 230-year recurrence interval.

Although this study does not include fossil corals from the west coast of Sumatra, sub-mm/yr interseismic vertical displacement rates indicate that coseismic displacements there may also be small. As with the interseismic case, uniform slip on a gently dipping plane that fits the observed displacement rates at the islands produces measurable displacements at the coast. But, again, the dip of the slab under the coast dips more steeply than 12 degrees, possibly as much as 50 degrees. Modifying the model from slip on a uniformly dipping plane to a more representative progressively steepening interface could minimize the discrepancy between model and observation.

4.3h. Segmentation and clustering

Two issues of interest in earthquake studies are the temporal clustering of events and the role of fault segmentation in defining coseismic rupture. The corals of Western Sumatra hint at the presence of possible clustering and suggest some degree of segmentation.

The 1833 earthquake apparently resulted from rupture of the Sumatran subduction zone from the Batus to Enggano, a distance of about 550 km (Newcomb and McCann, 1987). Newcomb and McCann have argued that this represents a distinct segment, structurally defined by two deep sediment-filled troughs near Enggano and by the Investigator Fracture Zone and the Pini Arch near the Batu Islands. I have found evidence of its occurrence throughout the Pagais and Sipora, over an area of about 200 km, parallel to the trench, by 30 km, orthogonal to the trench.

While the maximum extent of the segment is probably represented by the inferred 1833 rupture zone, the corals indicate that that large segment may often be subdivided into smaller segments, with smaller events occurring between the large segment-wide events. Preliminary indications are that the 1810 Sipora event had its southern extent between Sipora and North Pagai, since it does not appear in coeval corals on North Pagai.

Figure 4.29. Elastic dislocation model of 1833 coseismic slip versus distance from the subduction zone trench. Model describes vertical displacements at the surface for 13 m of uniform slip from the trench to 175 km down-dip, on a 12°-dipping plane. Estimated coseismic uplift derived from coral microatoll data from the Pagai and Sipora Islands is also plotted. The grey dot represents an estimate of the magnitude of coseismic emergence at the west coast of Sumatra. I did not study fossil corals there. However, the lack of significant interseismic vertical displacements recorded in living corals at that location suggests that coseismic displacements may also have been small. The model fits the island points reasonably well, but fails to account for the proposed small vertical displacements at the coast.

Vertical coseismic displacement (m) vs. Distance from the trench (km)
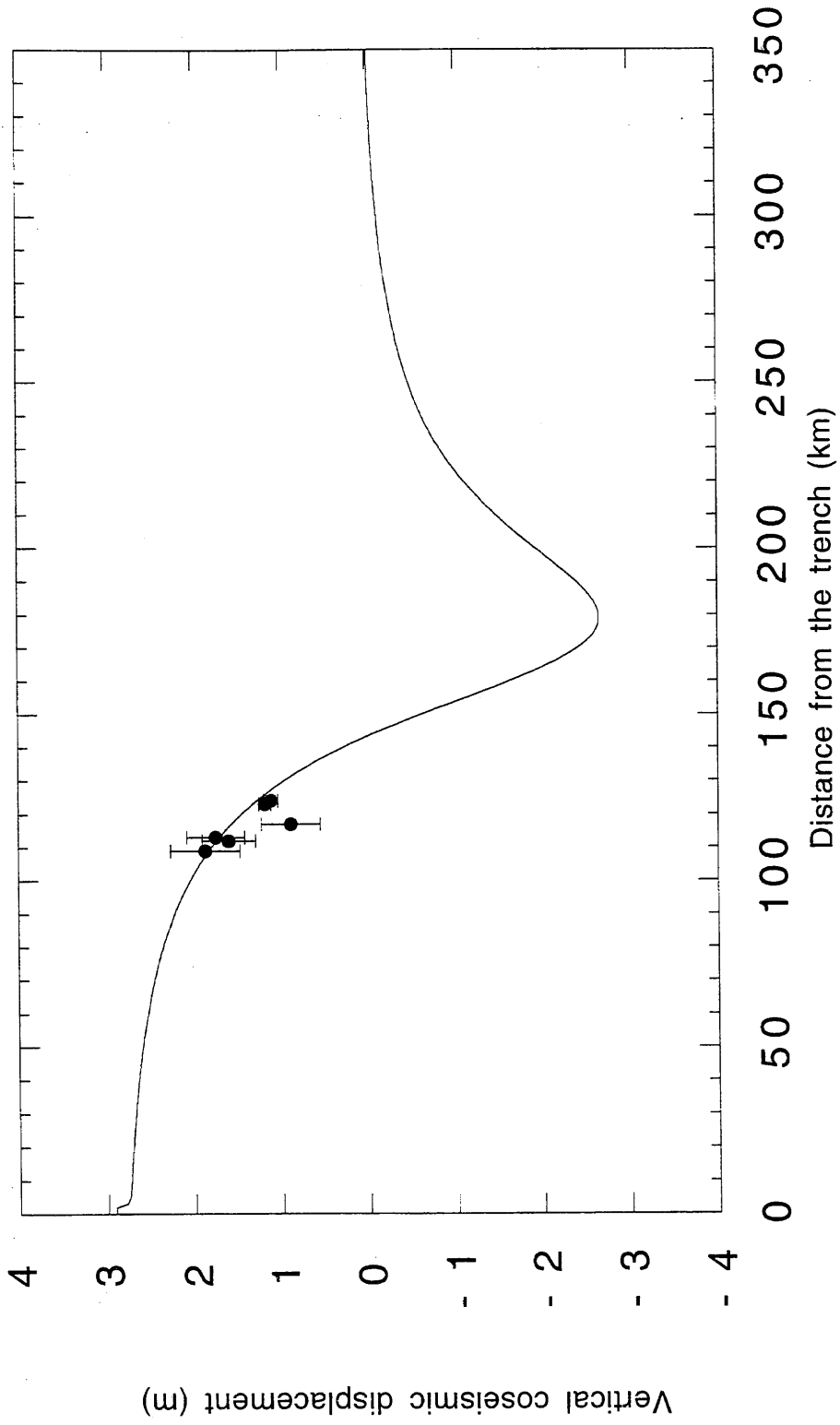
The 1790's event may have been limited to North Pagai. It may have affected southern Sipora and northern South Pagai slightly since the Si94-A-6 slab records an emergence of about 10 cm in 1789, and two northern South Pagai corals had death dates in the late 17th century. The Sipora emergence, much smaller than the estimated 70 cm emergence in southwestern North Pagai, may reflect the tapering-off of slip to the north. The geographic extent of earlier events is not well-established. Several corals throughout North and South Pagai may reflect a 1608 event, although uncertainties on many of those dates are high.

The issue of clustering in time can be only partially addressed too because the record still incomplete. Preliminary results suggest that the average recurrence interval between events affecting the whole plate segment is about 230 years. The late-18th-early-19th century events in North Pagai and Sipora occurred in rapid succession, with the smaller event preceding the larger event. There is some evidence from North Pagai (NP94-B) and South Pagai (P96-L and P96-M) of events in the 16th century, slightly before the 1608 event that had at least 50 cm of uplift and probably more. It may be that small events on sub-segments tend to cluster before a large segment-wide event. On the other hand, there is also evidence of events 80 and more years after the 1608 event that may have affected parts of the region. The possibility of clustered events here, while hardly definitive, is consistent with observations elsewhere of smaller, geographically circumscribed events shortly preceding a large segment-wide event, or of multiple similarly sized events clustering together in rapid succession followed by long periods of relative quiescence (Thatcher, 1990; Ambraseys and Finkel, 1991; Grant and Sieh, 1994; Pandolfi et al., 1994).

4.3i. Long-term vertical motion and implications for subduction zone deformation

Estimated elevations of regional mean sea levels for the last 10,000 years and elevations of mid-Holocene, 5000-8000 yr old, microatolls indicate a 0.1-0.3 mm/yr long-term submergence rate. The estimated HLS history for South Pagai (Figure 4.28b) over 700 years comes from four generations of coral. Relative elevation data reveal that each generation of coral is slightly lower than the last, from about 100-130 cm above 1996 HLS in about 1370 to 73 cm in 1608 to 62 cm in 1833. If I extrapolate the modern interseismic curve to 2060 (about 230 years, the estimated recurrence interval, after the last great earthquake), it appears the HLS then will be at about 42 cm. This does not account for the possibility that the submergence rate may speed up in the immediate preseismic period (Savage and Thatcher, 1992). The four-generation record suggests, if 100 cm elevation for the 14th-century corals is used, an emergence rate of 0.8 mm/yr over the last 700 years. If the upper limit of the 14th-century elevation range, 134 cm above living HLS, is used, the rate could be as high as 1.3 mm/yr. This possible slight emergence in recent centuries differs from the proposed slight submergence that has occurred on a time scale of thousands of years. The rates in both cases are low, however.

The slow net rate of elevation change contrasts strongly with the modern interseismic submergence rates of 0.5 to 1.0 cm/yr. It appears that elastic strains are many times larger than permanent strains. If this is so, then, the deformation of the Sumatran subduction zone at the latitude of the Pagais is essentially elastic, with coseismic slip fully recovered in the interseismic period.

Late Holocene rates of permanent vertical deformation at many other subduction zones are greater than the rates observed here. In Japan, average uplift rates along the coast parallel to the trench have been about 1-5 mm/yr over the last 5-6,000 years (Ota, 1985; Yonekura and Ota, 1986; Ota, 1986). Marshall and Anderson (1995) Holocene estimate tectonic uplift rates in Costa Rica at between 1.4 and 4.5 mm/yr. Ota and Berryman (1991) find uplifted marine terraces in New Zealand that have risen at rates of

3-8 mm/yr over the past 6700 years, although this uplift is occurring on subsidiary structures parallel to the subduction zone. Evidence from Alaska is ambiguous. Uplifted terraces at Middleton Island suggest rates of uplift as high as 10 mm/yr (Plafker and Rubin, 1967; 1978). Farther from the trench, in the region of coseismic subsidence, Plafker (1969) suggests Holocene subsidence at rates of 2 mm/yr. However, Savage and Plafker (1991) argue that almost all of this apparent subsidence may be due to eustatic sea-level rise and glacial isostatic rebound, so that there may be almost no net vertical deformation. The reasons for the variability are not immediately evident. Ota (1986), studying Quaternary and Holocene uplift rates at subduction zones around the world argued that permanent deformation is occurring at high rates at most subduction zones, except for those of the Marianas type. The Sumatran subduction zone appears not to fit that pattern, as it is marked by a high convergence rate, a high degree of coupling, and is clearly not of the Marianas-type, yet has very low deformation rates in the Holocene.

Further characterization of the subduction zone is limited by the lack of a complete documented coseismic step and of a postseismic record. Determining the magnitude of the coseismic step will clarify whether all or most of the strain release here occurs coseismically, or whether some fraction of it is released through creep or aseismic slip during the interseismic period. The postseismic behavior of the hanging wall and its relationship to the rest of the interseismic deformation has great implications for how the subduction zone is structured and whether deformation can be viewed as purely elastic or if a viscoelastic asthenospheric relaxation response dominates through some portion of the earthquake cycle. In estimating the coseismic step, I have assumed that interseismic strain accumulation has been linear, in other words that the interseismic deformation is a perfectly elastic response to the coseismic slip on the fault plane. Observations of high post-seismic deformation rates in Alaska and Japan have led various workers to suspect that there is a component of deformation due to asthenospheric relaxation after the event

in addition to the elastic signal (Thatcher and Rundle, 1984; Savage and Plafker, 1991; Savage and Thatcher, 1992). These workers find evidence for a very short-term (time constant ~5 yrs) component caused by continued slip down-dip of the main coseismic rupture zone and/or a longer-term component resulting from asthenospheric flow in the decades following the slip event. Obtaining the coral record for the postseismic period could help determine whether such a transient high-submergence rate is present in Sumatra.

4.4 Conclusions

Dead, emerged coral microatolls from the Mentawai Islands west of Sumatra illuminate the history of coseismic and interseismic vertical deformation in the hanging wall of the Sumatran subduction zone. The measurements of relative elevation of different generations of microatoll and stratigraphic analysis of coral slabs suggest that the precision afforded by the fossil microatoll HLS record approximates that of living microatolls. Furthermore, it exceeds that of most paleoseismic records from subaerial sites. With the corals, I was able to distinguish probable coseismic emergence events occurring 20 to 40 years apart, and provide constraints on the magnitudes of vertical displacements both accompanying and preceding those events.

Distinguishing paleoseismic events with this degree of precision depends strongly on the ability of obtaining precise absolute ages for the coral. This is possible with U-Th geochronometry, although in the Pagais, a high degree of contamination of many samples rendered dates of coral death too imprecise to distinguish some events.

HLS records from the fossil microatolls document the occurrence of one great earthquake in about 1833 that affected the full length of the Pagais and Sipora. Slabs from two South Pagai corals that died in about 1608 reveal a large emergence event, with more than 85 cm of uplift, which was preceded by submergence at rates of about 9-10 mm/yr.

This may have affected at least North and South Pagai. In addition, there is evidence for paleoseismic events between and before these large events that may have had a more limited geographic extent. The partial emergence of some 1833 corals in the decades prior to their final emergence suggests the occurrence of smaller emergence events at a few sites on Sipora and North Pagai, and possibly South Pagai too, in around 1810 and 1790. The possible occurrence of smaller events occurring shortly before larger events may indicate that events in the Mentawais cluster in time as they appear to elsewhere. There are indications of possible late Holocene events in the 17th, 16th, 14th, 12th and 2nd centuries, and about 100 BC. Lastly, six microatolls from South Pagai and Sipora suggest the occurrence of several mid-Holocene coseismic emergence events.

Stratigraphic analysis of coral slabs from seven corals that died in the 1833 event indicate the Mentawais were submerging at rates of about 0.5-1.0 cm/yr prior to the earthquake. These rates are similar to those inferred from analysis of living corals in the same area (Chapter 2). The 1833 corals all emerged fully in the earthquake so their fossil skeletons provide only a minimum estimate of the amount of coseismic uplift. The minimum emergence determined from the slabs is 29 cm. 1833-aged microatolls taller than 120 cm were observed but not slabbed. They suggest the coseismic step was much greater than 29 cm.

By comparing elevations and submergence rates of fossil corals with those of living corals, I have produced a tentative partial record of sea-level fluctuations over time which is representative of vertical tectonic displacement, oceanographic/climatic sea level changes aside. Linear extrapolation of modern submergence rates back to 1833 yields estimates of coseismic uplift between 100 and 190 cm, with higher estimates for sites closer to the subduction zone trench. The estimated uplift for earlier events is of the same order or somewhat greater. These uplifts are consistent with coseismic slip of about 13 m on the subduction interface.

The late Holocene HLS record reveals that there has been little net elevation change, or very slight emergence, over the time represented. Examination of mid-Holocene microatolls suggests this stability has prevailed throughout most of the Holocene. If that is so, it appears that the Sumatran subduction zone behaves primarily elastically, with coseismic emergence recouping essentially all of the interseismic submergence.

Chapter 5

Summary and Conclusions

Previous studies have indicated that coral microatolls, whose upward growth is limited by low water levels, retain in their skeletons records of past changes in relative sea level (Scoffin and Stoddart, 1978; Stoddart and Scoffin, 1979; Taylor et al., 1980, 1987). The coral is constrained to grow below its highest level of survival (HLS), which is usually a few centimeters or tens of centimeters above lowest low tide. Former HLS levels are recorded in the coral as flat surfaces where normal hemispheric, upward growth was inhibited by exposure above water. Annual growth bands, readily recognizable in x-radiographs of vertical slabs cut through the microatolls, provide temporal control, providing a means to document changes in HLS on a yearly basis. The temporal record provided by annual bands is relative; it depends on at least one ring in the coral having a known age, from which all other ring ages are determined by counting. The absolute age of that ring can be determined if the coral is alive (the outermost growth band has an age of zero) or if it can be dated. U-Th geochronometry can provide the absolute ages of individual coral rings in dead microatolls. Such microatolls and their HLS records have been used to document changes in relative sea level from both oceanographic/climatic and tectonic causes (Woodroffe et al., 1990a,b; Taylor et al., 1981, 1987). They have also been used to document paleoseismic events in which microatolls emerged above HLS as a result of coseismic uplift (Edwards et al., 1987c, 1988; Taylor et al., 1987, 1990).

In this study, I examined living and dead coral microatolls from the outer arc islands and coast of Western Sumatra, which overlie the Sumatran subduction zone. The islands are about 100-130 km from the trench and the coast is about 215 km away. This area has been the site of several large subduction zone earthquakes that have been documented in the past 300 years, including a Mw 8.7 earthquake in 1833 (Newcomb and McCann, 1987). Deformation on the subduction interface is likely to produce large vertical displacements, both coseismically and interseismically, in the region of the outer

arc rise. Thus, I studied the corals to see if they recorded such displacements, both modern and premodern. The nature of the microatoll records, with internal records of relative sea-level change on annual time scales and the possibility of precise dating of fossil corals, suggested that they could act as very precise paleoseismic and paleogeodetic recorders in an environment like the outer arc rise of a major subduction zone. The results of this study have largely borne out that contention.

I studied living microatolls to examine the quality, sensitivity and precision of coral microatolls as natural tide gauges, and to determine the nature of modern vertical deformation of the hanging wall of the subduction zone as recorded in those corals. I studied fossil microatolls, which I dated with U-Th geochronomtery, to analyze the quality of microatolls as paleoseismic and paleogeodetic recorders, and to determine the nature of past vertical displacements and the history of past earthquakes.

As an instrument, microatolls are capable of providing records of relative sea level change with a precision of a few cm and a few years. Stratigraphic analysis of vertical slabs cut through living microatolls showed that the history of interactions with HLS was similar between different coral heads. Emergences of a few centimeters, that should have affected all the corals, were recorded in all at the same time, within a year or two. Smaller emergences, and short, non-emergent impingements on the coral by HLS were less regular but most corals recorded them within a few years. The corals also recorded submergence, although constraints on this were less precise. New post-submergence HLS was only recorded after the coral grew up to the new level whereas emergences were recorded right away. Uncertainties in HLS elevation measurements in live corals were generated by uncertainty in establishing horizontal, erosion of former HLS surfaces, and uncertainties in identification of annual growth bands. Uncertainties in age came primarily from errors in ring identification. Absolute elevations of modern HLS, measured in a series of surveys, were usually within 20 cm of each other.

In fossil corals, the uncertainties increased to some extent, as might be expected. There was little difference from the living corals in the precision of relative ages and internal HLS elevations. In other words, the interior of a fossil coral is much the same as a living coral, so the uncertainties in ring identification, establishment of horizontal, measurement of relative elevations of rings and HLS surfaces, and determination of ages relative to one ring were the same. However, absolute constraints were less tight. Uncertainties in elevation derive from the fact that fossil corals may move after death, settle into a sandy substrate, be transported laterally by waves, without recording the change in their skeleton. Therefore while elevation changes internal to the coral are as precise as those living corals, comparing elevations between different coral heads, especially coral heads of different ages, does involve a greater uncertainty since one does not know if the observed relative elevations between two corals are their original elevations. If the corals are the same age this can be estimated by comparing the observed variation with that of living corals, but between corals of different ages, this constraint does not apply.

The uncertainties in absolute age are generally greater in fossil than living corals because the ^{230}Th age is not as well-known as the age of living coral. In principle, corals a few hundred years old could have U-Th uncertainties of only 3 or 4 years, which are similar to the uncertainties from ring identification in live corals. In that case, absolute age precision in fossil corals would be similar to that in living corals. However, in Sumatra, many of the fossil corals were highly contaminated with excess thorium, which was incorporated into the coral skeleton from a source other than radioactive decay of the coral's uranium. The contamination generates falsely old ages and higher analytical uncertainties. I corrected the ages for initial thorium contamination, but the correction factor is poorly constrained and has a wide range of possible values. The correction produces more accurate ages but with much greater uncertainties. Thus, in Sumatra, for a

large proportion of the corals, ages were much less well-constrained in fossil than live corals. This generated uncertainties in the dating of paleoseismic events. The quality of the paleoseismic record derivable from microatolls is thus strongly dependent on how well the ^{230}Th age can be constrained. High degrees of contamination can produce large uncertainties in distinguishing different events documented by different generations of coral with similar ages.

The results of the coral analysis constrain the nature and magnitude of modern and premodern vertical displacement histories and a record of paleoseismic events in the region. Stratigraphic analysis of the living slabs indicated the outer-arc islands have been submerging at rates between 5 and 10 mm/yr over the last few decades, while the west coast of Sumatra has remained relatively stable. The stratigraphic results are borne out by the morphological signature of other living corals that were not slabbed. The displacement rates are consistent with a high degree of interseismic locking of the shallow subduction interface below the islands.

Most fossil microatolls sat about half a meter higher than their living counterparts. Stratigraphic and morphologic analysis of the corals indicated they had died as a result of sudden emergence. Emerged corals that had died in the early to mid-1800's were ubiquitous throughout the Pagai and Sipora Islands. The number of such corals, their geographically broad distribution, and the known occurrence of a giant earthquake in 1833 in this area implied that the sudden emergence was caused by coseismic uplift in that earthquake. Thus, the emerged microatolls successfully recorded a paleoseismic event.

Stratigraphic analysis of slabs from corals that died in 1833 showed that they had been submerging at rates between about 5 and 10 cm/yr in the decades before emergence, rates similar to the observed interseismic rates in the modern period. There is some evidence that the rate might have increased slightly in the last two decades preseismic.

The magnitude of the coseismic emergence was not recorded. Slabs provided a minimum estimate of 29 cm of emergence, but the presence of numerous suddenly-emerged 1833 corals taller than 1 m suggested the emergence might be greater than that. I derived an estimate of the coseismic emergence by linearly extrapolating modern submergence rates back to 1833. This analysis suggested coseismic uplifts of 1 to 2 m in the islands, with smaller uplifts occurring in the south and farther from the trench.

Other, older corals also died in sudden emergence events that were probably paleoseismic events. A couple of events occurred just a few decades before the 1833 event, in the 1790's and 1810, and were documented as partial emergences in two 1833 corals. Other events occurred throughout the Late Holocene. One event, which occurred in about 1608, may have produced emergence over a meter throughout the islands. There was also evidence of a large event in South Pagai in the late 14th century.

By combining the displacement records from three generations of fossil coral with living coral, I obtained a tentative record of vertical displacement history spanning 700 years and three earthquake cycles. The recurrence interval suggested by these paleoseismic events is about 230 years. Accumulation of down-dip strain on the subduction interface over that interval is about 13 ± 4 m. Total relief of that accumulated strain by coseismic slip of 13 m on the interface is likely to produce about 1 to 2 m of uplift on the outer arc islands, consistent with what was observed. This suggests that coupling is nearly complete over the interseismic cycle and most slip accumulated during the interseismic period is recovered coseismically. This is consistent with the lack of accumulated vertical deformation over time. Mid-Holocene emerged microatolls found only slightly above 19th century corals suggests that net displacement rates in the Holocene have been less than 1 mm/yr. Therefore, the majority of the late-Holocene short-term displacement signal represents the elastic accumulation and relief of strain, not the construction of geological structure.

This study of coral microatolls confirms the belief that they can be used as paleoseismic and paleogeodetic recorders over hundreds and thousands of years. The accuracy and precision afforded by these records can be very high, significantly higher than that at most subaerial paleoseismic sites. Both interseismic and coseismic displacements can be documented. Because the corals provide annual records, not net records, they can resolve changes in displacement rates over the interseismic period, not just provide average rates. The records show that, if ^{230}Th ages are well-constrained, one can distinguish paleoseismic events that occurred only 30 or 40 years apart. Less well-constrained ages of course limit this resolution. However, it is safe to say that coral microatolls provide a strong tool for paleoseismological and paleogeodetic studies at subduction boundaries wherever coral microatolls grow.

References

Ambraseys, N. N., and C. F. Finkel, Long-term seismicity of Istanbul and of the Marmara Sea region, *Terra Nova*, 3, [5], 527-539, 1991.

Andersson, P. S., G. J. Wasserburg, D. A. Papanastassiou, and J. Ingri, ^{238}U-^{234}U and ^{232}Th -^{230}Th in the Baltic Sea and in river water, *Earth and Planetary Science Letters*, 130, [1-4], 217-234, 1995.

Atwater, B. F., Evidence for great Holocene earthquakes along the outer coast of Washington state, *Science*, 236, 942-944, 1987.

Atwater, B. F., and D. K. Yamaguchi, Sudden, probably coseismic submergence of Holocene trees and grass in coastal Washington State, *Geology*, 19, [7], 706-709, 1991.

Bard, E., B. Hamelin, and R. G. Fairbanks, U-Th ages obtained by mass spectrometry in corals from Barbados: sea level during the past 130,000 years, *Nature*, 346, 456-458, 1990.

Barnes, D. J., J. M. Lough, and B. J. Tobin, Density measurements and the interpretation of X-radiographic images of slices of skeleton from the colonial hard coral Porites, *J. Exp. Mar. Biol. Ecol.*, 131, 45-60, 1989.

Barnett, T. P., An attempt to verify some theories of El Niño, *J. Phys. Oceanogr.*, 7, 633-647, 1977.

Barnett, T. P., Recent changes in sea level and their possible causes, *Climatic Change*, 5, 15-38, 1983.

Beaudoin, T., O. Bellier, and M. Sebrier, Segmentation et aléa sismique sur la Grande Faille de Sumatra (Indonesie), *C.R. Acad. Sci. Paris.*, 321, [IIa], 409-416, 1995.

Beaudry, D., and G. F. Moore, Seismic stratigraphy and Cenozoic evolution of West Sumatra fore-arc basin, *Amer. Assoc. Petrol. Geol. Bull.*, 69, [5], 742-759, 1985.

Bellier, O., M. Sebrier, and S. Pramumijoyo, La grande faille de Sumatra: geometrie, cinematique et quantité de déplacement mises en évidence par l'imagerie satellitaire, *C.R. Acad. Sci. Paris*, 312, [II], 1219-1226, 1991.

Bloom, A. L., W. S. Broecker, J. M. A. Chappell, R. K. Matthews, and K. J. Mesolella, Quaternary sea-level fluctuations on a tectonic coast: new ^{230}Th /^{234}U dates from the Huon Peninsula, New Guinea, *Quaternary Research*, 4, 185-105, 1974.

Bryant, Last interglacial and Holocene trends in sea-level maxima around Australia: implications for modern rates, *Marine Geology*, 108, [2], 209-217, 1992.

Buddemeier, R. W., J. E. Maragos, and D. W. Knutson, Radiographic studies of reef coral exoskeletons: rates and patterns of coral growth, *J. Exp. Mar. Biol. Ecol.*, 14, 179-200, 1974.

Budhitrisna, T., and S. Andi Mangga, *Geology of the Pagai and Sipora Quadrangle*, Sumatra, 1 edition, Pusat Penelitian dan Pengembangan Geologi (Geological Research and Development Centre), Bandung, 1-21, 1990.

Buskirk, R., F. W. Taylor, W. P. O'Brien, P. Maillet, and L. Gilpin, Seasonal growth patterns and mortality of corals in the New Hebrides (Vanuatu), in *Fourth International Coral Reef Symposium*, vol. 2, pp. 197-200, Marine Sciences Center, Univ. Philippines, Quezon City, Philippines, 1981.

Byrne, D., D. M. Davis, and L. R. Sykes, Loci and maximum size of thrust earthquakes and the mechanics of the shallow region of subduction zones, *Tectonics*, 833-857, 1988.

Chappell, J., Geology of coral terraces, Huon Peninsula, New Guinea: a study of Quaternary tectonic movements and sea level changes, *Geol. Soc. Amer. Bull.*, 85, 553-570, 1974.

Chappell, J., and H. Polach, Post-glacial sea-level rise from a coral record at Huon peninsula, Papua New Guinea, *Nature*, 349, 147-149, 1991.

Chappell, J., A. Omura, T. Esat, M. Mcculloch, J. Pandolfi, Y. Ota, and B. Pillans, Reconciliation of late Quaternary sea level derived from coral terraces at Huon Peninsula with deep sea oxygen isotope records, *Earth and Planetary Science Letters*, 141, 227-236, 1996.

Chen, J. H., and G. J. Wasserburg, Isotopic determination of uranium in picomole and subpicomole quantities, *Anal. Chem.*, 53, 2060-2067, 1981.

Chen, J. H., G. J. Wasserburg, K. L. Von Damm, and J. M. Edmond, Pb, U, and Th in hot springs on the East Pacific Rise at 21°N and Guaymas basin, Gulf of California, *EOS, Trans. Amer. Geophys. Union*, 64, 724, 1983.

Chen, J. H., and G. J. Wasserburg, $^{234}U/^{238}U$ and lead isotopic compositions on the East Pacific Rise at 21°N, *Geol. Soc. Amer. Abstr. Prog.*, 16, 469, 1984.

Chen, J. H., R. L. Edwards, and G. J. Wasserburg, ^{238}U, ^{234}U and ^{232}Th in seawater, *Earth and Planetary Science Letters*, 80, 241-251, 1986.

Chen, J. H., H. A. Curran, B. White, and G. J. Wasserburg, Precise chronology of the last interglacial period: ^{234}U -^{230}Th data from fossil coral reefs in the Bahamas, *Geol. Soc. Amer. Bulletin*, 103, 82-97, 1991.

Clark, M. M., A. Grantz, and M. Rubin, Holocene activity of the Coyote Creek fault as recorded in sediments of Lake Cahuilla, *U.S. Geol. Surv. Prof. Paper*, 787, 112-130, 1972.

Clark, J. A., W. E. Farrell, and W. R. Peltier, Global changes in postglacial sea level: a numerical calculation, *Quaternary Research*, 9, 265-287, 1978.

Clarke, A. J., and X. Liu, Observations and dynamics of semiannual and annual sea levels near the eastern equatorial Indian Ocean boundary, J. Phys. Ocean., 23, 386-399, 1993.

Cobb, J.C., J.W. Norris, and D.R. Chestnut, Jr., Glacio-eustatic sea-level controls on the burial and preservation of modern coastal peat deposits, *GSA Abstracts with Programs*, 21 [6], A26, 1989.

Collins, L. B., Z. R. Zhu, K.-H. Wyrwoll, B. G. Hatcher, P. E. Playford, A. Eisenhauer, J. H. Chen, G. J. Wasserburg, and G. Bonani, Holocene growth history of a reef complex on a cool-water carbonate margin: Easter Group of the Houtman Abrolhos, Eastern Indian Ocean, *Marine Geology*, 115, [1-2], 29-46, 1993a.

Collins, L. B., Z. R. Zhu, K.-H. Wyrwoll, B. G. Hatcher, P. E. Playford, J. H. Chen, A. Eisenhauer, and G. J. Wasserburg, Late Quaternary evolution of coral reefs on a cool-water carbonate margin: the Abrolhos Carbonate Platforms, southwest Australia, *Marine Geology*, 110, [3-4], 203-212, 1993b.

Daly, M. C., M. A. Cooper, I. Wilson, D. G. Smith, and B. G. D. Hooper, Cenozoic plate tectonics and basin evolution in Indonesia, *Marine and Petroleum Geology*, 8, [February], 2-21, 1991.

Darwin, C.R., *The structure and distribution of coral reefs*, Smith, Elder and Co., London, 214 pp., 1842.

De Bièvre, K.J. Lauer, Y. Le Duigan, H. Moret, G. Muschenborn, J. Spaepen, A. Spernol, R. Vaninbroukx, and V. Verdingh, The half-life of U-234, in *Proceedings International Conference on Chemical Nuclear Data, Measurements and Applications*, edited by M.L. Hurrell, pp. 221-225, Institute of Civil Engineers, London, 1971

Detourbet, C., O. Bellier, and M. Sebrier, The Toba volcanic caldera and the Great Sumatran Fault (Indonesia) analyzed by SPOT imagery, *Comptes Rendus de l' Academie des Sciences Seire II Mecanique Physique Chimie Sciences de la Terre et de l' Univers*, 316, [10], 1439-1445, 1993.

Diament, M., H. Harjono, K. Karta, C. Deplus, D. Dahrin, M. T. Zen Jr., M. Gerard, O. Lassal, A. Martin, and J. Malod, Mentawai fault zone off Sumatra: a new key to the geodynamics of western Indonesia, *Geology*, 20, [March], 259-262, 1992.

Edwards, R. L., J. H. Chen, and G. J. Wasserburg, ^{238}U-^{234}U -^{230}Th -^{232}Th systematics and the precise measurement of time over the past 500,000 years, *Earth and Planetary Science Letters*, 81, 175-192, 1987a.

Edwards, R. L., J. H. Chen, T.-L. Ku, and G. J. Wasserburg, Precise timing of the last interglacial period from mass spectrometric determination of thorium-230 in corals, *Science*, 236, 1547-1553, 1987b.

Edwards, R. L., F. W. Taylor, J. H. Chen, and G. J. Wasserburg, High precision thorium-230 dating of corals using thermal ionization mass spectrometry: applications to paleoseismology, *USGS Open File Report*, 1987c.

Edwards, R. L., F. W. Taylor, and G. J. Wasserburg, Dating earthquakes with high-precision thorium-230 ages of very young corals, *Earth and Planetary Science Letters*, 90, 371-381, 1988.

Edwards, R. L., *High Precision Thorium-230 Ages of Corals and the Timing of Sea Level Fluctuations in the Late Quaternary*, Ph.D. thesis, pp., California Institute of Technology, 1988.

Edwards, R. L., J. W. Beck, G. S. Burr, D. J. Donahue, J. M. A. Chappell, A. L. Bloom, E. R. M. Druffel, and F. W. Taylor, A large drop in atmospheric 14C/12C and reduced melting in the Younger Dryas, documented with ^{230}Th ages of corals, *Science*, 260, 962-968, 1993.

Eisenhauer, A., G. J. Wasserburg, J. H. Chen, G. Bonani, L. B. Collins, Z. R. Zhu, and K. H. Wyrwoll, Holocene sea-level determination relative to the Australian continent: U/Th (TIMS) and 14C(AMS) dating of coral cores from the Abrolhos Islands, *Earth and Planetary Science Letters*, 114, 529-547, 1993.

Fallon, S. , Casey, R. , Ciccateri, A. , Cabrera, A. , Chomicz, L., Zarwell, L., Hill, V., Gutierrez, A., Fijian past climate recorded in tree rings and coral banding, *Abstracts with Programs - Geological Society of America*, 25 (6), p. 331, 1993.

Faure, G., *Principles of Isotope Geology*, 1 edition, John Wiley & Sons, New York, 1-464, 1977.

Fauzi, R. McCaffrey, D. Wark, Sunaryo, and P. Y. Prih Harydi, Lateral variation in slab orientation beneath Toba Caldera, northern Sumatra, *Geophysical Research Letters*, 23, 443-446, 1996.

Fitch, T. J., Plate convergence, transcurrent faults, and internal deformation adjacent to Southeast Asia and the Western Pacific, *J. Geophys. Res.*, 77, [23], 4432-4460, 1972.

Gallup, C. D., R. L. Edwards, and R. G. Johnson, The timing of high sea levels over the past 200,000 years, *Science*, 263, [5148], 796-800, 1994.

Gallup, C., *High-precision uranium-series analyses of fossil corals and Nicaragua Rise sediments: The timing of high sea levels and the marine delta U-234 value during the past 200,000 years*, Ph.D. thesis, pp., University of Minnesota, 1997.

Grant, L. B., and K. Sieh, Paleoseismic evidence of clustered earthquakes on the San Andreas Fault in the Carrizo Plain, California, *J. Geophys. Res.*, 99, [B4], 6819-6841, 1994.

Hudson, J. H., Long-term bioerosion rates on a Florida reef: A new method, in *Third Int'ernational Coral Reef Symp.*, Miami, FL, 491-497, 1977.

Imamura, A. On the chronic and acute earth-tilting in the Kii peninsula, *Jpn. J. Astron. Geophys.*,7, 31-45, 1929.

Imamura, A. Land deformations associated with the recent Tokaido earthquake, *Proc. Japan Academy*, 21, 193-196, 1945.

Inouchi, N. and H. Sato, Vertical crustal deformation accompanied with the Tonankai earthquake of 1944, *Bull. Geogr. Surv. Inst., Tokyo*, 21, 10-18, 1975.

Ivanovich, M., and R. S. Harmon eds., *Uranium-series Disequilibrium: Applications to Earth, Marine, and Environmental Sciences*, 2 edition, Oxford University Press, Oxford, 1992.

Izart, A., B. M. Kemal, and J. A. Malod, Seismic stratigraphy and subsidence evolution of the northwest Sumatra fore-arc basin, *Marine Geology*, 122, 109-124, 1994.

Jaffey, A.H., K.F. Flynn, L.E. Glendenim, W.C. Bentley and A.M. Essling, Precision measurements of half-lives and specific activities of U-235 and U-238, *Phys. Rev. C*, 4, 1889-1906, 1971.

Jouannic, C., C.-T. Hoang, W. S. Hantoro, and R. M. Delinom, Uplift rate of coral reef terraces in the area of Kupang, West Timor: preliminary results, *Paleaogeography, Palaeoclimatology, Palaeoecology*, 68, 259-272, 1988.

Karig, D. E., S. Suparka, G. F. Moore, and P. E. Hehanussa, Structure and Cenozoic evolution of the Sunda Arc in the central Sumatra region, *Amer. Assoc. Petr. Geol. Bull.*, 1979.

Karig, D. E., M. B. Lawrence, G. F. Moore, and J. R. Curray, Structural framework of the fore-arc basin, NW Sumatra, *J. Geol. Soc.*, London, 137, 77-91, 1980.

Katili, J. A., and F. Hehuwat, On the occurrence of large transcurrent earthquakes in Sumatra, Indonesia, *Osaka University Journal of Geoscience*, 10, 5-17, 1967.

Kato, T. and K. Tsumura, Vertical land movement in Japan as deduced from tidal record (in Japanese), Bull. Earthquake Res. Inst. Tokyo Univ.; 54, 559-628, 1979.

Kaufman, A., and W. S. Broecker, Comparison of ^{230}Th and ^{14}C ages for carbonate materials from lakes Lahontan and Bonneville, *J. Geophys. Res.*, 70, 4039, 1965.

Kawabe, M., Mechanisms of interannual variations of equatorial sea level associated with El Niño, *J. Phys. Oceanogr.*, 24, 979-993, 1994.

Kawasumi, H. Crustal deformation in the Shikoku district as deduced from tidal gauge records, second report (in Japanese), *Shikoku-Chiho Sogo Kaihatsu Shingikai*, 30-36, 1956.

Kieckhefer, R. M., G. F. Moore, and F. J. Emmel, Crustal structure of the Sunda forearc region west of central Sumatra from gravity data, *J. Geophys. Res.*, 86, [B8], 7003-7012, 1981.

Knutson, D. W., R. W. Buddemeier, and S. V. Smith, Coral chronometers: Seasonal growth bands in reef corals, *Science*, 177, 270-272, 1972.

Koide, M., and E. D. Goldeberg, *Uranium-234/uranium-238 ratios in sea water, in Progress in Oceanography*, vol. 3, pp. 173-178, Pergamon Press, Oxford and New York, 1965.

Ku, T. L., and Z. C. Liang, The dating of impure carbonates with decay-series isotopes, *Nucl. Instr. Meth.*, 223, 563-571, 1984.

Lambeck, K., and M. Nakada, Late Pleistocene and Holocene sea-level change along the Australian coast, *Palaeogeograph., Palaeoclimatol., Palaeoecol.*, 89, 143-176, 1990.

Lambeck, K., Glacial rebound, sea-level change and mantle viscosity, *Q. Jl. R. astr. Soc.*, 31, 1-30, 1990.

Lough, J. M., and D. J. Barnes, Possible relationships between environmental variables and skeletal density in a coral colony from the central Great Barrier reef, *J. Exp. Mar. Biol. Ecol.*, 134, 221-241, 1990.

Lounsbury, M. and R.W. Durham, The alpha half-life of U-234, in *Proceedings International Conference on Chemical Nuclear Data, Measurements and Applications*, edited by M.L. Hurrell, pp. 215-219, Institute of Civil Engineers, London, 1971.

Malod, J.-A., M. K. Badrul, M.-O. Beslier, C. Deplus, M. Diament, K. Karta, A. Mauffret, P. Patriat, M. Pubellier, H. Regnault, P. Aritonang, and M. T. J. Zen, Deformations du bassin d'avant-arc au Nord-Ouest de Sumatra: une reponse à la subduction oblique, *C.R. Acad. Sci. Paris*, 316, [II], 791-797, 1993.

Marone, C., and C. H. Scholz, The depth of seismic faulting and the upper transition from stable to unstable slip regimes, *Geophys. Res. Lett.*, 621-624, 1988.

Marshall, J.S. and R.S. Anderson, Quaternary uplift and seismic cycle deformation, Peninsula de Nicoya, Costa Rica, *Geol. Soc. Amer. Bulletin*, 107 [4], 463-473, 1995.

McCaffrey, R., Slip vectors and stretching of the Sumatran fore arc, *Geology*, 19, 881-884, 1991.

McCaffrey, R., Oblique plate convergence, slip vectors, and forearc deformation, *J. Geophys. Res.*, 97, [B6], 8905-8915, 1992.

Meadows, J.W., R.J. Armani, E.L. Callis, and A.M. Essling, Half-life of thorium-230, *Phys. Rev. C*, 22, 750-756, 1980.

Melbourne, T., I. Carmichael, C. DeMets, K. Hudnut, O. Sanchez, J. Stock, G. Suarez, and F. Webb, The geodetic signature of the M8.0 Oct. 9, 1995, Jalisco subduction earthquake, *Geophys. Res. Lett.*, 24, [6], 715-718, 1997.

Mitrovica, J. X., and W. R. Peltier, On postglacial geoid subsidence over the equatorial oceans, *J. Geophys. Res.*, 96, [B12], 20,053-20,071, 1991.

Miyake, Y., Y. Sugimura, and T. Uchida, Ratio U234/U238 and the uranium concentration in sea water in the western North Pacific, *J. Geophys. Res.*, 71, 3083-3087, 1966.

Moore, G. F., and D. E. Karig, Structural geology of Nias Island, Indonesia: Implications for subduction zone tectonics, *Amer. J. of Science*, 280, [March], 193-223, 1980.

Moore, G. F., H. G. Billman, P. E. Hehanussa, and D. E. Karig, Sedimentology and Paleobathymetry of Neogene Trench-Slope Deposits, Nias Island, Indonesia, *Journal of Geology*, 88, 161-180, 1980.

Moore, G. F., J. R. Curray, and F. J. Emmel, *Sedimentation in the Sunda Trench and foreac region, in Trench-Forearc Geology*, vol. Publication No. 10, edited by J. K. Leggett, Geological Society of London Spec., 1982.

Moran, S. B., J. A. Hoff, K. O. Buesseler, and R. L. Edwards, High precision [230]Th and [232]Th in the Norwegian Sea and Denmark Strait by thermal ionization mass spectrometry, *Geophys. Res. Lett.*, 22, 2589-2592, 1995.

Moran, S. B., M. A. Charette, J. A. Hoff, R. L. Edwards, and W. M. Landing, Distribution of [230]Th in the Labrador Sea and its relation to ventilation, *Earth and Planetary Science Letters*, 150, 151-160, 1997.

Muhs, D. R., and B. J. Szabo, New uranium-series ages of the Waimanalo Limestone, Oahu, Hawaii: implications for sea level during the last interglacial period, *Marine Geology*, 118, 315-326, 1994.

Nakada, M., Holocene sea levels in oceanic islands: implications for the rheological structure of the earth's mantle, *Tectonophysics*, 121, 263-276, 1986.

Nakada, M., and K. Lambeck, The melting history of the late Pleistocene Antarctic ice sheet, *Nature*, 333, 36-40, 1988.

Nakada, M., and K. Lambeck, Late Pleistocene and Holocene sea-level change in the Australian region and mantle rheology, *Geophys. J.*, 96, 497-517, 1989.

Nakada, M., and K. Lambeck, Late Pleistocene and Holocene sea-level change: evidence for lateral mantle viscosity structure?, in *Glacial Isostasy, Sea-Level and Mantle Rheology:*, vol. 334, edited by R. Sabadini Lambeck, K., Boschi, E., pp. 79-94, Kluwer Academic Publishers, Dordrecht, 1991.

Nakiboglu, S. M., and K. Lambeck, Secular sea-level change, in *Glacial Isostasy, Sea-Level and Mantle Rheology*, vol. 334, edited by R. Sabadini Lambeck, K., Boschi, E., pp. 237-258, Kluwer Academic Publishers, Dordrecht, 1991.

Neuzil, S. G., and C. B. Cecil, Evidence in peat of Late Quaternary climate and sea level change, western Indonesia, *Geol. Soc. Amer. Abstracts with Programs*, 24, [7], 50, 1992.

Newcomb, K. R., and W. R. McCann, Seismic history and seismotectonics of the Sunda Arc, *J. Geophys. Res.*, 92, [B1], 421-439, 1987.

Ota, Y., Marine terraces and active faults in Japan with special reference to co-seismic events, in *Tectonic Geomorphology*, edited by Morisawa and Hack, 1985.

Ota, Y., Marine terraces as reference surfaces in late Quaternary tectonics studies: examples from the Pacific Rim, *Royal Society of New Zealand Bulletin*, 24, 357-375, 1986.

Ota, Y., A. G. Hull, and K. R. Berryman, Cosesimic uplift of Holocene marine terraces in the Pakarae River area, Eastern North Island, New Zealand, *Quaternary Research*, 35, 331-346, 1991.

Ota, Y., J. Chappell, R. Kelley, N. Yonekura, E. Matsumoto, T. Nishimura, and J. Head, Holocene coral reef terraces and coseismic uplift on Huon Peninsula, Papua New Guinea, *Quaternary Research*, 40, [177-182], 1993.

Ota, Y., and K. Berryman, Tectonic geomorphology of Huon Peninsula, in *Study on Coral Reef Terraces of the Huon Peninsula, Papua New Guinea: Establishment of Quaternary Sea Level and Tectonic History*, edited by Y. Ota, pp. 11-20, 1994.

Ota, Y., ed., *Study on Coral Reef Terraces of the Huon Peninsula, Papua New Guinea: Establishment of Quaternary Sea Level and Tectonic History*, 1994.

Ota, Y., and J. Chappell, Late Quaternary coseismic uplift events on the Huon Peninsula, Papua New guinea, deduced from coral terrace data, *J. Geophys. Res.*, 101, [B3], 6071-6082, 1996.

Pandolfi, J., M. M. R. Best, and S. P. Murray, Coseismic event of May 15, 1992, Huon Peninsula, Papua New Guinea: comparison with Quaternary tectonic history, *Geology*, 22, [March], 239-242, 1994.

Peltier, W. R., Lithospheric thickness, Antarctic deglaciation history, and ocean basin discretization effects in a global model of postglacial sea level change: a summary of some sources of nonuniqueness, *Quaternary Research*, 29, 93-112, 1988.

Peltier, W. R., and A. M. Tushingham, Global sea level rise and the greenhouse effect: might they be connected, *Science*, 244, 806-810, 1989.

Peltier, W. R., and A. M. Tushingham, Influence of glacial isostatic adjustment on tide gauge measurements of secular sea level change, *J. Geophys. Res.*, 96, [B4], 6779-6796, 1991.

Perigaud, C., and P. Delecluse, Interannual sea level variations in the tropical Indian Ocean from Geosat and shallow water simulations, *J. Phys. Oceanogr.*, [23], 1916-1934, 1993.

Pirazzoli, P. A., Ecroches de corrosion marine dans l'arc héllenique, in Les indicateurs de niveaux marins, 5 edition, *Oceanis*, pp. 327-334, 1979.

Pirazzoli, P. A., Formes de corrosion marine et vestiges archéaologiques submerges: interpretation néotectonique de quelques exemples en Grèce et en Yougoslavie, *Annales de l'Institut Oceanographique*, 56, 101-111, 1980.

Pirazzoli, P. A., Marine Notches, in *Sea-Level Research: A Manual for the Collection and Evaluation of Data*, pp. 361-400, 1986.

Pirazzoli, P. A., U. Radtke, W. S. Hantoro, C. Jouannic, C. T. Hoang, C. Causse, and M. Borel Best, A one million-year-long sequence of marine terraces on Sumba Island, Indonesia, *Marine Geology*, 109, 221-236, 1993.

Plafker, G., Tectonic deformation associated with the 1964 Alaska earthquake, *Science*, 148, [3678], 1675-1687, 1965.

Plafker, G., and M. Rubin, Vertical tectonic displacements in south central Alaska during and prior to the great 1964 earthquake, *Geosci. Osaka City Univ.*, 10, 53-66, 1967.

Plafker, G. Tectonics of the March 27, 1964 Alaska earthquake, *U.S. Geol. Survey Prof. Paper* 543-I, 74 pp., 1969.

Plafker, G. and M. Rubin, Uplift history and earthquake recurrence as deduced from marine terraces on Middleton Island, Alaska, *U.S. Geol. Survey Open File Report* 78-943, 857-868, 1978.

Prawirodirdjo, L., Y. Bock, R. McCaffrey, J. Genrich, E. Calais, C. Stevens, S. S. O. Puntowedo, C. Subarya, and J. Rais, Geodetic observations of interseismic strain segmentation at the Sumatran subduction zone, in preparation, 1996.

Priess, K., B. A. Thomassin, G. A. Heiss, W.-C. Dullo, and G. Camoin, Variabilité de la croissance de *Porites* massifs dans les recifs coralliens de Mayotte, *C.R. Acad. Sci. Paris, Sciences de la vie*, 318, 1147-1154, 1995.

Sato, H., Crustal movements associated with the 1944 Tonankai earthquake, *J. Geol. Soc. Japan*, 15, 177-180 (in Japanese).

Savage, J. C., A dislocation model of strain accumulation and release at a subduction zone, *J. Geophys. Res.*, 4984-4996, 1983.

Savage, J. C., and G. Plafker, Tide gauge measurements of uplift along the south coast of Alaska, *J. Geophys. Res.*, 96, [B3], 4325-4335, 1991.

Savage, J. C., and W. Thatcher, Interseismic deformation at the Nankai trough, Japan, subduction zone, *J. Geophys. Res.*, 97, [B7], 11117-11135, 1992.

Savage, J. C., Interseismic uplift at the Nankai subduction zone, southwest Japan, 1951-1990, *J. Geophys. Res.*, 100, [B4], 6339-6350, 1995.

Schwarz, H. P., and A. G. Latham, Dirty calcites 1. Uranium-series dating of contaminated calcite using leachates alone, *Chem. Geol.*, 80, 35-43, 1989.

Scoffin, T. P., and D. R. Stoddart, The nature and significance of microatolls, *Phi☐osophical Transactions of the Royal Society London*, Series B, 284, 99-122, 1978.

Sieh, K., Pre-historic large earthquakes produced by slip on the San Andreas fault at Pallett Creek, California, *J. Geophys. Res.*, 83, 3907-3939, 1978.

Sieh, K., Neotectonic and Paleoseismic Studies in West and North Sumatra, (abstract) *AGU 1991 Fall Meeting Program & Abstacts*, 72, [No. 44], 460, 1991.

Sieh, K., J. Zachariasen, Y. Bock, R. L. Edwards, F. Taylor, and P. Gans, Active Tectonics of Sumatra, *Geol. Soc. Amer. Abstracts with Programs*, 26, [7], A-382, 1994.

Sieh, K., and D. H. Natawidjaja, Modern geometry and slip rates of the Great Sumatran Fault, in prep.

Spencer, T., Weathering rates on a Caribbean reef limestone: results and implications, *Marine Geology*, 69, 195-201, 1985.

Stein, M., G. J. Wasserburg, K. R. Lajoie, and J. H. Chen, U-series ages of solitary corals from the California coast by mass spectrometry, *Geochimica et Cosmochimica Acta*, 55, [12], 3709-3722, 1991.

Stein, M., G. J. Wasserburg, P. Aharon, J. H. Chen, Z. R. Zhu, A. Bloom, and J. Chappell, TIMS U-series dating and stable isotopes of the last interglacial event in Papua New Guinea, *Geochimica and Cosmochimica Acta*, 57, 2541-2554, 1993.

Stoddart, D. R., and T. P. Scoffin, Microatolls: review of form, origin and terminology, *Atoll Res. Bull.*, 228, 17 pp., 1979.

Taylor, F. W., B. L. Isacks, C. Jouannic, A. L. Bloom, and J. Dubois, Coseismic and Quaternary vertical tectonic movements, Santo and Malekula Islands, NewHebrides island arc, *J. Geophys. Res.*, 85, 5367-5381, 1980.

Taylor, F. W., C. Jouannic, and A. L. Bloom, Quaternary uplift of the Torres islands, Northern New Hebrides frontal arc: comparison with Santo and Malekula Islands, Central New Hebrides frontal arc, *Journal of Geology*, 93, 419-138, 1985.

Taylor, F. W., C. Frohlich, J. Lecolle, and M. Strecker, Analysis of partially emerged corals and reef terraces in the central Vanuatu arc: Comparison of contemporary coseismic and nonseismic with Quaternary vertical movements., *J. Geophys. Res.*, 92, [B6], 4905-4933, 1987.

Taylor, F. W., R. L. Edwards, and G. J. Wasserburg, Seismic recurrence intervals and timing of aseismic subduction inferred from emerged corals and reefs of the central Vanuatu (New Hebrides) frontal arc, *J. Geophys. Res.*, 95, [B1], 393-408, 1990.

Thatcher, W., and J. B. Rundle, A viscoelastic coupling model for the cyclic deformation due to periodically repeated earthquakes at subduction zones, *J. Geophys. Res.*, 89, [B9], 7631-7640, 1984.

Thatcher, W., The earthquake deformation cycle at the Nankai trough, Southwest Japan, *J. Geophys. Res.*, 3087-3101, 1984.

Thatcher, W., Order and diversity in the modes of circum-Pacific earthquake recurrence, *J. Geophys. Res.*, 95, [B3], 2609-2623, 1990.

Thurber, D. L., Anomalous $^{234}U/^{238}U$ in nature, *J. Geophys. Res.*, 67, 4518-1520., 1962.

Thurber, D. L., W. S. Broecker, R. L. Blanchard, H. A. Potratz, Uranium-series ages of Pacific atoll coral, *Science*, 149 (3679), 55-58, 1965.

Tregoning, P., F. K. Brunner, Y. Bock, S. S. O. Puntodewo, R. MCcCaffrey, J. F. Genrich, E. Calais, J. Rais, and C. Subarya, First geodetic measurement of convergence across the Java Trench, *Geophysical Research Letters*, 21, [19], 2135-2138, 1994.

Trupin, A. S., and J. M. Wahr, Constraints on long-period sea level variations from global tide gauge data, in *Glacial Isostasy, Sea-Level and Mantle Rheology*, vol. 334, edited by R. Sabadini Lambeck, K., Boschi, E., pp. 271-284, Kluwer Academic Publishers, Dordrecht, 1991.

Veron, J. E. N., *Corals of Australia and the Indo-Pacific*, 1993 edition, University of Hawaii Press/Angus and Robertson, Honolulu/North Ryde, NSW, Australia, 1-644 pp., 1986.

Verstappen, H. T., *A geomorphological reconnaissance of Sumatra and adjacent islands (Indonesia)*, Wolters-Noordhoff Publishing, Groningen, 1-192, 1973.

Vita-Finzi, C., and B. Situmorang, Holocene coastal deformation in Simeulue and Nias, Indonesia, *Marine Geology*, 89, 153-161, 1989.

Vita-Finzi, C., Pulses of emergence in the outer-arc ridge of the Sunda Arc, in *Journal of Coastal Research Special Issue No. 17: Holocene Cycles: Climate, Sea Levels, and Sedimentation, Journal of Coastal Research Special Issue*, pp. 279-281, 1995.

Wallace, R. E., Notes on stream channel offsets by the San Andreas Fault, southern Coast ranges, California, in *Proceedings, Conference on Geologic Problems of the San Andreas Fault system*, Stanford Univ. Publ. Geol. Sci., vol. 11, edited by W. R. D. a. A. Grantz, pp. 6-21, 1968.

Wallace, R. E., Profiles and ages of young fault scarps, north-central Nevada, *Geol. Soc. Amer. Bull.*, 88, 1267-1281, 1977.

Weber, J. N., and E. W. White, Caribbean reef corals Monastrea annularis and Monastrea cavernosa - long-term growth data as determined by skeletal X-radiography, *Amer. Assoc. Petrol. Geol.*, 4, 171-179, 1977.

Woodroffe, C., and R. McLean, Microatolls and recent sea level change on coral atolls, *Nature*, 344, 531-534, 1990.

Woodroffe, C., R. McLean, and E. Wallensky, Darwin's coral atoll: Geomorphology and recent development of the Cocos (Keeling) Islands, Indian Ocean, *National Geographic Research*, 6, [3], 262-275, 1990a.

Woodroffe, C., R. McLean, H. Polach, and E. Wallensky, Sea level and coral atolls: Late Holocene emergence in the Indian Ocean, *Geology*, 18, [January], 62-66, 1990b.

Woodroffe, C. D., H. H. Veeh, A. C. Falkland, R. F. McLean, and E. Wallensky, Last interglacial reef and subsidence of the Cocos (Keeling) Islands, Indian Ocean, *Marine Geology*, 96, 137-143, 1991.

Wyrtki, K., Sea level during the 1972 El Niño, J. *Phys. Oceanogr.*, 7, 779-787, 1977.

Wyrtki, K., The response of sea surface topography to the 1976 El Niño, J. Phys. Oceanogr., 9, 1223-1231, 1979.

Yeats, R. S., and C. S. Prentice, Introduction to special section: Paleoseismology, *J. Geophys. Res.*, 101, [B3], 5847-5853, 1996.

Yonekura, N., and Y. Ota, Sea-level changes and tectonics in the late Quaternary, *Recent Progress of Natural Sciences in Japan*, 11, 17-34, 1986.

Zachariasen, J., K. Sieh, F. Taylor, R. L. Edwards, and W. S. Hantoro, Paleoseismology of the Sumatran subduction zone: Records of coseismic and interseismic deformation, *EOS, Transactions of the American Geophysical Union*, 76, [46], F363, 1995.